Newcastle University

Identification of a Novel Cell Division Protein in *Bacillus subtilis*

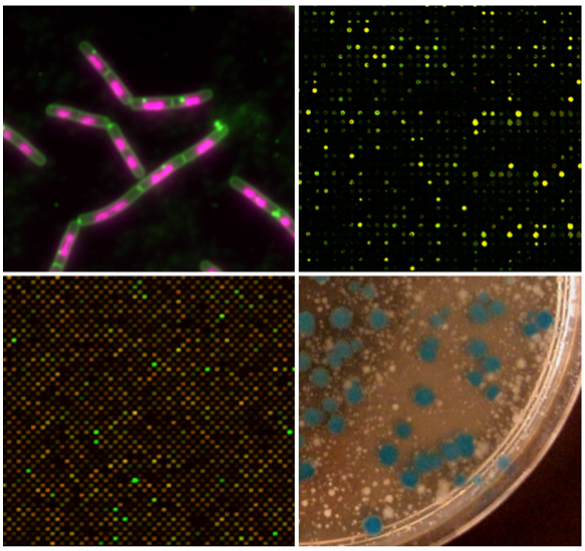

Katarína Šurdová

Thesis submitted for the degree of Doctor of Philosophy

Newcastle University
Faculty of Medical Sciences
Institute for Cell and Molecular Biosciences

September 2011

Abstract

FtsZ is a tubulin-like protein that polymerizes into a ring like structure at midcell, which is the first step in septum formation. The dynamics of FtsZ polymerization is regulated by a set of proteins, one of which is ZapA. ZapA is a non-essential positive regulator of FtsZ polymerization. In this study we have performed a screen for mutations in *Bacillus subtilis* that result in a cell division defect when combined with Δ*zapA*. Three such mutations were found in the *yvcL* gene. Since this gene is homologous to *whiA* from *Streptomyces coelicolor*, and the lack of both proteins imposes in some instances similar phenotypes, we proposed to rename the gene *whiA*. Mutation of *whiA* alone had only a mild effect on cells, which became 20-60% longer. However, the double mutant Δ*whiA* Δ*zapA* is filamentous and sick. Evidence is provided that the filamentation is caused by delocalization of FtsZ, and that WhiA is implemented in the early stage of cell division. Interestingly, WhiA localizes to the nucleoid and is important in cells that overinitiate replication. We also found that this protein is essential for survival after UV-induced DNA damage. Its binding sites on DNA were identified using a ChIP-on-chip method and the *dif* site, which is important for chromosome dimer resolution, was found to be a possible target of WhiA. A transcriptome analysis using whole genome microarray showed that WhiA does not function as transcriptional regulator. We conclude that WhiA is involved in both cell division and chromosome dynamics.

Acknowledgements

I would not have been writing this thesis without essential help from others. It is a great pleasure to thank everyone who has participated in my project, helped and encouraged me. I am earnestly grateful to my supervisors. Dear Leendert, thank you for leaving me (with) a space for my own thoughts and mistakes, and also for many discussions. Jeff, your everlasting enthusiasm for science is very infectious and has been inspirative for me. I have learned many things, and always got advised by former and also present members of the lab. I would like to thank Dennis, Yoshi, Stephan, Heath, Mark, Jan-Willem and Ling for sharing their support, guidance, strains and thorough help. Thank you also goes to our best, and only, technician Ian who is indisputably the most important person for all people performing 'wet work'. I am obliged to Dr. Richard Capper and Dr. Nigel Saunders who patiently supervised me in Oxford for two weeks. I would like to thank Imi and Katka. This work would not have been submitted without being read by Leendert, Nada, Richard and Kathrin whom I feel indebted for their useful comments and suggestions.

I would like to thank all the girls who were always there to listen to good news and also to my frustrations: Kathrin, Pamela, Nada, Robyn, Maki, Monika, Patri, Aurelie and others who joined for the girlie lunches and evening/night programmes. Many thanks for all the jokes and discussions to all the lab folks, who created fantastic and friendly atmosphere in and out of the lab. I must not leave out our associated Danish, Russian and German labs.

I am truly indebted to my parents who have supported me in becoming a molecular biologist. Many thanks to my partner Rasto, mainly for giving me the most precious 'present' in the world, our daughter Andrejka.

Table of Contents

	Table of Contents	i
	Abbreviations	1
1	**Introduction**	3
1.1	Cytokinesis in bacteria	4
1.1.1	Polymerization of FtsZ	4
1.1.2	FtsZ interacting proteins	9
1.1.3	Assembly of the divisome and completion of cell division in *E. coli* and *B. subtilis*	13
1.1.4	Cellular development - sporulation	15
1.1.4.1	Sporulation in *Streptomyces* spp.	17
1.2	Chromosome dynamics	19
1.2.1	Organization of the chromosomes in the cell	19
1.2.2	DNA replicatiom	20
1.2.3	Chromosome segregation	21
1.3	Coordination of cell division	25
1.3.1	Cell division and the growth rate	25
1.3.2	Cell division and chromosome dynamics	27
1.3.3	Coordination of chromosome replication	27
2	**Materials and methods**	29
2.1	Solutions and media	30
2.2	Strains and plasmids	30
2.3	Oligonucleotides	36
2.4	Media supplements	39
2.5	DNA manipulations	39
2.5.1	Oligonucleotides	39
2.5.2	Polymerase chain reaction (PCR)	39
2.5.3	Purification of PCR products	40
2.5.4	Plasmid purification	40
2.5.5	Agarose gel electrophoresis of DNA fragments	40

2.5.6	DNA modification reactions	40
2.5.6.1	Digestion with restriction enzymes	40
2.5.6.2	Dephosphorylation of 5' ends	40
2.5.7	Ligation reaction	40
2.5.8	DNA sequencing	41
2.5.9	Isolation of chromosomal DNA from *B. subtilis*	41
2.6	Protein manipulations	41
2.6.1	SDS-polyacrylamide gel electrophoresis	41
2.6.2	Coomassie brilliant blue staining	41
2.6.3	Western blot analysis	41
2.6.4	Purification of YvcL-His_6	42
2.6.5	Raising anti-YvcL- His_6 serum	42
2.6.6	Electrophoretic mobility shift assay - EMSA	43
2.7	*Escherichia coli* methods	43
2.7.1	Preparation of competent *E. coli* cells	43
2.7.2	*E. coli* transformation	44
2.7.3	Bacterial two hybrid system	44
2.8	*Bacillus subtilis* methods	44
2.8.1	Preparation of competent *B. subtilis* cells	44
2.8.2	*B. subtilis* transformation	44
2.8.3	Construction of strains	44
2.8.3.1	Construction of *yvcL* mutant strains	44
2.8.3.2	Construction of conditional mutants	45
2.8.3.3	Construction of GFP-fusions	47
2.8.4	Synthetic lethal screen	47
2.8.5	Suppressor screen for Δ*yvcL* Δ*zapA* doublemutant	50
2.9	Microscopic imaging	52
2.9.1	Phase contrast and fluorescence microscopy	52
2.9.1.1	Localization of YvcL	52
2.9.1.2	Determination of nucleoid morphology	52
2.9.2	Transmission electron microscopy	53
2.10	Microarray analysis	53
2.11	qPCR	53
2.11.1	Marker frequency analysis for *ori*/*ter* ratio measurement	53
2.11.2	Verification of microarray results	54
2.12	Determination of DNA binding sites of YvcL	54

3	**Identification and characterization of the new cell division protein YvcL**	56
3.1	Introduction	57
3.2	Results	60
3.2.1	Identification of YvcL in a synthetic lethal screen	60
3.2.1.1	Construction of strains for the synthetic lethal screen	60
3.2.1.2	Δ*zapA* is synthetically lethal with Δ*yvcL*	60
3.2.2	Excluding polar effects	61
3.2.3	Phenotypic characterization of the *yvcL* mutant	62
3.2.4	A Δ*yvcL* Δ*zapA* double mutant is disturbed in Z-ring formation	65
3.2.4.1	FtsZ concentration sensitivity	69
3.2.5	YvcL is important also for growth of other cell division mutants	70
3.2.5.1	Localization of GFP-FtsZ in Δ*yvcL* double mutants	73
3.3	Discussion	77
4	**Is WhiA a transcriptional regulator?**	82
4.1	Introduction	83
4.2	Results	84
4.2.1	Microarray analysis of the *whiA* mutant	84
4.2.2	Verification of microarray results using qPCR	85
4.3	Discussion	89
5	**WhiA is a DNA binding protein**	91
5.1	Introduction	92
5.2	Results	93
5.2.1	WhiA localizes to nucleoids *in vivo*	93
5.2.2	WhiA is not a nucleoid occlusion protein	98
5.2.3	Nucleoid morphology and positioning in a *whiA* mutant	99
5.2.3.1	Localization pattern of origins and termini of replication in a *whiA* mutant	101
5.2.4	The lack of WhiA causes sensitivity to increased DNA replication initiation and to DNA damage	105
5.2.5	Determination of WhiA binding sites using ChIP-on-chip	111
5.2.6	WhiA binds DNA *in vitro*	117
5.3	Discussion	119

6	**Identification of suppressor mutations of Δ*whiA***	122
6.1	Introduction	123
6.2	Results	124
6.2.1	Characterization of the Δ*whiA* Δ*zapA* suppressors	124
6.2.2	Shortening of cell length by mutations in *braB*, *ggaB*, *gtaB*, *pgcA* and *ugtP*	127
6.3	Discussion: Possible mechanisms of suppression	131
7	**Final remarks**	134
7.1	Summary	135
7.2	Possible dual implementation of WhiA	136
7.3	Future prospects	136
8	**References**	137
9	**Appendices**	159
9.1	Solutions	160
9.2	Growth media	162

Abbreviations

ATP	adenosine triphosphate
B. subtilis	*Bacillus subtilis*
BCAA	branched chain amino acid
C. crescentus	*Caulobacter crescentus*
CAA	casamino acids
ChIP	chromatin immunoprecipitation
DAPI	4,6-diamidino-2-phenylindole
dH_2O	deionised water
DNA	deoxyribonucleic acid
DTT	dithiothreitol
E. coli	*Escherichia coli*
EDTA	ethylenediaminetetraacetic acid
e. g.	*exempli gratia* (for example)
EMSA	Electrophoretic mobility shift assay
et al.	*et alii* (and others)
GFP	green fluorescent protein
Glc	glucose
GTP	guanosine triphosphate
h	hour
IPTG	isopropyl β-D-1-thiogalactopyranoside
kDa	kilo Dalton
LB	Luria-Bertani broth
LTA	lipoteichoic acid
min	minute
MOPS	3-(N-morpholino)-2-hydroxypropanesulphonic acid
NA	nutrient agar
OD_{600}	optical density; wavelength 600 nm
oriC	replication origin
PAB	Penassay broth
PAGE	polyacrylamide gel electrophoresis
PBP	penicillin binding protein

PBS	phosphate buffered saline solution
PCR	polymerase chain reaction
PG	peptidoglycan
RNA	ribonucleic acid
S. coelicolor	*Streptomyces coelicolor*
SD	standard deviation
SDS	sodim dodecyl sulfate
SLS	Synthetic Lethal Screen
SMM	Spizizen minimal medium
spp.	species (plural)
TAE	Tris, acetate, EDTA
TE	Tris, EDTA
Ter	DNA t*erm*inator
T. maritima	*Thermotoga maritima*
UDP	uridine diphosphate
UV	ultraviolet
vs.	versus
WB	western blot
WTA	wall teichoic acid
X-gal	5-bromo-4-chloro-3-indolyl-β-D-galactopyranoside

Chapter 1

Introduction

1.1 Cytokinesis in bacteria

Bacterial cell division is accomplished by a set of more than ten proteins, which assemble in a specific order, time and place within the cell. In rod shaped bacteria the earliest and crucial structure appearing during the division is a midcell positioned ring composed of the protein FtsZ. This so-called Z-ring attracts other cell division proteins that are responsible for the synthesis of the septal cell wall. FtsZ remains at the leading edge of the nascent septum.

1.1.1 Polymerization of FtsZ

FtsZ (Filamenting temperature sensitive mutant Z) is a tubulin-like protein that is essential in almost all bacteria (Erickson, 1995; Lowe and Amos, 1998; Romberg and Levin, 2003; Weiss, 2004). It can also be found in Archaea, in the mitochondria of some organisms, and in all chloroplasts (Margolin, 2000; Osteryoung and Pyke, 1998; Osteryoung *et al.*, 1998; Rothfield *et al.*, 1999). Both tubulin and FtsZ are cytoskeletal proteins and are very similar in their tertiary structures. However, their macromolecular organization shows fundamental differences. Tubulin forms a heterodimer composed of an α and β subunit (Krauhs *et al.*, 1981; Ponstingl *et al.*, 1981). Tubulin dimers polymerize head-to-tail into protofilaments in a GTP-dependent manner, and usually around 13 of these protofilaments align to form a microtubule (Li *et al.*, 2002; Lowe *et al.*, 2001; Nogales *et al.*, 1998). FtsZ does not form dimers, instead, FtsZ monomers polymerize into protofilaments in the presence of GTP. These protofilaments can assemble or disassemble bidirectionally while GTP is hydrolyzed (Fig. 1.1) (de Boer *et al.*, 1992; Huecas *et al.*, 2008; Lowe and Amos, 1998; Romberg *et al.*, 2001). Most of the FtsZ molecules in the protofilaments are bound to GTP (Mingorance *et al.*, 2001; Oliva *et al.*, 2004b; Romberg and Mitchison, 2004; Scheffers and Driessen, 2002). The energy acquired from GTP hydrolysis is not stored within the FtsZ molecule, but causes local destabilisation and results in curvature of protofilaments (Huecas and Andreu, 2004). The exchange of the FtsZ monomers in the protofilament is very dynamic. The Z-ring can reconstitute within a few seconds, by means of FRAP experiments the halftime of recovery after photobleaching is 8-30s (Anderson *et al.*, 2004; Stricker *et al.*, 2002). The GTPase active site is formed by two molecules of FtsZ, and is

sufficiently open to rapidly exchange nucleotides (Oliva *et al.*, 2004b; Scheffers *et al.*, 2002).

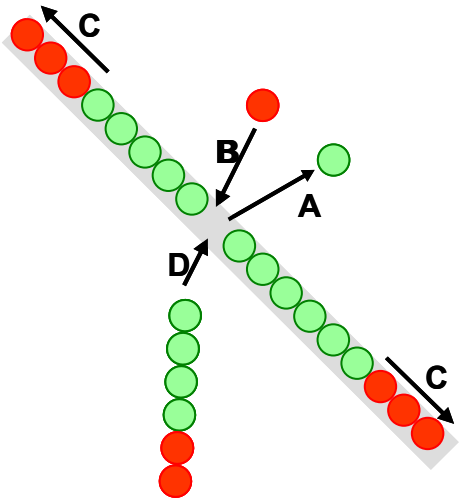

Fig. 1.1 FtsZ protofilament dynamics
(**A**) Any molecule can be relieved from the polymer (after GTP hydrolysis). (**B**) Polymerization by joining one or (**C**) more single molecules of FtsZ, or joining another nascent polymer (**D**). Green = preexisting polymer; Red = newly polymerized or joined FtsZ molecules.

The GTPase activity of FtsZ is Mg^{++} dependent and high concentrations of Mg^{++} can stimulate and stabilize protofilaments (Mohammadi *et al.*, 2009; Oliva *et al.*, 2004a; RayChaudhuri and Park, 1992). Biochemical and electron microscopy data have indicated that FtsZ protofilaments can be organized into bundles, sheets, rings, and other higher molecular structures depending on the conditions used (Bramhill and Thompson, 1994; Erickson *et al.*, 1996; Lowe and Amos, 1999; Mingorance *et al.*, 2005; Mukherjee and Lutkenhaus, 1994; Paez *et al.*, 2009). Although extensively studied, it is still unclear how the protofilaments are organized in living cells. The current view is that the cellular protofilaments are probably no more than 90 FtsZ molecules long and that the Z-ring is only around 3 protofilaments thick (Anderson *et al.*, 2004; Li *et al.*, 2007). In *E. coli*, *B. subtilis* and *C. crescentus* cells, FtsZ is organized into a helical structure (Z-helix) which spans the whole cell length (Peters *et al.*, 2007; Thanbichler and Shapiro, 2006; Thanedar and Margolin, 2004) (Fig. 1.2A). As the cell grows and becomes longer, the chromosomes segregate, the FtsZ moiety 'slides' along the helical trajectory from the distal cellular areas to the midcell where it forms the Z-ring (Peters *et al.,* 2007). It is not clear what mechanism directs the initial helical arrangement of FtsZ. Two mechanisms are thought to guide Z-ring positioning. First is the nucleoid occlusion system which allows coordination of septation with chromosome segregation. Second is the Min system which prevents the formation of septa at the cell poles.

Nucleoid occlusion

Cytokinesis must be coordinated with nucleoid replication and segregation to ensure the progeny inherits an intact copy of the genetic information. It has been speculated that the compacted chromosomal DNA at the centre of the cell, the nucleoid itself, prevents assembly of FtsZ into a Z-ring, and this phenomenon was called nucleoid occlusion (Mulder and Woldringh, 1989; Woldringh *et al.*, 1990). This was later confirmed by the discovery of the Noc protein in *B. subtilis* and SlmA in *E. coli* (Bernhardt and de Boer, 2005; Wu and Errington, 2004). Noc binds DNA and prevents septum formation in DNA-occupied regions (Fig. 1.2B). It was shown that deletion of *noc* causes formation of aberrant Z-rings over the nucleoids in sensitized cells (Wu and Errington, 2004). It is likely that Noc prevents the transition of Z-helix to Z-ring rather than the polymerization of FtsZ (Wu and Errington, 2004; Peters *et al.,* 2007). Direct interaction of Noc and FtsZ has not been shown and its *modus operandi* remains speculative. Noc recognizes a specific 14 bp repeat and was found to bind to 74 regions around the chromosome, except for the region close to the terminus (Wu *et al.*, 2009). Cell division is delayed when Noc is artificially forced to bind to the terminus region (Wu *et al.*, 2009). This suggests that cells form a Z-ring only after chromosome replication is completed and the Noc-bound DNA region is removed from the midcell area (Wu *et al.*, 2009). Despite this information, the exact localization of Noc in cells is not really clear since an active Noc-YFP fusion was found to be associated with the membrane (Wu *et al.* 2009). Although the *noc* mutant does not have an obvious phenotype, it has been speculated that beside Noc there is (are) more proteins(s) involved in nucleoid occlusion (Bernard *et al.*, 2010; Wu and Errington, 2004). *E. coli* SlmA shares no sequence homology with Noc. However, it acts in a similar way to Noc. It binds DNA and its overpoduction leads to cell division arrest. *In vitro*, SlmA was shown to interact directly with FtsZ and to promote formation of ribbon-like structures (Bernhardt and de Boer, 2005). In bacteria where no Min homologs are found (e. g. *C. crescentus*) cell division is thought to rely solely on nucleoid occlusion (Quardokus and Brun, 2002).

Min system

The Min system prevents the aberrant formation of Z-rings close to cell poles (de Boer *et al.*, 1989; Jacobs *et al.*, 1999). The active inhibitory complex constitutes two proteins: MinC and MinD. Their concentration is highest at the cell poles and decreases toward

the centre of the cell leaving the midcell free for Z-ring formation (Raskin and de Boer, 1997). MinC interacts directly with FtsZ, and was shown to prevent FtsZ polymerization (Hu *et al.*, 1999). Recent report showed that MinC causes loss of elasticity of the FtsZ assemblies (networks) presumably by weakening the longitudinal association of FtsZ monomers and also by inhibition of lateral interactions of FtsZ protofilaments (Dajkovic *et al.*, 2008). MinD is associated with the membrane through its amphipatic C-terminus (de Boer *et al.*, 1991), and is responsible for MinC activation (Cordell *et al.*, 2001; Hayashi *et al.*, 2001; Sakai *et al.*, 2001). In *E. coli* the concentration gradient of MinCD is assured by a third protein of the Min system, MinE (Rothfield and Zhao, 1996). Interestingly, MinCDE have been shown to oscillate from pole to pole (Hu and Lutkenhaus, 1999; Juarez and Margolin, 2010; Pichoff *et al.*, 1995). The mechanism of oscillation is complicated and not fully understood. However, MinD and MinE have been shown to spontaneously self-organize (in the presence of ATP) and form sliding waves on membrane surfaces *in vitro* (Loose *et al.*, 2008). When rod-shaped bacteria divide, the areas around the division site become new cell poles after cytokinesis. Recent microscopic studies using GFP fused MinD in *E. coli* suggested that the MinCD complex pauses at the midcell position late in the division, and then shortly after division it prevents the assembly of functional Z-rings at newly formed poles (Gregory *et al.*, 2008; Juarez and Margolin, 2010). This is supported also by microscopic experiments in *B. subtilis*, where GFP-fused MinC was found to colocalize with the assembled divisome (Gregory *et al.*, 2008).

Oscillation of the Min system was not observed in *B. subtilis*, and in fact this organism does not contain a MinE homologue (Marston and Errington, 1999; Marston *et al.*, 1998). Instead, the DivIVA protein, which binds to cell poles, is needed for the MinCD gradient (Fig. 1.2B) (Cha and Stewart, 1997; Edwards and Errington, 1997). DivIVA and MinE show no sequence homology (Zhang *et al.*, 1998). The interaction between DivIVA and MinD is mediated by MinJ (Bramkamp *et al.*, 2008; Patrick and Kearns, 2008). DivIVA is the main topological determinant of the Min system in *B. subtilis*. Two recent papers reported that DivIVA targets the cell poles because of its preference for negatively curved membranes (Lenarcic *et al.*, 2009; Ramamurthi and Losick, 2009). The curvatures produced with proceeding division septum formation attract DivIVA and, after septum enclosure, DivIVA becomes a constituent of newly formed cell poles (Edwards and Errington, 1997; Gamba *et al.*, 2009).

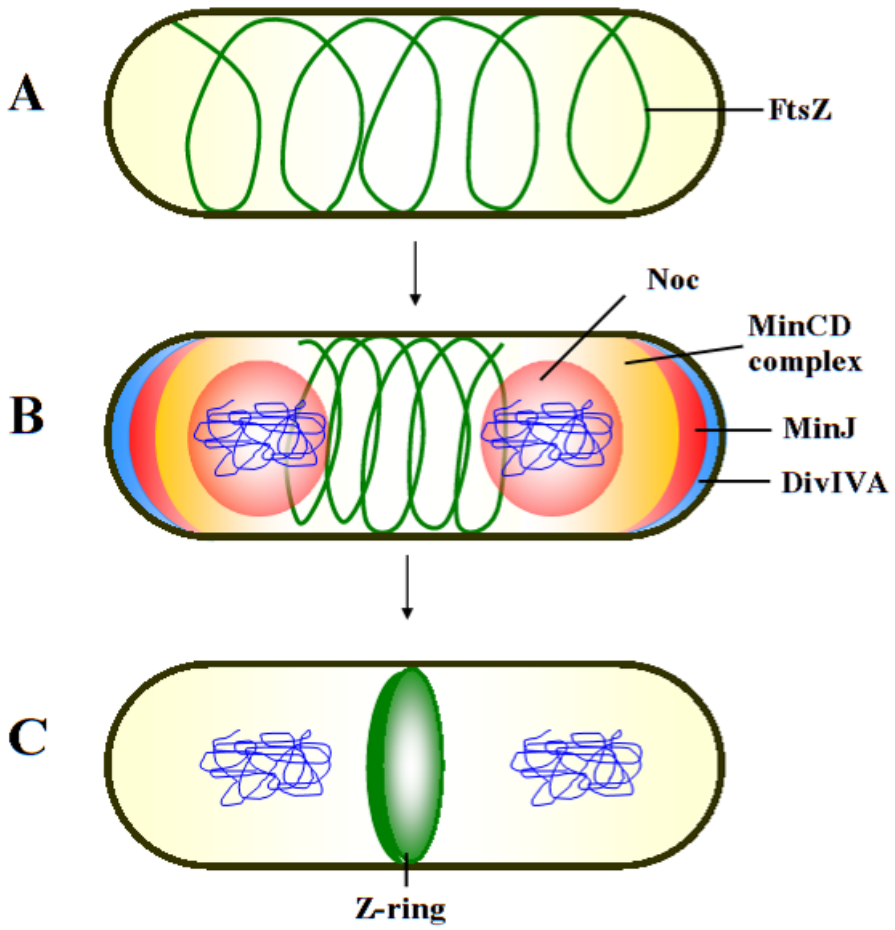

Fig. 1.2 An outline of the interplay between nucleoid occlusion and the *min* system during cell division in *B. subtilis*
(**A**) FtsZ (green) forms a helical structure. (**B**) FtsZ is remodelled and is more abundant at midcell. Nucleoid occlusion facilitated by Noc (binding to DNA) prevents the formation of a Z-ring in the proximity of the nucleoid. At the same time, a complex of proteins DivIVA, MinJ, MinD, and MinC prevent from the formation of Z-rings at the cell poles. (**C**) Z-ring is formed at midcell.

1.1.2 FtsZ interacting proteins

In addition to the Min and nucleoid occlusion systems, bacteria possess a number of other proteins that interact with FtsZ and modulate its activity. These 'additional' proteins are usually dispensable and may be specific to some bacterial species (reviewed in Adams and Errington, 2009).

FtsA is structurally related to actin (van den Ent and Lowe, 2000). Electron microscopy imaging revealed *S. pneumoniae* FtsA polymers form corkscrew-like helixes (Lara *et al.*, 2005). FtsA binds to the membrane through its C-terminal amphipatic helix which can be surprisingly exchanged by an unrelated membrane-targeting peptide, while FtsA remains functional (Shiomi and Margolin, 2008). FtsA also binds FtsZ and thus serves as a membrane anchor for FtsZ (Pichoff and Lutkenhaus, 2005). The gene for FtsA forms one operon with *ftsZ* in *B. subtilis* and in many other organisms (Nikolaichik and Donachie, 2000). The transcription of the *ftsAZ* operon is constitutive and the intracellular concentration of FtsA and FtsZ is constant during growth (Rueda *et al.*, 2003; Weart and Levin, 2003). However, during sporulation, *ftsAZ* expression is enhanced by the sigma factor SigH to secure a higher concentration of FtsZ required for sporulation (Gonzy-Treboul *et al.*, 1992; Levin and Losick, 1996). In *E. coli* the loss of FtsA is lethal, but *B. subtilis* is able to grow without FtsA, although cells are filamentous (Beall and Lutkenhaus, 1992; Jensen *et al.*, 2005). It appears that the balance of the protein ratio between FtsZ and FtsA is crucial for efficient cell division (100/1 in *E. coli* and 5/1 in *B. subtilis*) (Dai and Lutkenhaus, 1992; Dewar *et al.*, 1992; Feucht *et al.*, 2001; Rueda *et al.*, 2003). Biochemically FtsA binds triphosphates (preferentially ATP) which activate FtsA and, while *E. coli* FtsA exhibits weak (if any) hydrolytic activity, the *B. subtilis* FtsA was shown to hydrolyze ATP although the significance of this activity is unclear (Beuria *et al.*, 2009; Feucht *et al.*, 2001; Lara *et al.*, 2005).

ZipA is an essential protein in *E. coli*, however, no homologue is found in *B. subtilis*. ZipA was shown to interact with FtsZ (Hale and de Boer, 1997). ZipA contains a transmembrane helix and thus recruits FtsZ to the membrane (Hale *et al.*, 2000). *In vitro*, ZipA was shown to cause bundling of FtsZ protofilaments and it is thought to promote lateral interactions of FtsZ protofilaments (Hale *et al.*, 2000; RayChaudhuri, 1999). Localization of both ZipA and FtsA is dependent on FtsZ, but they act

independently on the targeting of the Z-ring to the membrane (Hale and de Boer, 1999; Liu *et al.*, 1999). Recent data have indicated that FtsA and ZipA are also required for recruitment of later cell division proteins to the division septum (Hale and de Boer, 2002; Pichoff and Lutkenhaus, 2002).

ZapA (Z-ring associated protein A) is a small (11.6 kDa) conserved protein that directly interacts with FtsZ and has a positive effect on Z-ring formation (Gueiros-Filho and Losick, 2002). It has been shown that overexpression of ZapA counteracts the division inhibition caused by MinCD overexpression (Gueiros-Filho and Losick, 2002). Although ZapA is not essential, lower FtsZ levels are lethal when ZapA is absent (Gueiros-Filho and Losick, 2002). The ZapA ortholog in *E. coli* is YgfE. It was shown that YgfE and ZapA inhibit GTP hydrolysis by FtsZ and both proteins stabilize FtsZ protofilaments (Gueiros-Filho and Losick, 2002; Low *et al.*, 2004; Small *et al.*, 2007). The crystal structure of ZapA from *Pseudomonas aeruginosa* (Fig. 1.3) shows that a tetramer is formed by two antiparallel dimers (Low *et al.*, 2004). The N-terminal domain of ZapA shows the highest conservation and it is thought to interact with FtsZ. ZapA probably acts as a 'clip' which joins FtsZ protofilaments side by side (Low *et al.*, 2004). This model is also supported by the fact that ZapA and YgfE promote bundling of FtsZ protofilaments *in vitro* (Gueiros-Filho and Losick, 2002; Small *et al.*, 2007).

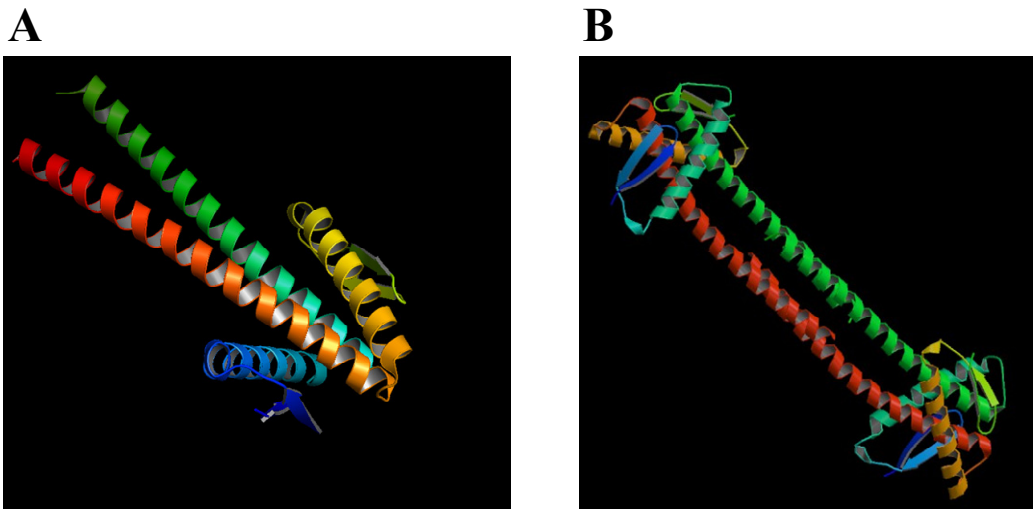

Fig. 1.3 The crystal structure of ZapA from *Pseudomonas aeruginosa* at 2.8 Å resolution (Low *et al.*, 2004)
(**A**) Formation of a ZapA dimer through its N-terminal region. (**B**) Tetramer is formed *in vitro* at high ZapA concentrations.

ZapB and **ZapC** are division proteins that have been recently identified in *E. coli*, and which are present in many Proteobacteria. ZapB localizes to the division site where it interacts with FtsZ and is presumably bridging FtsZ and YgfE (Galli and Gerdes, 2010). ZapB forms a coiled-coil structure and *in vitro* the protein forms long filaments (Ebersbach *et al.*, 2008b). The role of **ZapC** seems similar to ZapA or ZapB in that it binds FtsZ at the midcell and promotes lateral interactions of FtsZ protofilaments (Durand-Heredia *et al.*, 2011).

EzrA (Extra Z-ring Assembly) was found to be important for accurate Z-ring placement in *B. subtilis* (Haeusser *et al.*, 2007; Haeusser *et al.*, 2004; Levin *et al.*, 1999). *ezrA* mutants form multiple Z-rings and additional Z-rings at the cell poles (Haeusser *et al.*, 2004; Levin *et al.*, 1999). These structures sequester additional division proteins, resulting in a delay in septum completion and longer cell length (Chung *et al.*, 2004; Haeusser *et al.*, 2004; Levin *et al.*, 1999). Recent studies have indicated that EzrA is also involved in septum synthesis by recruiting PBP 1, a major transglycosylase and transpeptidase of peptidoglycan subunits, to the division septum (Claessen *et al.*, 2008). EzrA is essential in *Staphylococcus aureus* where it was also shown to fulfil a dual function in cell division and peptidoglycan synthesis (Steele *et al.*, 2011). *E. coli* does not encode an EzrA homologue but its membrane domain topology is similar to that of ZipA in that both proteins contain a transmembrane anchor at their N-temini. Whether they are functional homologues remains to be tested (Errington *et al.*, 2003a). An EzrA truncation lacking the N-terminus has been purified and was shown to interact directly with FtsZ and perturb FtsZ polymerization (Haeusser *et al.*, 2004). On the other hand, a seven amino acid stretch at the C-terminus is essential to direct EzrA to medially positioned Z-ring *in vivo* but is dispensable for FtsZ assembly dynamics *in vitro* (Haeusser *et al.*, 2007). In summary, EzrA has been shown to be involved in both the regulation of FtsZ assembly and septum biosynthesis; however, how these processes are linked is unclear.

SepF (Septum Forming) was discovered by two groups (Hamoen *et al.*, 2006; Ishikawa *et al.*, 2006). *sepF* mutants are delayed in cell division and their division septa are abnormally formed (Hamoen *et al.*, 2006; Ishikawa *et al.*, 2006). Loss of both *sepF* and *ezrA* leads to a synthetic lethal phenotype which does not result from the lack of the Z-rings. It was therefore suggested that SepF functions in a late step in septum formation (Hamoen *et al.*, 2006). On the other hand, the absence of *sepF* is also

synthetically lethal with an *ftsA* deletion, and in this case a conditional double mutant does not form Z-rings anymore. In addition, SepF overexpression stimulates Z-ring formation in an *ftsA* mutant, and it was suggested that SepF can take over the function of FtsA and it promotes the attachement of the Z-ring to the membrane (Ishikawa *et al.*, 2006). Yeast two hybrid and *in vitro* data have shown that SepF interacts directly with FtsZ, and promotes FtsZ polymerization (Hamoen *et al.*, 2006; Singh *et al.*, 2008). Electron microscopic images of purified SepF indicated that the protein oligomerizes into large rings (Gundogdu *et al.*, 2011). Moreover, these rings bundle FtsZ protofilaments into long tubular structures. This orderly arrangement was proposed to be important during synthesis of the septal wall, which is thicker in Gram-positive bacteria (Gundogdu *et al.*, 2011).

ClpX is one of the ATP-binding chaperones that provide substrate recognition for the ClpP protease. Interestingly, ClpX also affects cell division. A *clpX* mutation rescues cells that overexpress *minCD*, suggesting that ClpX is a negative regulator of FtsZ polymerization (Haeusser *et al.*, 2009; Weart *et al.*, 2005). *In vitro* experiments have shown that ClpX inhibits FtsZ polymerization and this activity is independent of its ATPase activity and does not require ClpP (Weart *et al.*, 2005). However, in *E. coli* the ClpXP complex does regulate cell division by means of FtsZ degradation (Camberg *et al.*, 2009, 2011). The N-teminus of *E. coli* ClpX is responsible for the recognition of the C-terminal patch of FtsZ where it competes with FtsA and ZipA for binding (Camberg *et al.*, 2009).

SulA is induced in *E. coli* by DNA damage (SOS response) and it is a potent inhibitor of cell division (Huisman and D'Ari, 1981; Huisman *et al.*, 1984). SulA stops cell division by directly interacting with FtsZ (Bi and Lutkenhaus, 1993; Justice *et al.*, 2000; Mukherjee *et al.*, 1998). It binds to the interface of the nucleotide-binding site of FtsZ thereby inhibiting its GTPase activity (Cordell *et al.*, 2003; Mukherjee *et al.*, 1998). This leads to destabilization of FtsZ polymers and elimination of Z-ring formation (Justice *et al.*, 2000). The cell division arrest induced by SulA provides the cells time to repair its DNA. The functional counterpart of SulA in *B. subtilis* is **YneA**. The primary sequences of SulA and YneA do not share sequence homology and there is no indication that YneA binds directly to FtsZ (Kawai *et al.*, 2003). Recent data have shown that YneA is anchored to the membrane via its transmembrane domain, which is essential for its function (Mo and Burkholder, 2010).

1.1.3 Assembly of the divisome and completion of cell division in *E. coli* and *B. subtilis*

The first set of proteins to localize at midcell are FtsZ, FtsA and ZapA/ZipA (Fig. 1.4) (summarized in Vicente and Rico, 2006). These proteins are referred to as early cell division proteins. In *E. coli*, the first protein to be recruited after the Z-ring is formed is **FtsK**. FtsK is a multifunctional protein that coordinates cell division with chromosome segregation (reviewed in Bigot *et al.*, 2007). FtsK is essential for the recruitment of the cell division proteins **FtsQ**, **FtsB** and **FtsL** (Buddelmeijer and Beckwith, 2004). These periplasmic proteins are tethered to the membrane by N-terminal membrane spanning domains and they form a complex that is required for the localization of proteins that synthesise the septal wall, which includes **FtsW** and **FtsI**. FtsW transports the precursors of cell wall (lipid II) through the membrane (Mohammadi *et al.*, 2011). FtsI is an essential septal transpeptidase that catalyzes cross-linking of peptidoglycan strands (Nguyen-Disteche *et al.*, 1998). One of the last proteins to localize to the septum is **FtsN**. FtsN is an essential protein that probably promotes septation by interacting with FtsI (Lutkenhaus, 2009).

The assembly of the divisome is similar in *B. subtilis*, although there are some fundamental differences. Instead of FtsK, it contains two translocases, **SftA** and **SpoIIIE** that act in concert to complete chromosome segregation. Mutations in either *sftA* or *spoIIIE* lead to a mild increase in the frequency of bisected chromosomes, and the proteins are dispensable for assembly of the divisome under normal growth conditions (Biller and Burkholder, 2009; Britton and Grossman, 1999; Kaimer *et al.*, 2009; Wu and Errington, 1994). After Z-ring assembly, a cluster of several proteins is simultaneously recruited to the division site. **DivIB**, **DivIC**, **FtsL** and **PBP 2B** are interdependent and this complex with the exception of PBP 2B is likely to be preformed before it localizes to the division site (Daniel *et al.*, 2006). DivIB presumably regulates the activity of FtsL (Daniel and Errington, 2000). DivIC and FtsL are unstable proteins but interact to form stable heterodimers (Daniel and Errington, 2000; Daniel *et al.*, 1998; Sievers and Errington, 2000). **PBP 2B** and other proteins, **FtsW** and **PBP 1**, are directly involved in the synthesis of septal wall. PBP 2B is a homolog of FtsI protein and is targeted to the septum by DivIB (Rowland *et al.*, 2010). FtsW probably functions as its *E. coli* counterpart to translocate peptidoglycan precursors through the membrane (Errington *et al.*, 2003b). *B. subtilis* does not encode a homologue of FtsN. PBP 1 acts

as a transglycosylase and transpeptidase (Pedersen *et al.*, 1999) and is also involved in the synthesis of the lateral cell wall (Pedersen *et al.*, 1999; Scheffers and Errington, 2004). Interestingly, PBP 1 is recruited to the septum by **EzrA** (Claessen *et al.*, 2008). Once the new poles had formed, PBP 1 is recycled from the septum back to the lateral wall by the action of **GpsB** (Claessen *et al.*, 2008). Thus, EzrA and GpsB proteins facilitate the switch from elongation (lateral wall growth) to the cell division mode of peptidoglycan synthesis. These proteins are not essential, therefore the presence of at least one of the counterparts is sufficient to fulfil this role (Claessen *et al.*, 2008). Division is finalized by specific hydrolases (autolysins) that separate the newly formed cells. These include LytC and LytD, that perform 95% of cell wall hydrolytic activity and also LytE, LytF and YwbG (reviewed in Smith *et al.*, 2000). However, a recent report suggests that only LytF is required for cell separation (Chen *et al.*, 2009).

In a recent paper, Gamba *et al.* (2009) have shown that the first proteins detectable at the division site are FtsZ, FtsA, ZapA and EzrA. The late division proteins PBP 2B, FtsL, DivIB, GpsB, FtsW and DivIVA, assemble after a considerable time delay (20% of the cell cycle). This is similar to *E. coli* data (Aarsman *et al.*, 2005; Gamba *et al.*, 2009). This delay cannot be altered by premature Z-ring assembly induced by FtsZ overexpression (Aarsman *et al.*, 2005; Gamba *et al.*, 2009).

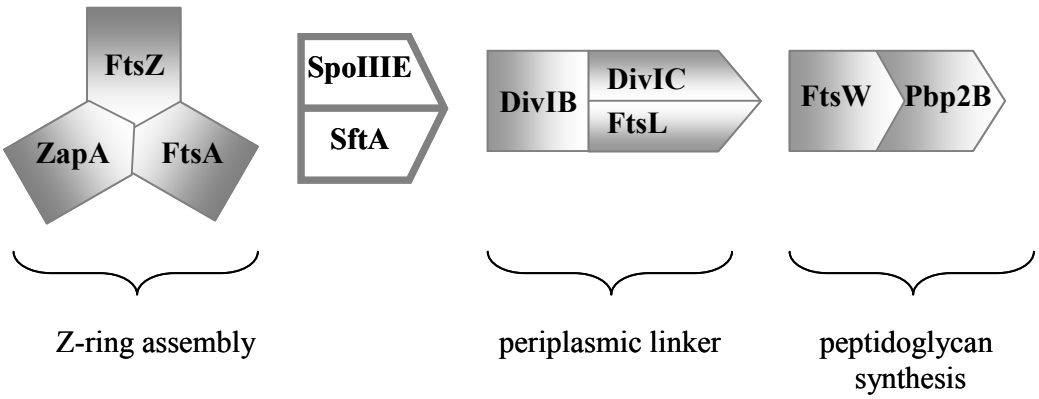

Fig. 1.4 Schematic presentation of the assembly of the divisome in *B. subtilis* (adapted and modified after Vicente and Rico, 2006)
The first group of proteins to arrive at midcell are FtsZ, FtsA and ZapA. The second group of proteins includes FtsQ, DivIB and DivIC. Finally, the peptidoglycan is synthesized by FtsW and Pbp 2B. References in text.

1.1.4 Cellular development - sporulation

One of the possibilities for *B. subtilis* to survive starvation is to form spores. The first morphological landmark of sporulation is the formation of an asymmetric septum, which is positioned close to one cell pole (Fig. 1.5) (Losick *et al.*, 1986; Piggot and Coote, 1976). This asymmetric division gives rise to two unequally sized cells with different fates; the smaller prespore matures into a spore, and the larger mother cell will eventually lyse and release the spore. *B. subtilis* forms a spore within the mother cell compartment (endospore). Spore formation is accomplished by a concerted and compartmentalized activation of spore-specific sigma factors (reviewed in Barak and Wilkinson, 2005; Errington, 2003; Hilbert and Piggot, 2004).

The key response regulator that directs the expression of many sporulation-specific genes is **Spo0A** (Burbulys *et al.*, 1991). Spo0A is activated by phosphorylation and it directs expression of 121 genes that are required for different stationary phase development processes (Molle *et al.*, 2003a). During sporulation the nucleoids are rearranged and form a so-called axial filament that stretches along the entire cell length (Bylund *et al.*, 1993). The chromosome in this conformation is attached to the cell pole by **RacA**, which binds to the *oriC* region of the chromosome and to the polar protein **DivIVA** (Ben-Yehuda *et al.*, 2003; Wu and Errington, 2003). This process also requires the **Soj/Spo0J** chromosome partitioning system (Ben-Yehuda *et al.*, 2003; Wu and Errington, 2003). In the initial stage of sporulation, FtsZ is rearranged from the medial position to both polar regions (Levin and Losick, 1996) via a helical intermediate that slides along the longitudinal axis of the cell (Ben-Yehuda and Losick, 2002). For an efficient asymmetric division expression of *ftsAZ* operon is required and this is established by the sigma factor SigH (Gholamhoseinian *et al.*, 1992; Gonzy-Treboul *et al.*, 1992). Spo0A activates expression of the bifunctional sporulation protein **SpoIIE** protein (Barak and Youngman, 1996; Feucht *et al.*, 1996). SpoIIE interacts with FtsZ and directs repositioning of FtsZ so that Z-rings are formed at both polar positions, but only one is destined to form asymmetric septum (Arigoni *et al.*, 1995; Barak *et al.*, 1996; Levin *et al.*, 1997; Lucet *et al.*, 2000). Usually the old pole is chosen for spore compartment formation (~ 75% of cells) (Dunn and Mandelstam, 1977). After the sporulation septum is formed, SpoIIE activates SigF in the prespore by facilitating the release of SigF from its anti-sigmafactor (Arigoni *et al.*, 1996; Duncan *et al.*, 1995). At this stage, the septum is not fully closed, but entraps one third of the

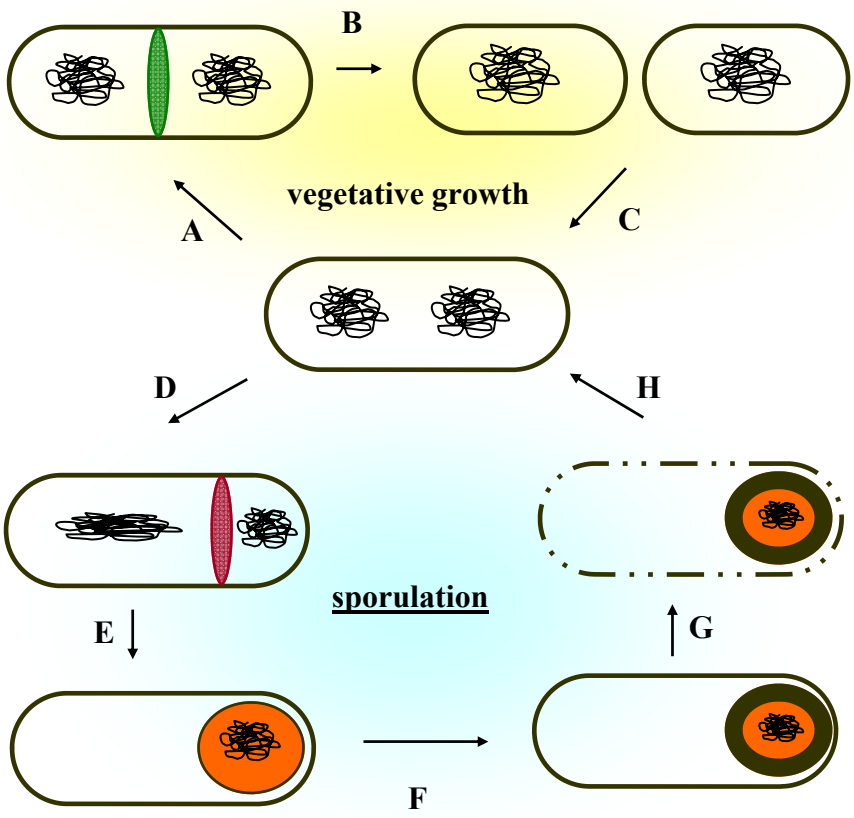

Fig. 1.5 Outline of the *B. subtilis* lifecycle (modified after Barak and Wilkinson, 2007)
During vegetative growth cells divide at midcell (**A**) and this gives rise to two equally sized daughter cells (**B**, **C**). Sporulation is accompanied by the formation of an asymmetric septum (**D**), engulfment of the endospore (**E**), maturation of the spore (**F**) and finally mother cell lysis and release of the dormant spore (**G**). Spore outgrowth occurs when the environmental conditions improve (**H**). Referenced in text.

chromosome in the prespore. The rest of the chromosome is pumped into the prespore compartment by the action of the **SpoIIIE** translocase that resides at the septum (Bath *et al.*, 2000; Wu and Errington, 1994). SigF directs the expression of genes responsible for proteolytic cleavage (processing) of pro-SigE and for its activation in the mother cell compartment (Karow *et al.*, 1995; Londono-Vallejo and Stragier, 1995; Stragier *et al.*, 1988). The next morphological change, engulfment of the prespore, is executed by genes under SigE control (Illing and Errington, 1991; Londono-Vallejo *et al.*, 1997). The late sporulation sigma factors, SigG and SigK are activated in the prespore and in the mother cell, respectively. They direct the final stages of cortex assembly and spore coat layers (Fukushima *et al.*, 2002; Henriques and Moran, 2000, 2007). The mother cell lyses, and releases a spore that is highly resistant to physical and chemical agents.

1.1.4.1 Sporulation in *Streptomyces* spp.

During my research I have studied a *B. subtilis* protein that shows a strong resemblance to the *Streptomyces coelicolor* sporulation protein WhiA, and therefore I will shortly review sporulation in this bacterium. While *B. subtilis* is an endospore former, *Streptomyces* spp. form exospores. During vegetative growth, *Streptomyces* grow as so-called substrate mycelium. When the decision to sporulate is made, long aerial hyphae (~50 μm in *S. coelicolor*) grow out of the substrate mycelium. The aerial hyphae are long cells with no septa. During sporulation the expression of FtsZ increases (Flardh *et al.*, 2000; Kwak *et al.*, 2001) and FtsZ-rings are evenly positioned between the nucleoids (Grantcharova *et al.*, 2005; Schwedock *et al.*, 1997). Interestingly, FtsZ follows the typical localization pattern seen in *B. subtilis* or *E. coli*, firstly accumulating at the membrane as intermediate helical structures that are then rearranged into Z-rings that lead to septation (Grantcharova *et al.*, 2005). It has recently been shown that the protein SsgB orchestrates Z-ring formation (Willemse *et al.*, 2011). So far, no Min or Noc orthologs have been found in *Streptomyces* spp. (Flardh, 2003).

FtsZ induction in the aerial hyphae is dependent on the products of the *whi* genes: *whiA, whiB, whiH, whiH, whiI* and *whiJ* (Flardh *et al.*, 2000). The ***whi*** genes are named after the white colonies these mutants produce, which results from their inability to produce a grey sporulation pigment (Chater, 1972; Kelemen *et al.*, 1998). ***whiG*** encodes a sigma factor Sig^{WhiG} (Chater *et al.*, 1989; Tan *et al.*, 1998), and this sigma factor seems to be the master regulator of sporulation (Ryding *et al.*, 1998; Tan *et al.*, 1998). In the early phase of sporulation, the aerial hyphae cease to grow but continue to

replicate their chromosomes. Based on the phenotype of the mutants, it is believed that during this stage, WhiA and WhiB are important (Flardh *et al.*, 1999). Mutants lacking ***whiA*** form unusually long aerial hyphae with dramatic twists and coils (Fig. 1.6) (Ainsa *et al.*, 2000; Chater, 1975; Flardh *et al.*, 1999). Moreover, the DNA in these aerial hyphae is not condensed into clear nucleoids (Flardh *et al.*, 1999). As sporulation-specific *ftsZ* expression is dependent on *whi* genes (Flardh *et al.*, 2000), the *whiA* mutant fails to form Z-rings (Grantcharova *et al.*, 2005; Schwedock *et al.*, 1997). Ainsa *et al*. (2000) have mapped the promoter region of *whiA* and showed that *whiA* possesses two promoters. The transcription from either promoter is very low and constant during vegetative growth. However, about the time sporulation commences, the transcriptional level of *whiA* mRNA from the more proximal promoter, which is probably Sig^{WhiG} independent, greatly increases, suggesting that WhiA is specifically overproduced during sporulation in *Streptomyces* (Ainsa *et al.*, 2000). In addition, a possible auto-regulatory loop was suggested since *whiA* mutants do not show strong transcriptional induction (Ainsa *et al.*, 2000). The function of *whiH* and *whiI* genes is to complete septation. The expression of the late sporulation sigma factor $\mathbf{Sig^F}$ depends on all *whi* genes, and controls maturation of the external capsule of the spores (Kelemen *et al.*, 1996; Potuckova *et al.*, 1995). The exact molecular mechanism by which the Whi proteins coordinate sporulation is yet unclear. Based on the primary sequence conservation they were predicted to be transcriptional regulators (see Flardh *et al.,* 1999).

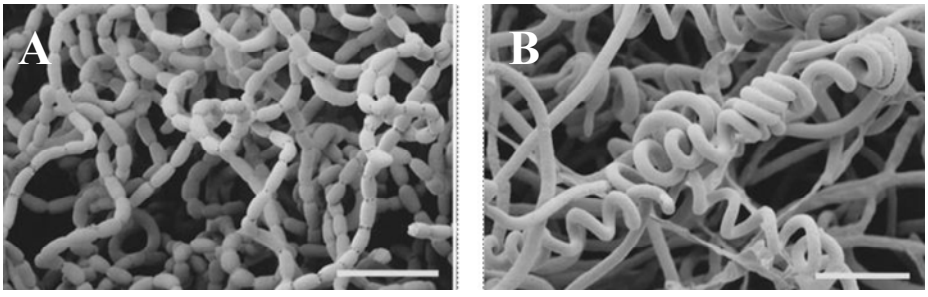

Fig. 1.6 Phenotype of wild type and Δ*whiA S. coelicolor* sporulating hyphae
Sporulating hyphae in wild type *S. coelicolor* (**A**) and a *whiA* mutant (**B**). Scale bars 10 μm. Adapted from Flardh *et al.,* 1999.

1.2 Chromosome dynamics

The cell division protein that became central to my PhD study was shown to be associated with the nucleoid and its mutation caused phenotypes that are detrimental when chromosome replication is altered. That is why chromosome organization, replication, and segregation are introduced in the following chapter.

1.2.1 Organization of the chromosomes in the cell

The bacterial cell is several μm long, while the chromosomal DNA is a few millimeters long. How do the cells maintain a structure that is ~1000-fold larger than their own size? The electron microscopy of isolated chromosomes from *E. coli* revealed a structure with loops protruding from the 'core', a so-called rosette (Delius and Worcel, 1974; Kavenoff and Bowen, 1976; Kavenoff and Ryder, 1976). Recent data suggest that *E. coli* DNA is divided into 450 loops that are assembled into the rosette by the action of proteins (domainins) that probably bear very little sequence specificity (Postow *et al.*, 2004). The loops are considered to be topological domains. The advantage of DNA partitioning into domains is that the introduction of nicks (gaps) leads to relaxation of only one domain, thereby limiting the affected region (Worcel and Burgi, 1972). The organization of DNA into such structure is essential since relaxation of the super-helicity of the chromosome is lethal (Gellert *et al.*, 1976; Worcel and Burgi, 1972; Zechiedrich *et al.*, 1997). The question of how the chromosomal DNA is organized into a rosette was partially answered by the discovery of the first topoisomerase (Trucksis and Depew, 1981; Wang, 1971). **Topoisomerases** are enzymes that are able to cut and then rejoin single or both strands of the DNA and introduce topological changes like relaxation or supercoiling and thus untangle the DNA (Vologodskii and Cozzarelli, 1994). This is important for processes like transcription and DNA replication (reviewed in Witz and Stasiak, 2010).

In *E. coli* another group of proteins that compact the chromosome include H-NS, HU, Fis, and IHF (Murphy and Zimmerman, 1997; Varshavsky *et al.*, 1977). These proteins do not show clear sequence specificity. H-NS was shown to dimerize and link two strands of DNA and it increases the rigidity of DNA (Dame *et al.*, 2000). HU, Fis and IHF have been shown to strongly bend DNA (reviewed in Dame, 2005) and HU is capable of introducing helical turns in the DNA (Rouviere-Yaniv *et al.*, 1979; Tanaka *et*

al., 1984). *B. subtilis* contains a homologue of HU called **HBsu**, an essential protein that is able to compact DNA *in vivo* (Kohler and Marahiel, 1997; Micka *et al.*, 1991). HBsu binds DNA, preferentially when it is distorted (ssDNA, gaps, and sharp bends) and has been shown to be involved in recombination (Rowland *et al.*, 2005). Another protein, LrpC has been shown to form DNA loops by bridging adjacent tracts of DNA (Tapias *et al.*, 2000). Other possible mechanisms that influence the nucleoid structure include supercoiling by the transcription machinery, certain stable RNAs, and transcription-translation coupled with the insertion of proteins into the membrane, a so-called transertion (Cabrera and Jin, 2003; Deng *et al.*, 2004, 2005; Lynch and Wang, 1993; Norris, 1995). Interestingly, proteins essential for the structural maintenance of chromosomes in eukaryotes, the SMC proteins, can also be found in most prokaryotes (Hirano, 2006; Nasmyth and Haering, 2005). In *B. subtilis* this protein is called **SMC**, and in *E. coli* it is called **MukB** (Soppa, 2001). SMC proteins form large V-shaped structures. Each arm of the V-shape consists of one molecule that is tagged together through two coiled-coil regions. (Haering *et al.*, 2002). The structure is flexible as the base of the 'V' acts as a hinge (Hirano and Hirano, 2002). The open ends constitute two ABC-type ATPase sites that mediate the interaction with the accessory proteins ScpA and ScpB (Hirano, 2002; Mascarenhas *et al.*, 2002; Soppa *et al.*, 2002). It is generally believed that the SMC structure can form a ring after the 'closure' of the open ends (Schleiffer *et al.*, 2003; Woo *et al.*, 2009). Because the arms are ~50 nm long, it is thought that SMC could enclose more than one DNA strand and could thus organize the DNA (Dame, 2005). In fact, SMC is also one of the key players during chromosome segregation (see more in section 1.2.3 Chromosome segregation).

1.2.2 DNA replication

To initiate replication, the bacterial initiation protein **DnaA** binds to the AT rich *oriC* region, melts the DNA, and loads the helicase DnaB and the primase DnaC (Marszalek and Kaguni, 1994; Wahle *et al.*, 1989; Zyskind and Smith, 1992). Two DnaB-DnaC complexes assemble to provide bidirectional replication (Fang *et al.*, 1999). The DNA polymerase III holoenzyme complex is recruited next. Recent data show that in *B. subtilis*, 11 proteins are required for the leading strand synthesis, and 13 proteins for the lagging strand synthesis (Sanders *et al.*, 2010). *B. subtilis* possesses two essential DNA polymerases: PolC which catalyzes synthesis of both leading and lagging strands

and DnaE, which is essential for lagging strand synthesis (Dervyn *et al.*, 2001; Sanders *et al.*, 2010). DnaE was found to be a slow polymerase with preference for RNA primers, implying that it catalyzes synthesis of short fragments and then 'hands over' to PolC which is highly processive (Sanders *et al.*, 2010).

1.2.3 Chromosome segregation

The positioning of the chromosome within bacterial cells does not seem to be random. In a newly born *E. coli* cell the origin of replication (*oriC*) is positioned at midcell and the left and right arms of the chromosome are distributed each into a separate cell half (Fig. 1.7) (Nielsen *et al.*, 2006b; Wang *et al.*, 2006). During replication, the duplicated origins move to quarter positions, which become midcell positions after cytokinesis (Nielsen *et al.*, 2006b; Wang *et al.*, 2006). However, in newly formed *B. subtilis* cells, the *oriC* and *ter* (terminus of chromosome) regions are localized bipolarly (Teleman *et al.*, 1998; Viollier *et al.*, 2004; Webb *et al.*, 1997; Wu and Errington, 1994). After replication initiation, the replication machinery and the *oriC* colocalize at the midcell (Lemon and Grossman, 1998; Migocki *et al.*, 2004) and eventually the duplicated origins move toward the old cell poles. After septum formation, the termini become located at the new cell poles.

The differing organizations of the nucleoid suggests that bacteria have evolved dedicated mechanisms to ensure correct positioning of nucleoids, but our current knowledge about this topic is limited. An elegant model for chromosome organization is proposed in *C. crescentus* (Fig. 1.7). This organism arranges the origins similarly to *B. subtilis* (Jensen and Shapiro, 1999), however, the replication machinery localizes to the pole, and is gradually sequestered to the midcell (Jensen *et al.*, 2001). The chromosome is organized through PopZ-ParB interaction. PopZ is a proline-rich protein that forms a network at the cell pole and draws in the ParB protein, which associates with the region around the origin (Bowman *et al.*, 2008; Ebersbach *et al.*, 2008a). Another rare example of chromosome positioning is the attachement of the chromosome (axial filament) by RacA-DivIVA proteins during sporulation in *B. subtilis*. RacA binds to a 600 kb region surrounding the origin and is attracted by DivIVA to the poles (Ben-Yehuda *et al.*, 2005; Ben-Yehuda *et al.*, 2003; Lenarcic *et al.*, 2009). However, RacA is expressed only during sporulation so it cannot be accounted for organizing the chromosome during vegetative growth (Ben-Yehuda *et al.*, 2003). In *B. subtilis* the

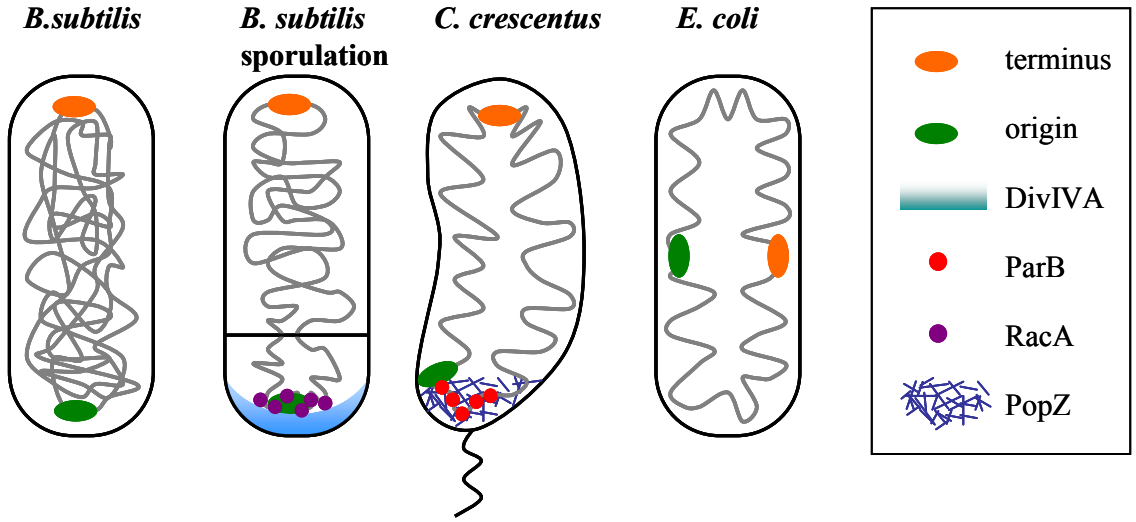

Fig. 1.7 Nucleoid arrangement in different bacteria (adapted from Toro and Shapiro, 2010)
B. subtilis has a bipolar orientation of *oriC* and terminus. During sporulation, the axial filament is attached to the polar membrane by RacA and DivIVA interaction, usually at the old pole. *C. crescentus* employs ParB-PopZ mediated anchoring of the origin-proximal region to the cell pole. ParB binds *parS* sites on the chromosome and PopZ forms a network of filaments at the cell pole. In *E. coli* the two arms of the chromosome are placed into opposite parts of the cell and the *oriC* and *ter* regions are located at midcell positions.

replication factory is placed at the midcell (Lemon and Grossman, 1998). The segregation in *E. coli* and *B. subtilis* was shown to be 'progressive', in that with ongoing replication the origin regions are moved away from midcell toward the poles (Fig. 1.8) (Nielsen *et al.*, 2006a; Viollier *et al.*, 2004). So far, two key players are known to be required for chromosome segregation: the *parABS* system and the SMC complex.

The ***parABS*** system was firstly observed to be encoded and used by plasmids (Austin and Abeles, 1983; Gerdes *et al.*, 1985; Ogura and Hiraga, 1983). The *parABS* system was later identified in bacterial genomes as well and although being distinct from their plasmid counterparts, the chromosomal *parABS* do share the main features (Ireton *et al.*, 1994; Mohl and Gober, 1997; Ogasawara and Yoshikawa, 1992). When *parABS* is deleted, an increase in the formation of anucleate cells is observed (Ireton *et al.*, 1994; Mohl and Gober, 1997). In addition, *parABS* is able to facilitate inheritance of an otherwise unstable plasmid (Dubarry *et al.*, 2006; Godfrin-Estevenon *et al.*, 2002; Yamaichi and Niki, 2000). The *parABS* system consists of the protein couple ParA and ParB and a specific DNA sequence, the *parS* site. The *parS* sites are usually positioned proximal to the origin (Lin and Grossman, 1998; Livny *et al.*, 2007). ParB is a DNA-binding protein with a high affinity for *parS* where it binds and then spreads along the DNA (Breier and Grossman, 2007; Murray *et al.*, 2006; Rodionov and Yarmolinsky, 2004). ParA proteins are ATPases and the plasmid ParA can form polymers that oscillate from pole to pole (reviewed in Gerdes *et al.*, 2010). Although *E. coli* lacks chromosomal homologues of *parABS* system, a functional *parABS* is essential in *C. crescentus* (Gerdes *et al.*, 2000; Ireton *et al.*, 1994; Mohl and Gober, 1997). In *C. crescentus*, the ParB-*parS* complex is initially tethered to the old pole by PopZ (Bowman *et al.*, 2008; Ebersbach *et al.*, 2008a). TipN, which is localized at the new pole, interacts with ParA (Ptacin *et al.*, 2010). The ParB-*parS* complex causes dissociation of ParA from the ends of the ParA polymer, and so the protein-DNA complex is being pulled from the old pole towards the new pole (Ptacin *et al.*, 2010). Ten *parS* sites were identified close to *oriC* on the chromosome of *B. subtilis* (Lin and Grossman, 1998). Mutations in *parA* or *parB* mutants, which in *B. subtilis* are better known as *soj* and *spo0J*, respectively, have pleiotropic characteristics. Soj has been found to affect the activity of the key replication initiation protein DnaA (Murray and Errington, 2008). Deletion of *spo0J* has only a mild effect on chromosome organization and segregation but the strain is defective in sporulation which is a consequence of accumulation of active Soj (Autret *et al.*, 2001; Ireton *et al.*, 1994). Two independent studies have shown that SMC is recruited to the origins in a Spo0J-dependent

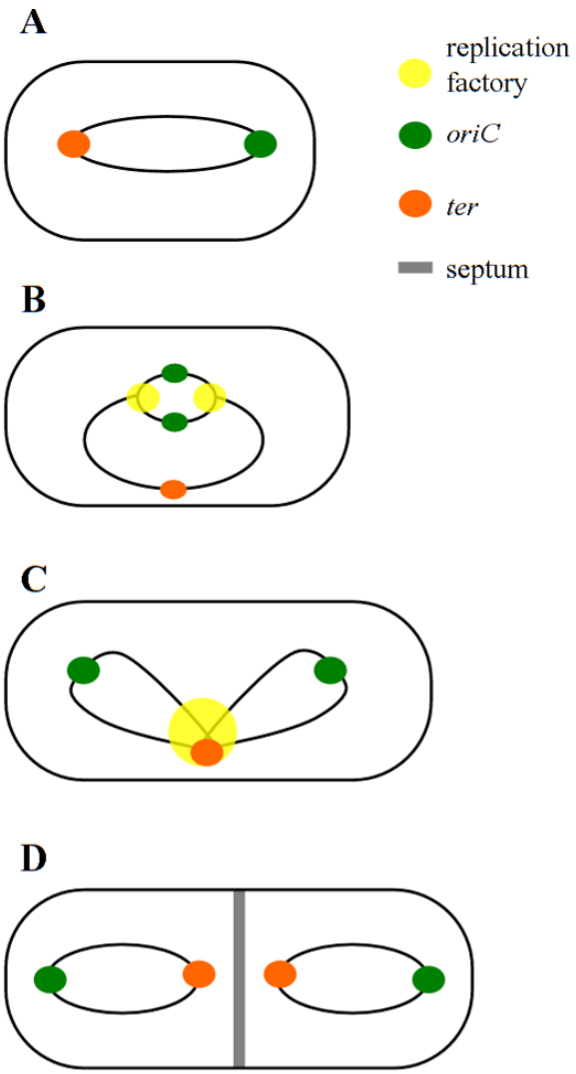

Fig. 1.8 Segregation of chromosomes in *B. subtilis*
(**A**) Origin and terminus of replication are placed at the opposite poles in newly born cells. (**B**) After replication is initiated, the replication machinery (yellow circle), origin and terminus of replication move to midcell. (**C**) Newly replicated origins (green) are moved towards the poles, while the replication machinery remains at midcell position. (**D**) The Z-ring forms just before the termination of DNA replication, so that after the DNA is replicated, the septum (grey) divides the cell.

manner and a proper localization of SMC is essential for efficient chromosome segregation (Gruber and Errington, 2009; Sullivan *et al.*, 2009). It was proposed that the SMC complex organizes the origin region, however, the precise function of SMC in chromosome segregation remains unclear (Sullivan *et al.*, 2009).

There are also reports that **MreB**, a bacterial actin homologue (Jones *et al.*, 2001; van den Ent *et al.*, 2001) is involved in chromosome segregation (Gitai *et al.*, 2005; Kruse *et al.*, 2006). However, this idea is controversial since inactivation of MreB causes strong deformation and leads to round cells and experiments performed in *E. coli* did not detect any segregation phenotype in MreB-depleted cells (Shaevitz and Gitai, 2010).

In *E. coli*, the DNA translocase **FtsK** was shown to play an important role during the final stages of chromosome segregation. At the end of replication, chromosome dimers must be resolved. FtsK activates the XerD recombinase that promotes Holliday junction formation at a specific *dif* site, and the chromosomes are finally untangled by the action of the XerC recombinase (Yates *et al.*, 2006). This process is coupled with the FtsK-catalyzed translocation of DNA from the septal region (Grainge *et al.*, 2011). *B. subtilis* encodes two DNA translocases that both accumulate at the dividing septum. Recently identified **SftA** localizes to the constricting septum where it pumps DNA away from the division site (Biller and Burkholder, 2009; Kaimer *et al.*, 2009). Second translocase **SpoIIIE** acts later in division to resolve trapped DNA in the septum. SpoIIIE forms channels in septa and translocates the remaining part of the chromosome into the cell (Burton *et al.*, 2007). Neither SpoIIIE nor SftA is essential for cell division but SpoIIIE is essential for the development of the spore (Fleming *et al.*, 2010; Liu *et al.*, 2006; Sharp and Pogliano, 2003).

1.3 Coordination of cell division

It has been shown that cells maintain a constant DNA/cell mass ratio (Sargent, 1975; Schaechter *et al.*, 1958; Sharpe *et al.*, 1998; Weart *et al.*, 2007). Thus, DNA replication and division must be coordinated with cell growth.

1.3.1 Cell division and the growth rate

It has been known for a long time that bacteria are longer in nutrient-rich media (Cooper and Helmstetter, 1968; Sargent, 1975; Sharpe *et al.*, 1998), and the formation of the

Z-ring is modulated by the growth rate (Den Blaauwen *et al.*, 1999; Weart and Levin, 2003). In *B. subtilis*, **UgtP** was identified to act as a global regulator of cell size and cell division (Fig. 1.9) (Weart *et al.*, 2007). UgtP is a UDP-glucose diacylglycerol glucosyltransferase involved in the biosynthesis of the lipoteichoic acids (LTA) (Jorasch *et al.*, 1998). In fast growing bacteria, UgtP localizes at the septum (Nishibori *et al.*, 2005; Weart *et al.*, 2007) and inhibits the cell division. It was shown that the protein inhibits lateral assembly of FtsZ-filaments *in vitro* (Weart *et al.*, 2007). In nutrient poor conditions, the concentration of UDP-glucose decreases and UgtP detaches from the cell division site and no longer inhibits Z-ring formation. In *ugtP* mutants division occurs even when the cells have not reached the desired cell length, and *ugtP* mutant cells are shorter than wild type cells. A similar phenotype was observed when *pgcA* and *gtaB*, involved in the UDP-glucose synthesis, were disrupted (Lazarevic *et al.*, 2005; Weart *et al.*, 2007). Interestingly, *pgcA* and *ugtP* mutations increase the frequency of Z-rings over the nucleoids, and with some frequency bisected chromosomes were observed in strains that also lacked *spoIIIE* (Weart *et al.*, 2007). These results suggest that UgtP and PgcA may be important for the coordination of cell division with chromosome segregation (Weart *et al.*, 2007).

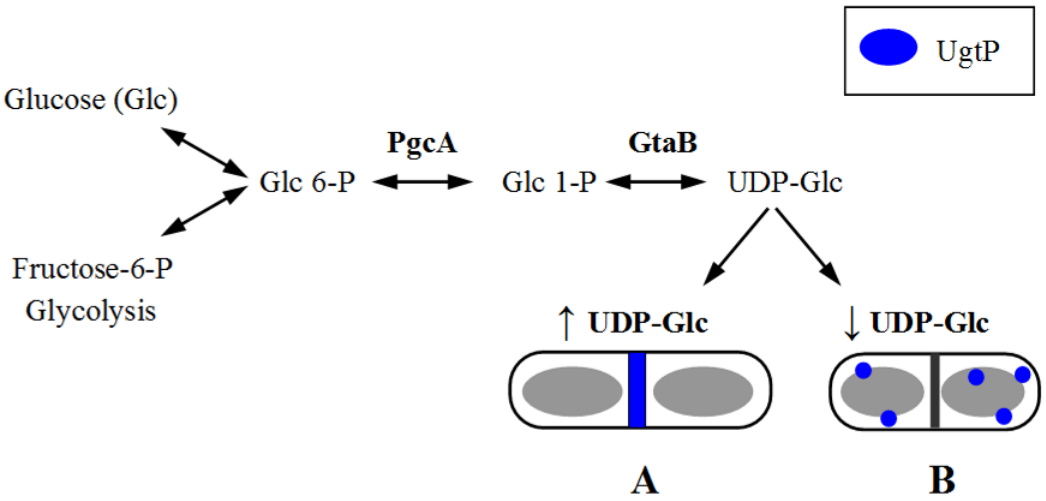

Fig. 1.9 Outline of the link between glucose metabolism and cell division
Glucose (Glc) or Fructose-6-P are converted to Glucose-6-P (Glc 6-P) which is converted to UDP-Glucose by PgcA and GtaB proteins. (**A**) In nutrient rich conditions the UDP-Glucose concentration increases and UgtP (blue) localizes to the midcell where it blocks Z-ring assembly. (**B**) In nutrient poor conditions, UDP-glucose concentration drops, UgtP becomes delocalized and the Z-ring is formed.

1.3.2 Cell division and chromosome dynamics

It has been proposed that replication might serve as a checkpoint for cytokinesis. (Harry *et al.*, 1999). This was based on the observation that cells that are blocked in replication are delayed in cell division. It is now known that this delay is related to the fact that DnaA inhibits *ftsL* transcription (Goranov *et al.,* 2005).

In *C. crescentus*, chromosome replication is strictly coordinated with cell division (Marczynski, 1999). Before the division begins, the origin of replication is attached to the old cell pole (Jensen and Shapiro, 1999). **MipZ** belongs to the *parA* family of ATPases, binds the ParB/*parS* complex close to the origin (Figge *et al.*, 2003; Mohl and Gober, 1997; Thanbichler and Shapiro, 2006). Soon after replication is initiated and the origin replicated, the complex splits into two, one remains attached to the old pole and the other follows ParB to the new cell pole. Importantly, MipZ protein is also a negative regulator of FtsZ polymerization and the Z-ring forms at the only place that is left out unocuppied by MipZ, the midcell (Thanbichler and Shapiro, 2006).

B. subtilis Noc protein, which is responsible for nucleoid occlusion, might also be a transducer of the information that the replication has proceeded into a stage suitable for cell division initiation (Wu *et al.*, 2009), or that the segregation of chromosomes has relieved the midcell from nucleoid occlusion (Corbin *et al.*, 2002; Yu and Margolin, 1999). This assumption was based on an experiment where cells became elongated when an array of Noc binding sites was placed near the terminus of replication, which is normally devoid of Noc and is positioned proximal to the prospective division site (Wu *et al.*, 2009). However, cells with intact initiation of replication but with inhibited replication elongation are still able to form midcell positioned Z-rings (Regamey *et al.*, 2000).

1.3.3 Coordination of chromosome replication

The cell cycles of bacteria grown in rich media are shorter than the time needed for chromosome replication. A solution to this problem is a multi-fork replication (Cooper and Helmstetter, 1968). Cells initiate another round of replication before the previous round has come to an end and as a result, the cells possess more origins of replication. Yet it remains unclear what the signal is for the initiation of replication. Cell division is an unlikely checkpoint since cells replicate DNA when cell division is perturbed (Bates

and Kleckner, 2005). The most recent view is that temporal control of initiation seems to be dependent on multiple factors relating to the growth rate (Wang and Levin, 2009).

The intracellular concentration and the activity of DnaA, an essential protein allowing the replisome to assemble, are the key determinants of the initiation rate. In nutrient-rich conditions the increase in DnaA synthesis causes overinitiation (Ogura *et al.*, 2001; Skarstad *et al.*, 1989; Xu and Bremer, 1988). The rate of DnaA transcription is inhibited by **(p)ppGpp** which is produced by the stringent response protein RelA when cells are starved for aminoacids or carbon sources (Chiaramello and Zyskind, 1990). The activity of DnaA is also regulated by **DiaA** and **Hda** in *E. coli* and **Soj** and **YabA** in *B. subtilis* (Keyamura *et al.*, 2007; Murray and Errington, 2008). In *B. subtilis* **YabA** was shown to promote sequestration of DnaA molecules by DnaN thereby inhibiting its activity (Cho *et al.*, 2008; Noirot-Gros *et al.*, 2006; Soufo *et al.*, 2008). Recent data show that YabA directly binds DnaA at *oriC* and lowers the amount of DnaA bound to DNA (Merrikh and Grossman, 2011). DnaA regulates the expression of *nrdAB* gene, which encodes the enzyme for the synthesis of dNTPs, and as such affects the pool of dNTPs available for DNA polymerization (Augustin *et al.*, 1994; Gon *et al.*, 2006; Sun and Fuchs, 1994). (p)ppGpp not only regulates DnaA expression but it directly inhibits DnaC, which is essential for replication, and causes replication fork arrest (Wang *et al.*, 2007). Finally, Jannière *et al* have shown an interesting genetic connection between nutrient availability and replication elongation (Janniere *et al.*, 2007). Mutants in the three-carbon part of the glycolysis pathway were found to suppress conditional mutants in the polymerase DnaE (Dervyn *et al.*, 2001; Sanders *et al.*, 2010). The mechanism of such suppression remains unclear (Janniere *et al.*, 2007). Importantly, DnaA also regulates the expression of FtsL, an essential component of the divisome, and thus coordinates DNA replication and cell division (Goranov *et al.,* 2005).

Chapter 2

Materials and Methods

2.1 Solutions and media

The composition of solutions and media is listed in Appendix 1.

2.2 Strains and plasmids

Bacterial strains and plasmids used in this study are summarized in Table 2.1 and Table 2.2.

Table 2.1 Summary of bacterial strains used in this study

Strain ***B. subtilis***	**Relevant genotype**	**Source, construction, comment**
1282	*trpC2 noc*::*tet*	(Wu and Errington, 2004)
1283	*trpC2 noc*::*spc*	(Wu and Errington, 2004)
1356	*trpC2* Δ*zapA-yshB*::*tet*	(Feucht and Errington, 2005)
1801	*trpC2* chr:: pJSIZDpble (P_{spac}-*ftsZ ble*)	(Marston *et al.*, 1998)
2020	*trpC2 amy*E::(P_{xyl}-*gfpmut1-ftsZ spc*)	J. Sievers (unpublished)
3309	*trpC2 minCD*::*kan*	JE laboratory stock
3362	*trpC2 ezrA*::*tet*	(Hamoen *et al.*, 2006)
4221	*trpC2 gpsB*::*kan*	(Claessen *et al.*, 2008)
BFA2863	*trpC2 sepF*::(pMut *erm*)	
HM3	*trpC2* P_{rtp}-*rtp-gfp cat*	(Murray *et al.*, 2006)
HM41	*trpC2* Δ*spo0J*::*neo*	(Murray and Errington, 2008)
HM31	*trpC2* Δ*soj*Δ*spo0J*::*tet*	(Murray and Errington, 2008)
HM160	*trpC2 soj* P_{spo0J}-*spo0J-gfpmut2 neo yyaC*	(Murray and Errington, 2008)
HM161	*trpC2* Δ*soj*::*neo*	(Murray and Errington, 2008)
LH4042	*trpC2* Δ*divIVA*::*cat*	L. Hamoen, unpublished
JJS142	*trpC2* Δ*upp* Δ*yabA*	(Noirot-Gros *et al.*, 2006)
JWV042	*trpC2 amy*E::P_{HBsu}-HBsu-*gfp cat*	J.W.Veening, unpublished
KS2	*trpC2* 0168 ED	wild-type for this study
KS6	*trpC2* Δ*zapA-yshB*::*tet*	KS2::chr. DNA 1356
KS44	*trpC2 ezrA*::*tet*	KS2::chr. DNA 3362
KS50	*trpC2* Δ*lacA*::*cat* Δ*zapA-yshB*::*tet* pLOSS-ZapAB	This work

KS90	*trpC2* Δ*divIVA*::*cat* Δ*zapA-yshB*::*tet* pLOSS-ZapAB	This work, Δ*divIVA* comes from LH4042
KS115	*trpC2* Δ*divIVA*::*cat* pLOSS-ZapAB	LH4042::pLOSS-ZapAB
KS162	*trpC2* Δ*zapA-yshB*::*tet* P_{spac}-*ftsZ ble*	KS6::chr. DNA 1801
KS180	*trpC2 amy*E::P_{xyl}-*gfp-yvcL spc*	KS2::pSG1729YvcL, this work
KS207	*trpC2* Δ*yvcL*::(pMut *erm*)	This work
KS263	*trpC2 sepF*::(pMut *erm*)	KS2::chr. DNA BFA2863
KS267	*trpC2 yvcL*::TnYLB-1 (pos.171 bp)	This work
KS268	*trpC2* P_{spac}-*ftsZ ble*	KS2::chr. DNA 1801
KS338	*trpC2 minCD*::*kan*	KS2::chr. DNA 3309
KS340	*trpC2 sepF*::(pMut *erm*) Δ*yvcL*::*kan*	KS400::KS263
KS345	*trpC2 noc*::*spc*	KS2::chr. DNA 1283
KS381	*trpC2* Δ*spoIIIE*::*aphA-3*	JE collection strain 647
KS382	*trpC2* Δ*spo0J*::*neo*	KS2::HM42
KS383	*trpC2* Δ*soj*::*neo*	KS2::HM161
KS384	*trpC2 amy*E::(P_{xyl}-*gfpmut1-ftsZ spc*)	KS2::chr. DNA 2020
KS394	*trpC2 amy*E::P_{xyl}-*yvcL-gfpmut1*	KS2::pSG1154YvcL
KS400	*trpC2* Δ*yvcL*::*kan*	This work
KS404	*trpC2 gpsB*::*kan*	KS2::chr. DNA 4221
KS414	*trpC2 gpsB*::*kan yvcL*::(pMut *erm*)	This work
KS420	*trpC2* P_{spo0J}-*spo0Jgfp*	KS2::chr. DNA HM160
KS421	*trpC2* Δ*yvcL*::*erm* P_{spo0J}-*spo0Jgfp*	KS420::chr. DNA KS207
KS438	*trpC2 yvcL*::P_{spac}-*yvcL erm*	This work
KS439	*trpC2 crh*::P_{spac}-*crh erm*	This work
KS559	*trpC2* Δ*spoIIIE*::*kan* Δ*yvcL*::*erm*	KS381::chr. DNA KS207
KS560	*trpC2* Δ*spo0J*::*neo* Δ*yvcL*::pMut *erm*	KS382::KS207
KS562	*trpC2* Δ*soj*::*neo* Δ*yvcL*::pMut *erm*	KS383::KS207
KS696	*trpC2 yvcL*	This work
KS701	*trpC2 yneA-yneB-ynzC*::*tet*	KS2::chr. DNA YK03
KS702	*trpC2* Δ*noc*::*spc yneA-yneB-ynzC*::*tet*	1283::chr. DNA YK03
KS703	*trpC2 yvcL yneA-yneB-ynzC*::*tet*	KS696::chr. DNA YK03
KS742	*trpC2* Δ*lacA*::*cat* Δ*zapA-yshB*::*tet* Δ*yvcL* pLOSS-YvcL	This work; Δ*yvcL* originated from KS696
KS745	*trpC2 yvcL amy*E::(P_{xyl}-*gfpmut1-ftsZ spc*)	KS696::chr. DNA 2020
KS748	*trpC2 yvcL* P_{spac}-*ftsZ ble*	KS696::chr. DNA 1801
KS749	*trpC2* Δ*yvcL*::*kan amy*E::P_{xyl}-*gfp-yvcL*	KS180::chr. DNA KS400,

	spc	This work
KS752	*trpC2* Δ*yvcL*::*kan amy*E::P_{xyl}-*gfpmut1-yvcL*	This work, KS394::chr. DNA KS400
KS754	*trpC2 yvcL*::P_{spac}-*yvcL erm* Δ*zapA-yshB*::*tet amy*E::P_{xyl}-*gfp-ftsZ*(*spc*) pMAP65(*lacI*,*kan*)	This work
KS755	*trpC2 yvcL*::P_{spac}-*yvcL erm* Δ*noc*::*cat amy*E::P_{xyl}-*gfp-ftsZ*(*spc*) pMAP65(*lacI*,*kan*)	This work
KS859	*trpC2 yvcL*::P_{spac}-*yvcL erm* Δ*zapA-yshB*::*tet aprE*::*lacI spc*	This work
KS873	*trpC2 ezrA*::*tet yvcL*::P_{spac}-*yvcL erm aprE*::*lacI spc*	This work
KS877	*trpC2 ggaB*::TnYLB-1 (*kan*) *yvcL*::P_{spac}-*yvcL erm* Δ*zapA-yshB*::*tet aprE*::*lacI spc*	This work
KS878	*trpC2 pgcA*::TnYLB-1 (*kan*) *yvcL*::P_{spac}-*yvcL erm* Δ*zapA-yshB*::*tet aprE*::*lacI spc*	This work
KS880	*trpC2 yusB*::TnYLB-1 (*kan*) *yvcL*::P_{spac}-*yvcL erm* Δ*zapA-yshB*::*tet aprE*::*lacI spc*	This work
KS883	*trpC2 braB*::TnYLB-1 (*kan*) *yvcL*::P_{spac}-*yvcL erm* Δ*zapA-yshB*::*tet aprE*::*lacI spc*	This work
KS887	*trpC2 speD*::TnYLB-1 (*kan*) *yvcL*::P_{spac}-*yvcL erm* Δ*zapA-yshB*::*tet aprE*::*lacI spc*	This work
KS888	*trpC2 amy*E::P_{xyl}-*gfp spc*	This work; used pSG1729
KS891	*trpC2 yvcL*::P_{spac}-*yvcL erm aprE*::*lacI spc*	KS438::pAPNC213
KS902	*trpC2 gtaB*:: TnYLB−1 *kan* Δ*yvcL*::*erm*	This work
KS903	*trpC2 pgcA*:: TnYLB−1 *kan* Δ*yvcL*::*erm*	This work
KS904	*trpC2 braB*:: TnYLB−1 *kan* Δ*yvcL*::*erm*	This work
KS905	*trpC2 speD*:: TnYLB−1 *kan* Δ*yvcL*::*erm*	This work
KS907	*trpC2 yvcL*::P_{yvcL}-*yvcL-gfp-mut1* (*cat*)	This work
KS925	*trpC2 ezrA*::*tet gtaB*::TnYLB-1 (*kan*) *yvcL*::P_{spac}-*yvcL erm aprE*::*lacI spc*	This work
KS927	*trpC2 ezrA*::*tet pgcA*:: TnYLB−1 *kan yvcL*::P_{spac}-*yvcL erm aprE*::*lacI spc*	This work
KS930	*trpC2* P_{spac}-*ftsZ ble amy*E::P_{HBsu}HBsu-*gfp cat*	This work; using JWV042

KS931	*trpC2* Δ*yvcL* P_{spac}-*ftsZ ble amy*E::P_{HBsu}-HBsu-*gfp cat*	This work; using JWV042
KS991	*trpC2* P_{spac}-*ftsZ ble* P_{spo0J}-*spo0J-gfp* (*kan*)	KS268::chr. DNA HM160
KS993	*trpC2* Δ*yvcL* P_{spac}-*ftsZ ble* P_{spo0J}-*spo0J-gfp* (*kan*)	This work
KS1012	*trpC2 crh*::P_{spac}-*crh erm aprE*::*lacI* (*spc*)	KS439::pAPNC213
KS1013	*trpC2 crh*::P_{spac}-*crh erm* Δ*zapA-yshB*::*tet aprE*::*lacI* (*spc*)	This work
KS1015	*trpC2* Δ*yvcL*::*erm* Δ*ugtP*::*neo*	KS207::chr. DNA PG237
KS1016	*trpC2* P_{spac}-*ftsZ ble* P_{rtp}-*rtp-gfp cat*	KS268::chr. DNA HM3
KS1017	*trpC2* Δ*yvcL* P_{spac}-*ftsZ ble* P_{rtp}-*rtp-gfp cat*	This work
KS1025	*trpC2* Δ*yvcL*::*erm ggaB*:: TnYLB−1 *kan*	This work
KS1026	*trpC2* Δ*yvcL*::*erm yusB*:: TnYLB−1 *kan*	This work
KS1050	*trpC2 ugtP*::*neo yvcL*::P_{spac}-*yvcL erm* Δ*zapA-yshB*::*tet aprE*::*lacI spc*	KS859::chr. DNA PG237
KS1063	*trpC2* Δ*yabA yvcL*::P_{spac}-*yvcL erm* pMAP65	This work
KS1064	*trpC2* Δ*yabA crh*::P_{spac}-*crh erm* pMAP65	This work, Δ*yabA* comes from JJS142
KS1069	*trpC2 ugtP*::*spc* Δ*yabA yvcL*::P_{spac}-*yvcL erm* pMAP65	This work
KS1070	*trpC2 ugtP*::*spc* Δ*yabA crh*::P_{spac}-*crh erm* pMAP65	This work
KS1071	*trpC2 pgcA*::*tet* Δ*yabA yvcL*::P_{spac}-*yvcL erm* pMAP65	This work, *pgcA* mutation comes from SSB122
KS1072	*trpC2 pgcA*::*tet* Δ*yabA crh*::P_{spac}-*crh erm* pMAP65	This work
KS1077	*trpC2 yvcL*::P_{spac}-*yvcL erm* Δ*zapA-yshB*::*tet aprE*::*lacI spc amyE*::P_{xyl}-*ftsZ cat*	This work; P_{xyl}-*ftsZ* comes from YK059
KS1098	*trpC2 yvcL*::P_{spac}-*yvcL erm* Δ*ezrA*::*tet aprE*::*lacI* (*cat*) *amyE*::P_{xyl}-*gfp-ftsZ*(*spc*)	This work
KS1099	*trpC2 yvcL*::P_{spac}-*yvcL erm* Δ*minCD*::*kan aprE*::*lacI* (*cat*) *amyE*::P_{xyl}-*gfp-ftsZ*(*spc*)	This work
KS1102	*trpC2* Δ*soj*Δ*spo0J*::*tet yvcL*::P_{spac}-*yvcL erm* pMAP65	This work, Δ*soj*Δ*spo0J* comes from HM31

KS1116	*trpC2* Δ*soj*Δ*spo0J*::*tet crh*::P_{spac}-*crh erm* pMAP65	This work
PG237	*trpC2 ugtP*::*neo*	Pamela Gamba, unpublished
PG253	*trpC2 ugtP*::*spc*	Pamela Gamba, unpublished
SSB122	*pgcA*(*yhxB*)::*tet*	(Branda *et al.*, 2006)
YK03	CRK6000 *yneA-yneB-ynzC*::*tet*	(Kawai *et al.*, 2003)
YK059	CRK6000 *amyE*::P_{xyl}-*ftsZ cat*	(Kawai and Ogasawara, 2006)
Strain - *E. coli*		
BTH101	F - *cya-99 araD139 galE15 galK16 rpsL1 (str^R) hsdR2 mcrA1 mcrB1*	(Karimova *et al.*, 1998)
DH5α	F - φ80*lacZ*ΔM15 Δ(*lacZ*YAargF) U196 *recA1 endA1 hsdR17* (r_K - , m_K+) *phoA supE44* λ - *thi1 gyrA96 relA1*	Invitrogen
XL1Blue	*recA1 endA1 gyrA96 thi1 hsdR17 supE44 relA1 lac* [F′ proA$^+$B$^+$ *lacI^q*ZΔM15 Tn10 (Tet^R)]	Stratagene
KS432	XL1Blue::pQE60EYvcL	This work

The antibiotic resistance gene names are abbreviated as follows: *bla* (ampicillin), *cat* (chloramphenicol), *erm* (erythromycin), *kan* (kanamycin), *neo* (neomycin / kanamycin), *spc* (spectinomycin), *tet* (tetracycline).

Table 2.2 Summary of plasmids used in this study

Plasmid	**Relevant genotype/comment**	**Source, construction, comment**
pAPNC213	*bla aprE5' spc lacI* P_{spac}-mcs *aprE3'*	(Morimoto *et al.*, 2002)
pBEST501	bearing the kanamycin cassette	(Itaya *et al.*, 1989)
pKT25	*kan* P_{lac} *cya* $^{1-672}$ *-mcs*	(Karimova *et al.*, 1998)
pLOSS*	*bla spc* P_{spac}-mcs P*divIVA-lacZ lacI* rep_{pLS20} (GA→CC)	(Claessen *et al.*, 2008)
pLOSS-ZapAB	pLOSS* containing *zapA-yshB*	This work
pLOSS-YvcL	pLOSS* containing *yvcL*	This work
pMAP65	pUB110 P_{pen}-*lacI (kan)*	(Petit *et al.*, 1998)
pMarB	*bla erm* P_{ctc}Himar1 *kan* (TnYLB−1)	(Le Breton *et al.*, 2006)
pMutin4	*bla erm lacZ lacI*	(Vagner *et al.*, 1998)

pMutin4YvcL	integrates into *yvcL* gene	This work
pMutin4YvcLKO	pMutin4 containing 3' fragment of *yvcK* and 5' fragment of *yvcL*	This work
pMut4YKO	pMutin4YvcLKO introducing a stop codon and *Eco*RI site into *yvcL*	Used for construction of a markerless *yvcL* mutant (KS696). This work
pMutiCrh	used for construction of a *crh* conditional mutant	This work
pMutiYvcL	used for construction of an *yvcL* conditional mutant	This work
pQE60	expression vector for C-terminal His-Tag fusions	Qiagen
pQE60E	derived from pQE60, allows selection for *erm*^{R} in *B. subtilis*	L. Hamoen, unpublished data
pQE60EYvcL	pQE60E containing C-terminally fused *yvcL-his*$_6$	This work
pSG1151	*bla cat gfpmut1*	(Lewis and Marston, 1999)
pSG1151YvcL	used to construct a transcriptional *yvcL-gfp* fusion	This work
pSG1154	*bla amy*E3' *spc* P$_{xyl}$-'*gfpmut1 amy*E5'	(Lewis and Marston, 1999)
pSG1154YvcL	*bla amy*E3' *spc* P$_{xyl}$-*yvcL-gfpmut1 amy*E5'	This work, C-terminal GFP fusion
pSG1729	*bla amy*E3' *spc* P$_{xyl}$-*gfpmut1*' *amy*E5'	(Lewis and Marston, 1999)
pSG1729YvcL	*bla amy*E3' *spc* P$_{xyl}$-*gfpmut1-yvcL amy*E5'	This work, N-terminal GFP fusion
pUT18	*bla* P$_{lac}$ *cya* $^{673-1197}$	(Karimova *et al.*, 1998)
pUT18C	*bla* P$_{lac}$ *cya* $^{673-1197}$ *-mcs*	(Karimova *et al.*, 1998)
p25-N	*kan* P$_{lac}$ *-mcs-cya* $^{1-672}$	(Claessen *et al.*, 2008)

2.3 Oligonucleotides

The oligonucleotides were designed primarily using Clone Manager software (www.scied.com). Oligonucleotides used in this study are listed in Table 2.3.

Table 2.3 List of oligonucleotides used in this study

Name	Restriction site	Sequence (5'-3')	Reference/ comment
*fts*ZqPCR-F		CATTAACAGTCGGCGTTGTG	(Leaver *et al.*, 2009)
*fts*ZqPCR-R		ATCCACCGCTTCTTTCATTG	(Leaver *et al.*, 2009)
km3	*Bam*HI	GGGGGATCCAAGACGAAGAGGATGAAG	*kan*^{R} amplification
km4	*Eco*RI	CCCGAATTCAGAGTATGGACAGTTGCG	*kan*^{R} amplification
KS80		GTACAGGTCTTTCTGTATTG	
KS83		GGCGCTCTGACATGACCATC	
KS84	*Eco*RI	CGGACAGAATTCACCGTCACTTTAAAATAAC	
KS89	*Bam*HI	TGAGGTGGATCCATGTCATTTGCATCAGAAA	pQE60EYvcL construction
KS90	*Bgl*II	TCTTTAAGATCTTTTTAAAGTGACGGTTTGC	pQE60EYvcL construction
KS94	*Hind*III	GCTAAGCTTGCATTCTTCCCAATTTGCTC	pMutiYvcL construction
KS95	*Bam*HI	GATGGATCCCTCATTTCAAGGCTTCATTC	pMutiYvcL construction
KS96	*Hind*III	GCTAAGCTTTAATTGGCGCTCACAATTCG	pMutiCrh construction
KS97	*Bam*HI	GATGGATCCTTACGGTTATTTTAAAGTG	pMutiCrh and pLOSSYvcL constructions
KS98	*Kpn*I	GATCCTCGAGTAAAGTGACGGTTTGCCCTG	pSG1154YvcL construction
KS99	*Bgl*II	GATCAGATCTTAAAGTGACGGTTTGCCCTG	pQE60EYvcL construction
KS120		AATTCTGATAACTGGAAGTGAAGGACTG	pMut4YKO construction
KS121		CCAGTTATCAGAATTCTTTTTTTGTTTCTGATG	pMut4YKO construction
KS128	*Noc*I	ACTGAAAGCGGCCGCCCTTGAAATGAGGTG	pLOSSYvcL

		GC	construction
KS129	*Kpn*I/*Asp*718	GATCGGTACCTAATGAAACAGCCAACTTAAAC	pSG1151YvcL construction
KS130	*Hind*III	GCTAAGCTTTTTTAAAGTGACGGTTTGCC	pSG1151YvcL construction
KS185		AATGGAGACTGGATTGCTGTAG	*xynD* qPCR
KS186		TTACCGTCTGCACTGTCGAG	*xynD* qPCR
KS187		ATACGCGCAGCATCTTAACG	*ynfF* qPRC
KS188		GTATTTCTTGCGGCGTCCAC	*ynfF* qPCR
KS198		TCTGAGCCAGAACCTGATCC	*spoVID* qPCR
KS199		AGTCTCCGCTGGAGAGTCTG	*spoVID* qPCR
KS200		GATACTAAATCCGCCGGAAAC	*acoC* qPCR
KS201		TCAAATGTCAGGCTGAGTGG	*acoC* qPCR
KS268		GGAAGTGACGCTGAAAGAGC	*yvcL* Fw qPCR
KS269		CTGTTCTGCGATTTCGTCAA	*yvcL* Rw qPCR
KS270		ATACCGGTCTTTGCATGAGC	RTP Fw qPCR
KS271		AGCTTGGCAGCTTCGTAATC	RTP Fw qPCR
KS272		AACGACATTGATACAGAACC	*ilvA* Fw qPCR
KS273		ACCTTTGTATCAGGAGACAC	*ilvA* Rw qPCR
KS274		CTGTCGAAACGCTTGATTGA	*pyrK* Fw qPCR
KS275		CGTCAGCTGTTGCCACATAC	*pyrK* Rw qPCR
KS276		GATCAAACGGTGAAGGGAAA	*oppA* Fw qPCR
KS277		CGGATAACACCGCCTGATAC	*oppA* Fw qPCR
KS278		GGAACGTCAAATCCGTAAGC	*yvyD* Fw qPCR
KS279		TGTCATCCTGAACCGCAATA	*yvyD* Rw qPCR
KS280		CATCCAAGCCCATAAAGACG	*ywaA* Fw qPCR
KS281		TCACCGTTGTTGATCGAAAG	*ywaA* Rw qPCR
KS282		CATTTGTGATCTGCCAGTCG	*ytxK* Fw qPCR
KS283		TTGGTATGCTTGACGCTCTG	*ytxK* Rw qPCR
KS284		ACGTCCTGCTGCTTTGTTTG	*crh* Fw qPCR
KS285		CTTACCGCAAGGCTCATCA	*crh* Rw qPCR
KS288		CTGAAACACGTGCGAAAGAA	*rplQ* Fw qPCR
KS289		GGATGTATGCAGCAGCTTGA	*rplQ* Rw qPCR
KS290		GCTTTCGGCATCCAGAATTA	*yktD* Fw qPCR
KS291		AGATGACCCGGAATTGTCAG	*yktD* Rw qPCR
KS292		AACACTCGGCATTGTGACAG	*ysfC* Fw qPCR
KS293		ATGTCCGATACCGTTTGAGC	*ysfC* Rw qPCR
KS294		TCTATCCCGGCTGAGAGATG	*truA* Fw qPCR

KS295		TTTGACTGCGCTAAATCGTG	*truA* Rw qPCR
KS296		CCAATGCCTCAAGAACACTG	*glpK* Fw qPCR
KS297		TGAGAGGACGGCTTCACTTC	*glpK* Rw qPCR
KS298		TGTCGCTTTATTATTTGGACGA	*ylxM* Fw qPCR
KS299		GCATTGCTTCTGTTCGTTTG	*ylxM* Rw qPCR
OIPCR1		GCTTGTAAATTCTATCATAATTG	(Le Breton *et al.*, 2006)
OIPCR2		AGGGAATCATTTGAAGGTTGG	(Le Breton *et al.*, 2006)
OIPCR3		GCATTTAATACTAGCGACGCC	(Le Breton *et al.*, 2006)
qORI-F		GATCAATCGGGGAAAGTGTG	(Murray and Errington, 2008)
qORI-R		GTAGGGCCTGTGGATTTGTG	(Murray and Errington, 2008)
qTER-F		TCCATATCCTCGCTCCTACG	(Murray and Errington, 2008)
qTER-R		ATTCTGCTGATGTGCAATGG	(Murray and Errington, 2008)
STG101		ATACCGCGGAGATACACGAG	*scpB* Fw qPCR
STG102		TTTGACGGCACTTCAATCAG	*scpB* Rw qPCR
STG410		TTGACGACAAGCGTGAAAAG	*rplC* Fw qPCR
STG411		TTcatACGcatCcatTTCCA	*rplC* Rw qPCR
yshA-F	*Noc*I	GATGCGGCCGCCACTTTTCGCTGTATATACC	pLOSS-ZapAB construction
yshB-R	*Bam*HI	GATGGATCCGACGTTCACATATGTTTCCATC	pLOSS-ZapAB construction
yvcL-C5	*Xho*I	GCCTTGGGTACCGGTGGCTATATGTCATTTG	pSG1154YvcL construction
yvcL-F1	*Hind*III	GCTAAGCTTAAACCGCCATCTCGTACTC	pMutin4YvcL construction
yvcL-R1	*Bam*HI	GATGGATCCAATTGACGAGGCGGTTGACC	pMutin4YvcL construction
yvcL-N5	*Hind*III	GCCTTGAAGCTTGGTGGCTATATGTCATTTG	pSG1729YvcL construction
yvcL-N3	*Eco*RI	GAACTTGAATTCTCTGTTGAACCATAAGATC	pSG1729YvcL construction

Fw = forward primer; Rw = reverse primer

2.4 Media supplements

Media supplements are indicated in Table 2.4.

Table 2.4 Media supplements

Supplement	*B. subtilis*	*E. coli*
ampicillin		100 µg/ml
chloramphenicol	5 µg/ml	
erythromycin	1 µg/ml	
glucose		0.4-0.8 %
kanamycin	5 µg/ml	
phleomycine	2 µg/ml	
spectinomycin	50 µg/ml	
tetracycline	12 µg/ml	
X-gal	160 µg/ml	
IPTG	0.5-1 mM unless otherwise indicated	
xylose	0.025-1 %	

2.5 DNA manipulations

2.5.1 Oligonucleotides

Oligonucleotides were purchased from Eurogentec, and stored at -20ºC as 100 µM stocks.

2.5.2. Polymerase chain reaction (PCR)

A typical PCR reaction contained 2.5 µM dNTPs, 1 µM primers, supplemented with appropriate reaction buffer. For cloning, either Pfu Ultra polymerase (Stratagene) or Expand High Fidelity PCR System (Roche) was used. As for colony PCR, GoTaq (Promega) polymerase was used routinely to select for recombinants.

2.5.3. Purification of PCR products

The PCR products were purified using a PCR purification kit (Qiagen). In some cases, the DNA was separated firstly on agarose gel and purified using Qiagen Gel Extraction kit. The DNA was eluted in water.

2.5.4. Plasmid purification

Plasmids were purified from overnight cultures grown at 30ºC following manufacturer's manual (Qiagen Miniprep kit).

2.5.5 Agarose gel electrophoresis of DNA fragments

DNA samples were mixed with a STOP dye before loading on gel. The electrophoresis of DNA fragments in agarose gels was performed using 0.8 % agarose gels supplemented with 0.5 mg/ml ethidium bromide, run in TAE buffer (90-130 V), and visualized using a UV transilluminator.

2.5.6. DNA modification reactions

2.5.6.1 Digestion with restriction enzymes

DNA was digested for 3-6 h in conditions suggested by the manufacturer. The enzymes were heat-inactivated by 15 *min* incubation at 65ºC, when possible, and the DNA was cleaned using the QIAquick purification kit (Qiagen).

2.5.6.2. Dephosphorylation of 5' ends

Linearized plasmids were dephosphorylated using alkaline phosphatase (calf intestine phosphatase, CIP, Roche). The restriction reaction was directly supplemented with CIP buffer and heated to 50ºC for 2min; usually 1 unit of the enzyme was added and the reaction was incubated for 20-30 *min* at 37ºC. The procedure of heating (50ºC for 2 *min*), adding the alkaline phosphatase and 20-30 *min* incubation at 37ºC was repeated. The DNA was cleaned using QIAquick purification kit.

2.5.7 Ligation reaction

DNA fragments were ligated using 1 unit of T4 DNA ligase (Roche) per reaction. The ligation volume was usually 20 µl and the aliquots were incubated overnight at 4ºC in a bucket filled with water (~21ºC initial temperature).

2.5.8 DNA sequencing

Sequencing analysis of plasmids or PCR products was performed by Dundee Sequencing service.

2.5.9 Isolation of chromosomal DNA from *B. subtilis*

For preparation of chromosomal DNA from *B. subtilis*, 2 ml culture was harvested (best grown overnight at 30ºC to avoid formation of spores) and resuspended in 750 µl TES buffer. The suspension was mixed with 20 µl of lysozyme solution (10 mg/ml), incubated at 37ºC until the solution was cleared, then 50 µl of pronase solution and 30 µl of sarkosyl were added, mixed, and incubated for 30 - 60 *min* at 37ºC. Then 250 µl of phenol and 250 µl of chloroform were added to the cell lysate, mixed vigorously and centrifuged for 4 *min* at 13,000 rpm to separate the phases. The top aqueous layer was transferred into a new tube, 500 µl of chloroform was added, and again the aqueous layer (600 µl) was extracted. Then 1200 ul ethanol was added, the tube was inverted a few times until a cloud of DNA precipitated, which was washed two times with 70 % ethanol. After the remains of ethanol were removed, the DNA was resuspended in 500 µl of MilliQ water, heated for 10 *min* at 55ºC, and stored at -20ºC.

2.6 Protein manipulations

2.6.1 SDS-polyacrylamide gel electrophoresis

The protein samples were mixed with loading dye (supplied by the manufacturer), incubated for 10 *min* at 95ºC, and applied to pre-cast Novex Midi Gels 4-12 % Bis-Tris (Invitrogen). The electrophoresis was perfomed at 90-150 V in one of the buffers supplied by the manufacturer.

2.6.2 Coomassie brilliant blue staining

The protein bands on SDS-PAGE gels were visualized by incubating the gels in a solution P (40% methanol, 12% acetic acid) supplemented with 0.025% Coomassie brilliant blue dye and subsequently destained in solution P.

2.6.3 Western Blot analysis

Before blotting, the SDS-PAGE gels were rinsed with dH_2O and placed onto a PVDF (HybondP) membrane. The transfer was performed using a BioRad apparatus run at 30 mA overnight in transfer buffer. The membrane was then washed 2x 10 *min* with

PBSTM, and blocked in blocking buffer for 6 h. The primary antibody was added to the blocking buffer and the membrane was incubated for 1 h while shaking. Membrane was washed 3-4x in PBSTM and soaked in blocking buffer supplemented with the secondary antibody. After 1 h, the membrane was washed 3x in PBSTM and 2x in PBST. Finally, ECL Plus Western Blotting Detection System (GE Healthcare) was used for autoradiography.

2.6.4 Purification of YvcL-His$_6$

Strain KS432 was used for purification of YvcL-His$_6$. The growth media had to be supplied with >0.4 % glucose to allow tighter repression of the promoter on the plasmid pQE60EYvcL. To construct this plasmid, an amplified 967 bp DNA fragment (using primers KS89 and KS99) was digested with *Bam*HI and *Bgl*II, and cloned into pQE60E digested with the same enzymes. *E. coli* XL1Blue was used as a host both for cloning and protein expression. A fresh culture was inoculated into 600 ml LB supplemented with ampicillin and 0.8 % glucose and grown to OD_{600}~0.5 at 37ºC. Expression was induced by addition of IPTG to a final concentration of 0.025 mM, for 1 h at 30ºC. We used short induction and low temperature, since otherwise the protein had a tendency to aggregate into inclusion bodies and we were aiming for a soluble protein (although at lower concentrations). The cells were cooled on ice and harvested. The cell pellet was resuspended in 8 ml buffer A and stored at -20ºC.

YvcL-His$_6$ fusion protein was purified using a one-step purification protocol. The cell pellet was sonicated until the cells were lysed and the debris was removed by ultracentrifugation at 40,000 rpm for 30 *min*. The supernatant was loaded onto a Ni^{2+}-charged 2 ml sepharose column equilibrated in buffer AK. The protein was eluted using a linear gradient of KCl (using buffer BK). We used KCl because we thought it is less likely to interfere with DNA-protein reactions than imidazole. The protein peak was present in fractions corresponding to ~250 mM KCl. Despite our attempts to keep YvcL-His$_6$ fusion protein in solution (increasing salt/glycerol concentration, pH change, modifying the storage temperature) it precipitated within a few hours.

2.6.5 Raising anti-YvcL-His$_6$ serum

Strain KS432 was inoculated into 300 ml LB supplemented with ampicillin and glucose (0.8%). After the cell density of the culture had reached OD_{600} ~0.5, the expression of the fusion protein was induced by adding 1 mM IPTG. The culture was grown for 3.5 h before harvesting. Cells were pelleted and resuspended in 1.2 ml of buffer (100 mM

NaCl, 50 mM Tris-Cl pH8.0), and sonicated. After ultracentrifugation, the pellet containing inclusion bodies was resuspended in 1.2 ml 1 x sample buffer, the samples were heated for 10 *min* at 95ºC and run on a 12 % SDS-PAGE gel. The protein bands were excised from the gel and were used to raise anti-YvcL-His_6 antibodies in a rabbit (Eurogentec, Ltd). We used a standard 3-months immunisation programme. For western blot analysis, the α-YvcL-His_6 was used at a dilution of 1:10 000 to detect YvcL in lysates from 10 x concentrated *B. subtilis* cultures.

2.6.6 Electrophoretic mobility shift assay (EMSA)

To perform gel-shift assay using YvcL-His_6, a fresh protein preparation was used. DNA probes to test the DNA-binding ability of YvcL-His_6 were amplified from chromosomal *B. subtilis* DNA using primers *yvcL*-F1 and *yvcL*-R1 (571 bp) and KS94 and KS95, (412 bp) which comprised the *yvcL* region and a region just upstream of *yvcL* (7 bp from start codon), respectively. For all reactions, 5 µl 4x Binding buffer, 8 µl of DNA and different concentrations of purified YvcL-His_6 (7, 3.5, and 1 µl corresponding to ~1.75, 0.875 and 0.25 µg) were used per reaction. The sample volumes were adjusted to 20 µl. The reaction was incubated for 25 *min* at 30ºC and run on 1.5 % agarose gel in TAE buffer at 4ºC. The DNA in the gel was visualized by staining in a solution of ethidium bromide (0.5 mg/ml).

2.7 *Escherichia coli* methods

2.7.1 Preparation of competent *E. coli* cells

To prepare competent cells a modified method of Inoue *et al.,* 1990 was used (Inoue *et al.*, 1990). In brief, an overnight cell culture was diluted 100 x into fresh LB supplemented with 15 mM $MgSO_4$ and 15mM $MgCl_2$ and grown to OD_{600} ~0.3. The flask containing the culture was cooled on ice, and the cells were gently harvested by 10 *min* centrifugation at 2250 rpm. The cell pellet was resuspended in 15 ml TB buffer and incubated on ice for 10 *min*. Then the cells were harvested and resuspended gently in 2 ml of TB, and incubated on ice for another 10 *min*. After the addition of DMSO to a final concentration of 7 %, cells were kept on ice for 10 *min* prior to dividing the suspension into small aliquots that were flash frozen in liquid nitrogen and stored at -80ºC.

2.7.2 *E. coli* transformation

To transform DNA into *E. coli* cells, the competent cells that were thawed on ice were mixed with DNA and incubated for 40 *min* on ice. After a heat-shock (42ºC 45 s) 600 µl of LB was added to the mixture and the cells were regenerated by vigorous shaking at 37ºC for 1 h. Transformants were selected on media with appropriate supplements.

2.7.3 Bacterial two hybrid system

The plasmids for this study were a kind gift from Dr. Robyn Emmins, and from Dr. Heath Murray (Murray and Errington, 2008). Pairwise combinations of plasmids pUT18C/pKT25 or p25-N/pKT18 (Claessen *et al.*, 2008; Karimova *et al.*, 1998) bearing target genes were transformed into competent BTH101 cells, plated onto NA plates supplemented with ampicillin, kanamycine, and X-gal. No IPTG was used to express WhiA since it was toxic for *E. coli*. A positive control was pUT18C-Zip x pKT25-Zip cotransformation. A negative control was pUT18C x pKT25 cotransformation. Blue colony formation after 48 h at 30 ºC indicated an interaction.

2.8 *Bacillus subtilis* methods

2.8.1 Preparation of competent *B. subtilis* cells

To prepare competent cells of *B. subtilis*, 5 ml overnight culture in competence medium was diluted 10-fold into fresh competence medium and grown for 3-4 h at 37ºC, after which an equal volume of starvation medium was added and the cells were starved for another 1-2 hours at 37ºC.

2.8.2 *B. subtilis* transformation

To transform DNA into *B. subtilis* cells, usually 10 µl of chromosomal or plasmid DNA was added to 500 µl of competent cells (in a 2 ml test tube). The cells were subsequently incubated for 1 h at 37ºC and plated on selective media.

2.8.3 Construction of strains

2.8.3.1 Construction of *yvcL* mutant strains

Three *yvcL* mutant strains were constructed (Fig. 2.1). Mutant KS207 contains an insertion of pMutin4YvcL in *yvcL* that disrupts *yvcL* expression. A 581 bp DNA fragment, acquired by PCR using primers *yvcL*-F1 and *yvcL*-R1 and wild type

chromosomal DNA as a template, was digested with *Hind*III and *Bam*HI and ligated with dephosphorylated pMutin4 plasmid cut with the same enzymes. Then correct plasmid (pMutin4YvcL) was integrated in *B. subtilis* by Campbell integration, which was checked by PCR.

In strain KS400 *yvcL* is deleted and substituted by a kanamycin resistance cassette. To construct strain KS400, the DNA fragments outside of *yvcL* were amplified using primer pairs KS80, KS95 and KS84, KS83 (resulting in 940 bp and 984 bp DNA fragments). The kanamycin resistance cassette was amplified from pBEST501 (Itaya *et al.*, 1989) with primers km3 and km4. After all three fragments were digested with suitable restriction enzymes (*Bam*HI, *Eco*RI), they were ligated, and the mixture was transformed into *B. subtilis*. Recombinants were selected using a PCR.

Strain KS696 is a markerless *yvcL* mutant strain. To generate it, firstly pMutin4YvcLKO was constructed. A 1094 bp fragment, comprising the 3' end of *yvcK* and 5' end of *yvcL*, was amplified using primers KS94 and *yvcL*-R1, and was cloned into pMutin4 after digestion with *Hind*III and *Bam*HI. Site-directed mutagenesis on the plasmid was performed using primers KS120 and KS121 that introduced an *Eco*RI site and a stop codon in the beginning of *yvcL* (32 bp from start codon). The resultant plasmid, pMut4YKO was transformed into *B. subtilis* cells, and selected for erythromycine resistance and blue colonies on NA+Xgal+*erm* plates. One of the transformants was then grown in the competence medium for ~10 generations without any antibiotic pressure, in order to excise the plasmid, and~1000 colonies were plated on NA+X-gal. White colonies that were also Ery-sensitive (11 out of 30 white colonies) were cultured and the chromosomal DNA inspected for the *Eco*RI insertion site *yvcL* gene. The *yvcL* region was sequenced.

All three *yvcL* mutants were also tested for the synthetic phenotype when combined with Δ*zapA* (data not shown).

2.8.3.2 Construction of conditional mutants

The conditional mutants in *crh* and *yvcL* were constructed using plasmids pMutiCrh and pMutiYvcL, respectively. For both plasmids, ~400 bp regions upstream of either *crh* or *yvcL* were amplified using primer pairs KS96, KS97 or KS94, KS95, respectively. The fragments and plasmids were cut with *Hind*III and *Bam*HI and cloned into pMutin4 plasmid digested with corresponding enzymes. The plasmids were transformed into *B. subtilis* and selected for single cross-over events that led to insertion of the IPTG-inducible P_{spac} promoter upstream of either *crh* or *yvcL* (strains KS439 and

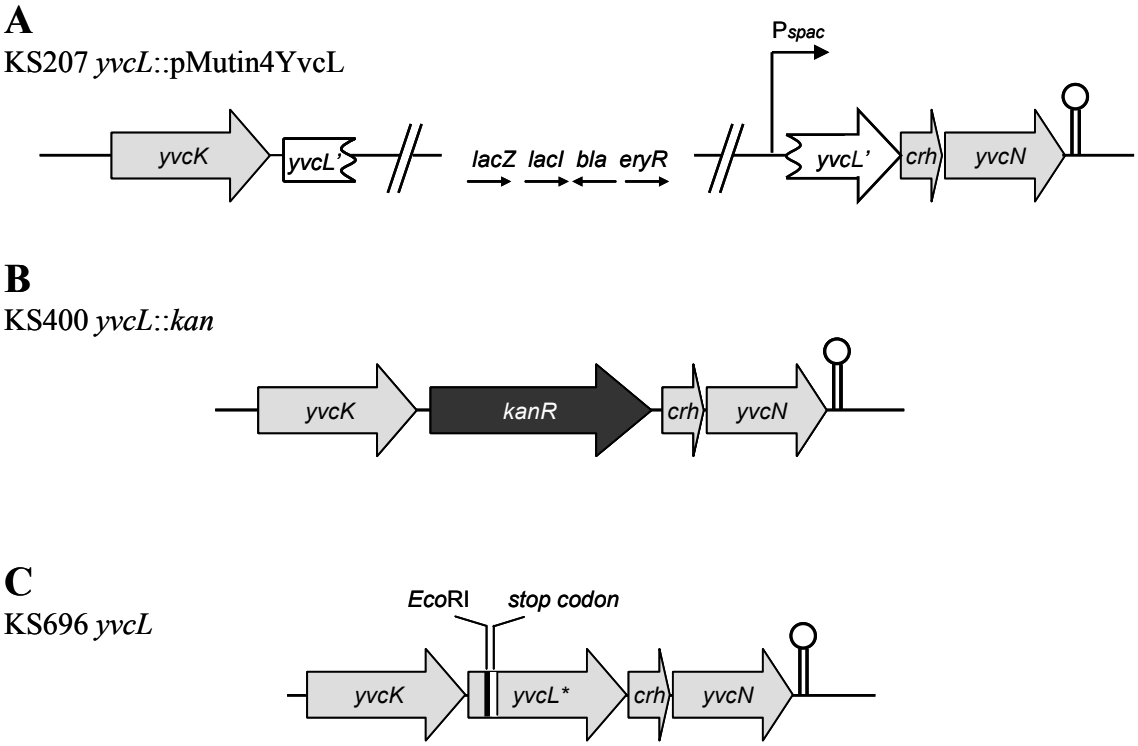

Fig. 2.1 Outline of *yvcL* mutants constructed
(**A**) Strain KS207 contains a single cross-over insertion of pMutin4YvcL plasmid in the coding region of *yvcL*. This causes disruption of the gene. (**B**) Strain KS400 was constructed using a *kan*^{R} marker and outside flanking regions homologous to the up- and downstream regions of *yvcL*. These fragments of DNA were ligated and then introduced into cells of *B. subtilis* by double cross-over. (**C**) The markerless mutant KS696 was created using plasmid pMut4YKO that contained a fragment of *yvcK* and *yvcL* genes, but also an *Eco*RI site and a *stop* codon at the beginning of *yvcL*. *B. subtilis* cells were transformed with this plasmid, single cross-over recombinants were selected that formed blue colonies on X-gal plates containing erythromycin. This strain was subsequently grown and selected for a second, but this time a double cross-over event. This resulted in the escape of the plasmid from the cells, as a result of which the strain formed white and erythromycin sensitive colonies. There is no marker or residual DNA in this strain except for the *stop* codon and an *Eco*RI site that enables a PCR check of the strain.

KS438, respectively). To allow tight regulation of *yvcL* expression, an extra copy of *lacI* was introduced by pAPNC213 (Morimoto *et al.,* 2002), which integrates into *aprE* locus, into strains KS439 and KS438, resulting in strains KS1012 and KS891, respectively.

2.8.3.3 Construction of GFP-fusions

To construct a xylose-inducible GFP-YvcL fusion, plasmid pSG1729YvcL was generated by ligating the *amy*-integration vector pSG1729 and a 1020 bp PCR fragment (primers *yvcL*-N5 and *yvcL*-N3) that were both digested with *Hind*III and *Eco*RI. Plasmid pSG1729YvcL was transformed into *B. subtilis* resulting in a strain KS180 with a xylose-inducible GFP-YvcL fusion at the *amy*E locus. This *amy*E::P_{xyl}-*gfp-yvcL spc* allele was combined with a *yvcL* mutation (strain KS400) so that *gfp-yvcL* is the only copy of *yvcL* in the cell (strain KS749).

YvcL-GFP fusion was constructed similarly. To generate pSG1154YvcL, a 976 bp PCR fragment (primers KS98 and *yvcL*-C5) and pSG1154 were digested with *Kpn*I and *Xho*I and ligated. Plasmid pSG1154YvcL was transformed into *B. subtilis* resulting in strain KS394 and subsequently *yvcL* gene was deleted resulting in strain KS752.

To clone *yvcL-gfp* under its endogenous promoter, plasmid pSG1151YvcL was constructed. For this, a 293 bp 5' fragment of *yvcL* was amplified using KS129 and KS130 primers and cloned into pSG1151 plasmid (using Asp718 and *Hind*III). *B. subtilis* cells were transformed with pSG1151YvcL and Campbell recombinants were checked by PCR, resulting in a strain KS907.

2.8.4 Synthetic lethal screen

To perform a synthetic lethal screen with Δ*zapA* (Fig. 2.2), we used the methods described by Claessen *et al.* (Claessen *et al.*, 2008). In brief, the *zapA-yshB* genes were amplified using yshA-F and yshB-R primers, and cloned into the instable plasmid pLOSS*. The resulting plasmid pLOSS-ZapAB was tested for functionality. It recovered growth of a double Δ*divIVA* Δ*zapA* mutant (which is not viable) (Gueiros-Filho and Losick, 2002) and normal colonies were formed (Fig. 2.3). Importantly, from the blue colour of the colonies it is clear that the plasmid is maintained without antibiotic pressure. In a background where only *zapA* is deleted the plasmid is quickly lost, resulting in white colonies (Fig. 2.3, strain KS50). The plasmid was transformed

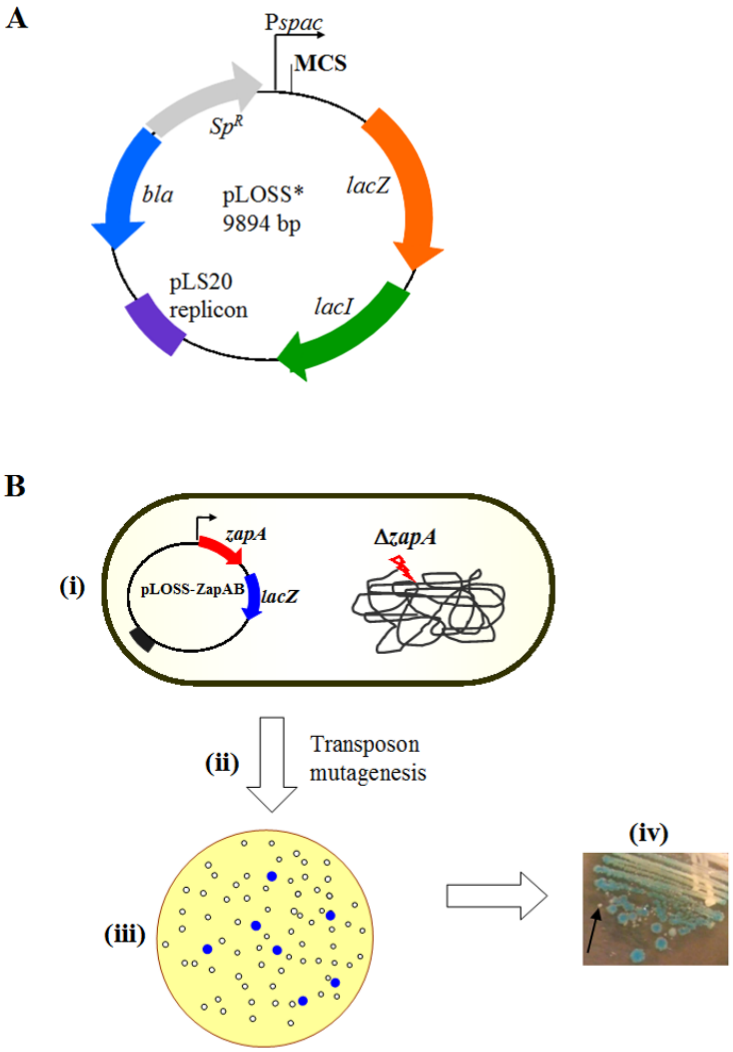

Fig. 2.2 A schematic outline of the synthetic lethal screen
(**A**) The unstable plasmid pLOSS* used for synthetic lethal screening (Claessen *et al.*, 2008). (**B**) In our experimental setup, deletion of *zapA* is complemented by expression of *zapA* from pLOSS-ZapAB (**i**). Then, transposon mutagenesis is performed to generate a library of transposon mutants (**ii**). This library is subsequently screened for blue colonies (on X-gal plates) indicating that the plasmid in stably maintained (**iii**). The possible synthetically lethal mutants are then streaked to search for those that form uniform blue colonies, or a mixture of blue colonies and minute white colonies (**iv**, see arrow).

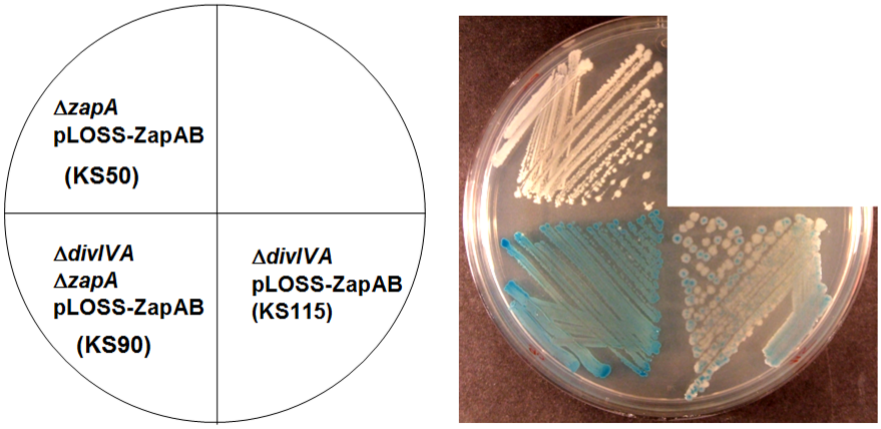

Fig. 2.3 Functionality of pLOSS-ZapAB
Strains were streaked on X-gal plates and grown at 37°C. Blue colonies contain the plasmid. The synthetic lethality of a deleterious strain lacking both *divIVA* and *zapA* (KS90) causes pressure to maintain the plasmid. In a *divIVA* mutant some cells retain the plasmid as well, which might be explained by a partial amelioration of *divIVA* mutant by ZapA overexpression from pLOSS-ZapAB.

into cells with a *zapA-yshB* deletion (strain KS6), and subsequently a *lacA* deletion was introduced (D. Claessen, unpublished) resulting in a strain KS50. This strain was transformed by pMarB, which carries a transposon TnYLB-1 (Le Breton *et al.*, 2006), and transposon mutagenesis was perfomed that acquired a library of transposon mutants. To screen for synthetically lethal mutants, the library was plated on NA plates supplemented with X-gal and 1 mM $MgSO_4$ and incubated for 8 h at 50ºC without antibiotic pressure so that plasmid would be lost during segregation. Magnesium was added to media since it seemed to enhance blue colony formation, data not published. Only in case the transposon inserts into a gene that makes ZapA essential will pLOSS-ZapAB be maintained and the colony expresses ß-galactosidase. Blue colonies were picked and streaked on fresh NA+X-gal. In this step, we were aiming for clones that formed uniformly blue colonies or a mixture of normal-sized blue colonies and tiny white colonies (with perturbed cell division resulting from loss of the plasmid). The chromosomal DNA of these positive clones was then backcrossed systematically into strain KS50 to check whether the transposon caused again the stability of pLOSS-ZapAB plasmid. To map the transposon insertions, 5 µl of chromosomal DNA was digested with TaqI for 4 hours at 65ºC in a 20 µl total volume. After DNA purification, the DNA fragments were circularized by ligation in a (diluted) 100 µl total volume, and purified (elution in 50 µl). For the inverse PCR, 20 µl template DNA, and primers OIPCR1 and OIPCR2 were used. The chromosomal position of the transposon was mapped by sequencing using primer OIPCR3 (Le Breton *et al.*, 2006).

2.8.5 Suppressor screen for Δ*yvcL*Δ*zapA* double mutant

To select for transposon mutants that would suppress the lethal phenotype of a Δ*yvcL*Δ*zapA* double deletion, the following steps were carried out (Fig. 2.4) Firstly, the instable plasmid pLOSS-YvcL was constructed by cloning *yvcL* (amplified by KS128 and KS97) into pLOSS*. Leaky transcription from the P_{spac} promoter gave sufficient levels of YvcL to prevent cell death in the Δ*yvcL*Δ*zapA* background (strain KS742). Nevertheless, we used 0.1 mM IPTG and spectinomycine during construction of the strains. This strain also contained a *lacA* deletion to prevent transposon insertions that would activate the native *B. subtilis* ß-galactosidase.

A transposon mutagenesis using pMarB (Le Breton *et al.*, 2006) was performed yielding 34,000 clones. The library was then screened on NA plates supplemented with X-gal, 0.1 mM IPTG and 1 mM $MgSO_4$ and incubated at 37ºC (the 50ºC incubation step was skipped). White colonies were restreaked to check for whiteness, presence of

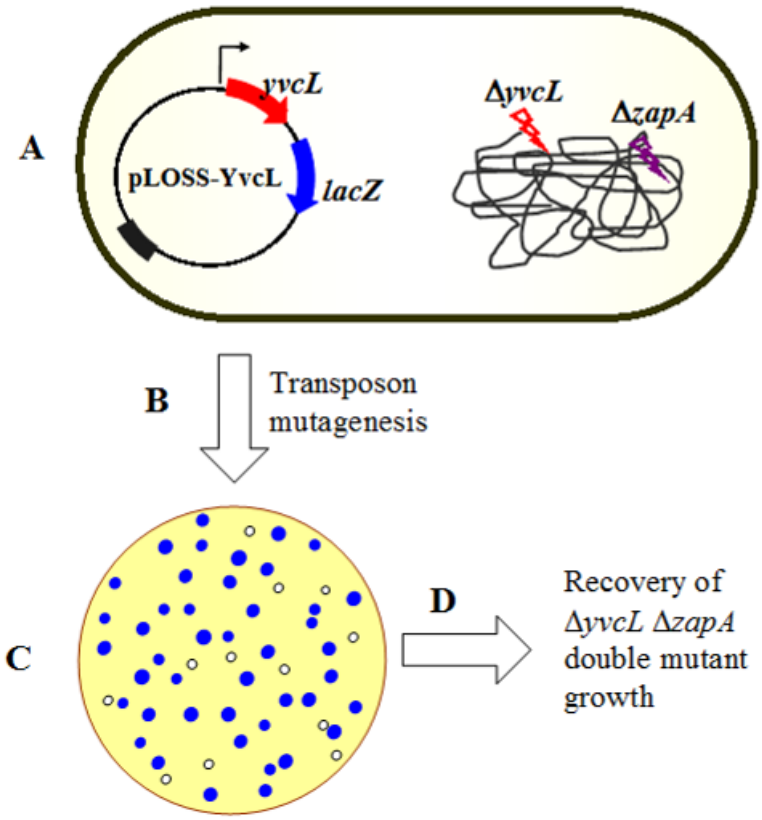

Fig. 2.4 Use of the synthetic lethal screen 'the other way around' to search for suppressor mutations

The parental strain containing two mutations that are synthetically lethal (*yvcL* and *zapA*), retains pLOSS-YvcL without antibiotic selection (**A**). A library of transposon mutants (**B**) is generated and screened for the loss of pLOSS-YvcL marked by appearance of white colony formation on media with X-gal (**C**). Possible clones containing suppressors are checked for the amelioration of a Δ*yvcL* Δ*zapA* mutant (**D**).

the plasmid (Spc^R) and the transposon (Kan^R Ery^S). The chromosomal DNA of 82 positive clones was purified and transformed into the conditional *yvcL*⁻ *zapA*⁻ mutant strain (KS859). Suppressor mutations that were able to recover growth of KS859 in the absence of IPTG were mapped as described for the synthetic lethal screen.

2.9 Microscopic imaging

2.9.1 Phase contrast and fluorescence microscopy

To prepare cells for light microscopy, the slides were covered with a thin layer of 1.5% agarose solution. For fluorescence microscopy, also 1 mM $MgSO_4$ and 0.5% glucose were added to the agarose to nourish the cells.

Membranes were stained by either Nile Red (Molecular Probe) (1-2 µl of 12.5 mg/ml solution added to 1 ml of cell culture) or with FM5-95 (4 µl of 200 µg/ml solution added to 800 µl agarose). To stain nucleoids, 4 µl of DAPI (1 mg/ml, Sigma) was mixed with 800 µl agarose. Zeiss Axiovert 200M microscope combined with Sony CoolSnap HQ cooled CCD camera (Roper Scientific) was used to capture images. For analyses of the pictures ImageJ software (http://rsb.info.nih.gov/ij/) was used.

Spinning disc microscopy was performed using a Nikon Eclipse Ti inverted microscope (coupled to a laser source), equipped with a Yokogawa spinning disc (CSU22) and a Cool-Snap HQ2 camera (Photometrics).

2.9.1.1 Localization of YvcL

To examine the localization of GFP-tagged YvcL, the strains KS749 and KS752, harbouring a P_{xyl}-*gfp-yvcL* or P_{xyl}-*yvcL-gfp* allele, respectively, were grown at 30 ºC, diluted to an OD_{600} ~0.05, and induced with 0, 0.01, 0.05, 0.1 and 0.5 % xylose. After two hours cells were observed using fluorescence microscopy. Strain KS907 was used to examine YvcL-GFP expressed from the *yvcL* promoter. In this case cells were grown in SMM+ medium, diluted to OD_{600} ~0.05 and grown to OD_{600} ~0.2, and spinning disc microscopy was employed to acquire the images since it allowed shorter excitation times.

2.9.1.2 Determination of nucleoid morphology

Strains were grown in the absence of IPTG for two hours to deplete for FtsZ after which epifluorescent images were acquired. The DNA binding protein HBsu, fused to GFP (construct from J. W. Veening, unpublished), was used as a fluorescent marker for the

nucleoid (Kohler and Marahiel, 1997). To quantify potential differencies in nucleoids, the fluorescence signal intensity along the longitudinal axis of cells was measured. In three independent experiments, at least 10 graphs were acquired from different cells. To assess the spacing of *oriC* and *ter* regions, a comparable approach was used but this time the position of Spo0J-GFP or RTP-GFP foci was measured in the longitudinal axes of the cells.

2.9.2 Transmission electron microscopy

The samples of exponentially growing cells in LB were fixed in 2 % glutaraldehyde solution and further processing was performed by the Electron Microscopy Research Service of Newcastle University. These steps included overnight fixation in Sorenson's phosphate buffer (TAAB Laboratory Equipment), pH 7.4, then 1 h fixation in 1% osmium tetroxide (Agar Scientific), dehydration in an acetone graded series, and finally, impregnation with a graded series of epoxy resin (TAAB Laboratory Equipment) in acetone. The cell material was embedded in 100 % resin and incubated at 60° C for 24 h. The material was sectioned and stained with 2 % uranyl acetate and lead citrate (Leica). The imaging was performed using a Philips CM100 Compustage Transmission Electron Microscope (FEI) attached to an AMT CCD camera (Deben).

2.10 Microarray analysis

RNA isolation, cDNA preparation, hybridization and microarray analyses were performed as previously described (Gamba *et al.*, 2009). For the RNA samples, overnight cultures of strains KS2 (wt) and KS400 (Δ*yvcL*::*kan*) were diluted 100 x and grown to OD_{600} ~0.6 in LB medium. Then 5 ml cultures were used for the isolation of RNA. The cDNA transcribed from the RNA was poly(T)-tailed and the dye-specific capture sequences were ligated only subsequently to minimize the loss of fluorescence (N. Saunders, unpublished).

2.11 qPCR

2.11.1 Marker frequency analysis for *ori*/*ter* ratio measurement

To assess the *ori*/*ter* ratio in cells, marker frequency analysis was performed. The DNA isolation and quantitative PCR (qPCR) were performed as previously described (Murray and Errington, 2008). In brief, cells were grown in CH medium to exponential phase (OD_{600} ~0.2) and 0.5 % sodium azide was added to 1 ml of cell suspension. The DNA

was isolated using DNeasy Blood and Tissue Kit (QIAGEN). Following primers were used: qORI-F, qORI-R, qTER-F, qTER-R. For each PCR reaction, 2 µl of the primer pair (3 µM), 10 µl of SYBR Green PCR Master Mix (Applied Biosystems), and 8 µl of 400 x diluted chromosomal DNA were mixed. The qPCR was performed using Roche Light Cycler 480 instrument. Spores DNA where the ori/*ter* ratio is expected to be 1 was used to normalize the qPCR reaction. The relative ori/*ter* ratio was calculated from the difference in the CP (the cycle number when the fluorescence crosses an arbitrary line; crossing point).

2.11.2 Verification of microarray results

To verify microarray results quantitative PCR of reverse transcripts was performed. Cells were grown in LB to OD_{600} ~0.6 and the total RNA was purified using FastRNA® Pro Kit (BIO 101 Systems). The RNA was then further cleaned and DNase-treated using RNeasy Mini Kit and RNase-Free DNase Set (both Qiagen). The quality of RNA was checked using Agilent RNA 6000 Nano Kit (Agilent Technologies). The cDNA was acquired using a cDNA Reverse Transcription Kit (Applied Biosystems) and 1 µg of RNA. qPCR reaction conditions were similar as described above. The data analysis was based on the difference in CP (curvature point). Primers used for this include *ftsZ*qPCR-F and *ftsZ*qPCR-R, and primers KS270-KS299. The efficiency of ftsz qPCR was used as a normalizer.

2.12 Determination of DNA binding sites of YvcL

To determine where on the chromosome YvcL would bind, a Chip-on-chip analysis was performed, as described by (Gruber and Errington, 2009). In brief, cells were grown in competence medium (SMM+) at 37 ºC and fixed in the exponential growth phase (OD_{600} ~0.1) with formaldehyde. Protoplasts were prepared by lysozyme treatment, and DNA was sheered by sonication. Chromatin immunoprecipitation was performed with α-YvcL antibody bound to Protein A coated magnetic Dynabeads (Invitrogen). Beads were washed, and the DNA was eluted by 1% SDS treatment at 65ºC, and purified by phenol-chloroform extraction. Then the immunoprecipitated DNA (IP DNA) was purified by phenol-chloroform method.

For the qPCR, the total DNA was diluted 1:1000 and the IP DNA 1:25, and the reaction conditions were used as described for marker frequency analysis. The primers

used are listed in Table 2.3. Second derivative function was used to calculate the CP (curvature point).

For hybridization, Roche NombleGen (v3.1) protocol was followed. Total DNA (input) and IP DNA were purified using Qiagen PCR purification column, and 10 ng of DNA was used for random amplification using Sigma WGA2 kit. The Cy3- and Cy5-9-mers were used to label 400 ng of amplified DNA. The labelled DNA (4.7 μg of each) was hybridized onto *Bacillus subtilis* Nimblegen-custom-made chip (~383 k probes). The probes (~50 bp) covered both strands of the whole genome with the exception of repetitive sequences. NimbleGen (v 3.1) protocol was used for data analysis.

Chapter 3

Identification and characterization of the new cell division protein YvcL

3.1 Introduction

Assembly of the FtsZ-ring is the first key event in bacterial cell division. In *B. subtilis*, the proteins ZapA, SepF and EzrA interact with FtsZ to promote formation of the Z-ring at midcell. One of the first proteins to interact with FtsZ is ZapA. It is a small 11 kDa protein and is conserved in most bacterial species. Although ZapA appears to stimulate Z-ring formation, the protein is not essential for growth (Gueiros-Filho and Losick, 2002). *In vitro* experiments including pull-down, light scattering and pelleting assays for polymerization have shown that ZapA directly interacts with FtsZ, and electron microscopy corroborated that it is capable of promoting the lateral bundling of FtsZ protofilaments (Gueiros-Filho and Losick, 2002; Low *et al.*, 2004; Small *et al.*, 2007). In a recent paper, Monahan and co-workers (Monahan *et al.*, 2009) have shown that a temperature-sensitive mutant of *ftsZ* which lacks the capability to form lateral associations and filaments is viable when ZapA is overproduced. It is therefore assumed that ZapA confers stability to the cell division machinery. Concurrently with ZapA, EzrA is another protein co-localizing with the Z-ring (Gamba *et al.*, 2009; Levin *et al.*, 1999). EzrA is a membrane protein that is localized throughout the membrane but appears at the division site together with FtsZ (Levin *et al.*, 1999). It has a positive impact on Z-ring formation since disruption of *ezrA* expression results in a longer cell length and filamentation (Chung *et al.*, 2004). However, it is a negative regulator of FtsZ assembly. Contrary to ZapA, when EzrA is not produced, cells are able to divide at lower FtsZ concentrations and also form mislocalized Z-rings (Levin *et al.*, 1999). Moreover, the effect of *minCD* overproduction can be counteracted by disruption of *ezrA* (Levin *et al.*, 2001). Additionally to its role during Z-ring formation, EzrA cooperates with GpsB to shuttle PBP 1, a protein involved in septum biogenesis, in and out of the septal position (Claessen *et al.*, 2008). Another important protein for Z-ring assembly is SepF. The mechanism of its function is as yet unclear since the data indicate that it has a dual role. Early in division, SepF apparently assists FtsA in tethering the Z-ring to the membrane because when SepF is overexpressed, it is able to take over the function of FtsA (Ishikawa *et al.*, 2006). *In vitro*, SepF forms large polymeric rings, and stacks FtsZ protofilaments into long tubular structures (Gundogdu *et al.*, 2011). SepF is also required for normal septum formation since its lack results in aberrant septa (Hamoen *et al.*, 2006). None of the mentioned proteins are individually

essential, however, strains carrying double deletions of *sepF* and *ezrA* or *ftsA* are not viable (Gundogdu *et al.*, 2011; Ishikawa *et al.*, 2006).

The timing of the Z-ring assembly and its midcell localization are essential for efficient septation. At least two known systems direct the Z-ring to the midcell position; nucleoid occlusion and the *min* systems. A nucleoid occlusion protein, Noc, was observed to bind specific regions at the DNA covering both chromosomal arms, with the exception of the region around chromosomal terminus (Wu *et al.*, 2009). *In vivo*, the fluorescent fusion protein Noc-YFP localizes to the nucleoid region omitting the terminus region. It seems that the protein is dynamic since the fluorescence signal moves over time (Wu *et al.*, 2009). The mechanism of how exactly it fulfils its role as an inhibitor of cell division remains so far unclear (Wu *et al.*, 2009). Cells lacking *noc* are more prone to bisect their chromosomes under certain stress conditions, e.g. disruption of the *min* system (Wu and Errington, 2004). The *min* system in *E. coli* has been shown to oscillate from pole to pole, however, the components of *B. subtilis min* seem to be more static (Hu and Lutkenhaus, 1999; Juarez and Margolin, 2010). The *min* system effector, MinC, interacts with FtsZ and inhibits FtsZ assembly (de Boer *et al.*, 1989). MinC is activated by MinD (Cordell *et al.*, 2001; Hayashi *et al.*, 2001; Sakai *et al.*, 2001). In *B. subtilis* the determinant of *min* localization is DivIVA protein that localizes primarily to poles and late in the division to the newly formed septa, presumably because it has a preference for curved membranes (Hamoen and Errington, 2003; Lenarcic *et al.*, 2009). DivIVA binds MinJ, which is recognized by the MinCD complex (Bramkamp *et al.*, 2008; Patrick and Kearns, 2008). As a result, MinC localizes predominantly to the cell poles.

Interestingly, ZapA overexpression suppresses the cell division block induced by MinC overproduction. This further supports the idea that ZapA is a positive regulator of Z-ring assembly, however a *zapA* deletion does not cause any detectable phenotype and it is unclear whether this is because other proteins take over the function of ZapA or complement it. The aim of this project was to search for such cell division proteins. To do this we used the newly developed synthetic lethal screening system for *B. subtilis* (Claessen *et al.*, 2008). This type of a genetic screen has firstly been used in yeast (Bender and Pringle, 1991), and also became available for *E. coli* (Bernhardt and de Boer, 2004) and *B. subtilis* (Claessen *et al.*, 2008). Central to the synthetic lethal screen is an unstable plasmid pLOSS*, that is easily lost from the cells. To identify mutations that would be synthetically lethal in combination with a *zapA* mutation, *zapA* was

cloned into the pLOSS plasmid and introduced into a strain carrying a chromosomal deletion of *zapA*. Subsequent transposon mutagenesis resulted in some mutations that were synthetically lethal with Δ*zapA* and as a result, these cells retained the plasmid and could be detected by blue/white selection since the plasmid carries a *lacZ* marker. Using this synthetic lethal screen, we identified the gene *yvcL*. Double deletion of *yvcL* and *zapA* led to a strong filamentation phenotype of *B. subtilis* cells. Sequence analysis revealed that the protein is conserved amongst Gram-positive bacteria and is homologous to *whiA* of *Streptomyces coelicolor*. In this bacterium, deletion of *whiA* leads to a sporulation defect, supposedly because of an inability to form Z-rings (Ainsa *et al.*, 2000; Flardh *et al.*, 1999). It is assumed that WhiA acts as a transcriptional regulator, but the exact function of WhiA is unclear. We set out to investigate the function of YvcL in *B. subtilis* and found that a *yvcL* deletion is lethal in combination with mutations in the cell division genes *ezrA*, *minCD* or *noc*, suggesting that it constitutes a novel component of the cell division machinery in *B. subtilis*.

3.2 Results

3.2.1 Identification of YvcL in a synthetic lethal screen

In the synthetic lethal screen developed for *B. subtilis*, the gene of interest is deleted from the chromosome and placed on the segregationally instable plasmid pLOSS* (for Lethal or Synthetic Sick) (Claessen *et al.*, 2008). Subsequently, a random mutagenesis with the TnYLB-1 (pMarB) transposon is performed (Le Breton *et al.*, 2006). When the transposon disrupts a gene that is lethal when *zapA* is not present, the pLOSS-ZapAB plasmid has to be maintained in the cell to confer viability. pLOSS* also harbours a constitutively expressed *lacZ* reporter so the presence of the plasmid can easily be detected on X-gal plates.

3.2.1.1 Construction of strains for the synthetic lethal screen

ZapA is encoded in an operon with *yshB* (Gueiros-Filho and Losick, 2002). Only ZapA is involved in FtsZ polymerization and nothing is known about the function of YshB. Therefore, the complete *zapA-yshB* operon, including the promoter region, was cloned into pLOSS* resulting in pLOSS-ZapAB. For the screen a strain (KS6) was used in which the complete *zapA-yshB* operon was replaced by a tetracycline resistance marker (Feucht and Errington, 2005). The strain used for the screen (KS50) also contained a deletion in the *B. subtilis lacA* gene (D. Claessen, unpublished), which prevents false-positives that activate the endogenous β-galactosidase (encoded by chromosomal *lacA*) and would thus interfere in the blue-white screen.

3.2.1.2 Δ*zapA* is synthetically lethal with Δ*yvcL*

After transposon mutagenesis with transposon TnYLB-1 (Le Breton *et al.*, 2006), about 60,000 colonies were screened for increased blue colour on X-gal plates. 65 colonies were selected and checked by backcrossing isolated chromosomal DNA into the parental strain KS50. We found four mutants that formed a mixture of normally-sized blue colonies and small white colonies that seemed to have lost the plasmid (Fig. 3.1C, arrow). When a Δ*zapA* mutant was transformed with chromosomal DNA from these

four clones, only very small colonies were formed after 48 hours and the cells from these colonies were very filamentous and showed increased cell lysis (Fig. 3.1B, F). This phenotype suggests a major defect in cell division. However, when a wild type background was transformed with the mutant DNAs, normal colonies were obtained and cells looked normal (Fig. 3.1A, E). When the transposon insertion sites of these four strains were mapped by reversed PCR, all transposons had inserted in the gene *yvcL*. Two clones had inserted at bp positions 171 and the other at bp 459 and 481bp (full length *yvcL* gene n = 948 bp).

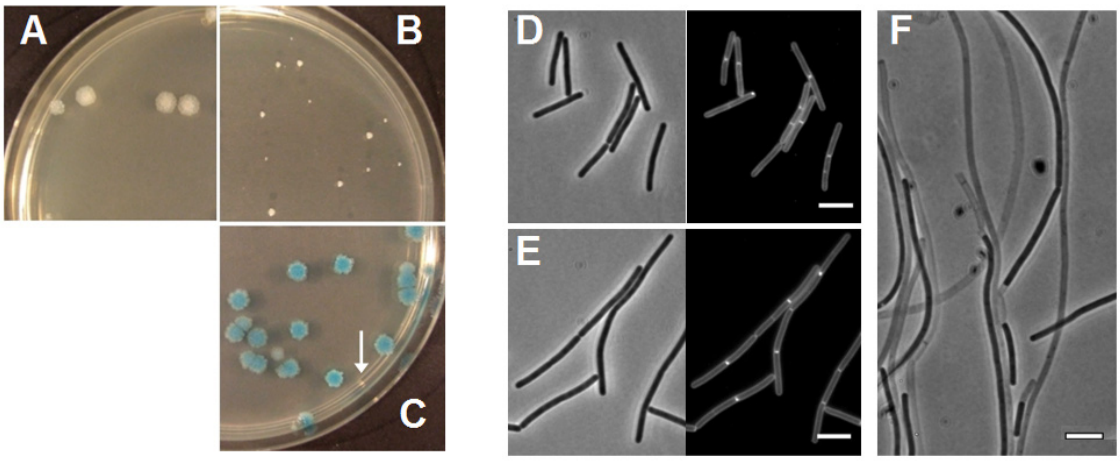

Fig. 3.1 Double deletion of *yvcL* and *zapA* results in a division defect
(**A-C**) Backcross of chromosomal DNA from a successful candidate from the synthetic lethal screen into (**A**) wild type cells (KS2), (**B**) Δ*zapA* (KS6), and (**C**) parental strain Δ*zapA-yshB* Δ*lacA* pLOSS-ZapAB (KS50). The arrow indicates a small white colony that has lost the plasmid. Phenotypes of (**D**) wild type, (**E**) Δ*yvcL* and (**F**) Δ*yvcL* Δ*zapA-yshB*. Membranes were stained with FM5-95. Scale bars 5µm.

3.2.2 Excluding polar effects

yvcL is the fourth gene in an operon consisting of six genes (Fig. 3.2A). The operon includes genes *yvcI*, *yvcJ*, *yvcK*, *yvcL*, *crh* and *yvcN*. The genes *yvcI* and *yvcN* encode proteins of an unknown function. YvcJ was shown to be involved in the regulation of expression of competence genes (Luciano *et al.*, 2009). YvcK plays a role in gluconeogenesis and cell wall maintenance (Foulquier *et al.*, 2011; Gorke *et al.*, 2005) and Crh is involved in catabolite regulation (Warner and Lolkema, 2003). To exclude the possibility that the transposon insertion caused a polar effect on the genes downstream of *yvcL*, an IPTG-inducible P_{spac} promoter was placed either up- or

downstream of *yvcL* (strains KS891 and KS1012, respectively) (Fig. 3.2A). These alleles were introduced into the Δ*zapA* mutant strain. For an efficient repression of the P_{spac} promoter, an extra copy of *lacI* was introduced into the *aprE* locus using plasmid pAPNC213 (Morimoto *et al.*, 2002). As seen in Fig. 3.2B, only the Δ*zapA* strain with P_{spac} upstream of *yvcL* grew poorly and showed a filamentous phenotype without IPTG (Fig. 3.2E). Thus, the synthetic phenotype is related to *yvcL* and not an altered expression of the downstream located genes *crh* or *yvcN*.

3.2.3 Phenotypic characterization of the *yvcL* mutant

To further confirm that the *yvcL* gene disruption caused by the transposon insertion was responsible for the observed phenotype, we constructed a markerless *yvcL* mutant (KS696) that contained a stop codon at 32 bp of the coding region and also rendered the open reading frame out of frame (see Materials and Methods). Cells of this *yvcL* mutant are significantly longer than wild-type cells ($p<0.001$) (Fig. 3.3A, B). Furthermore, they grow slower than wild type cells in LB or in competence (SMM+) and CH medium (Fig. 3.3C and data not shown). This phenotype was comparable to transposon mutants acquired from the synthetic screen, and other two mutants we constructed (strains KS207 and KS400, data not shown).

It has been shown that *yvcL* of *Streptomyces coelicolor* (called *whiA*) and *Streptomyces ansochromogenes* (*sawC*) are essential for sporulation (Ainsa *et al.*, 2000; Flardh *et al.*, 1999; Xie *et al.*, 2007). To test whether YvcL plays a role in sporulation in *B. subtilis*, we used four different *yvcL* mutants to secure consistent results. *yvcL* mutants were grown in DSM medium, a nutrient-limiting sporulation medium (Schaeffer *et al.*, 1965), for 24-hours and sporulation efficiency was determined by counting percentages of phase-bright spores using light microscopy. As seen in Fig. 3.4A, two of the *yvcL* mutant strains (KS207, KS696) sporulated less efficiently, but these changes were statistically insignificant (mutants sporulated with 38-48% efficiency, wild type with 67 %). These mutants contain a pMutin4 insertion in *yvcL*, or a 'silent' markerless *yvcL* mutation, respectively. However, a significant decrease in sporulation efficiency was observed in a mutant *yvcL*::*kan* (KS400) carrying a deletion of the whole *yvcL* gene by substitution with a kanamycin cassette (16%, $p<0.01$) and in a mutant *yvcL*::Tn which contains a TnYLB-1 transposon insertion (39%, $p<0.05$). We think these two strains show a significant decrease due to a polar effect of the antibiotic

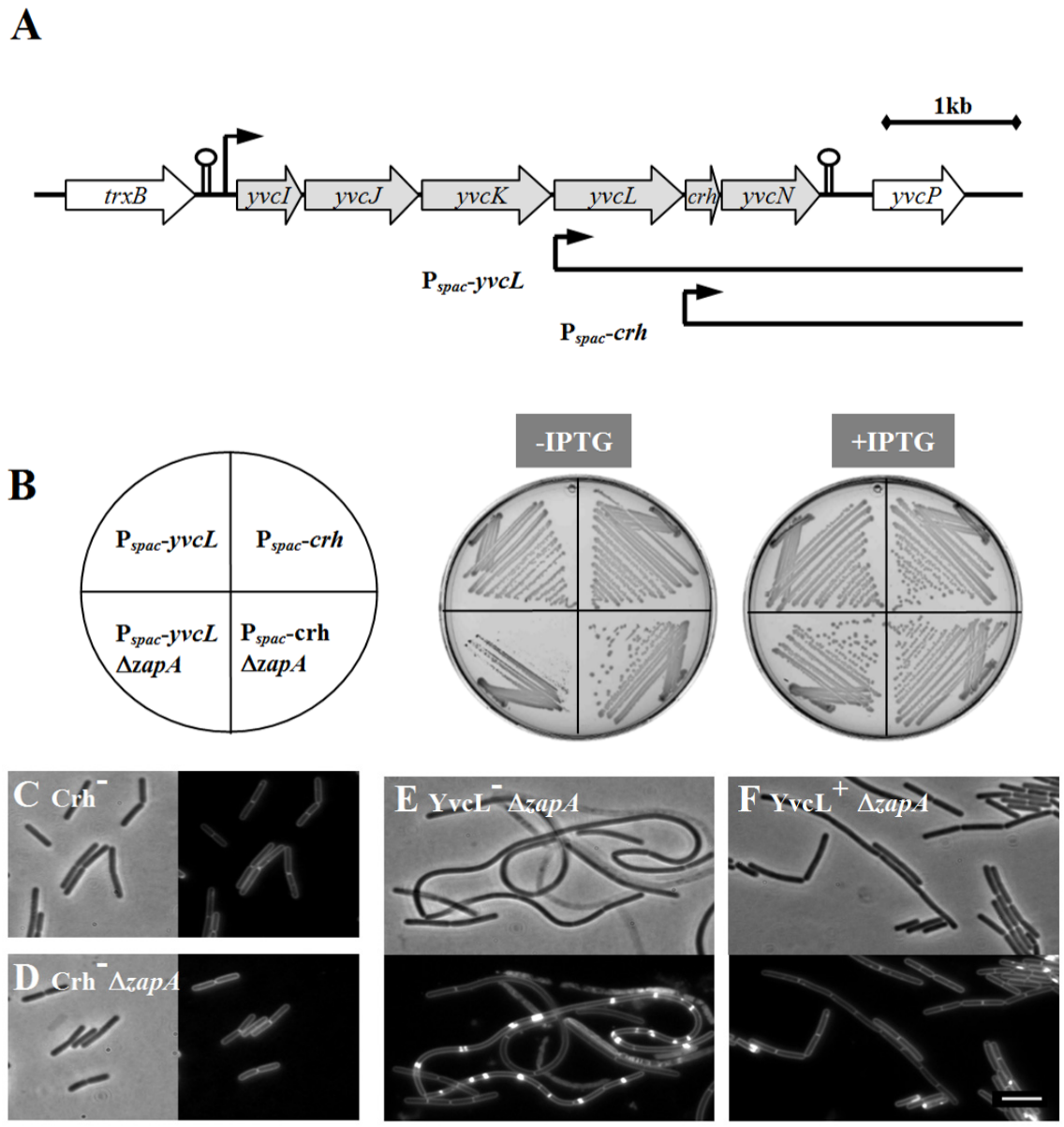

Fig. 3.2 The synthetically lethal phenotype of Δ*yvcL* and Δ*zapA* mutations is not due to polar effects

(**A**) An outline of the *yvcI-N* locus and the conditional mutants in either *yvcL* (P_{spac}-*yvcL*; KS891) or *crh* (P_{spac}-*crh*; KS1012). The strains were constructed by the introduction of an IPTG-dependent P_{spac} promoter up or downstream of *yvcL*. The strains also encode an additional copy of the *lacI* at the *aprE* locus (*aprE*::pAPNC213). (**B**) Test of polar effects. The deletion of *zapA* (*zapA-yshB*::*tet*) was introduced into strains KS891 and KS1012 resulting in strains KS859 and KS1013, respectively. Strains were tested for growth on plates with or without IPTG. Only strain KS859 (P_{spac}-*yvcL* Δ*zapA*) was sensitive for IPTG levels, suggesting the expression of *crh* and the downstream *yvcN* is not important for the growth of a *zapA* mutant. (**C-F**) Phenotypes of depleted strains. Phase contrast and fluorescence microscopic pictures of cells grown with (**F**) or without IPTG (**C-E**) and stained with membrane dye nile red. All strains except for KS859 (E), which is filamentous and lyses, seem to divide efficiently in the absence of IPTG. Strain KS859 recovers when grown on plates with IPTG (F). Scale bar 5 µm.

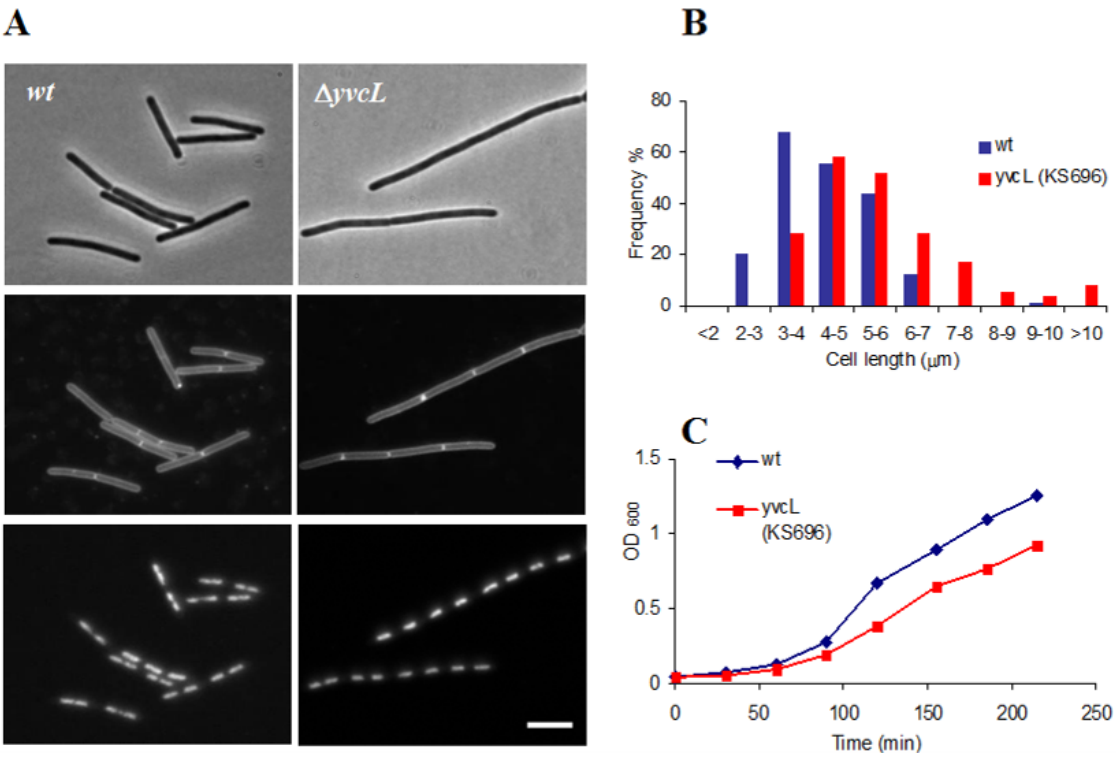

Fig. 3.3 *yvcL* mutation causes slower growth and cell elongation
(**A**) Exponentially growing cells of wild type and *yvcL* mutant (KS696) were stained with nile red to visualize the membranes and with DAPI to visualize nucleoids. From top to the bottom: phase contrast, membrane, and nucleoid stain. Scale bar 5 μm.
(**B**) Histogram of wild type (blue) and *yvcL* (red) mutant cells dimensions.
(**C**) Growth curve of wild type and *yvcL* mutant grown in LB. The lack of YvcL causes slower increase in cell mass (OD_{600}). The same result was observed in CH or SMM+ medium, data not shown.

cassette (kanamycin), as described later for strain KS400 in chapter 4.2 (Microarray). In summary, *yvcL* mutant cells tend to sporulate less well than wild type cells. It may be that they are affected in sporulation indirectly. Nevertheless, it is clear that deletion of *yvcL* in *B. subtilis* does not block sporulation which is in contrast to what has been found in *Streptomyces*. The reason for this may be that *B. subtilis* forms endospores, while *Streptomyces* produce exospores out of sporulation hyphae.

We were also curious when YvcL is expressed in cells. The autoradiograph using α-YvcL-Ab in Fig. 3.4B shows that a band corresponding to YvcL is present in the overnight culture lysate and also in exponentially growing cells and cells in stationary phase. This is in contrast with what has been found for $WhiA^{Sco}$, which is primarily expressed in the aerial hyphae during sporulation (Ainsa *et al.*, 2000).

The aerial hyphae of *Streptomyces* contain rows of nucleoids (>50) that become separated by septal walls during sporulation. The lack of $whiA^{Sco}$, the *yvcL* ortholog, perturbs this process. Possibly, YvcL is involved in septum synthesis in *B. subtilis*. To gain more insight into the morphology of the division septa in a Δ*yvcL* mutant we examined the cells by electron microscopy. As shown in Fig. 3.4C, the septa of Δ*yvcL* mutant cells are comparable to the septa in wild type cells, indicating that YvcL does not play a role in the actual synthesis of the *B. subtilis* division septa.

3.2.4 A Δ*yvcL* Δ*zapA* double mutant is disturbed in Z-ring formation

The Δ*yvcL* Δ*zapA* synthetic effect and the longer cell length of *yvcL* mutants suggest that YvcL is involved in cell division. To examine whether YvcL affects Z-ring formation we introduced the *yvcL* deletion into a strain that contained a *gfp-ftsZ* fusion under the control of an inducible P_{xyl}-promoter at the *amy* locus (J. Sievers, unpublished). Fluorescence microscopy showed similar pattern of the GFP signal in wild-type and *yvcL* mutant backgrounds (Fig. 3.5), although the latter contained slightly less Z-rings per cell.

To test whether Z-rings were still formed when both YvcL and ZapA are absent we used a Δ*zapA* mutant strain that could be depleted for YvcL, using the inducible promoter P_{spac}. This strain (KS754) also contained the pMAP65 plasmid that encodes *lacI* to provide a tighter regulation of the P_{spac} promoter. In the presence of 0.5 mM IPTG strain KS754 grew like wild type with normally localized FtsZ-GFP rings (Fig. 3.6A). When the culture was grown without IPTG, cells became elongated and the

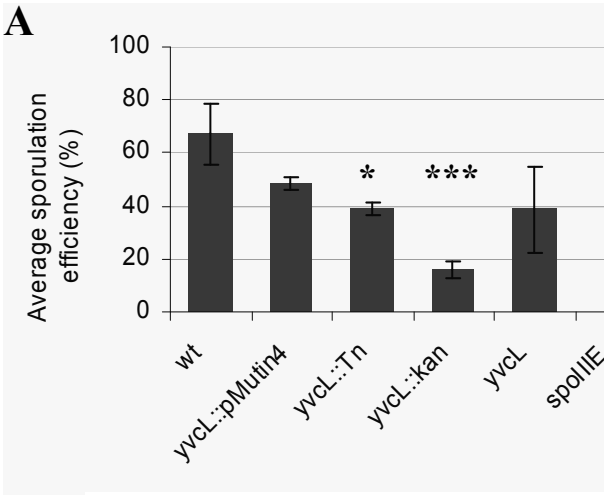

Strain	Average sporulation efficiency ± SD
KS2 (*wt*)	67.1 ± 11.5
KS207 (*yvcL*::pMutin4)	48.2 ± 2.5
KS267 (*yvcL*::*Tn*)	39.2 ± 2.4
KS400 (*yvcL*::*kan*)	16.1 ± 3
KS696 (*yvcL*)	38.8 ± 16.3
KS383 (*spoIIIE*)	0 ± 0

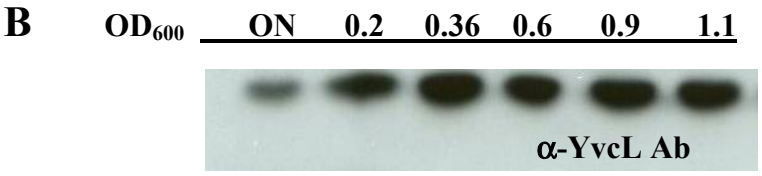

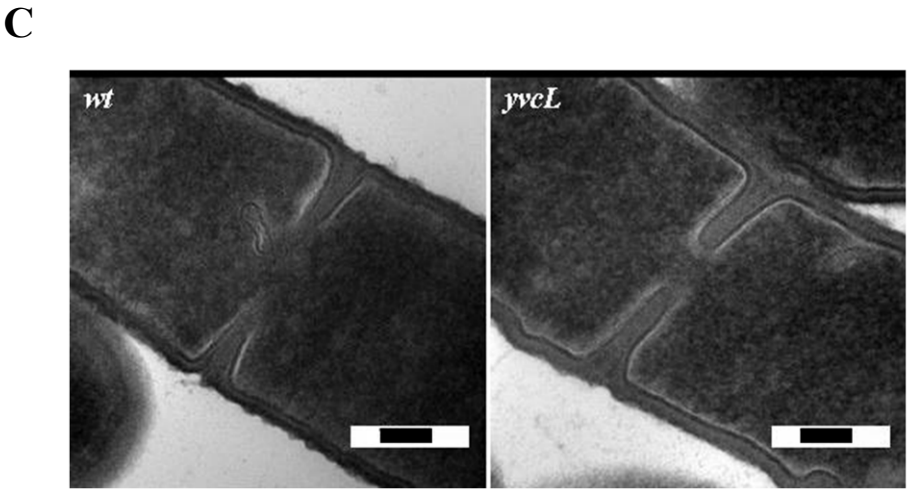

Fig. 3.4 Phenotype of *B. subtilis yvcL* mutants
(A) Sporulation efficiency. Sporulation was induced in DSM medium for 24 hours. The percentage of phase-bright spores was counted using light microscopy in two biological and two technical replicates. More than 800 cells per experiment were counted. The results suggest that *yvcL* mutant does sporulate less well than a wild type. In case of strains KS400 ($p<0.01$) and KS267 ($p<0.05$) the sporulation efficiency differs significantly, which is indicated by asterisks. (**B**) Detection of YvcL in cell lysates using Western blot analysis (α-YvcL-Ab). The OD_{600} of cell cultures used for sample preparation is indicated on top of the autoradiograph. ON = overnight culture. YvcL is present throughout the growth cycle. (**C**) Transmission electron microscopy of *yvcL* mutant cells. Exponential cells of wild type and KS400 (*yvcL*::*kan*) were prepared for transmission electron microscopy as described in Materials and Methods. We have not observed any noticeable difference in the morphology of the septum within two independent experiments. Scale bars 100 nm.

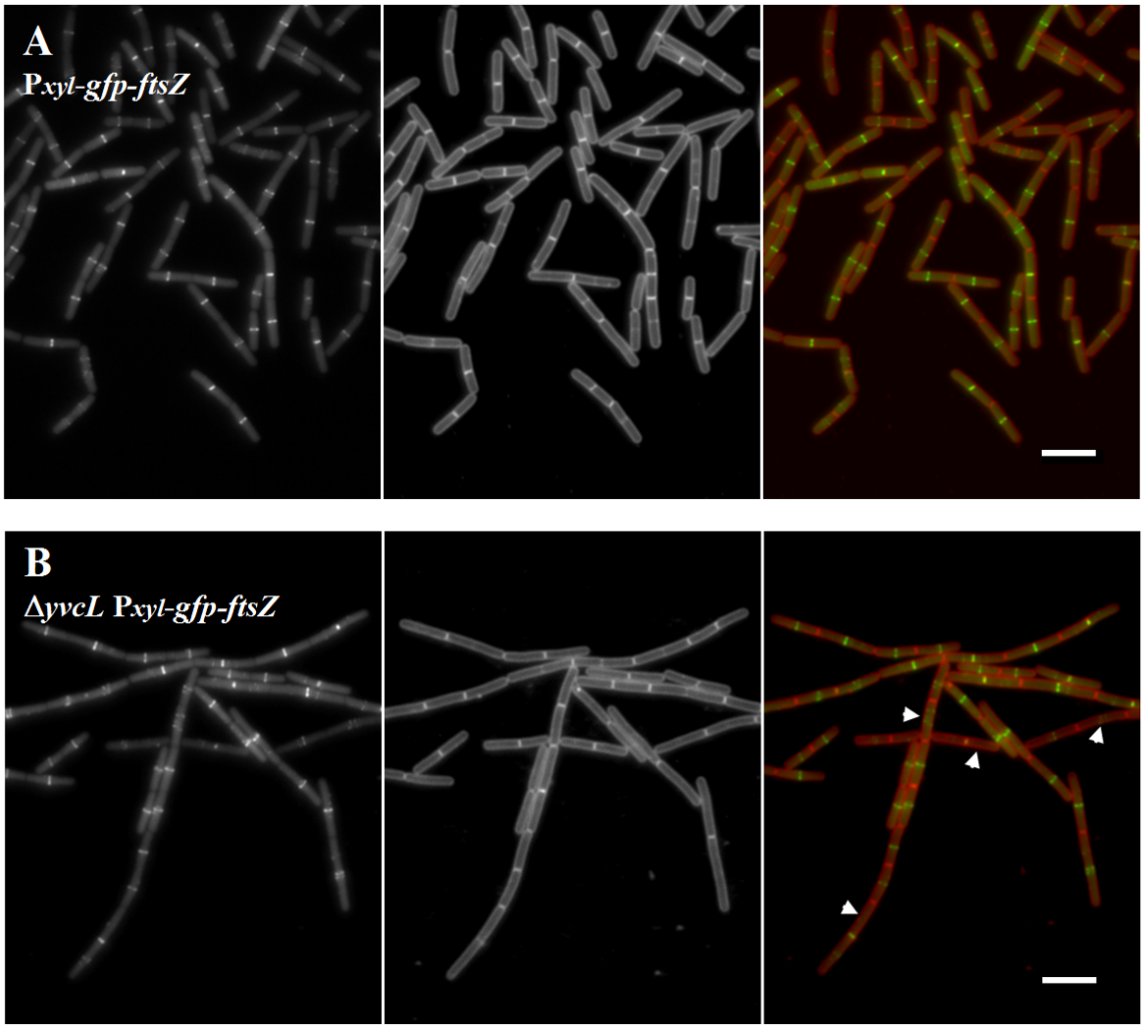

Fig. 3.5 GFP-FtsZ localization in a *yvcL* mutant
Exponentially growing cells of (**A**) KS384 (*amy*E::P_{xyl}-*gfp-ftsZ*) and (**B**) KS745 (Δ*yvcL amy*E::P_{xyl}-*gfp-ftsZ*) were induced (0.05% xylose) for two hours. From left to the right, GFP, membrane (stained with nile red) and the overlay of both GFP (green) and membrane (red) channels. The localization of GFP-FtsZ is not very impaired in a *yvcL* mutant, although there is a ~13% decrease in the occurence of Z-rings. Arrowheads point towards incomplete Z-rings or cells lacking Z-rings. Scale bars 5 µm.

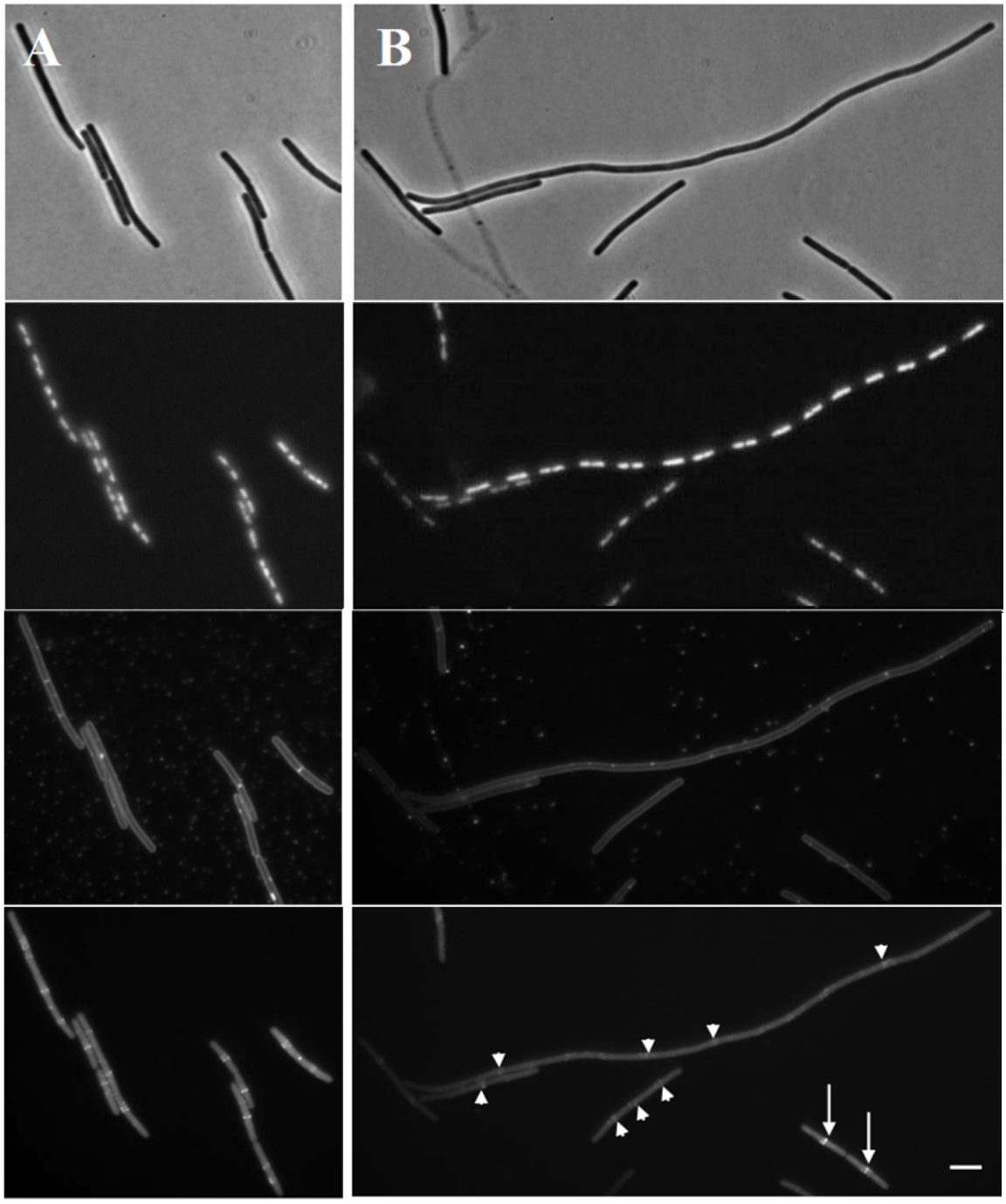

Fig. 3.6 Localization of GFP-FtsZ in Δ*zapA-yshB* cells depleted of YvcL
An overnight culture of strain KS754 (Δ*zapA yvcL*::P_{spac}-*yvcL amy*E::P_{xyl}-*gfp-ftsZ* pMAP65(*lacI*)) was washed and grown with (**A**) or without 0.5 mM IPTG (**B**). From top to bottom: phase contrast, DNA stain (DAPI), membrane stain (nile red), and GFP fluorescence. Cells depleted of YvcL do not form septa. The weak localization of GFP-FtsZ (arrowheads) suggests that FtsZ has difficulties forming functional Z-rings (B, arrowheads). In some cells, Z-rings are formed, presumably due to incomplete depletion of YvcL (arrows). Scale bar 5 μm.

number of Z-rings strongly decreased and they became irregular in appearance (Fig. 3.6B). Apparenly, the filamentation of a Δ*yvcL* Δ*zapA* double knockout results from a defect in Z-ring formation, suggesting that YvcL is involved in an early step in the cell division process.

3.2.4.1 FtsZ concentration sensitivity

The intracellular FtsZ concentration is strictly regulated (Weart and Levin, 2003) and changes in the FtsZ concentration can inhibit division (Dai and Lutkenhaus, 1992). If YvcL is required for the polymerization of FtsZ into a Z-ring, it is likely that a *yvcL* mutant will be sensitive for low FtsZ concentrations. To test this, we introduced an IPTG-inducible *ftsZ* allele into the *yvcL* mutant (strain KS748). Serial dilutions of exponentially growing cultures were spotted on NA plates containing different IPTG concentrations. In agreement with previous findings (Gueiros-Filho and Losick, 2002), a Δ*zapA* mutant is very sensitive to reduced FtsZ levels (Fig. 3.7). The Δ*yvcL* mutant was clearly less sensitive than the Δ*zapA* mutant; however, compared to the wild type the size of the colonies was strongly reduced. These data provide further evidence that YvcL plays a role in cell division in *B. subtilis* but yet it is unclear whether this has to do with a direct effect on FtsZ activity.

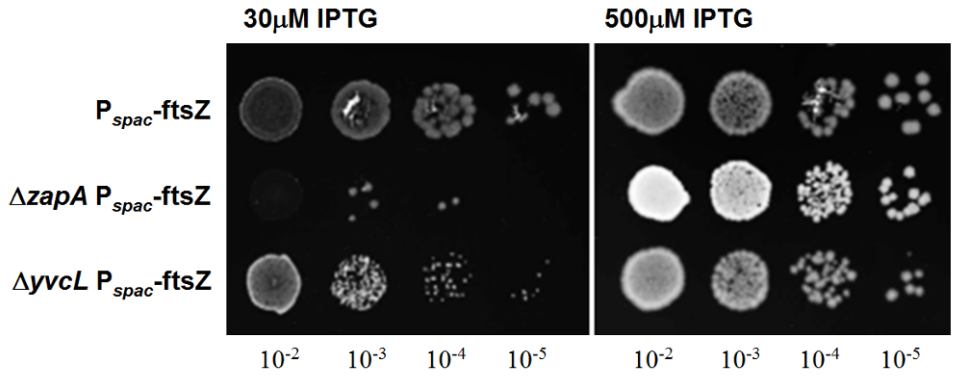

Fig. 3.7 A *yvcL* mutant displays increased sensitivity to low FtsZ concentrations.
Strains KS268 (P_{spac}-*ftsZ*), KS162 (Δ*zapA* P_{spac}-*ftsZ*) and KS748 (Δ*yvcL* P_{spac}-*ftsZ*) were tested for sensitivity to low FtsZ concentration. The cell cultures were grown with 0.2 mM IPTG, and after reaching OD_{600}~0.5, 10 µl volumes of 10-fold serial dilutions were spotted on NA plates supplemented with 30 µM or 500 µM IPTG. While 30µM IPTG is sufficient for growth of the wild type background strain, the Δ*zapA* background is unable to grow, which is in agreement with published data (Gueiros-Filho and Losick, 2002). The growth of *yvcL* mutant is impaired at low FtsZ concentration. Growth of all strains is recovered on plates with 500 µM IPTG.

The Δ*zapA* background strain forms dense colonies on NA with 500 µM IPTG. This was a constant feature of Δ*zapA* mutant colonies (Δ*zapA*::*tet*, strain KS6). We noticed that this strain grew faster than wild type (in liquid LB medium) and that is why the colonies have such a morphology.

If YvcL influenced polymerization of FtsZ into the Z-ring, it might be that overexpression of FtsZ would rescue the filamentation of a Δ*yvcL* Δ*zapA* mutant. To examine this, an extra copy of *ftsZ* driven by the P_{xyl} promoter (Kawai and Ogasawara, 2006), was introduced into strain KS859 that carries a deletion in *zapA* and a conditional *yvcL* mutation. The resulting strain KS1077 was grown on NA plates supplemented with increasing concentrations of xylose. As shown in Fig. 3.8, increasing FtsZ (xylose) concentration stimulates colony formation in the conditional *yvcL* Δ*zapA* mutant (Fig. 3.8A, right panel), although the colonies are small compared to the single *yvcL* or single *zapA* mutants. When examined by microscopy, cells looked normal at high xylose concentrations (Fig. 3.8B). Since *ftsZ* overexpression partially recovers the Δ*yvcL* Δ*zapA* phenotype, this suggests that YvcL is important for Z-ring formation. On the other hand, as the growth rate is still decreased, it implies that YvcL is also important for other process than Z-ring formation.

3.2.5 YvcL is important also for growth of other cell division mutants

The results so far suggest that YvcL affects an early step in cell division but it is not yet clear whether the protein regulates FtsZ assembly. To gain a better idea of the function of YvcL in cell division we combined a *yvcL* deletion with other cell division mutants. When the Δ*yvcL* strain (KS207) was transformed with chromosomal DNA from an *ezrA*, *minCD*, *noc* or *minJ* mutant, the resulting transformants formed tiny colonies (data not shown) and in case of *minJ*, no transformants were acquired. Microscopic analysis of cells from these colonies showed very filamentous cells and substantial lysis (Fig. 3.9, D-F). This phenotype is similar to the Δ*yvcL* Δ*zapA* double mutant. EzrA, MinCD and Noc have a negative effect on FtsZ polymerization (de Boer *et al.*, 1989; Haeusser *et al.*, 2004; Wu *et al.*, 2009), whereas ZapA stimulates Z-ring formation (Gueiros-Filho and Losick, 2002). The data clearly suggest that YvcL influences the activity of FtsZ, but it is not a simple negative or positive regulatory role.

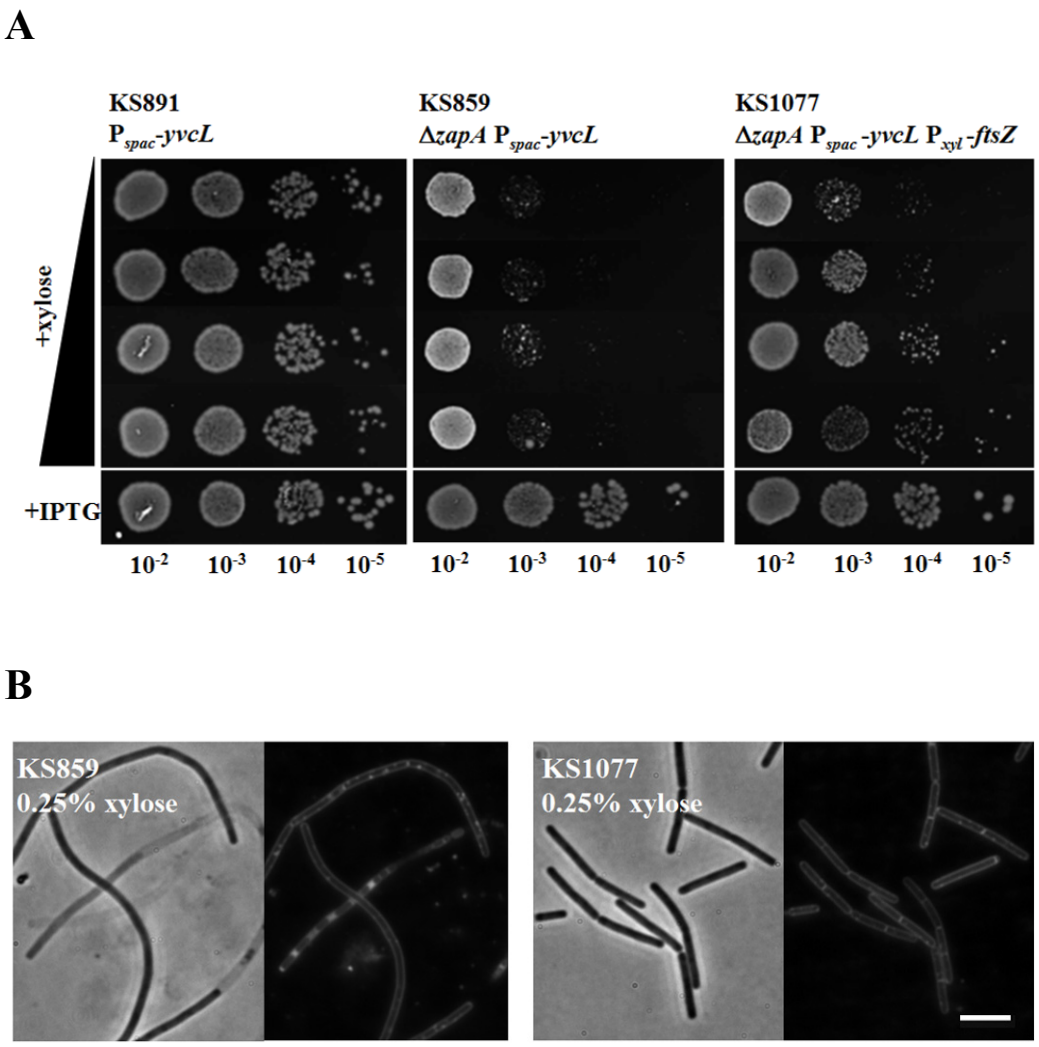

Fig. 3.8 FtsZ overexpression partially suppresses a Δ*yvcL* Δ*zapA* double mutant phenotype

(**A**) Strains KS891 (P_{spac}-*yvcL*), KS859 (Δ*zapA* P_{spac}-*yvcL*), and KS1077 (Δ*zapA* P_{spac}-*yvcL* P_{xyl}-*ftsZ*) were grown in the presence of IPTG and serial dilutions were spotted on NA agar plates with 0, 0.05, 0.125 and 0.25% xylose and with only IPTG. Strain KS859 is almost unable to grow without IPTG. However, overexpression of FtsZ from P_{xyl}-*ftsZ* in an isogenic strain (KS1077) results in an improved colony formation (right panel). (**B**) Phase contrast and membrane stain images of cultures grown on 0.25% xylose plates. FtsZ overexpression in strain KS1077 leads to amelioration of the Δ*yvcL* Δ*zapA* filamentous phenotype. Cells were stained with FM5-95. Scale bar 5 µm.

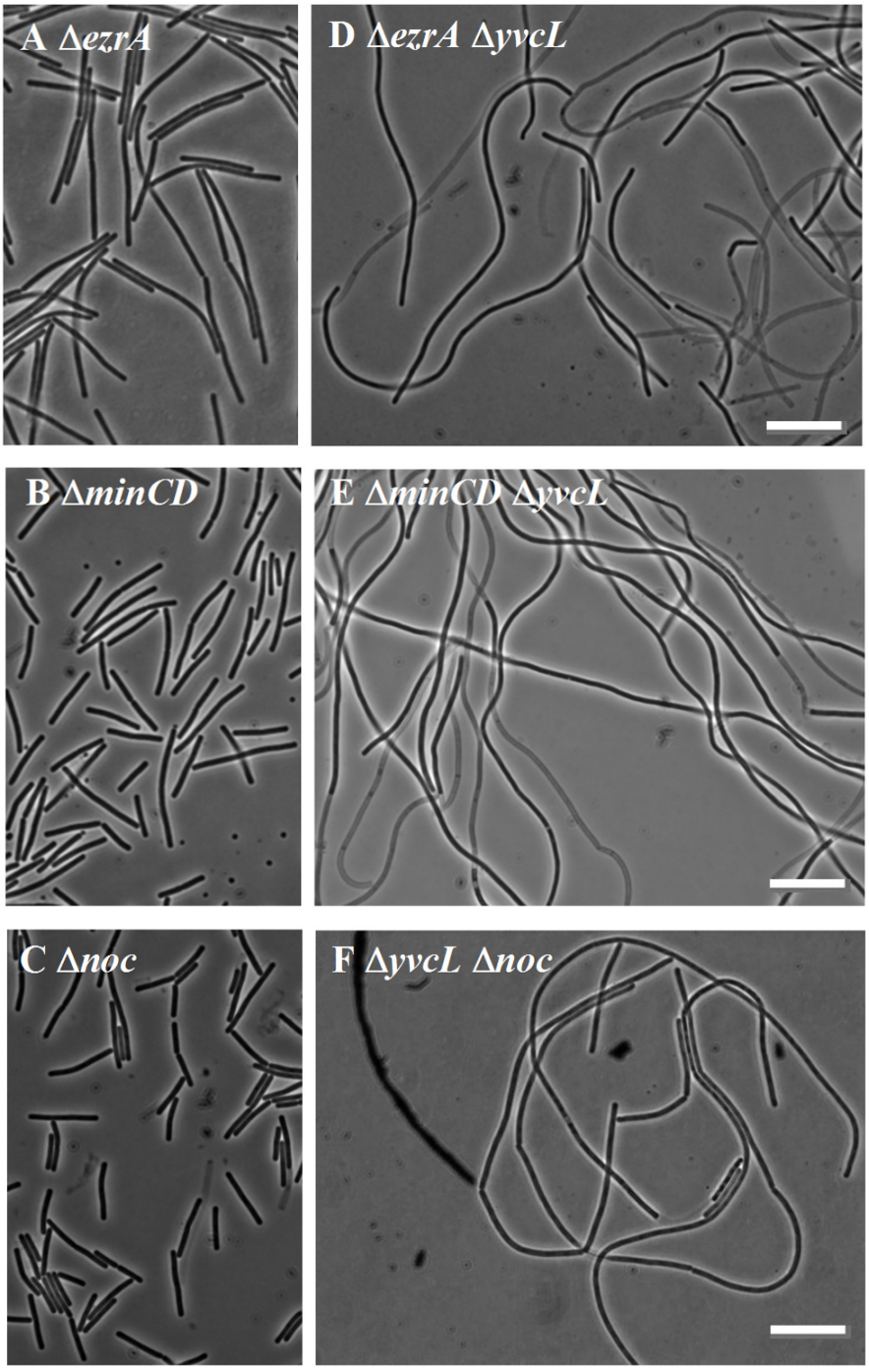

Fig. 3.9 Deletion of *yvcL* in combination with other early cell division proteins leads to cell filamentation
Single cell division mutants (**A**) *ezrA*::*tet* (KS44), (**B**) *minCD*::*kan* (KS338), (**C**) *noc*::*spc* (KS345) were combined with a *yvcL* deletion (KS207). Only a few minute colonies grew on the transformation plates and the cells were very filamentous. Shown are cells of (**D**) Δ*ezrA* Δ*yvcL*, (**E**) Δ*minCD* Δ*yvcL*, and **(F)** Δ*noc* Δ*yvcL* double mutants. Scale bars 10 µm.

ZapA and EzrA are early cell division proteins and assemble simultaneously with FtsZ at midcell (Gamba *et al.*, 2009). GpsB and SepF are required for normal septum development (Claessen *et al.*, 2008; Hamoen *et al.*, 2006; Ishikawa *et al.*, 2006) and assemble later at the Z-ring. When a *gpsB* or *sepF* deletion was introduced into a *yvcL* mutant, no obvious effect on growth and cell size was detected (Fig. 3.10), confirming that YvcL functions early in the cell division process.

3.2.5.1 Localization of GFP-FtsZ in Δ*yvcL* double mutants

Since FtsZ is delocalized in the Δ*yvcL* Δ*zapA* double mutant, we were curious whether this also occurred in *yvcL* mutants that lacked *ezrA*, *minCD* or *noc*. To test this we used the same IPTG-inducible *yvcL* strain as previously used (3.2.4), with minor changes (instead of pMAP65, *lacI* copy at the *aprE* locus was used to regulate the expression of *yvcL* in *ezrA* and *minCD* mutant backgrounds). As shown in Fig. 3.11B, Fig. 3.12B and D, in all three mutant strains the cells became filamentous as a result of YvcL depletion and in all cases the Z-rings eventually disappeared.

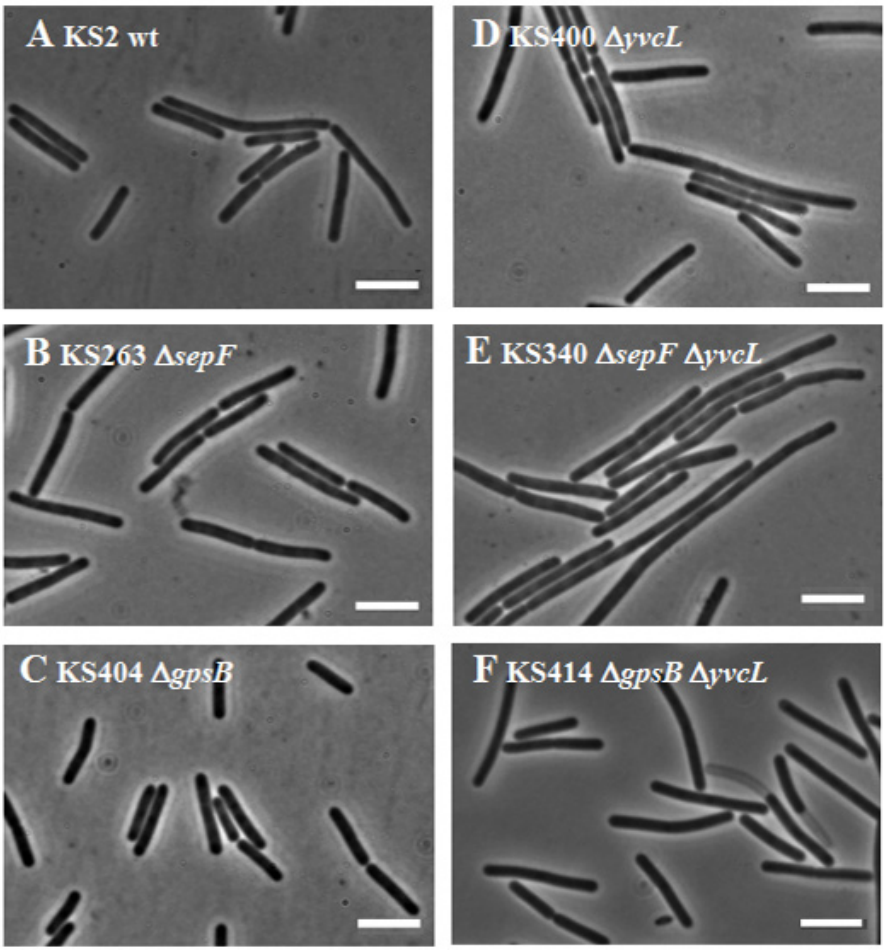

Fig. 3.10 The double mutants Δ*sepF* Δ*yvcL* and Δ*gpsB* Δ*yvcL* do not display a cell division phenotype
The wild type strain, *sepF*, *gpsB* and *yvcL* single mutants (**A-D**) and the double mutants Δ*sepF* Δ*yvcL* and Δ*gpsB* Δ*yvcL* (**E, F**) are not very distinct in their phenotypes. Scale bar 5 µm.

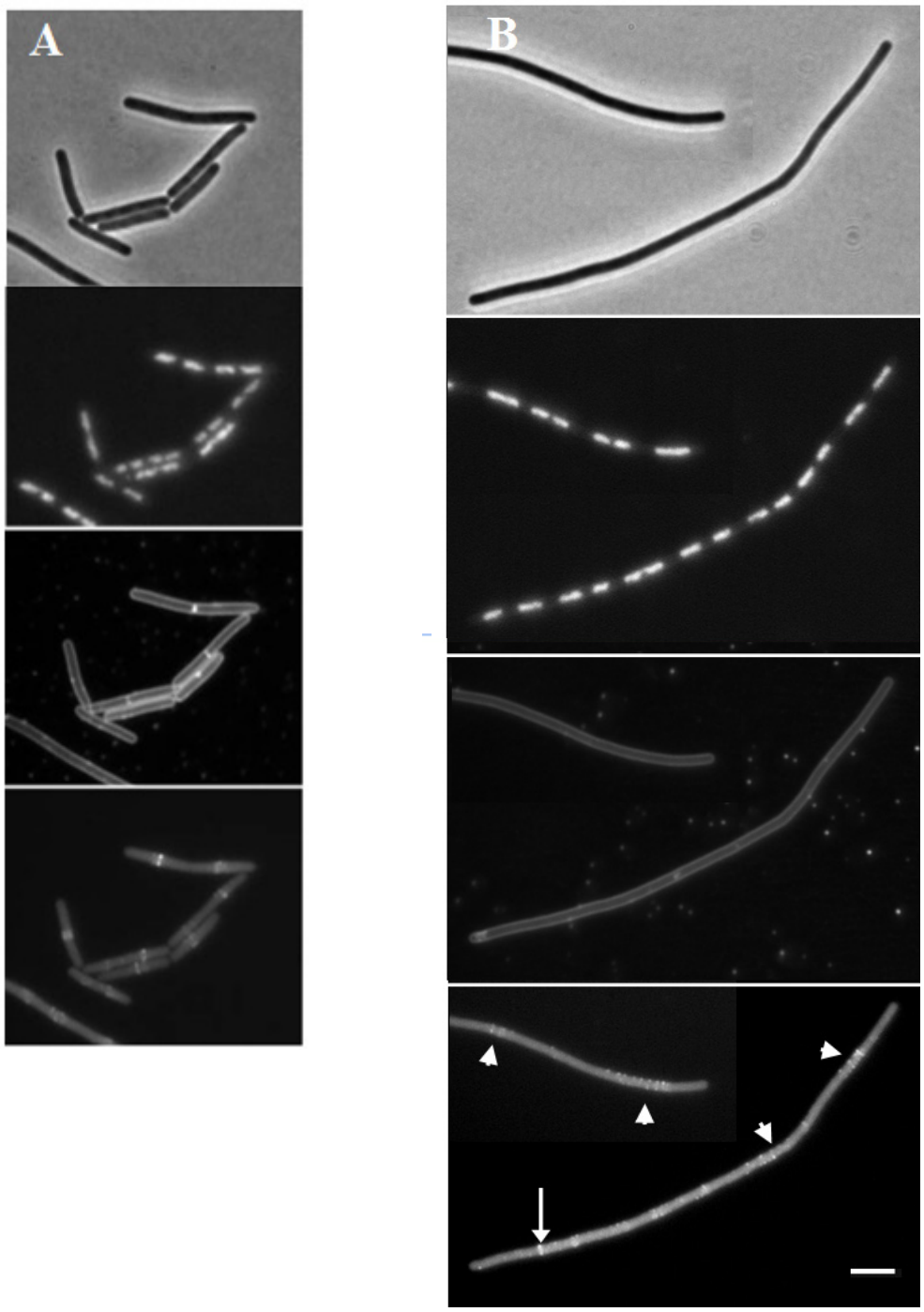

Fig. 3.11 Mislocalization of GFP-FtsZ in a Δ*noc* mutant strain depleted of YvcL

Strain KS755 (Δ*noc yvcL*::P_{spac}-*yvcL amy*E::P_{xyl}-*gfp-ftsZ* pMAP65(*lacI*)) was grown in the presence (**A**) or absence (**B**) of 1 mM IPTG. Without IPTG cells became filamentous as a result of the lack of proper Z-rings (arrowheads). Only a few normally looking Z-rings could be observed (arrow). Scale bar 5 µm.

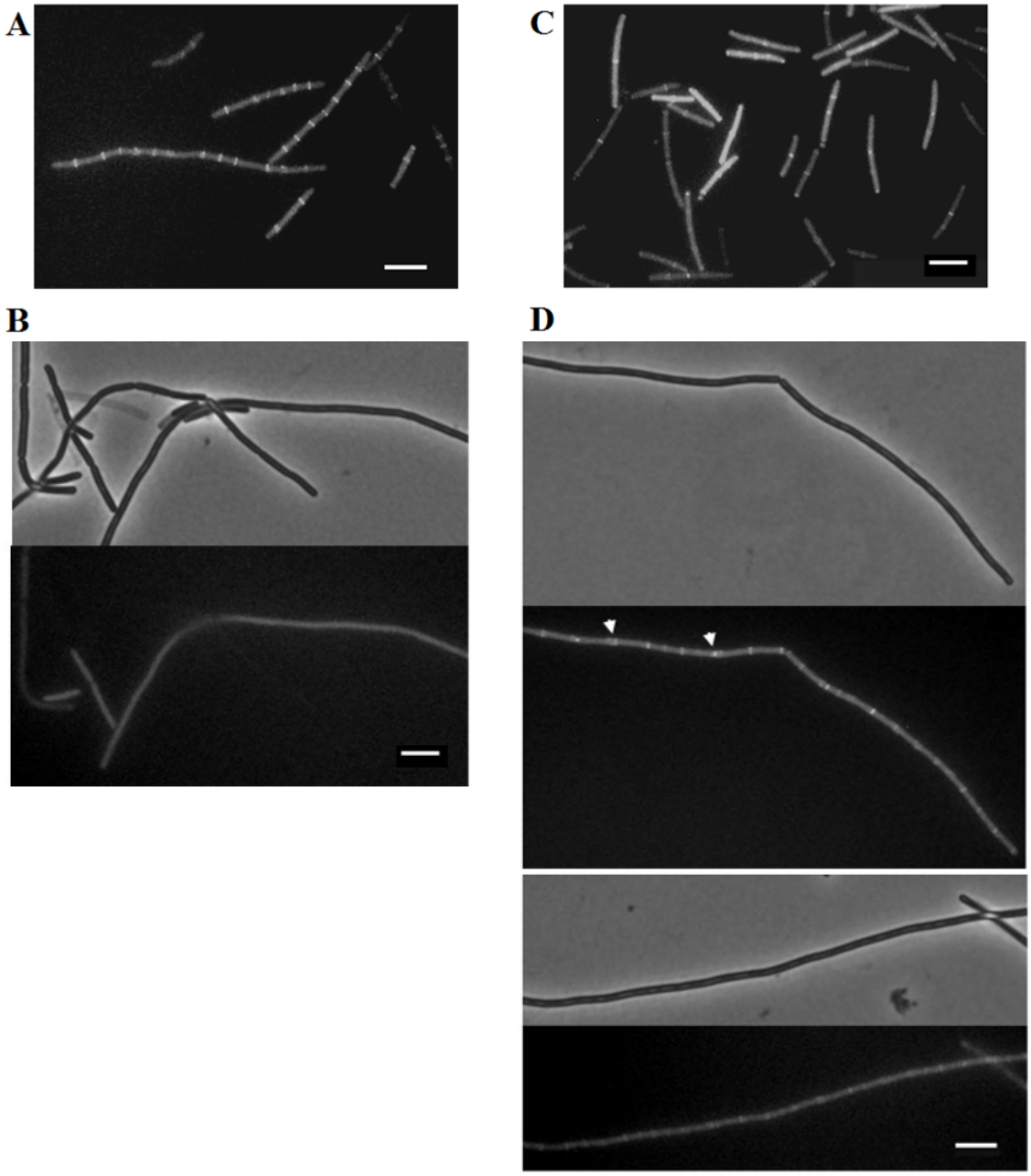

Fig. 3.12 Mislocalization of GFP-FtsZ in Δ*ezrA* and Δ*minCD* mutants depleted of YvcL

Strains KS1098 (**A**, **B**) and KS1099 (**C**, **D**) were used to assess localization of GFP-FtsZ in an *ezrA* or a *minCD* mutant in which YvcL was depleted. Overnight cultures on LB plates supplemented with 0.5 mM IPTG were inoculated into a fresh LB medium with (A, C) or without 0.5 mM IPTG (B, D). The expression of GFP-FtsZ was induced by 0.05% xylose, and the cultures were grown at 30 ºC for two hours before examination by fluorescence microscopy. Arrowheads point toward aberrant GFP-FtsZ structures. Scale bars 10 μm.

3.3 Discussion

We have identified a new cell division regulator in *B. subtilis*; the protein YvcL. *yvcL* and the gene order of its adjacent genes are conserved in Gram-positive bacteria (Ainsa *et al.*, 2000) (Fig. 3.13). In *B. subtilis*, the operon consists of six genes. The first gene, *yvcI*, has been annotated as an uncharacterized nudix hydrolase (BLAST). Nudix hydrolases are enzymes that prevent incorporation of oxidized nucleotides into the DNA during replication (reviewed in McLennan, 2006). The second gene *yvcJ* codes for a protein which can hydrolyze nucleotides, and it somehow stimulates the induction of competence development (Luciano *et al.*, 2009). The third gene, *yvcK*, is essential for normal cell shape when cells are grown on gluconeogenic substrates (Foulquier *et al.*, 2011; Gorke *et al.*, 2005). YvcK was shown to localize in a helical pattern in the cell and acts as an additional cytoskeletal protein besides MreB (Foulquier *et al.*, 2011). The *yvcL* gene (fourth in the operon) is followed by *crh*. Crh is a well known metabolic regulator. In *B. subtilis*, the central catabolite control protein is CcpA (reviewed in Lorca *et al.*, 2005 or Fujita, 2009). CcpA usually binds to DNA at catabolite-responsive elements (CRE) (Hueck *et al.*, 1994; Miwa *et al.*, 2000), and is activated by interaction with phosphorylated HPr or Crh proteins. The phosphorylation is mediated by an HPrK kinase. Crh is a homologue of HPr and is important for cells during growth on media with alternative carbon sources such as glutamate or succinate (Warner and Lolkema, 2003). The protein sequence of YvcN, encoded by the last gene in the operon, shares similarities with arylamine N-acetyltransferases that transfer the acetyl group from Acetyl Coenzyme A on to arylamine. In *Mycobacterium tuberculosis* the deletion of N-acetyltransferase gene causes perturbed cell wall synthesis (Abuhammad *et al.*, 2010; Sim *et al.*, 2008). YvcL is presumably not involved in the production of cell wall material as it retains a rod-shape and its septa look normal. So far we have no evidence that the activity of YvcL is related to that of one of the other proteins encoded by the *yvcI-N* operon. Apart from a slower growth and an increased cell length, Δ*yvcL* showed no serious growth defect in the different media that we have tested (NA, LB±5 µM Mg^{2+}, SMM+, DSM, PAB, data not shown). Furthermore, the *yvcL* mutant forms normal septa as judged by electron microscopy and does not display aberrant cell shapes that would point towards disturbed cell wall synthesis.

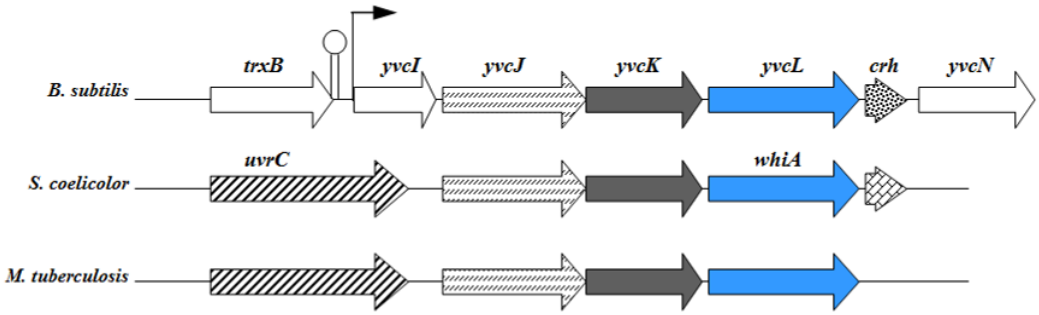

Fig. 3.13 The *yvcL* region
Conservation of the *yvcL* region in different organisms. Similar genes are shown in the same shades. After Ainsa *et al.,* 2000.

YvcL belongs to a conserved family of proteins (Knizewski and Ginalski, 2007) (see phylogram in Fig. 3.14 and also Fig. 3.15) that are assumed to function as transcription factors since they possess a characteristic helix-turn-helix domain similar for sigma-70 family of sigma factors (Kaiser *et al.*, 2009). Despite this structural information, not much is known about the biological activity of the WhiA protein family. The best characterized member of this family of proteins is WhiA from *Streptomyces coelicolor* ($WhiA^{Sco}$). The *whiA* locus has been identified as a sporulation mutation and the name was derived from mutants that formed white colonies, as a result of the inability to synthetize grey sporulation pigment (Chater, 1972). *whiA* is only expressed in the aerial hyphae (Ainsa *et al.*, 2000; Xie *et al.*, 2007) and the sporulation deficiency of a *whiA* mutant appears to be a consequence of the lack of Z-rings and transverse septa in the aerial hyphae that precede spore formation (Flardh *et al.*, 1999; Grantcharova *et al.*, 2005). Western blot analyses revealed that YvcL is expressed during logarithmic and also late stationary phase. Furthermore, sporulation is not blocked in a *yvcL* mutant, which sets YvcL apart from $WhiA^{Sco}$. *B. subtilis* is an endospore former, while *Streptomyces* divide the aerial hyphae into numerous exospores. Actually this is the only time for this organism to form cells containing only one chromosome, since their vegetative mycelia contain many chromosomes and only a few crosswalls (Chater, 2001). The mutants in $whiA^{Sco}$ do not cease longitudinal growth of the aerial hyphae, suggesting $whiA^{Sco}$ is important for the division of these compartments. Furthermore, the lack of Z-ring formation in a $whiA^{Sco}$ mutant strongly resembles the division phenotype of Δ*yvcL* Δ*zapA* (and other) double mutations, and since both proteins share

25% identical and 50% similar amino acid residues we propose to rename *yvcL* as *whiA*, and we will refer to it as *whiA* from here on.

Our data indicate that WhiA is a novel cell division protein. The sensitivity to FtsZ levels of *whiA* mutant cells and the lack of functional Z-rings in division mutants depleted of WhiA suggests that WhiA acts at the level of Z-ring formation. Deletions of cell division proteins with promoting or inhibiting activities during Z-ring assembly have fatal impacts on *whiA* mutant cells, and this suggests that WhiA affects FtsZ assembly indirectly or that the regulation of Z-ring assembly by WhiA is not straight-forward. Nevertheless, WhiA is important for the formation of Z-rings in *B. subtilis*.

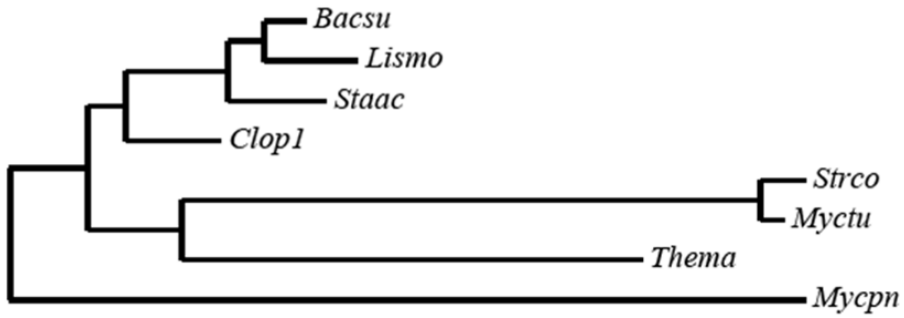

Fig. 3.14 Phylogram of WhiA-like proteins
The aminoacid sequences of WhiA proteins from *Bacillus subtilis (Bacsu), Listeria mo*noc*ytogenetes (Lismo), Staphylococcus aureus (Staac), Clostridium perfringens (Clop1), Streptomyces coelicolor (Strco), Mycobacterium tuberculosis (Myctu), Thermotoga maritima (Thema) and Mycoplasma pneumoniae (Mycpn)* were used to generate a phylogenetic tree using PHYLOGENY.FR programme (Dereeper *et al.*, 2008).

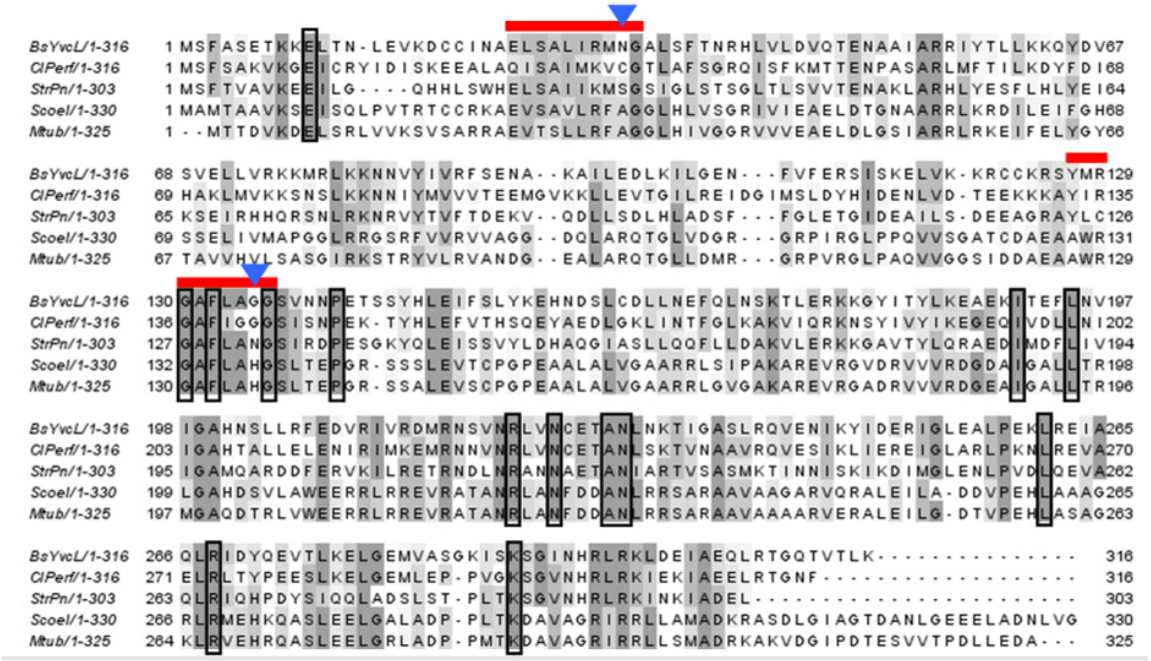

Fig. 3.15 Multiple sequence alignment of WhiA-like proteins
The protein sequences were aligned using ClustalW and the alignment was coloured using JalView programme (Waterhouse *et al.*, 2009). WhiA-like proteins from the following organisms were aligned: BsYvcL, *Bacillus subtilis*; ClPerf, *Clostridium perfringens*; StrPn, *Streptococcus pneumoniae*; Scoel, *Streptomyces coelicolor*; Mtub, *Mycobacterium tuberculosis*. The multiple sequence alignment of the amino acid sequences shows conserved residues in boxes that are invariable. The two LAGLIDADG motifs are indicated by red lining. Blue triangles point towards positions that are occupied in homing endonucleases by acidic residues that are required for DNA cleavage. However, in WhiA-proteins they are absent. After(Kaiser *et al.*, 2009).

Chapter 4

Is WhiA a transcriptional regulator?

4.1 Introduction

It has been suggested that WhiA proteins in *Streptomyces* spp. act as transcriptional regulators (reviewed in Kaiser *et al.*, 2009). During sporulation in these species there is a cascade of different transcriptional factors that regulates this process and $WhiA^{Sco}$ is considered to be one of them (Flardh *et al.*, 1999). An *in vitro* study suggested that $WhiA^{Sco}$ regulates its own expression (Ainsa *et al.*, 2000). Additionally, the crystal structure of WhiA from *Thermatoga maritima* has revealed that the conserved C-terminal domain shows structural similarity to sigma-70 sigma factors (Kaiser *et al.*, 2009) (Fig. 4.1). Because of this WhiA might be a transcription factor and to test this we performed a whole-genome microarray analysis.

Fig. 4.1 Crystal structure of WhiA from *Thermotoga maritima* (Kaiser et al., 2009)
The crystal structure of the full-length $WhiA^{Tm}$ (2.6 Å resolution) shows that the protein consists of a large N-terminal domain with two LAGLIDADG motifs (on the left, see also Fig. 3.15) connected to the C-terminal part by a long stretch of two α-helices. The C-terminal domain shows similarities to sigma-70 factors. The structure accessible under PDB code 3HYI is visualized using the Jmol programme.

4.2 Results

4.2.1 Microarray analysis of the *whiA* mutant

This experiment was performed with a kind help and supervision of Dr. Nigel Sauders and Dr. Richad Capper, Oxford University.

We compared the gene expression profiles of a wild type strain with that of a *whiA*::*kan* mutant (strain KS400). Each microarray slide consisted of three amplicons of 4000 different oligonucleotides covering all annotated open reading frames in the *B. subtilis* genome. The assay was performed, with minor changes, as previously described by Whitehead *et al.*, 2007 (see also Materials and Methods). The cells were grown in LB medium and harvested when they reached an OD_{600}~0.6. RNA was isolated in independent experiments and three slides were prepared. After hybridization the slides were analyzed using the BASE programme (www.cbrg.ox.ac.uk). The results are summarized in Table 4.1.

56 changes in gene expression were detected with a p-value cut-off of 0.001. In 18 cases gene expression decreased and 38 cases were upregulated. The expression of *rtp* was, with 4.64 fold difference, mostly decreased (p=0.0002). RTP is the replication termination protein (Sahoo *et al.*, 1995) that also plays a role in the inhibition of DNA replication during the stringent response (Autret *et al.*, 1997). Two other genes that showed clear differences in gene expression, *crh* and *yvcN*, were likely affected by the the upstream kanamycin resistence cassette used to delete the *whiA*, which reads in the same direction. Crh is involved in catabolite repression (Galinier *et al.*, 1997). We have been able to link some of the other candidate genes to catabolite repression (e. g. *ilvH, lacR, gntZ*), hence the changes in their expression profiles were probably due to Crh overexpression. YvcN is a probable acetyltransferase involved in Acetyl-CoA metabolism but otherwise its function remains unknown. Altogether, 13 of the identified genes are involved in sugar metabolism, 5 in aminoacid metabolism, 10 genes are part of a large ribosomal operon, 2 genes encode secretion proteins, 3 genes encode putative transporters, 3 genes encode proteins with predicted DNA binding motives.

4.2.2 Verification of microarray results using qPCR

To verify the results of the microarray analysis, a quantitative PCR was employed. This time we included a 'clean' *whiA* mutant (KS696) which contains a stop codon at the beginning of its reading frame, so we could correct for the effect of the kanamycin marker. The most relevant fifteen genes from the microarray dataset were tested. As shown in Table 4.2, the expression of most genes is not significantly changed, and if there is a change, it is less than a two-fold. The data is also graphically presented in Fig. 4.2. In strain KS696, the mRNA for *whiA* is present (the functional protein is not produced as judged by α-WhiA western blot analysis and the phenotype of this strain). Surprisingly, *rtp* does not show a significant change in the expression pattern (~2-fold upregulation), and it does not correlate with a clear downregulation found by microarray. In the *whiA* deletion mutant (KS400), *crh* showed a 10-fold increase in expression, however, in a 'silent' mutant the level of expression remained only slightly changed (~90% of the wild type expression level). Although both these changes are significant ($p<0.01$), we conclude that in KS400 the insertion of the kanamycin cassette causes overexpression of downstream genes, whilst in KS696 their expression remains constant or changed only slightly. The second biggest change found with qPCR was identified in *pyrK* expression, which increased about ~4-fold. However, these data do not correspond to the microarray data, and the change is insignificant ($p>0.1$). Both microarray and qPCR results indicate that *ilvA*, *oppA* and *yvyD* are downregulated in *whiA* mutants. These changes are only mild (~2-fold decrease) but in case of *oppA* and *ilvA* they are significant at least in one of the strains.

A Upregulated genes

gene	fold-change
yvcN	7.58
crh	6.49
manA	4.88
rplQ	4.59
yktD	4.08
rpsK	4.02
truA	3.91
ysfC	3.86
rpsM	3.66
rpmD	3.51
yjdF	3.51
rbsC	3.45
ysfD	3.39
yfmQ	3.29
glpK	3.28
ywsB	2.98
gntP	2.96
rbsB	2.94
adk	2.85
ylxM	2.69
tasA	2.65
gntZ	2.63
ctaO	2.59
rpmJ	2.57
ydzA	2.54
ffh	2.53
rpmI	2.44
yrzI	2.43
rplT	2.37
rpsG	2.25
map	2.21
rpoA	2.18
trmD	2.18
ykvJ	2.16
spoI	2.16
mleA	2.1
ydhR	2.05
yheH	2.05

B Downregulated genes

gene	fold-change
yvcL	30.96
rtp	4.64
ilvA	4.59
pyrK	3.84
pyrA	3.71
oppA	3.06
yvyD	3.04
ywaA	2.88
ybbH	2.82
yhaA	2.70
ytxK	2.64
oppC	2.57
ybbI	2.42
ycsG	2.25
ywfH	2.24
serA	2.12
ypmP	2.08
ybbE	2.08

Table 4.1 Microarray analysis of a *whiA* mutant
List of the genes that were found to be up-regulated (**A**) and down-regulated (**B**) in a *whiA*::*kan* mutant (KS400) in a microarray study. Only genes that fulfilled the following criteria are listed: the expression changed in all three microarray slides, it was at least 2-fold, and with the $p<0.001$.

A Genes upregulated in the microarray

gene	fold change		corresponding to MA
	strain KS400	strain KS696	
crh	10.31	0.9	+/-
rplQ	1.4	1.47	-
yktD	1.37	1.36	-
ysfC	1.4	1.39	-
truA	0.86	1.02	-
glpK	0.82	0.94	-
ylxM	0.35	0.47	-

B Genes downregulated in the microarray

gene	fold change		corresponding to MA
	strain KS400	strain KS696	
yvcL	63 000	1.03	+
rtp	0.40	0.45	-
ilvA	1.49	2.13	+
pyrK	0.27	0.26	-
oppA	1.54	2.5	+
yvyD	1.92	2.38	+
ywaA	0.99	1.12	-
ytxK	0.70	0.68	-

Table 4.2 Verification of microarray results using qPCR
Three strains for qPCR analysis were used: wild-type, KS400 (*whiA*::*kan*) and KS696 (clean *whiA* mutant). KS400 was previously used for microarray analysis. Three independent biological replicates were prepared for RNA isolation. After RNA purification and reverse transcription, the corresponding primer pairs were used for quantitative PCR. The qPCR was performed using SybrGreen dye. CP values were calculated and normalized for *ftsZ*. MA=microarray.
Significant change when compared to wild type ($p<0.01$; t-test).

A Genes upregulated in the microarray

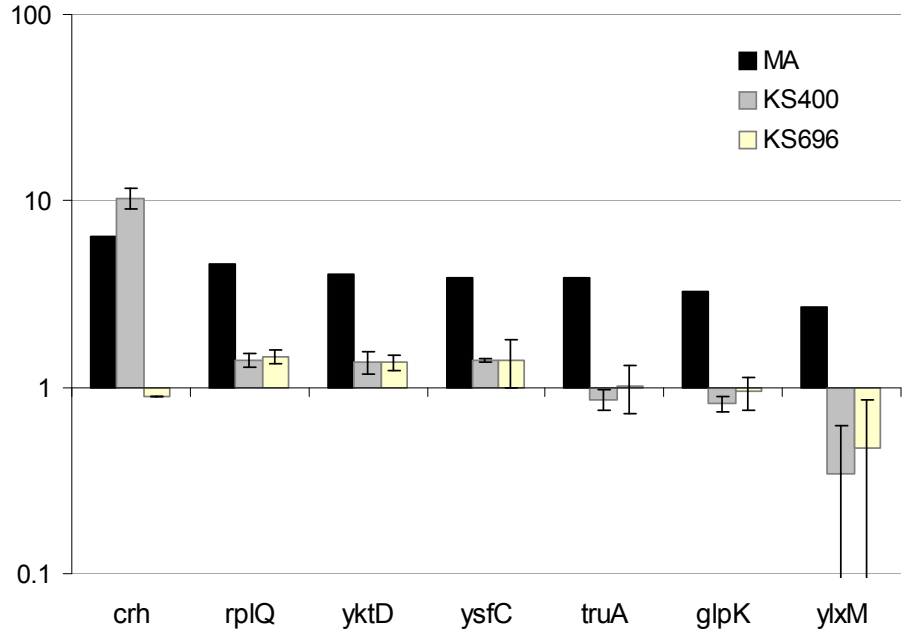

B Genes downregulated in the microarray

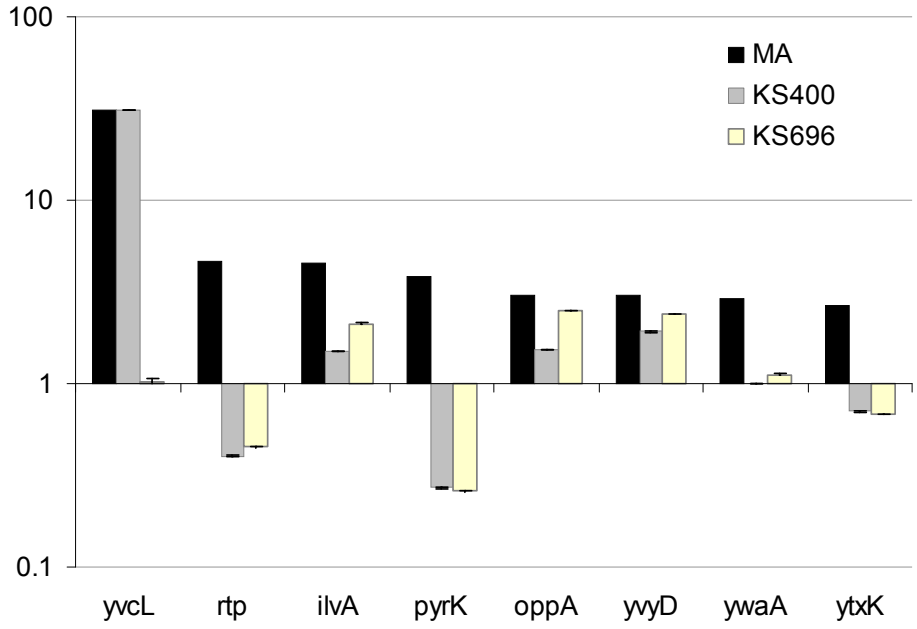

Fig. 4.2 Graphical representation of the verification of microarray data by qPCR.
The mean fold-change values of three independent biological replicates were plotted on the logarithmic y-scale. Scale bars represent standard deviation calculated as of three replicates. MA = microarray readout, KS400 and KS696 = qPCR results. (**A**) Upregulated genes in MA, fold change = increase. (**B**) Downregulated genes in MA, fold change = decrease in expression in *whiA* mutants.

4.3 Discussion

WhiA is a 316 amino acid long protein with a predicted pI of 9.27. The structure of WhiA from *Thermotoga maritima* ($WhiA^{Tm}$) has been solved using X-ray crystallography (Kaiser *et al.*, 2009) (Fig. 4.1). As indicated in Fig. 3.15, the protein can be divided into two parts: an N-terminal domain that possesses two LAGLIDADG motifs typical for homing endonucleases, and a C-terminal domain with a helix-turn-helix fold. It has been proposed that both these domains bind DNA. The main difference between WhiA and homing endonucleases is that WhiA lacks the key residues that are essential for DNA cleavage (Knizewski and Ginalski, 2007) (see Fig. 3.15).

In *Streptomyces,* $WhiA^{Sco}$ was shown to activate its own expression, and at least three other genes: *ftsZ* (Flardh *et al.*, 2000), *whiB* which encodes another sporulation-specific factor (Ainsa *et al.*, 2000), and *parAB* locus whose products are involved in chromosome segregation (Jakimowicz *et al.*, 2006; Kim *et al.*, 2000). These data suggested that $WhiA^{Sco}$ regulates the expression of a protein or several proteins that are required for the proper assembly of Z-rings in the aerial hyphae. However, our microarray analysis of *B. subtilis whiA* mutant does not show an apparent gene regulation effect and we cannot conclude that in *B. subtilis* WhiA functions as a transcriptional regulator. The moderate changes in the expression that we do observe (*oppA*, *ilvA* and *yvyD*), are unlikely causes of the synthetic phenotype of a Δ*whiA* Δ*zapA* mutant. *oppA* is part of an operon that codes for an oligopeptide transporter, which is involved in the initiation of sporulation and competence (Goodell and Higgins, 1987; LeDeaux *et al.*, 1997; Perego *et al.*, 1991; Rudner *et al.*, 1991). In Gram-negative bacteria such transporter has also been implicated in the recycling of peptide cell wall precursors (Goodell and Higgins, 1987). The expression of *oppA* is regulated by catabolite repression in *B. subtilis* (Lorca *et al.*, 2005). IlvA is threonine dehydratase involved in isoleucine biosynthesis and its expression is under the control of the global regulator CodY (Mader *et al.*, 2004; Molle *et al.*, 2003b). In the microarray study some other genes involved in the synthesis of branched chain aminoacids showed lower expression levels in a *whiA* mutant as well (*ilvBHC, ilvD*). Normally these genes are induced upon entry into stationary phase when the available aminoacid pool becomes limited and *de novo* synthesis of aminoacids is required (Molle *et al.*, 2003b). Whether the slower growth of a *whiA* mutant is caused by or results into the lower expression in these genes, we do not know. YvyD is probably involved in modulation of Sig^{L} levels

(*B. subtilis* sigma-54 factor) (Drzewiecki *et al.*, 1998). The expression of *yvyD* was found to be Sigma-B and SigmaH dependent and furthermore, it is also produced upon amino acid starvation (Bernhardt *et al.*, 1997; Drzewiecki *et al.*, 1998; Wendrich and Marahiel, 1997). Importantly, as we show later in a ChIP on chip analysis, WhiA does not bind to the promoter regions of *oppA*, *ilvA* or *yvyD* and together with our microarray it seems that in *B. subtilis* WhiA does not function as a transcription factor. Although a *whiA* mutation does show an altered gene expression, there is no biochemical evidence that WhiA binds to the promoter sites of these genes, and we suppose the changes might be induced indirectly. Furthermore, $WhiA^{Sco}$ might have a divergent activity in *Streptomyces*. Our data suggest that it is now important to verify this.

Chapter 5

WhiA is a DNA binding protein

5.1 Introduction

Most of the reported cell division genes act directly at the septum but there are some that bind to DNA. These include proteins involved in nucleoid occlusion (*noc*, *slm*). Based on the regulatory role of WhiA in *S. coelicolor*, and the crystal structure of the WhiA homolog in *T. maritima*, it is assumed that WhiA binds DNA and functions as a transcriptional regulator (Ainsa *et al.*, 2000; Flardh *et al.*, 1999; Kaiser *et al.*, 2009). However, using a transcriptome experiment we did not find a clear direct effect of WhiA on gene regulation in *B. subtilis*. To gain more information we examined whether WhiA binds to DNA. Here we show that WhiA localizes to DNA in the cell and we determine where on the chromosome WhiA binds, and propose a consensus sequence for its binding. Based on our findings we speculate that WhiA might be involved in chromosome orchestration.

5.2 Results

5.2.1 WhiA localizes to nucleoids *in vivo*

To test whether WhiA binds DNA and localizes to the nucleoid, we constructed fluorescently labelled WhiA by fusing the gene to *gfp* (both C-and N-terminal fusions). The constructs were placed under the control of the xylose-inducible P_{xyl} promoter at the *amy*E locus (strains KS749 and KS752). Both C- and N- terminal fusions appeared to be functional since their expression restored normal growth to the otherwise sick Δ*whiA* Δ*zapA* mutant strains (data not shown). In fact the GFP fusion protein complemented a *whiA* mutation even without the addition of xylose. Apparently, the leakiness of the xylose promoter provides the cell with enough GFP-WhiA, indicating that small amounts of WhiA are sufficient for cell division. The localization pattern of a C-terminal WhiA-GFP fusion was identical to the N-terminal fusion pattern (data not shown). The microscopic observations were performed using exponentially growing cells in media with different concentrations of xylose. Fig. 5.1 and Fig. 5.2 show the localization of GFP-WhiA (strain KS749). It is apparent that WhiA localizes to the nucleoid. However, the distribution of the GFP-signal is dependent on the amount of the inducer (xylose) used. When the protein was expressed at low levels, faint but distinct foci could be observed (Fig. 5.1A). These foci appeared to be on the nucleoid. When the protein was overexpressed, the GFP signal covered the whole nucleoid region (Fig. 5.1D, Fig. 5.2). Spreading of the fluorescence signal from distinct spots to a compact area covering the nucleoid suggests that WhiA might have a preference for some DNA motifs but that it is also able to bind DNA non-specifically. Overexpression of GFP-WhiA (Fig. 5.1D) does not lead to an apparent phenotype.

The expression levels of *gfp-whiA* determine the localization pattern of GFP-WhiA. To achieve a more faithful impression of WhiA localization, a transcriptional fusion of *whiA-gfp* was constructed at its native locus (strain KS907). Under these conditions, *whiA-gfp* is expressed from its endogenous promoter. In this case the more sensitive spinning disc microscope was employed which allowed shorter exposure times (500 ms instead of 20 s). As seen in Fig. 5.3C the GFP signal formed spots in the nucleoid-occupied area. This localization pattern is comparable with the punctuate

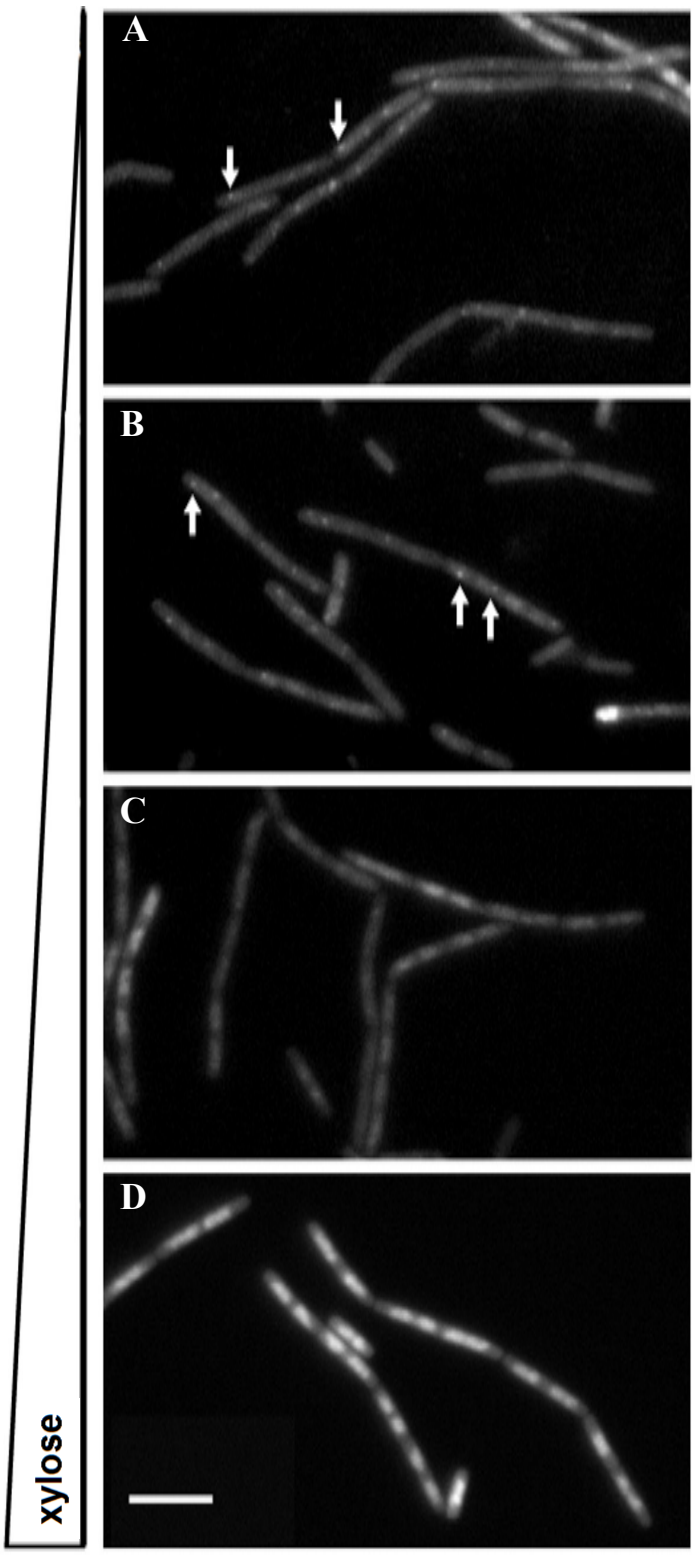

Fig. 5.1 Distinct GFP-WhiA localization
The cellular localization of GFP-WhiA was visualized using strain KS749 (Δ*whiA amy*E::P_{xyl}-*gfp*-*whiA*). Cells were grown in SMM+ at 30 ºC, diluted into OD_{600}~0.05, followed by the addition xylose. After two hours of induction cells were imaged by fluorescence microscopy. Four different xylose concentrations were used: (**A**) 0, (**B**) 0.01, (**C**) 0.1 and (**D**) 1%. The fluorescent signal emerges as distinct dots (arrows in A, B) and eventually spreads out over the DNA-occupied area, covering the whole nucleoid (D). The fluorescence was weak and long exposure times were necessary (20 s in A). Scale bar 5 µm.

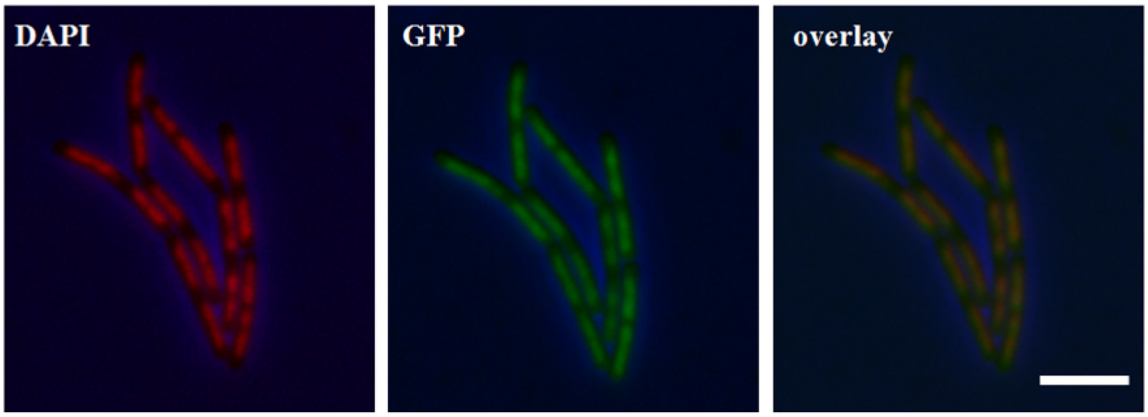

Fig. 5.2 GFP-WhiA localizes to nucleoids
Cells of strain KS749 were grown in LB, and expression of the GFP-WhiA fusion was induced for 2 hours by 1 % xylose. The cells were stained by DAPI to visualize nucleoids before subjecting to microscopy. The background is false-coloured in blue. Scale bar 5 μm.

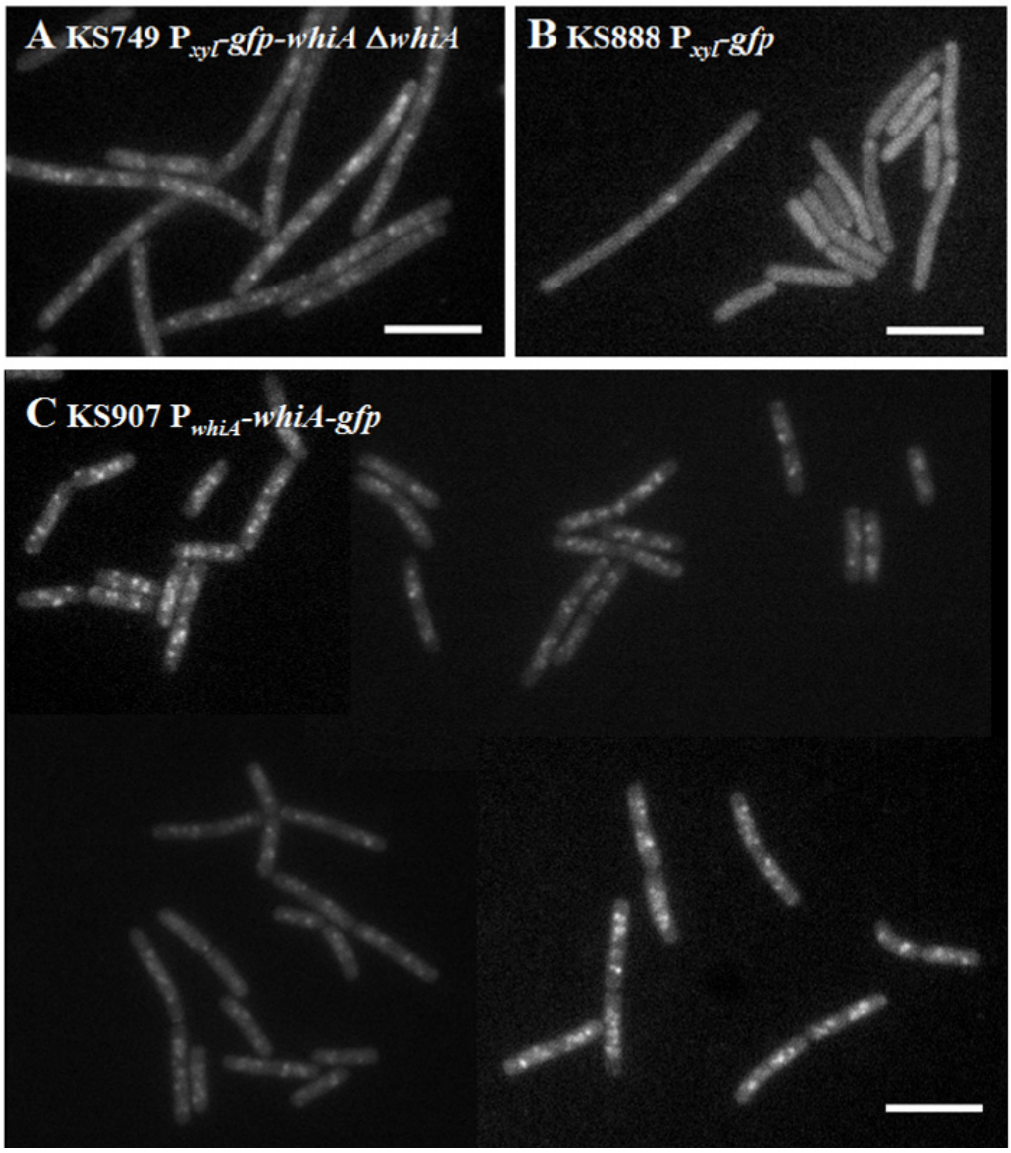

Fig. 5.3 High resolution microscopy shows discrete foci of GFP-WhiA over the nucleoids

To improve the quality of images, strains (**A**) KS749 Δ*whiA amy*E::P$_{xyl}$-*gfp*-*whiA*; (**B**) KS888 *amy*E::P$_{xyl}$-*gfp* and (**C**) KS907 *whiA*::P$_{whiA}$-*whiA*-*gfp* were inspected using a spinning disc microscope. In strain KS907 WhiA-GFP is expressed from its endogenous promoter. Spots of GFP signal, most probably positioned on or in the vicinity of the nucleoid, can be seen with both fluorescent WhiA fusions (A, C). In a control strain KS888 (*amy*E::P$_{xyl}$-*gfp*) where GFP alone is expressed (B), most of the signal is dispersed in the cytoplasm. The randomly localized spots are rare and can be seen after contrast enhancement of the pictures. Cells were grown in SMM+ medium at 30 ºC and the strain KS749 was supplemented with 0.05% xylose. Exposure times were 500 ms. Scale bars 10 μm.

localization of P_{xyl}-driven GFP-WhiA fusion at low xylose concentration (Fig. 5.1A). Whether there is a constant number of foci per cell is unclear. The control strain that expressed GFP only formed very few fluorescent foci (Fig. 5.3B).

To check whether the protein levels of both fluorescent WhiA fusions were comparable to wild type WhiA, the expression levels were investigated with Western Blot analysis using α-WhiA antibody. As seen in Fig. 5.4, addition of 0.05% xylose gives wild type levels of WhiA (lanes 1 and 5, respectively). This corresponds to a localization pattern where fluorescently tagged WhiA forms foci over nucleoids (Fig. 5.3A). The results also show that the intracellular levels of P_{whiA}- driven WhiA-GFP fusion (lane 3) is lower compared to wild type (lane 1). This discrepancy might be a consequence of an insufficient transcription of the *gfp*-fusion, instability of the mRNA, unprocessive translation or degradation of the protein. However, since the intensities of GFP in strains KS749 and KS907 are comparable it is likely that the GFP fusion in KS907 masks an epitope and the efficiency of α-YvcL-Ab binding is lowered. We have not tested yet whether this is the case. This fusion protein also migrates more slowly in the gel and, even though it is 0.55 kDa smaller than the N-terminal GFP fusion, we are not sure what the reason for the change in the mobility is. However, all the *gfp*-fusions complemented the Δ*whiA* Δ*zapA* double mutant (data not shown) suggesting that the levels of WhiA are sufficient.

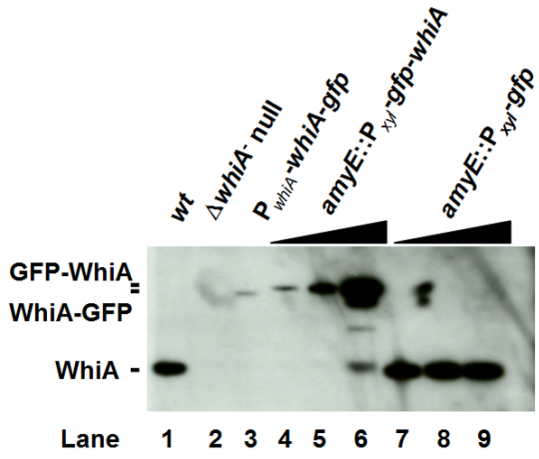

Fig. 5.4 Western Blot analysis of fluorescent WhiA fusions
Wild type (KS2) (lane 1), *whiA*-null mutant (KS400) (lane 2), P_{whiA}-*whiA-gfp* (KS907) (lane 3), Δ*whiA amy*E::P_{xyl}-*gfp-whiA* (KS749) (lanes 4-6) and a control strain KS888 (*amy*E::P_{xyl}-*gfp*) (lanes7-9) were grown in SMM+ medium supplied with xylose (0, 0.05 or 0.5%; lanes 4-6 or 7-9), 20 µg of total protein extract was applied on the gel and the blot was analysed using α-WhiA antibodies. The expression of WhiA reaches wild type levels in strain KS749 (0.05% xylose) (lane 5).

5.2.2 WhiA is not a nucleoid occlusion protein

Since WhiA localizes to the nucleoid and affects cell division, it was possible that WhiA was involved in nucleoid occlusion. The Δ*noc* Δ*whiA* double mutant grows as filaments and FtsZ is delocalized, so we could not examine whether the cells lose the nucleoid occlusion system. To examine this in detail we looked at the bisection of chromosomes by division septa after mitomycin C treatment. In cells that lack Noc and YneA, chromosomes are frequently bisected when these cells are treated with mitomycin C. This compound induces DNA damage; mainly double strand breaks that block replication. This results in the bisection of chromosomes since Noc no longer repels FtsZ from the nucleoid occupied area. To observe this it was necessary to mutate *yneA* as well to permit cell division. YneA is induced during the SOS response and it would otherwise have blocked cell division (Kawai *et al.*, 2003). If WhiA was involved in nucleoid occlusion, we should find a comparable effect to the *noc* mutant. However, it appeared that mitomycin C does not induce increased formation of bisected chromosomes in Δ*whiA* Δ*yneA* double mutant cells, suggesting that WhiA is not involved in nucleoid occlusion (Table 5.1).

Importantly, we also found that the double mutant of *whiA* and *yneA* (strain KS703) is 47 % longer than wild type strain, suggesting that the increase of cell length of *whiA* mutants is independent of YneA.

strain	genotype	% of bisected nucleoids	cell length of uninduced vs. induced cells (μm)
KS701	Δ*yneA*::*tet*	17	5.4 / 5.1
KS702	Δ*noc*::*spc* Δ*yneA*::*tet*	34	4.6 / 4.4
KS703	*whiA** Δ*yneA*::*tet*	8.8	6.6 / 7.2
KS2	wild type	-	4.5 / -
KS696	*whiA**	-	6.5 / -

Table 5.1 Mitomycin C does not induce increased bisection of chromosomes in a *whiA* mutant
An exponentially growing culture (OD_{600}~0.1) was divided and one sample was treated with mitomycin C (1 μg/ml) for 40 *min*. Then the cells were harvested and stained with DAPI and nile red. On the far right, the mean cell dimensions are indicated.

5.2.3 Nucleoid morphology and positioning in a *whiA* mutant

Based on the observation that in *S. coelicolor* aerial hyphae of a *whiA*^{Sco} mutant the DNA is dispersed throughout the whole cell, Ainsa *et al*. suggested that WhiA^{Sco} might be a part of the chromosome partitioning system (Ainsa *et al.*, 2000). In the case of the *B. subtilis whiA* mutant, however, nucleoids appear normal as judged by DAPI staining. However, to compare the nucleoids of wild type and a *whiA* mutant in more detail, we visualized them using a HBsu-GFP fusion. HBsu is a histone-like protein that binds non-specifically to DNA (reviewed in Dame, 2005) and allows for a better resolution of DNA than using DNA-specific DAPI staining (J.W.Veening, personal communication). We measured the internucleoid spaces and the length of the nucleoids in wild type and *whiA* mutant backgrounds in which filamentation had been induced artificially by depleting FtsZ (strains KS930 and KS931, respectively). The use of filamented cells enabled us to minimize the impact of cell division problems and to evaluate large number of nucleoids. The results in Table 5.2 and Fig. 5.5 show that in a *whiA* mutant the nucleoids are on average 14% longer than in the wild type cells. Importantly, they are considerably more widely separated, on average by 44%. While in wild type cells there is, on average, one nucleoid per each 2.2 (+/-0.37) μm, nucleoids are less frequent in the *whiA* mutant, with a nucleoid appearing each 2.86 (+/-0.17) μm, which is a 24 % decrease. This could indicate a delay in chromosome segregation.

	nucleoid length (μm)	internucleoid space length	nucleoid length/cell length ratio	**no. of nucloids per 1 μm**
KS930 FtsZ$^-$ HBsu-GFP	1.17 ± 0.13	1.04 ± 0.25	0.53 ± 0.03	**0.46 ± 0.07**
KS931 Δ*whiA* FtsZ$^-$ HBsu-GFP	1.33 ± 0.10	1.49 ± 0.23	0.48 ± 0.06	**0.35 ± 0.02**
fold change	1.138	1.436	0.9	**0.76**

Table 5.2 Nucleoid morphology in *ftsZ*-depleted cells
The strains used contained a HBsu-*gfp* fusion for the visualization of DNA, an inducible *ftsZ* allele, and in case of KS931, a disruption of *whiA*. Cells were depleted of FtsZ at 37° C for 140 minutes before subjecting to fluorescence microscopy. For strains KS930 and KS931, in total 955 μm and 948 μm of filaments were analyzed, respectively. The means were deduced from the averages of three independent experiments. The last row of the table indicates fold changes relative to wild type levels.

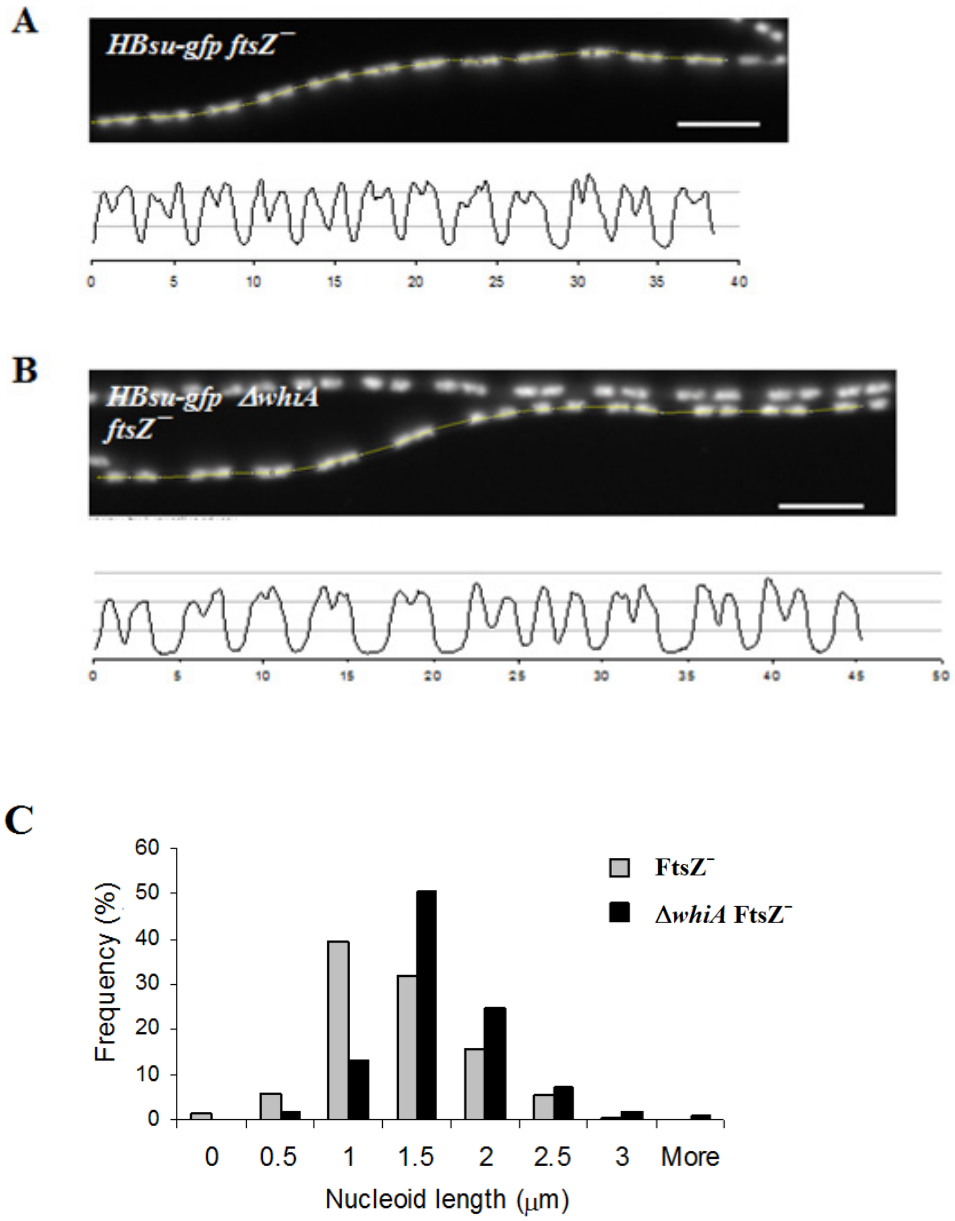

Fig. 5.5 Nucleoids are longer in a *whiA* mutant
Analysis of HBsu-GFP labelled nucleoids in FtsZ-depleted cells. FtsZ was depleted in wild type (**A**) and *whiA* mutant (**B**) backgrounds (strains KS930 and KS931, respectively), both of which also carry the *amy*E::P_{HU}-HBsu-*gfp* allele. For a relative quantification of the results, a line passing through the middle of nucleoids was drawn and the signal intensity was plotted against the cell length measurement. The resulting graphs (below microscopic figures) represent the intensity of GFP. A peak above the mean GFP intensity was considered as being a nucleoid, whilst the area below this line was considered to be an internucleoid space. The length of each nucleoid was measured. In three independent experiments, at least 10 graphs were acquired (altogether ~950 μm per strain). Scalebar 5 μm. (**C**) Histogram of the nucleoid dimensions in wild type (grey bars) and *whiA* mutant (black bars) FtsZ depleted cells.

5.2.3.1 Localization pattern of origins and termini of replication in a *whiA* mutant

The nucleoids in the *whiA* mutant appear longer, which might be a consequence of an increased DNA content and over-initiation of replication. To test this hypothesis we visualized *oriC* regions in the *whiA* mutant using fluorescently labelled Spo0J as a marker of the origin. Spo0J takes part in chromosome partitioning and binds to several areas at and around *oriC* (Lin and Grossman, 1998; Lin *et al.*, 1997). We introduced a *spo0J-gfp* fusion (source HM160) into a wild type and a Δ*whiA* strain that could also be depleted for FtsZ. To evaluate the localization of Spo0J-GFP in filamentous cells, these were depleted of FtsZ and subjected to fluorescence microscopy (Fig. 5.6). After measuring the distances between Spo0J-GFP it appeared that this distance increased in a *whiA* mutant which formed 23% less visible foci per 1 μm of cell length. These data correlate well with the 24% decrease in the number of nucloids in a *whiA* mutant, as judged by HBsu-GFP localization (Fig. 5.5). This suggests the *whiA* mutant initiates replication at the same rate as wild type.

Additionally, we also determined the number of nucleoid termini that can be marked by an RTP-GFP fusion. RTP is a non-essential replication termination protein that binds to *ter* sites near the chromosome terminus (Lemon *et al.*, 2001). There were 24% less RTP-GFP- marked terminal regions of DNA in a *whiA* mutant depleted of FtsZ than in wild type, which is consistent with the *oriC* localization data (23% less *oriC* per 1μm) (Fig. 5.7).

To exclude the possibility (although unlikely) that FtsZ depletion was responsible for the increased inter-nucleoid distances in a *whiA* mutant, we inspected cells that were not depleted of FtsZ. We found that in a *whiA* mutant there were 26% less RTP-GFP foci per cell length than in wild type cells (data not shown), which is in agreement with previous results using the FtsZ depleted strain. Interestingly, in exponentially growing cells without FtsZ depletion, the *whiA* mutant seemed to contain 13% more Spo0J-GFP foci per cell and was on average 28% longer than wild type (Fig. 5.8). This means that the *whiA* mutant contains 12 % less Spo0J-GFP foci per cell length, which is slightly more compared to situation where FtsZ is also depleted (Fig. 5.6). The nascent *oriC* regions might be difficult to distinguish microscopically since the region covered by Spo0J is relatively large (Lin and Grossman, 1998). That is why we performed marker

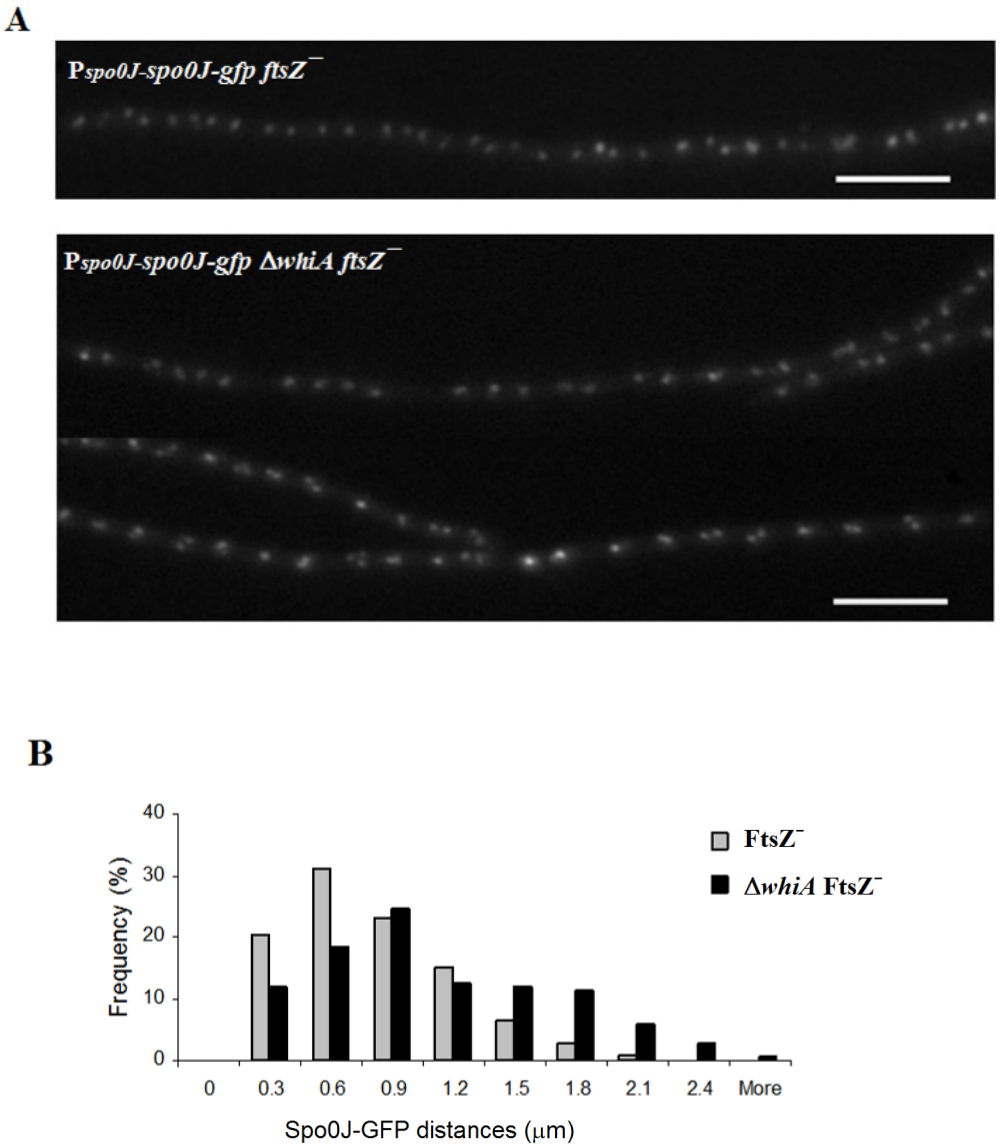

Fig. 5.6 Increased spacing between Spo0J-GFP foci in a filamentous *whiA* mutant

(**A**) Strains KS991 (P_{spo0J}-*spo0J-gfp* P_{spac}-*ftsZ*) and KS993 (P_{spo0J}-*spo0J-gfp* P_{spac}-*ftsZ* Δ*whiA*) were depleted for FtsZ. Similar to Fig. 5.4, the Spo0J-GFP foci were connected with a line and the signal intensities were plotted into a graph. Each peak reaching above the median was counted as one *oriC* region. Two independent experiments were performed. Scale bars 5 µm. Graph (**B**) shows the histogram of the frequencies of the distances between Spo0J-GFP foci in both strains.

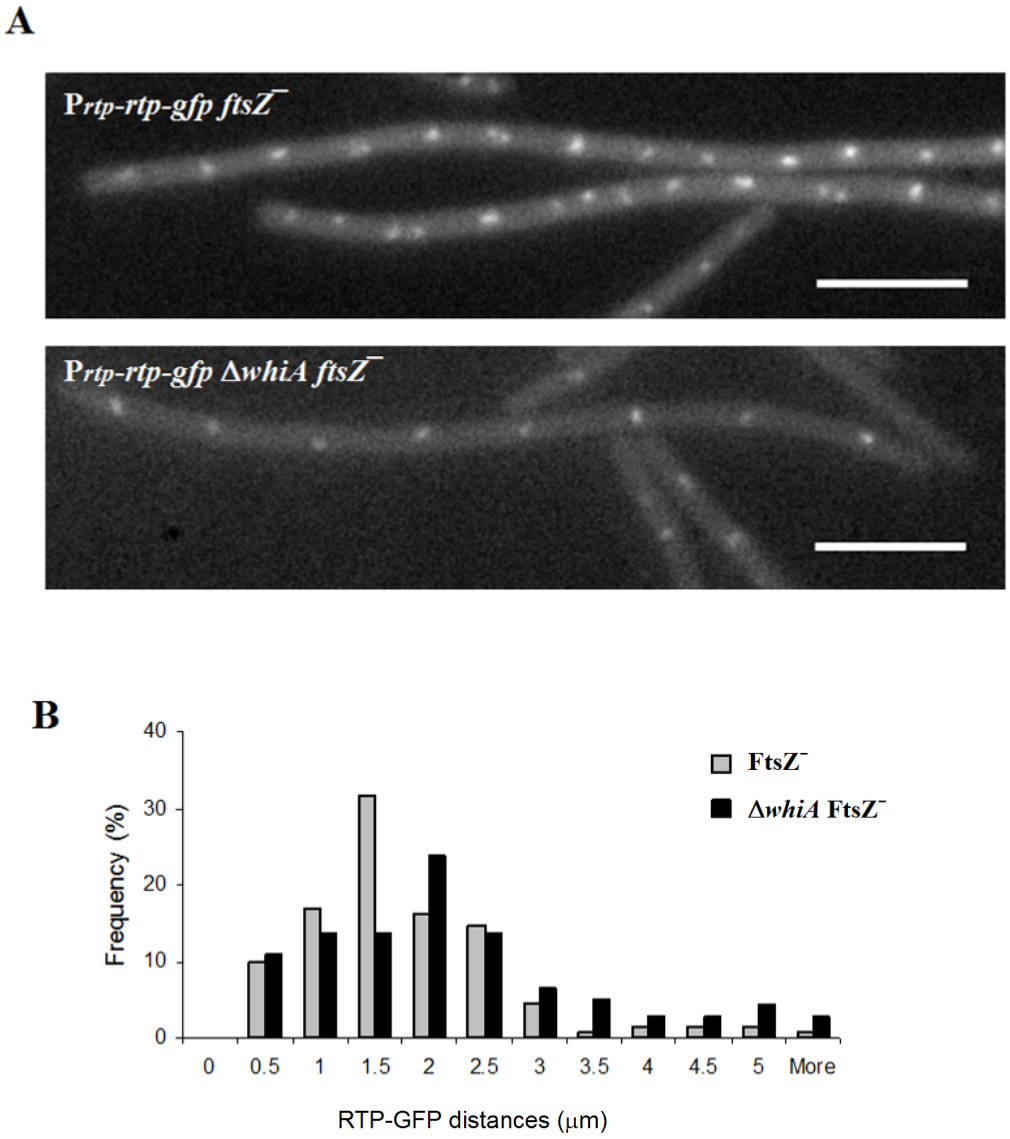

Fig. 5.7 RTP-GFP spacing increases in filamentous *whiA* mutant cells
(**A**) Localization of RTP-GFP expressed from its endogenous promoter in strains KS1016 (P_{RTP}-*rtp-gfp* P_{spac}-*ftsZ*) and KS1017 (P_{RTP}-*rtp-gfp* P_{spac}-*ftsZ* Δ*whiA*) after FtsZ depletion. Scale bars 5 μm. (**B**) Histogram shows the distribution of frequencies of the interfocal distances.

A

Strain	Genotype	Average number of Spo0J-GFP foci per cell	Average cell length (μm)	Number of foci per 1 μm
KS420	*spo0J-gfp*	2.56 ± 0.86	3.44 ± 0.86	0.74
KS421	*spo0J-gfp whiA*::*erm*	2.88 ± 1.04	4.4 ± 1.32	0.65

B

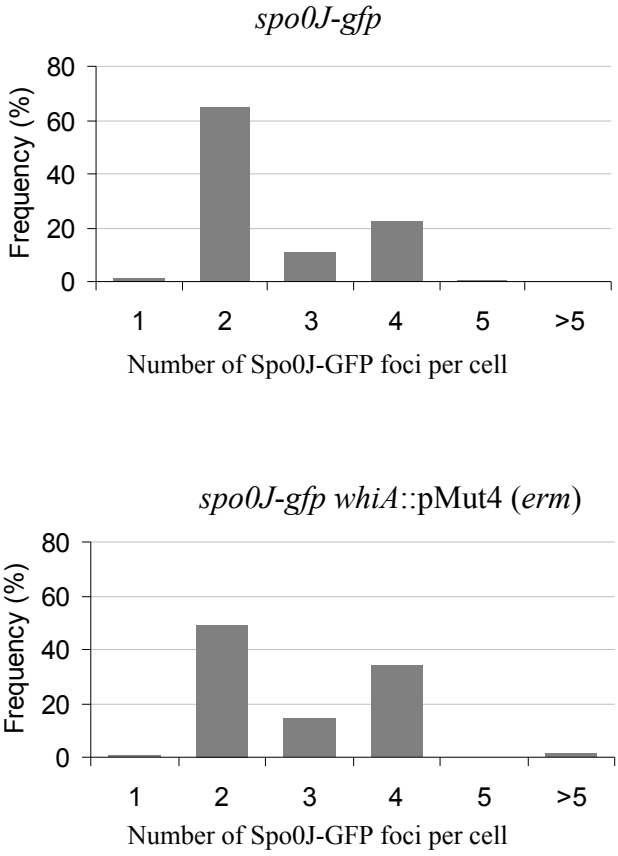

Fig. 5.8 Analysis of Spo0J-GFP distribution in a *whiA* mutant
Transcription of *spo0J-gfp* fusion used in this experiment is driven from its endogenous promoter. Cells were grown in SMM+ medium at 30º C to OD~0.2 (exponential growth) when microscopic pictures of membrane stained cells (nile red) were taken. Numbers of Spo0J-GFP foci per cell were counted and the cell lengths were measured. Cumulative results of two independent experiments are shown, 736 and 638 cells were examined for KS420 and KS421, respectively. (**A**) Table shows the average number of Spo0J-GFP foci per cell. Although statistically significant (p=0.025), the change between strains KS420 (*spo0J-gfp*) and KS421 (Δ*whiA spo0J-gfp*) is only 13 %. (**B**) Histograms of the distributions of Spo0J-GFP foci.

frequency analysis, which is a more precise approach. Chromosomal DNA from wild type and *whiA* mutants cells was purified, and primer sets binding to the *oriC* or *ter* regions were used to perform quantitative PCR. As indicated in Fig. 5.9, *whiA* mutants show a slight decrease in *oriC*/*ter* ratio, varying from 5% in the 'clean' *whiA* mutant (KS696) to 19% in the *whiA* deletion mutant (KS400). However, these changes are not statistically significant ($p>0.1$). On the other hand, a control strain of a *spo0J* mutant (KS382) that had previously been shown to overinitiate replication (Murray and Errington, 2008) shows a 57% increase of *oriC*:*ter* ratio ($p<0.01$). The relatively unchanged *oriC*/*ter* ratio in *whiA* mutants suggests that replication initiation remains unchanged.

In summary the *whiA* mutant contains less nucleoids per cell length, but cells initiate replication at the same rate or efficiency as wild type cells. The longer internucleoid spacing suggests that WhiA may influence chromosome separation.

5.2.4 The lack of WhiA causes sensitivity to increased DNA replication initiation and to DNA damage

In *B. subtilis*, the partitioning (*par*) system, required for chromosome replication and segregation, is represented by Soj (ParA) and Spo0J (ParB) proteins (Autret *et al.*, 2001; Ireton *et al.*, 1994). However, deletion of their encoding genes does not impose radical changes in nucleoid positioning (Autret *et al.*, 2001). Taking into account the changes in the nucleoid spacing of *whiA* mutants, we were interested whether the absence of Soj or Spo0J would have an additional effect. Indeed, when the *whiA* deletion was introduced into *spo0J* and *soj* mutants, only tiny colonies were obtained, the cells were filamentous and often lysed (Fig. 5.10A). Spontaneous suppressor mutations appeared frequently, similarly to Δ*whiA* Δ*zapA* double mutant. To be able to examine the phenotype more closely, a double Δ*soj*/*spo0J* mutation was combined with an IPTG inducible *whiA*::P_{spac}-*whiA* allele. The resulting strains KS1102 also contained plasmid pMAP65, which carried an additional copy of *lacI* to ensure tight regulation of the P_{spac} promoter. The strain was tested for growth in the presence and absence of the inducer. As shown in Fig. 5.10B, Δ*soj*/*spo0J* cells depleted for WhiA failed to form colonies on plates and were blocked in cell division. The presence of WhiA expression (IPTG presence) restored growth of this strain. The control strain, containing an IPTG inducible *crh* gene, shows no difference in the absence or presence of IPTG (strain KS1116). These

A

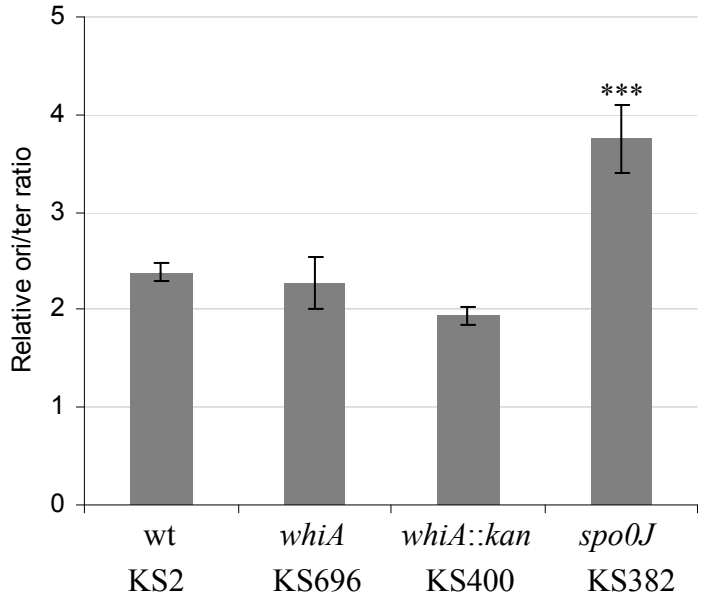

B

	Average ori/*ter* ratio
wild type	2.39 ± 0.10
KS696 *whiA*	2.27 ± 0.27
KS400 *whiA*::*kan*	1.94 ± 0.10
KS382 *spo0J*	3.75 ± 0.35

Fig. 5.9 Marker frequency analysis of *oriC* and ter regions
(**A**) Chromosomal DNA from wild type, KS696 (markerless *whiA* mutant), KS400 (*whiA*::*kan*) and KS382 (*spo0J* mutant) strains was purified and a quantitative PCR was performed using *oriC*/*ter* specific primer pairs. Two replicates were collected for DNA purification (in case of KS696 four replicates). The exact numbers are shown in table (**B**).

data show that the lack of Soj and Spo0J negatively affects the growth of a *whiA* mutant.

One of the effects of a *soj* and *spo0J* deletion is overinitiation of DNA replication (Murray and Errington, 2008). Since these proteins affect replication initiation and many other processes, we wondered whether it is the increased replication initiation causing lethal effects in a *whiA* mutant. To test this, we used a *yabA* deletion strain. YabA is a known inhibitor of the initiation of DNA replication, and its deletion causes rapid overinitiation (Noirot-Gros *et al.*, 2002). Attempts to construct a double mutant of *yabA* and *whiA* were not successful; we obtained only a few transformants that formed minute colonies after more than 48 h incubation. Therefore we used again the inducible *whiA*::P_{spac}-*whiA* construct and combined it with a *yabA* mutation. Fig. 5.10C shows this strain tested for growth on plates with and without IPTG. Similarly to Δ*soj*/*spo0J* mutant, Δ*yabA* strain depleted of WhiA (KS1063) fails to grow without IPTG. The cells became longer and lysed frequently (Fig. 5.10D). However, the control strain KS1064 in which *whiA* is intact forms normal colonies. These data suggest that the lethality of the double mutant strains Δ*yabA* Δ*whiA* and Δ*soj*/Δ*spo0J* Δ*whiA* is probably due to replication overinitiation.

Using a bacterial two hybrid system, we found that WhiA interacts with Spo0J and Soj (Fig. 5.11). WhiA levels were kept low in *E. coli* cells because of its toxicity for *E. coli*. This might be the reason why the interactions are not strong. This result suggests that WhiA may directly cooperate with Spo0J. Furthermore, WhiA did not interact with cell division proteins Noc, ZapA, and MinC/D.

During the construction of strains we noticed that *whiA* mutants transformed less well than a wild type. The microarray analysis has not revealed changes in the transcriptional profile that would indicate decreased competence. That is why we thought that Δ*whiA* might be impaired in the incorporation of DNA, which requires a recombination event. It has been known that *rec* mutants that cannot recombine are also sensitive to DNA damage since they cannot repair the DNA (Howard-Flanders *et al.*, 1969; Munakata, 1974). To test whether *whiA* mutation affects sensitivity to DNA damage, a dose of UV radiation was applied on cells and tested for survival. As seen in Fig. 5.12, wild type strain shows ~2-3 log decrease in cell survival. However, *whiA* mutant cells completely fail to grow (>5 log decrease) similarly to a *recA* mutant strain. SOS response induces

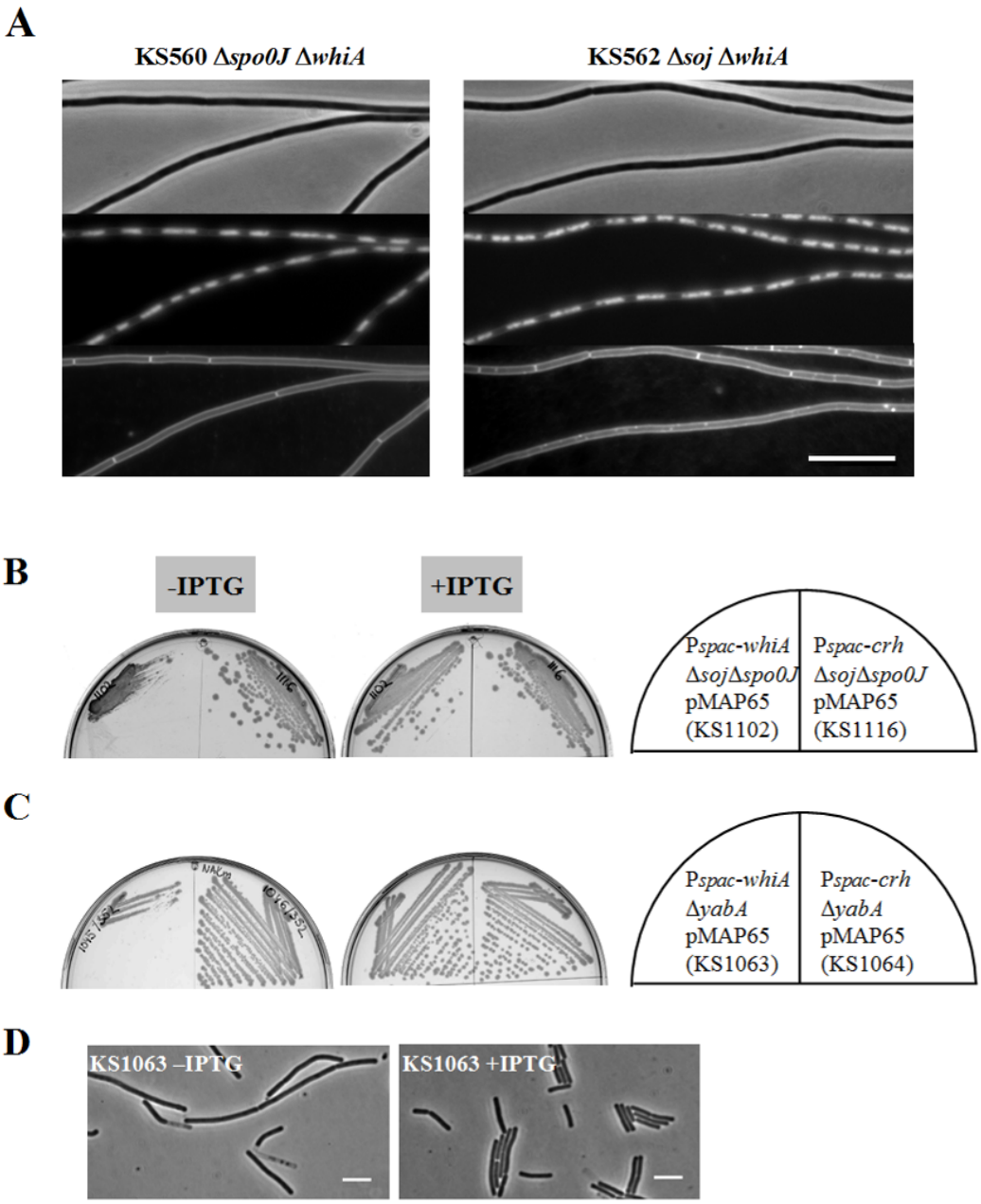

Fig. 5.10 Deletion of the *par* system (*soj*/*spo0J*) or *yabA* in a *whiA* mutant has a detrimental effect on cell growth

(**A**) Phenotype of strains KS560 (Δ*spo0J*::*neo* Δ*whiA*::pMut *erm*) and KS562 (Δ*soj*::*neo* Δ*whiA*::pMut *erm*) stained with DAPI (nucleoids) and nile red (membranes). Scale bar 10 µm. (**B**) Strains KS1102 and KS1116 lack *soj* and *spo0J*, and carry an inducible copy of either *whiA*::P_{spac}-*whiA* (left) or *crh*::P_{spac}-*crh* (right), respectively. Tight regulation of the P_{spac} promoter is secured by the presence of the non-integrative pMAP65 plasmid that encodes *lacI*. Growth of the *soj*/*spo0J* mutant depends on the presence of WhiA. The control strain (KS1116) grows independently of IPTG. (**C**) Strains KS1063 and KS1064 are isogenic strains to KS1102 and KS1116, but instead of *soj*/*spo0J*, the *yabA* gene is deleted. Cells lacking YabA and WhiA have difficulties to grow, but the growth is restored when 0.1 mM IPTG is added. (**D**) Phenotype of strain KS1063 (Δ*yabA whiA*::P_{spac}-*whiA* pMAP65) without (-IPTG) and with (+IPTG) WhiA. Scale bars 5 µm.

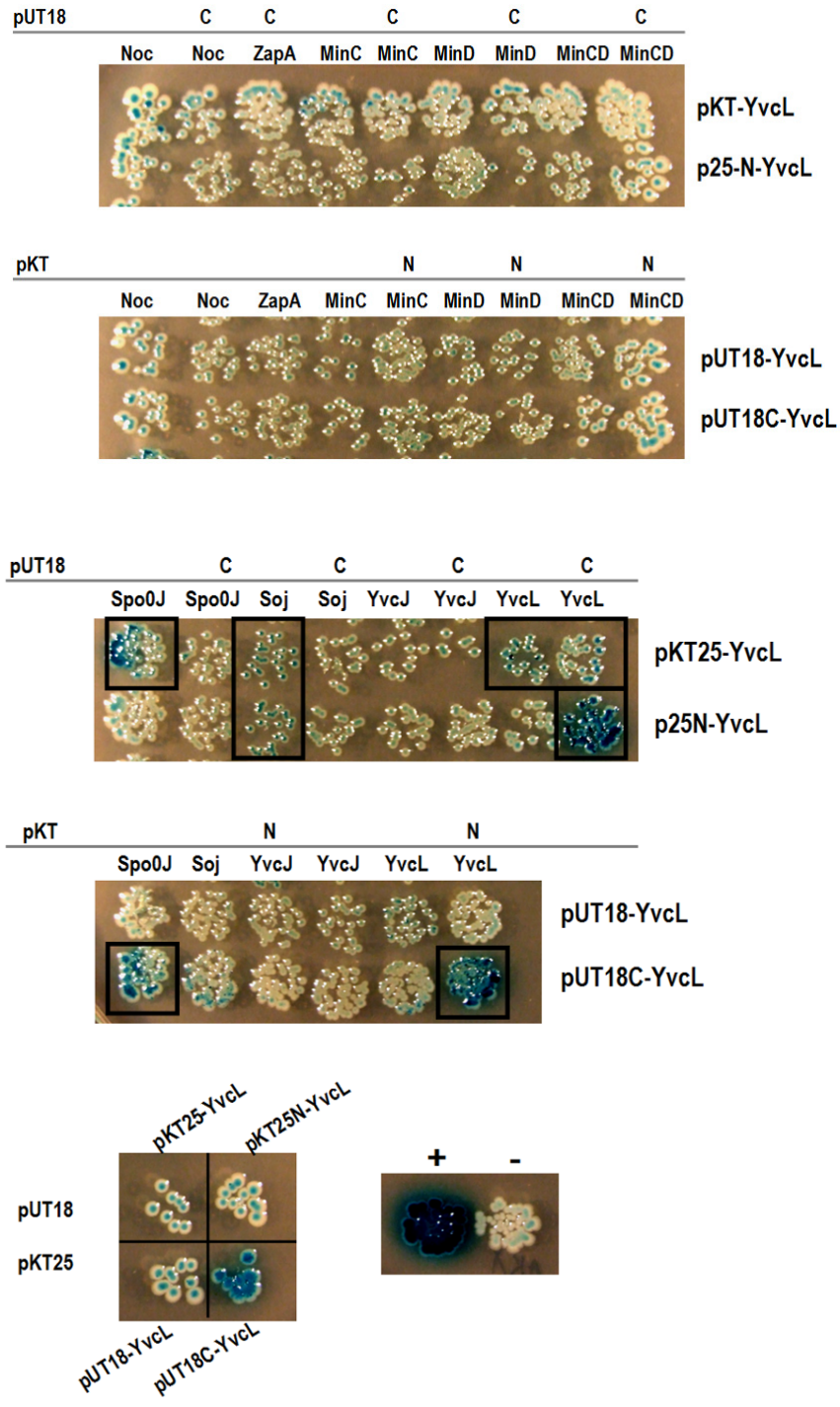

Fig. 5.11 Bacterial two hybrid system shows WhiA interacts with Spo0J and Soj

WhiA was fused to the N- or C- terminus of either T18 or T25 fragment of adenylate cyclase protein. Boxes indicate an interaction of proteins. WhiA interacts weakly with Spo0J, Soj, and also self-interacts.

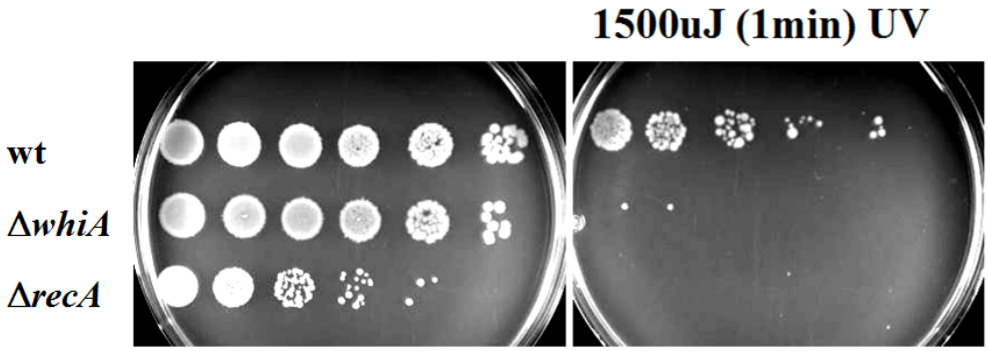

Fig. 5.12 The *whiA* mutant is hypersensitive to UV irradiation
Wild type strain (KS2), the Δ*whiA*::*kan* mutant (KS400) and a Δ*recA* mutant were grown to OD_{600}~0.5, diluted, and spotted onto NA plates. On the right, the plate was subjected to UV radiation, and it is clear that both the Δ*whiA* and Δ*recA* strains cannot recover from DNA damage.

expression of YneA, which is a negative regulator of Z-ring assembly (Kawai *et al.*, 2003). There is a possibility that production of YneA interferes with the lack of *whiA*, which inhibits division, however, this must be tested further.

5.2.5 Determination of WhiA-binding sites using ChIP-on-chip

To find out which DNA regions the WhiA protein associates with, we performed a ChIP-on-chip assay. We found that the α-WhiA antibody is of a good quality, and specific enough that DNA can be detected in the immunoprecipitate (IP) fraction by qPCR (e. g. primer pair STG410 and STG411 for *rplC*). The crosslinked DNA (input) of the wild type strain was subjected to Chromatin ImmunoPrecipitation (ChIP). Input and immunoprecipitated DNA were amplified, labelled and applied onto Nimblegen-custom-made chip (~54.000 50bp oligonucleotides) which was a kind gift from Dr. Richard Daniel. The data was processed as suggested by the manufacturer.

The intensity plot in Fig. 5.13A shows enrichment of WhiA binding in several regions of the chromosome. Both chromosome arms contain apparent WhiA-binding sites. Only positions 2 - 2.8 Mb on the chromosomal map seem to be devoid of binding signal. Most of the binding seems to occur around strongly transcribed regions like rRNA and tRNA genes (Fig. 5.13C). The strongest binding signals were verified in an independent ChIP followed by qPCR and confirmed WhiA binding to the *rplC*, *acoC*, *spoVID*, and *xynD* regions (Fig. 5.13B). The highest peak indicating binding to the *scpB* gene was shown to be a result of contamination, since in an independent control ChIP, qPCR for this region showed similar values as that of *ter*, which is a region not occupied by WhiA, using the wild type and Δ*whiA* lysates (Fig. 5.13B). Many of the WhiA-binding peaks seemed to cover coding regions of genes, suggesting that WhiA does not preferentially bind to promoter regions (Fig. 5.13D-F).

To search for WhiA-specific peaks, the ChIP-on-chip profile of WhiA was compared to the profile of SMC (Gruber and Errington, 2009), Spo0J (L.J.Wu, unpublished) and Noc (Wu *et al.*, 2009) and the peaks specific for WhiA (highlighted in red in Fig. 5.13A and C) were subjected to further analysis. Sequences were chosen, each containing a potential WhiA binding region. These sequences were analysed using a MEME programme (Bailey *et al.*, 2009) to find a possible consensus binding sequence. In the 12 sequences analysed, MEME identified a 15 bp sequence motif AG[CGA][TA][GC]A[AT][AT]CG[GTC][CA][TA]GC (Fig. 5.14).

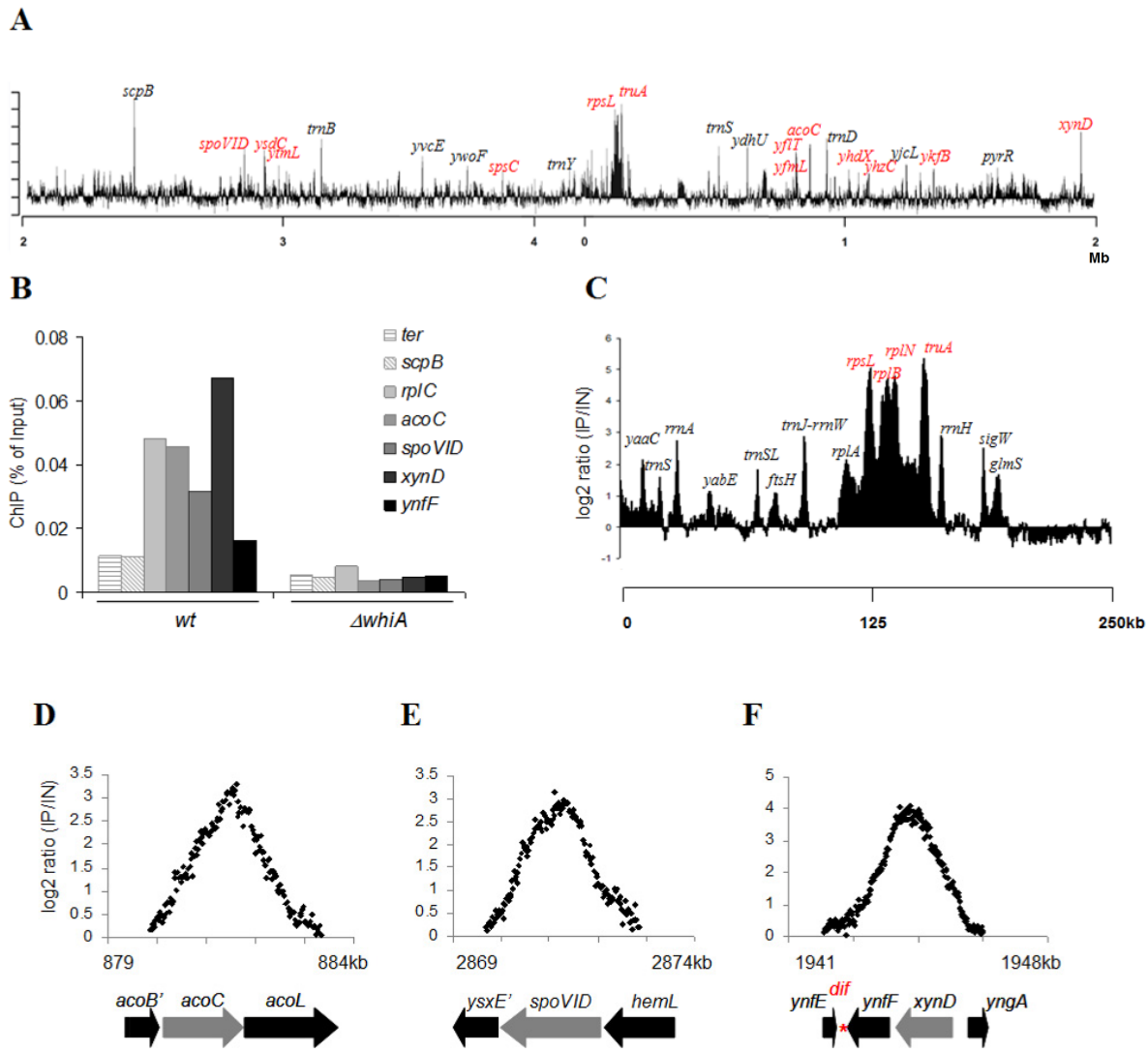

Fig. 5.13 Determination of the WhiA binding sites on the chromosome of *B. subtilis*
(**A**) ChIP on chip analysis of WhiA distribution on the chromosome. Cells of a wild type strain (KS2) were grown in SMM+ medium, and after ChIP the fragmented DNA was applied on a microarray slide containing genomic-wide probes. The results show averaged immunoprecipitated/total DNA (IP/IN) ratios. WhiA binds to highly expressed regions (rRNA and tRNA) and also to coding regions. The profile of microarray analysis was compared to that of the SMC, Spo0J and Noc (referenced in text), and WhiA-specific binding sites are highlighted in red.
(**B**) Verification of ChIP on chip data in an independent ChIP experiment. Cells of wild type (KS2) and a *whiA* mutant (KS696) were subjected to ChIP and qPCR. As seen in the graph, *rplC* (next to *rplB*), *acoC*, *spoVID* and *xynD* are enriched in the wild type sample eluate. However, using the *whiA* mutant lysate only residual DNA is detected in the eluate.
(**C**) Abundant distribution of WhiA at the region with high transcriptional activity (position 0-250 bp).
(**D-F**) Detailed distribution of WhiA binding sites around *acoC*, *spoVID* and *xynD* regions. The maxima of the peaks fall into their coding regions (in grey).

A

gene	sequence		
xynD	ACCGGGTAGA	AGCTGAAACGTTTGC	TTGGAATGGA
spsC	GGACTTCATC	AGCTGAAACGGCTGG	ATGATATGCA
yhdX	AAAGAATTAA	AGCCGAAACGGATGC	TGAAATGCAA
spoVID	ACGTTGGAGC	AGAAGAATCGCCTGC	TTTGGAAGCT
yhzC	TCCGCCATTG	ACGTGAATCGTCTGC	CCTGTGACGT
ytmL	GTGTAGATAA	AGGCCAAACGGAAGC	GGCGTACAGT
yflT	ATCAAAATTA	AGGAGAAGCCGCTGC	ACGGAGCACA
truA	TCTCCCGATG	AGGTGAAATCCATGC	TGGAAGCGAA
yfmLM	CAAGACCGGC	AGCGCATACGCCAGC	GTCTTCCCTG
ysdC	CCGGCGGCGG	AACTGATTCGGGTGC	CATCCATTTG
rpsL	GTTTTTGTGG	AGAAGATACGTTAGT	GTGCTCTTTT
acoC	ACACGCTCTG	TGATCAAATGTCAGG	CTGAGTGGCA

B

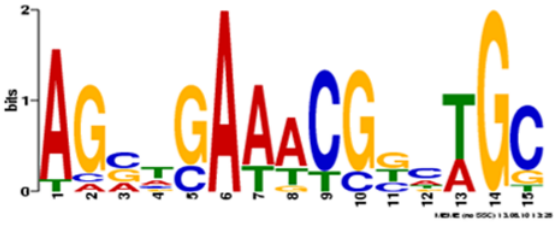

Fig. 5.14 Analysis of WhiA binding sites on DNA
(**A**) The sequences of different WhiA binding sites were collected, whereby sites that were also found to be bound by Smc, Noc and Spo0J, were ignored. Sequence analysis using the MEME programme (Bailey *et al.*, 2009) showed a potential recognition sequence of 15 bp in length (in colour). (**B**) The sequence conservation of a possible binding site of WhiA (E value = 7,6 x 10^{-30}).

As seen in Fig. 5.15A, WhiA binds also near the *yvcI-N* operon, in the region of the upstream *trxB* and *yvcE* genes. However, the maximum binding omits the promoter of *yvcI-N* operon, which is located just before the *yvcI* gene. This is in agreement with our result showing that WhiA does not regulate its own expression (Fig. 4.2B, strain KS696). Interestingly, this region is occupied also by SMC, which is a protein required for the maintenance of chromosomes (Gruber and Errington, 2009). We also saw no binding of WhiA to the the promoters of *ftsAZ* and *soj-spo0J* operons, which correlates with the microarray data. (Fig. 5.15B, C).

In summary, WhiA binds about 12 regions on the chromosome of *B. subtilis* that are not occupied by SMC, Spo0J or Noc proteins. However, there are other WhiA-bound regions that are recognized by at least one of these proteins. In the case of Spo0J, they may bind the same DNA sequences since we found WhiA to interact with Spo0J in a bacterial two hybrid system. Nevertheless, amongst WhiA-specific sequences a 15 bp binding motif was identified, but further experimental data is needed to investigate what is the significance of this sequence.

One of the highest peaks was found near the *xynD* gene (Fig. 5.13F), which neighbours a specific *dif* site which is important for chromosome dimer resolution to segregate chromosomes (Kuempel *et al.*, 1991; Sciochetti *et al.*, 2001). Since the nucleoids of a *whiA* mutant are longer, and WhiA might be involved in recombination, possibly at *dif*, we tested the effect of *spoIIIE* deletion on a *whiA* mutant. SpoIIIE can pump trapped chromosomes in the septum (Wu and Errington, 1994), resulting from corrupt chromosome segregation, which would be a consequence of inadequate chromosome recombination. The double mutant of *spoIIIE* and *whiA* was easily obtained, showed no marks of chromosome bisection or formation of anucleate cells (Fig. 5.16). This result suggests that WhiA is dispensable for chromosome resolution, or it may be an indication of a functional redundancy.

An interesting question also is, whether WhiA would bind the same chromosomal regions if placed in *trans*. In fact, we constructed mutants in *acoC*, *spoVID* and *xynD* genes (that show WhiA binding) and aimed to place the genes into an ectopic locus, *amyE* (which shows no WhiA binding). It would be interesting to see whether WhiA still binds these DNA fragments but further investigation is needed. Unpublished

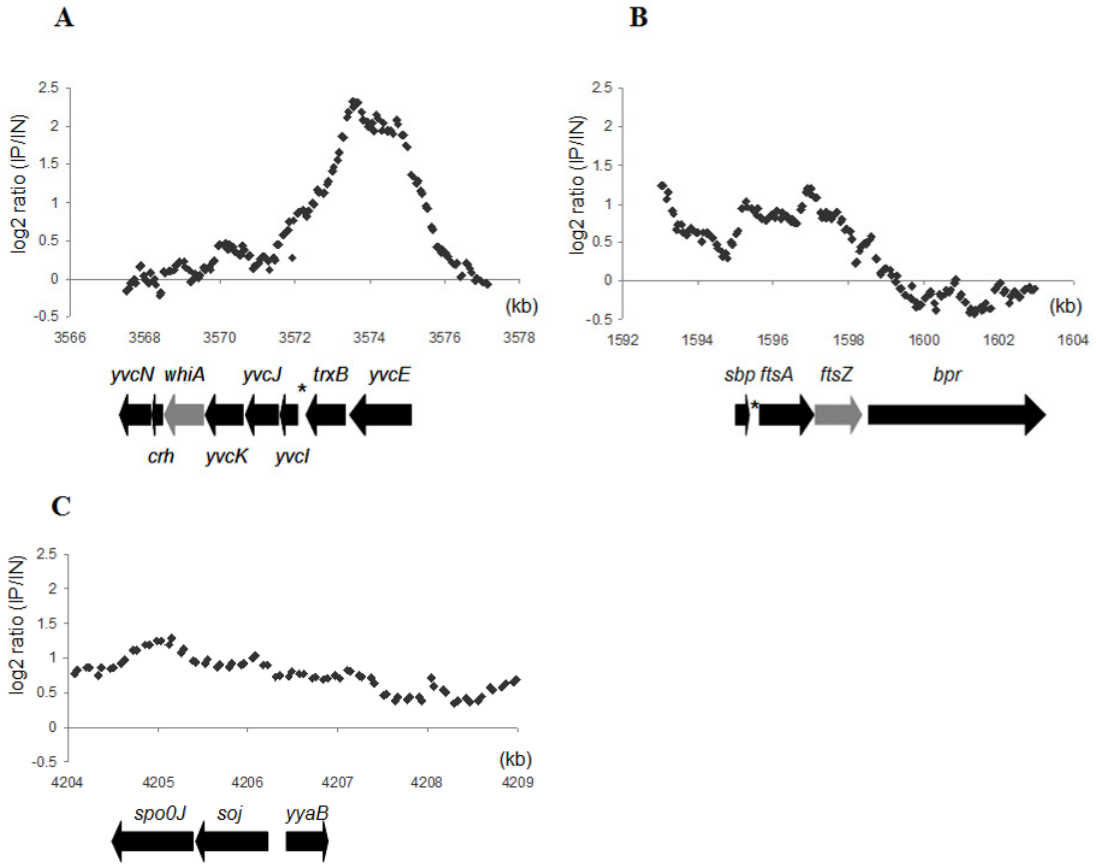

Fig. 5.15 Detailed distribution of WhiA near the *yvcI-N* (A), *ftsAZ* (B) and the *soj-spo0J* (C) operons

The promoter regions of the operons are marked by asterisks.The signal in graph (**A**) is concentrated in the region of *yvcE* and *trxB* genes. The protein does not seem to bind to the *ftsAZ* (**B**) or *soj-spo0J* (**C**) regions.

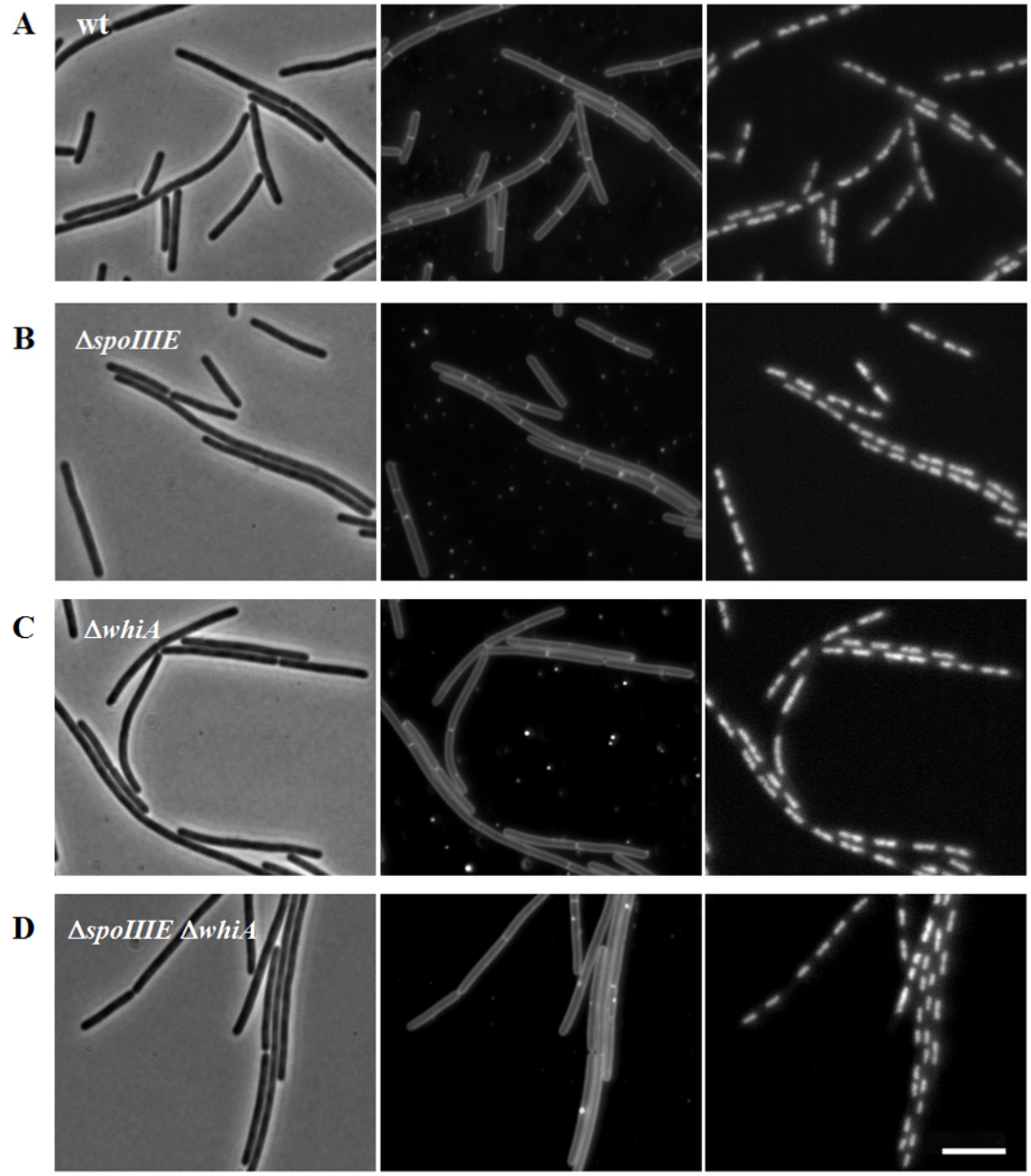

Fig. 5.16 Deletion of spoIIIE does not alter the *whiA* mutant phenotype
Exponentially growing wild type (**A**), Δ*spoIIIE* (**B**), Δ*whiA* (**C**), and Δ*spoIIIE* Δ*whiA* (**D**) cells in LB medium at 37 ºC were stained with nile red (membrane, middle panels) and DAPI (DNA, right panels) and subjected to fluorescent microscopy. Strains used for this study: KS2, KS381, KS207, KS559. Scale bar 5 µm.

evidence from Dr. Stephan Gruber suggest that *trnS* (tRNA), which is bound by WhiA, attracts WhiA when it is placed on pLOSS* plasmid. These initial results imply that WhiA binds to specific regions with no regard to the topological context (either plasmid or out-of locus location), suggesting it recognizes specific DNA motifs and binds them. It would be interesting to experimentally test the proposed consensus sequence for WhiA binding, mainly *in vivo* (using truncated versions of DNA fragments, placing them on e. g. pLOSS plasmid).

5.2.6 WhiA-His6 binds DNA *in vitro*

To determine whether WhiA binds DNA directly, we purified the protein as a WhiA-His_6 tagged fusion in *E. coli*. We found that WhiA-His_6 is toxic for *E. coli* and precipitates from solutions easily. In addition, purified protein always carried contaminant DNA from *E. coli*. However, by preparing freshly purified WhiA-His_6 it was possible to perform an EMSA (electrophoretic mobility shift assay) experiment. After elution, the fraction containing the highest WhiA-His_6 concentration (~0.2 mg/ml on SDS PAGE gel) was used for EMSA using an agarose gel (Fig. 5.17). At this stage of our research, we had not yet obtained the ChIP-on-chip data results, and that is why the DNA fragments used for EMSA corresponded to the region upstream of *whiA* (A) and the *whiA* intragenic region (B). As shown in Fig. 5.17A, the mobility of DNA fragments correlated with the amount of protein added, suggesting a direct binding of the DNA by WhiA-His_6. The fusion protein is not fully functional since it does not recover growth of the Δ*whiA* Δ*zapA* double mutant strain, and such strain is filamentous. Furthermore, the DNA sequences used for EMSA were later not found to be enriched by WhiA in a ChIP-on-chip experiment (Fig. 5.15A), suggesting that the WhiA-His_6 binds DNA unspecifically. However, further experiments are required to elucidate this.

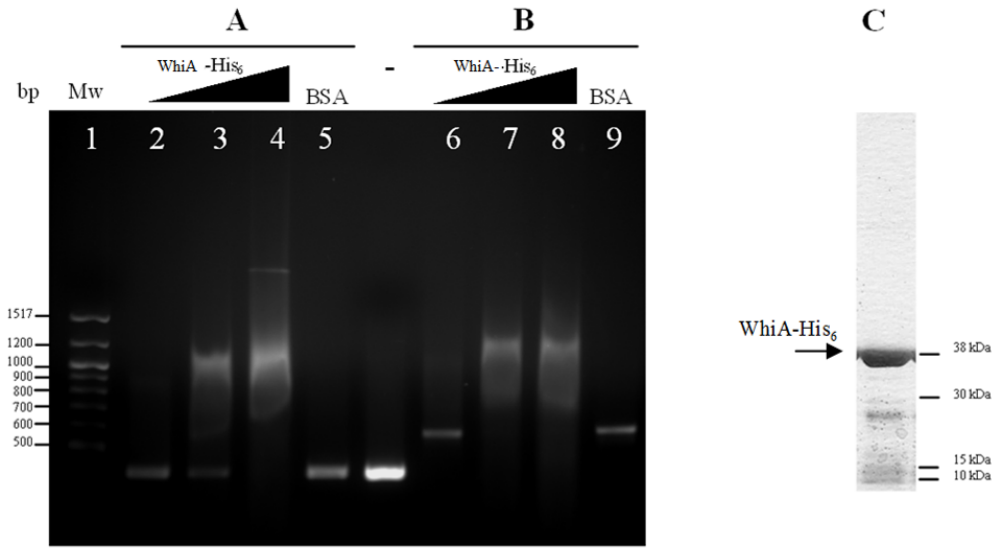

Fig. 5.16 WhiA^{His6} binds DNA *in vitro*
(**A**) The 412-bp DNA fragment upstream of *whiA* and (**B**) the 571-bp *whiA* intragenic regions were mixed with an increasing amount of the protein (lanes 2-4 and 6-8) (described in Materials and Methods) and used for EMSA in 1.5 % agarose gel. BSA was added to DNA as a negative control (lanes 5 and 9). A DNA shift is not observed at the lowest WhiA^{His6} concentration (lanes 2,6). With increasing protein concentrations the DNA bands disappear and in (A) there is a new low mobility band visible. (**C**) A fraction of the purified WhiA^{His6} used for EMSA analysis run on PAGE.

5.3 Discussion

In the *whiA* mutant, when forced to grow as filament by FtsZ depletion, the nucleoids are widely spaced when compared to wild type (44%). This result strongly implies that the lack of WhiA leads to a delay in nucleoid segregation or to a defect in nucleoid architecture.

The lack of known segregation proteins, Spo0J or SMC, leads to formation of anucleate cells resulting from corrupted segregation (Britton and Grossman, 1999; Ireton *et al.*, 1994), however *whiA* mutant does not form anucleate cells. This might be due to presence of other redundant/functional counterpart(s) of WhiA. We sought to uncover this by deleting *spoIIIE*, encoding a translocase that pumps trapped chromosomes through the divisome machinery and thus rescues unsegregated chromosomes from bisection (Britton and Grossman, 1999; Sharpe and Errington, 1995). However, we did not notice any striking phenotype of a Δ*spoIIIE* Δ*whiA* mutant, indicating that the WhiA effect on segregation is not strong enough to be unmasked by *spoIIIE* deletion. SftA is another protein with similar function to SpoIIIE (Biller and Burkholder, 2009; Kaimer *et al.*, 2009), but presumably acts earlier than SpoIIIE, yet before septum closure (Kaimer *et al.*, 2009). It may be possible that SftA is capable to avoid bisection of chromosomes in a Δ*spoIIIE* Δ*whiA* mutant. It would be interesting to test the phenotype of a triple Δ*sftA* Δ*spoIIIE* Δ*whiA* mutant.

The other speculation, that WhiA might be involved in chromosome architecture is based on the nucleoid dimensions in *whiA* mutant cells. Furthermore, in the sporogenic hyphae of *S. coelicolor*, the lack of $WhiA^{Sco}$ causes delocalization of ParB and the DNA becomes dispersed (Flardh *et al.*, 1999), suggesting a role for $WhiA^{Sco}$ in chromosome organization. In *B. subtilis*, however, the mutation of *whiA* does not induce dislocalization of Spo0J and the nucleoids are only mildly affected when compared to $whiA^{Sco}$ mutant. This discrepancy may have to do with the linearity of chromosomes of *S. coelicolor*, or multiplicity of nucleoids (>50 per one aerial hypha).

It has been shown that proteins implicated in chromosome architecture are also important in, for example, recombination, since it often requires DNA bending (Rowland *et al.*, 2005). This would correspond with detected increased sensitivity to UV and lower genetic competence of a *whiA* mutant. However, these results must be tested further, particularly whether DNA damage is lethal for *whiA* mutant

independently of YneA, and to show whether lowered competence is imposed by defects in recombination.

The evidence implicates the chromosome replication rate as important in cells lacking WhiA due to the synthetic lethal effects of Δ*whiA* Δ*spo0J*/*soj* and Δ*whiA* Δ*yabA* double mutants. In these strains the DNA segregation is not disrupted since we have not observed anucleate cells or frequently bisected chromosomes. WhiA also does not seem to alter the replication initiation rate since the occurence of *oriC* and *ter* sites is concurrently decreased (23-24%) in *whiA* mutant cells depleted of FtsZ, and marker frequency analysis has shown similar *ori*/*ter* ratios in wild type and *whiA* mutant cells. This suggests that the block in division in these double mutants is not caused by interference and hyperinitiation of replication. Nevertheless, WhiA becomes essential upon DNA overinitiation.

We also considered that WhiA might influence the progression of replication. In vegetatively growing 'healthy' cells the replication machinery becomes stalled frequently in every cell cycle and replication must be reactivated (reviewed in Cox *et al.*, 2000; Kreuzer, 2005). Recently, Bernard *et al*. have shown that the introduction of a replication roadblock into the chromosome induces cell and nucleoid elongation and the nucleoids fill the cellular volume (Bernard *et al.*, 2010). Similarly, *whiA* mutant cells and their nucleoids are longer. Mutation of *priA*, which is responsible for replication restart, has pleiotropic effects including poor cell viability and sensitivity to UV radiation (Polard *et al.*, 2002). WhiA was not found to be a part of the complex of proteins around PriA (Costes *et al.*, 2010). Moreover, the ratio of *ori*/*ter* in *whiA* mutants is not altered, suggesting the replication is not slowed down rapidly. These data suggest that the lack of WhiA probably does not decrease the efficiency of stalled replication forks reactivation.

The *dif* site is near the terminus of replication and is essential for resolution of chromosome dimers that arise from recombination between sister chromatids (Kuempel *et al.*, 1991). We think WhiA might be involved in this process. Firstly, ChIP-on-chip analysis revealed that WhiA binds to the region of *xynD* region which is close to the *dif* site (1915 bp) and may become even more proximal to the *dif* as the DNA bends. In *B. subtilis*, the two recombinases essential for chromosome dimer resolution are CodV and RipX (Sciochetti *et al.*, 2001; Sciochetti *et al.*, 1999). The absence of these proteins or the *dif* site results in filamentous cells and frequently unsegregated chromosomes

(14-25% of cells with partitioning defects) and they also form anucleate cells (0.83-1.6%) (Sciochetti *et al.*, 2001). We have not observed such a phenotype in *whiA* mutants, suggesting WhiA may fulfil only additional function during this process. Secondly, longer nucleoids separated by longer distances in a *whiA* mutant might be due to a delay in chromosome resolution. Thirdly, WhiA may be involved in recombination since it does not recover growth after exposure to UV radiation, although we must analyze whether YneA induction during SOS response does not exaggerate the division phenotype of a *whiA* mutant. Further investigation is needed to explore implementation of WhiA in chromosome dimer resolution.

B. subtilis translocase SpoIIIE is dispensable for recombination at *dif* site (Sciochetti *et al.*, 2001). This might be the reason why we did not detect a partitioning defect when *spoIIIE* and *whiA* genes were deleted.

WhiA contains two DNA-binding domains, and both are required for sufficient DNA binding (Fig. 3.15 and Fig. 4.1) (Kaiser *et al.*, 2009; Knizewski and Ginalski, 2007). The N-terminal domain contains two LADLIDADG motifs and a unique N-terminal α-helix that makes contacts with them (Kaiser *et al.*, 2009). The C-terminal domain which shares a helix-turn-helix fold is also very conserved (Knizewski and Ginalski, 2007). We have constructed several WhiA truncations (fused to GFP) to determine whether both domains are required for the function of WhiA in cell division (data not shown). However, all were dysfunctional and showed a dispersed GFP signal (truncations of WhiA which is 316 amino acid full length: 39-316, 138-316, 184-316, 1-279, 1-255, 1-202). Western blot analysis indicated that the fusions were degraded. These preliminary data suggest that a full length WhiA is required for its function; however, this must be tested further. It was indicated that DNA must be bent to allow binding by the helix-turn-helix of WhiA (Kaiser *et al.*, 2009). The authors concluded that it is possible that WhiA utilizes the N-terminal domain for this purpose, and the inability to construct functional truncations of WhiA supports this notion. It would be interesting to investigate point mutants in the conserved amino acid residues of WhiA (Fig. 3.15, in boxes).

Chapter 6

Identification of suppressor mutations of Δ*whiA*

6.1 Introduction

To gain more insight into the function of WhiA we set out to search for mutations that suppress the deleterious Δ*whiA* Δ*zapA* double mutant phenotype. In fact the Δ*whiA* Δ*zapA* double mutant forms spontaneous mutants with high frequencies. It is unlikely these spontaneous mutants are revertants since we used complete gene knock-outs. We tried to use transposon mutagenesis to map these mutations but with no success. We therefore employed our synthetic lethal screen but this time selected for mutants that would have lost the pLOSS plasmid and would be white on X-gal plates. We took the Δ*whiA* Δ*zapA* double mutant which was kept fit by the presence of the pLOSS plasmid that contained *yvcL (whiA)*, and thus formed blue colonies on X-gal plates. This strain was then subjected to a transposon mutagenesis, with the aim of identifying white colonies, in which the pLOSS-YvcL was no longer essential.

6.2 Results

We used strain KS742 that contained a markerless *whiA* deletion, a tetracycline resistance cassette that replaced the entire *zapA-yshB* operon, the pLOSS-YvcL plasmid and a deletion of the *lacA* gene. Following transposon mutagensis, 36, 000 colonies were screened on X-gal plates. 82 white colonies were selected and their chromosomal DNA was backcrossed into a conditional *whiA* Δ*zapA* mutant strain (KS856). Seven clones contained a mutation that enabled strain KS856 to grow in the absence of IPTG (Fig. 6.1). The transposon insertions were mapped by reversed PCR, as previously described, and the genes that contained a transposon insertion are listed in Table 6.1.

gene	function	cellular process
braB	possible branched aminoacid transporter	amino acid metabolism
ggaB	sugar transferase	glycosylation of teichoic acids
gtaB (found 2x)	UTP-glucose-1-phosphate uridyltransferas	glc1-P→UDP-glc conversion
pgcA	phosphoglucomutase	couples cell division to cell mass
speD	S-adenosyl-methionine decarboxylase	aminoacid transport & metabolism
yusB	methionine transporter	amino acid metabolism

Table 6.1 Summary of supressor mutations of Δ*whiA* Δ*zapA* found in the suppressor screen
Two different transposon insertions were found in the *gtaB* gene. References in text.

6.2.1 Characterization of the Δ*whiA* Δ*zapA* suppressors

To check whether the suppressor mutations restored normal cell division, the strains were grown in LB without IPTG and examined by microscopy (Fig. 6.2). The strongest restoration of cell division (cell length) was observed with the transposon insertions in *pgcA* and *gtaB*. These genes have been shown to be involved in the coordination of growth rate and cell division (Weart *et al.*, 2007), and they are involved in maintaining UDP-Glucose levels, which is a precursor of wall teichoic and lipoteichoic acids

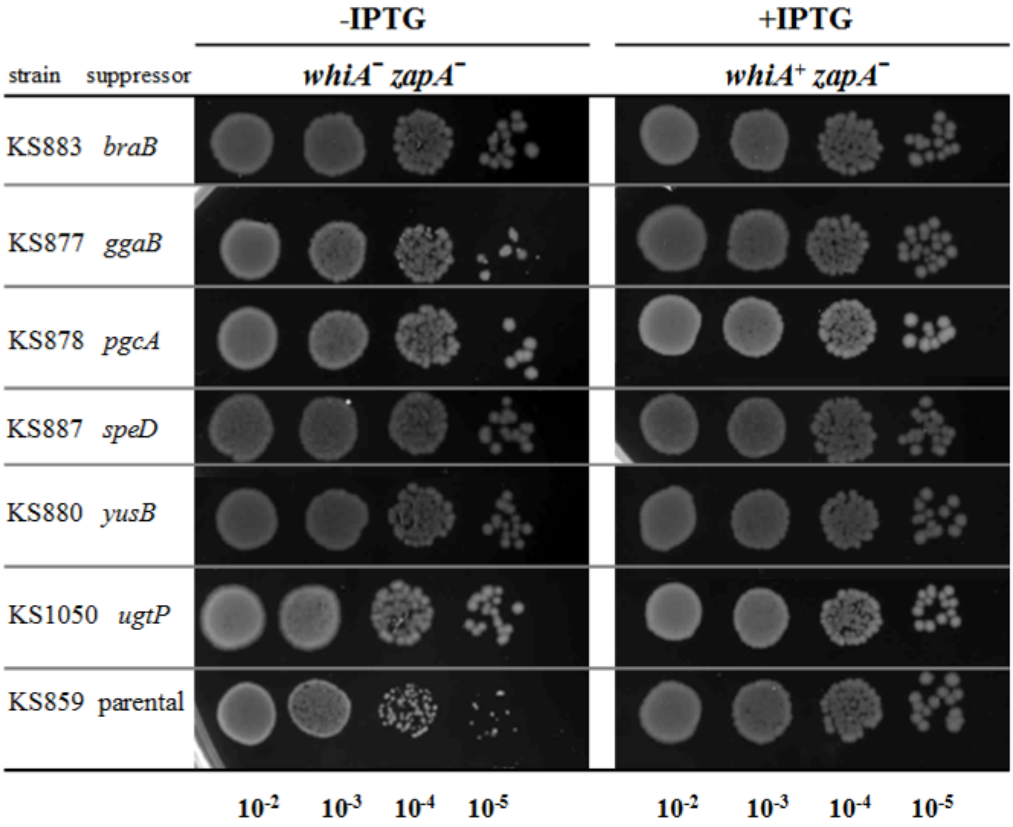

Fig. 6.1 Suppressors of Δ*whiA* Δ*zapA*
Suppressor mutations were introduced into strain KS859 (Δ*zapA* P_{spac}-*whiA aprE*::*lacI*) and tested for colony formation on plates with or without IPTG. All strains grow well in the presence of IPTG (*whiA*$^+$ background). The introduction of transposon mutations in *braB*, *ggaB*, *pgcA*, *speD*, and *yusB*, recovered growth of KS859 despite the absence of IPTG (left panel). Introduction of a *ugtP* mutation gave similar results.

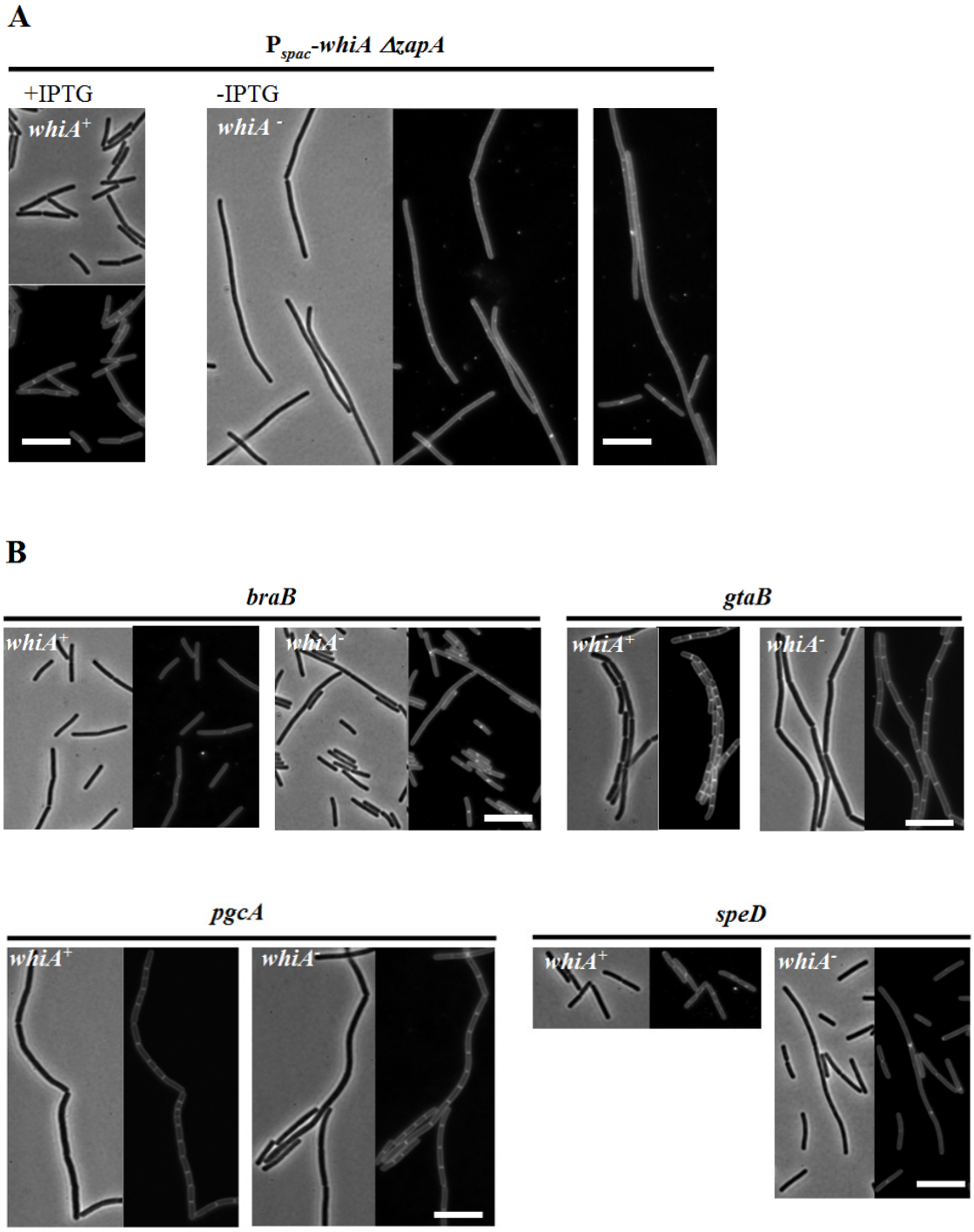

Fig. 6.2 Phenotypes of suppressed Δ*whiA* Δ*zapA* mutants
Strains were depleted for WhiA in liquid LB medium. (**A**) Formation of filamentous cells in parental strain KS859 (P_{spac}-*yvcL* Δ*zapA aprE*::*lacI*) in the absence of IPTG. The cells lack septa as judged from a membrane stain (nile red). (**B**) Introducing transposon insertions in *braB*, *gtaB*, *pgcA* or *speD* (strains KS883, KS875, KS878, KS887, respectively) recovered the ability to form septa when grown without IPTG. Scale bars 10 µm.

(Lazarevic *et al.*, 2005) (Fig. 1.9 and 6.5). The key regulator in this pathway is UgtP. This is a multifunctional protein that is a sugar transferase involved in the synthesis of an anchor for the lipoteichoic acids (Jorasch *et al.*, 1998; Lazarevic *et al.*, 2005), it catalyzes the last step in the synthesis of glycolipids (Jorasch *et al.*, 1998; Price *et al.*, 1997) and it also binds directly to FtsZ and inhibits assembly of protofilaments (Weart *et al.*, 2007). Mutations in *pgcA*, *gtaB* and *ugtP* result in an increase in division frequency and shorter cells (Lazarevic *et al.*, 2005; Weart *et al.*, 2007). Since we found transposon insertions in *pgcA* and *gtaB*, we wondered whether a deletion of *ugtP* would have a similar effect. An *ugtP* mutation was introduced into strain KS859 and tested for IPTG dependency. As shown in Fig. 6.1, deletion of *ugtP* suppresses the reduction in growth of a Δ*whiA* Δ*zapA* mutant as well. These data suggest that the synthetic lethality of a Δ*whiA* Δ*zapA* might originate from a disability to coordinate cell-division timing with the cellular metabolic status. At this stage however, we cannot definitely exclude that the suppression is imposed by altered cell wall structure.

6.2.2 Shortening of cell length by mutations in *braB*, *ggaB*, *gtaB, pgcA, and ugtP*

As shown above (Fig. 3.3), *whiA* mutants form longer cells, presumably as a result of delayed division. We examined whether the transposon suppressors were able to stimulate division and reduce the average cell length of a *whiA* mutant. As shown in Table 6.2, it is clear that Δ*whiA* cells are shorter in the presence of disruptions of *braB*, *ggaB*, *gtaB*, *pgcA* or *ugtP*.

Since most suppressors reduce the length of *whiA* mutant cells, the question arises as to whether the transposon mutations would suppress the other filamentous double mutants including Δ*ezrA* Δ*whiA* and Δ*minJ* Δ*whiA*. To test this we constructed strains bearing an inducible P_{spac}-*whiA*, one of the transposon mutations, and a deletion of *ezrA* or *minJ*. From the combinations tested, only mutations in *pgcA* and *gtaB* were able to restore normal growth in an *ezrA* mutant depleted of WhiA (Fig. 6.3). The recovered cells form minicells, which we have not observed in suppressed Δ*whiA* Δ*zapA* backgrounds. We have not yet tested the *ugtP* mutation but it is very likely that it would also rescue Δ*ezrA* Δ*whiA* mutant.

strain	genotype	cell length (μm)	±SD	% relative to wt
KS2	wt	4.92	1.16	100
KS696	Δ*whiA*	7.48	3.50	152
KS904	Δ*braB* Δ*whiA*	4.44	1.18	90
KS1025	Δ*ggaB* Δ*whiA*	5.27	1.66	107
KS902	Δ*gtaB* Δ*whiA*	4.69	1.13	95
KS903	Δ*pgcA* Δ*whiA*	4.48	1.19	91
KS905	Δ*speD* Δ*whiA*	6.80	4.10	138
KS1015	Δ*ugtP* Δ*whiA*	3.99	1.00	81
KS1026	Δ*yusB* Δ*whiA*	5.81	4.42	118

Table 6.2 Cell lengths of *whiA* mutants combined with suppressor mutations
Exponentially growing cells were stained with the fluorescent membrane stain (FM5-95) for cell length measurement. SD = standard deviation.

Next, we examined whether the strongest suppressors, Δ*pgcA* and Δ*ugtP*, would be able to suppress the lethal Δ*yabA* Δ*whiA* combination as well. Mutations in either *pgcA* or *ugtP* were introduced into strains KS1063 and KS1064 and the resulting strains were tested for IPTG dependency. As shown in Fig. 6.4, neither Δ*pgcA* (KS1071) nor Δ*ugtP* (KS1069) were able to rescue Δ*yabA* mutant cells depleted of WhiA. We noticed that strain KS1071 does not grow well on media with IPTG. It was shown that the loss of *pgcA* leads to an increased frequency of bisected nucleoids, which is a consequence of uncoupled Z-ring assembly from chromosome segregation (Weart *et al.*, 2007). Possibly the combination of Δ*pgcA* with the DNA replication overinitiation caused by Δ*yabA* poses a severe pressure on the coordination of chromosome segregation and cell division. However, a control strain where the WhiA expression remained intact (strain KS1072), grows well. We think the Δ*pgcA* Δ*yabA* mutant requires also optimal WhiA levels for growth, but this must be tested further.

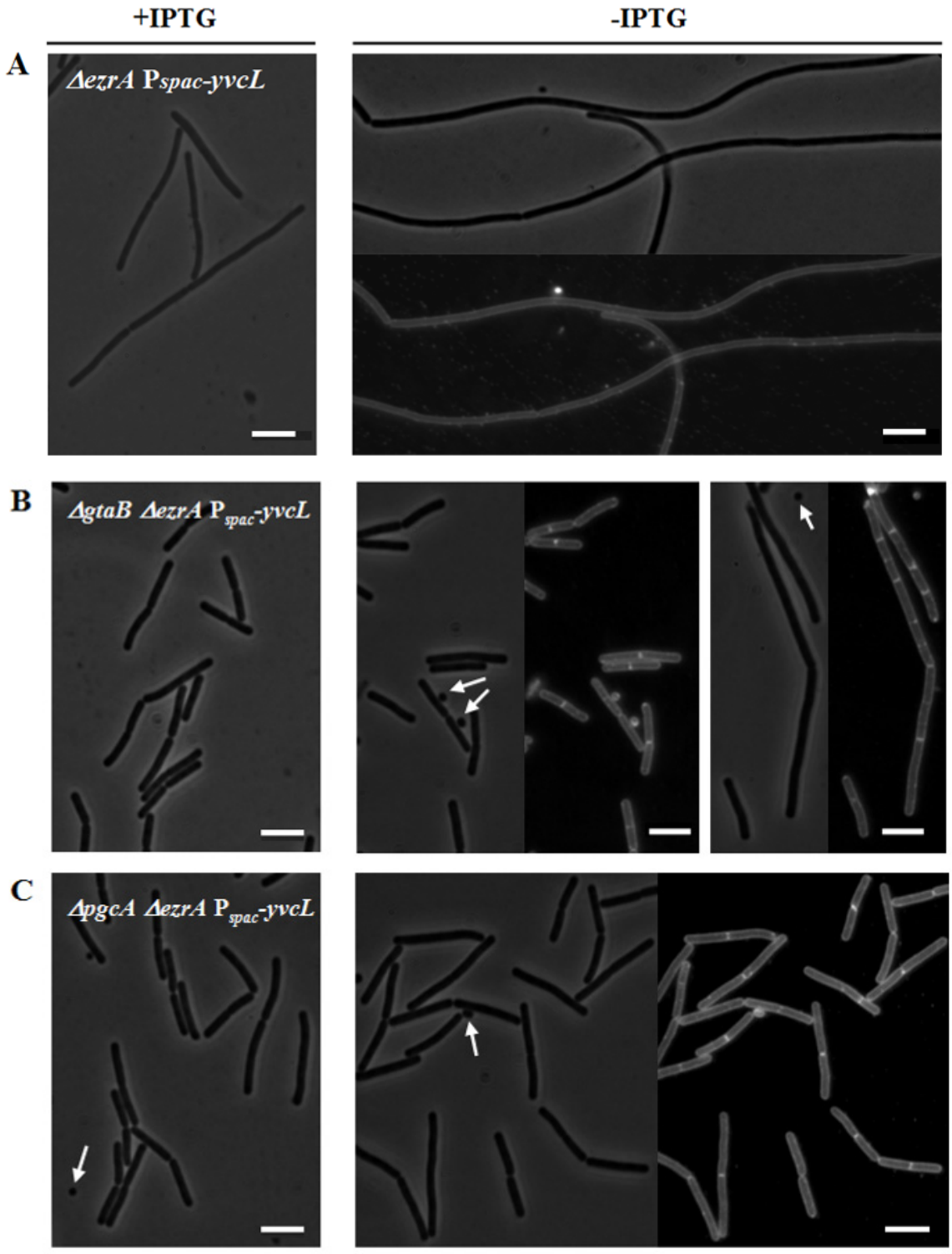

Fig. 6.3 Deletions of *pgcA* and *gtaB* rescue the Δ*ezrA* Δ*yvcL* double mutant
(**A**) Parental strain KS873 (Δ*ezrA* P_{spac}-*yvcL lacI*), (**B**) KS925 bearing also transposon insertion in *gtaB*, and finally (**C**) KS927 carrying a transposon insertion in *pgcA*. Cells were grown in LB with IPTG (left panels), or without IPTG (right panels). Suppressor mutations *gtaB* and *pgcA* reverse the filamentous phenotype of Δ*ezrA* Δ*whiA* double mutant (B) and (C). Minicells are indicated by arrows. Scale bars 5 μm.

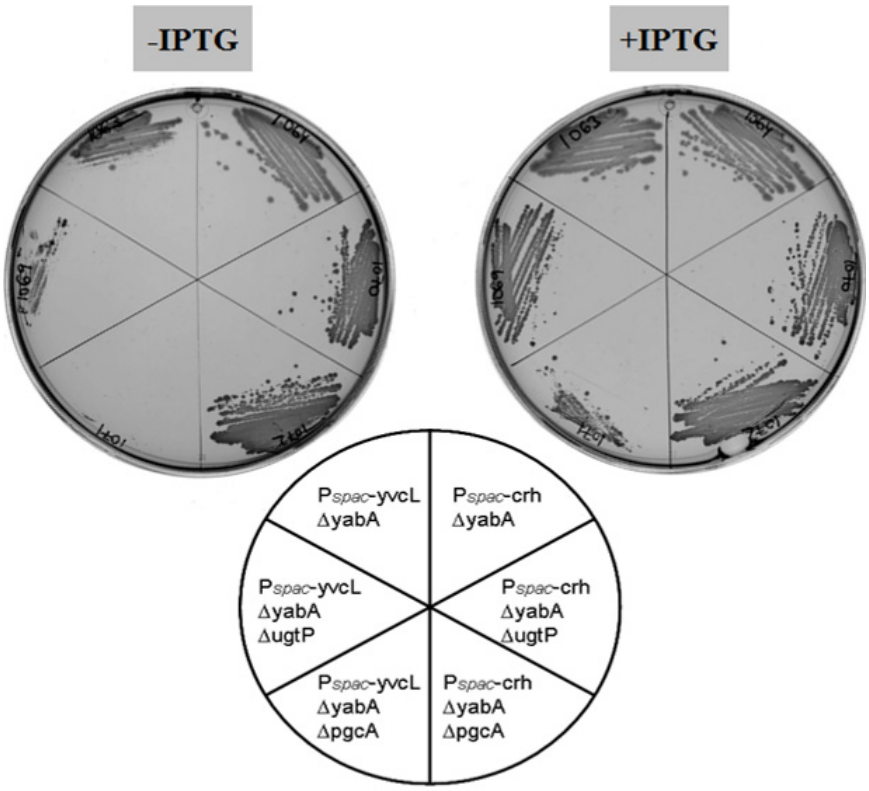

Fig. 6.4 Disruption of *pgcA* or *ugtP* does not rescue the Δ*whiA* Δ*yabA* double mutant
Strains containing a *yabA* deletion and P_{spac}-*whiA* or P_{crh}-*crh* were streaked on plates with or without IPTG (clockwise: KS1064, KS1070, KS1072, KS1071, KS1069, KS1063).

6.3 Discussion: Possible mechanisms of suppression

PgcA and GtaB are directly involved in the conversion of Glucose 6-P to UDP-Glucose (UDP-Glc), which is the substrate for the synthesis of cell wall polymers such as minor and major wall teichoic acids (WTA) (Honeyman and Stewart, 1989; Lazarevic *et al.*, 2002; Lazarevic *et al.*, 2005; Mauel *et al.*, 1991) and it is a precursor for synthesis of the membrane anchor of the lipoteichoic acids (LTA) catalyzed by UgtP (Jorasch *et al.*, 1998) (Fig. 6.5). The availability of UDP-Glc modulates the cellular localization of UgtP. At high UDP-Glc concentration UgtP localizes to the midcell where it inhibits the Z-ring formation by a direct interaction with FtsZ (Weart *et al.*, 2007) (see Fig. 1.9). The GgaB protein is involved in a process that utilizes UDP-Glc for glycosylation of teichoic acids (Freymond *et al.*, 2006) and is thus functionally linked to the UgtP-mediated regulation of FtsZ polymerization. It seems that uncoupling cell division from the sensing of the internal UDP-Glc concentration by mutations in *pgcA*, *gtaB*, *ugtP* or *ggaB* forces the otherwise filamentous double mutant Δ*whiA* Δ*zapA* cells to divide.

BraB is a putative branched chain aminoacid transporter. The transposon insertion in the coding region of *braB* might have affected the expression of the neighbouring convergently transcribed gene *ezrA*. The reading direction of the kanamycin marker of the transposon runs in the opposite direction of the *ezrA* gene so it was possible that the *ezrA* expression had been altered. We found that, unlike the *ezrA* mutant (Claessen *et al.,* 2008), the *braB* transposon mutant is not sensitive to high salt concentrations, suggesting that it is unlikely that the transposon insertion inhibits the expression of *ezrA* (data not shown). Moreover, a reduction in *ezrA* expression would make a *whiA* mutant sick. Branched chain aminoacids (BCAA) (leucine, isoleucine, valine) are the most frequent aminoacids in proteins (Shivers and Sonenshein, 2004; Tojo *et al.*, 2005) and are utilized also for the synthesis of membrane lipids (reviewed in Fujita, 2009). They also modulate the activity of a global transcriptional regulator CodY (Shivers and Sonenshein, 2004) by a direct interaction (Tojo *et al.*, 2005). However, we found no medium dependency of the Δ*whiA* Δ*zapA* double mutant (data not shown), suggesting that amino acid availability is an unlikely cause of this synthetic effect.

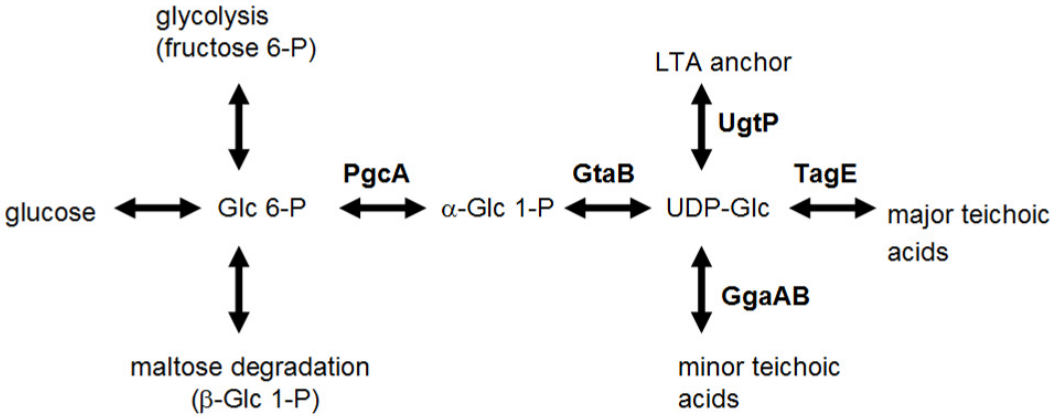

Fig. 6.5 Schematic representation of the metabolic pathway leading to regulation of cell division through UDP-Glucose (UDP-Glc) and UgtP
Glucose 6-P (Glc 6-P) is converted into α-Glc 1-P which is metabolized into uridine-5'-diphosphoglucose (UDP-Glc). UDP-Glc is utilized by various proteins, one of them is UgtP. UgtP is a negative regulator of FtsZ assembly and its cellular localization depends on the concentration of UDP-Glc (see also Fig. 1.9). Hence, UDP-Glc serves as a signal to postpone cell division at high levels of nutrients. Referenced in text. Adapted after (Lazarevic *et al.*, 2005) and (Weart *et al.*, 2007).

Another bypassing mutation was a transposon insertion in *speD*. SpeD is an S-adenosinemethionine decarboxylase involved in the production of spermidine (Sekowska *et al.*, 2000). Spermine and spermidine are important polyamines for DNA synthesis, gene expression and protection of cells from free radicals. The last transposon insertion was identified in a *yusB* gene, encoding for an ABC transporter for methionine that becomes essential for cells grown at low methionine concentrations (Hullo *et al.*, 2004). We have not yet tested these two suppressors in great detail.

The deletion of *whiA* in *B. subtilis* is not manifested by a strong phenotype but it is synthetically sick when combined with mutations in cell division genes. At least in the case of Δ*whiA* Δ*zapA* double mutant, this phenotype can be ameliorated by overexpression of FtsZ. The filamentous phenotype can also be suppressed by the introduction of *pgcA* or *ugtP* mutations which were previously shown to cause recovery of a strain with MinC overexpression (Weart *et al.*, 2007). Since we have found that transposon mutations in these genes suppress the Δ*whiA* Δ*zapA* mutant, this provides more ammunition for a model in which WhiA acts at the level of Z-ring formation.

Our screen for suppressor mutations has not been completed yet and there are more possible adepts to be verified. These preliminary candidates include: *zwf, adaB, lytD* and *gltT* and it might be interesting to inspect them in a detail.

Chapter 7

Final remarks

7.1 Summary

More than a dozen proteins have been shown to regulate the assembly of the FtsZ-ring, which marks the first step in bacterial cell division. In this study, we focused on cell division in the Gram-positive model organism, *B. subtilis*. The aim was to find novel cell division protein(s) using a genetic approach developed in our laboratory. Using this tool called synthetic lethal screen that is based on the instability of a plasmid, we succeeded in discovering a novel cell division protein in *B. subtilis*: YvcL. Based on the strong sequence homology with the *S. coelicolor* protein WhiA^{Sco}, we proposed to rename YvcL to WhiA. We found that WhiA is important for Z-ring formation, and thus acts early in cell division. This was supported by several lines of evidence. Firstly, mutations in other cell division mutants (*zapA*, *ezrA*, *minCD* or *noc*) have detrimental effect when combined with a *whiA* knockout, and this was caused by a strong reduction in Z-rings in these double mutants. Secondly, the *whiA* mutant is hypersensitive when FtsZ is expressed at low levels. Thirdly, FtsZ overexpression restores division of the Δ*whiA* Δ*zapA* double mutant. And fourthly, deletion of *ugtP*, encoding a negative regulator of Z-ring assembly, ameliorates the Δ*whiA* Δ*zapA* double mutant. The deletion of *whiA*^{Sco} in *S. coelicolor* has been associated with sporulation deficiency (Ainsa *et al.*, 1999; Flardh *et al.*, 1999). In *B. subtilis*, however, deletion of *whiA* does not block sporulation. Moreover, we found that WhiA is constitutively expressed. WhiA^{Sco} has been postulated to be a transcriptional regulator (Ainsa *et al.*, 2000; Knizewski and Ginalski, 2007) so we tested whether this was the case for WhiA. The whole genome microarray analysis of a *B. subtilis whiA* mutant and the conjoined verification results do not support a role for WhiA as a transcriptional regulator. Nevertheless, WhiA binds DNA, and *in vivo* fluorescently labelled WhiA forms faint spots occupying the nucleoid area. Using ChIP-on-chip analysis several DNA binding sites were revealed. They covered both chromosome arms and only positions 2-2.8 Mb on the chromosomal map were lacking strong WhiA binding. Many strong peaks on the array corresponded to strongly transcribed regions around *oriC*. WhiA binds near the *dif* site, which is essential for resolution of chromosome dimers. We proposed a possible consensus sequence for WhiA binding. We also found that deletion of *whiA* causes sensitization to DNA overreplication since introduction of mutations in *soj*/*spo0J* and *yabA* into *whiA* mutant cells had detrimental effects on cell growth. Moreover, cells lacking WhiA display morphological changes in the size and positioning of nucleoids that become

longer and are separated by wider spaces. We think that WhiA regulates processes that are important for maintenance of chromosomes or chromosome segregation, but how this is related to cell division we do not know.

7.2 Possible dual implementation of WhiA

Based on our results, we think that WhiA is a protein with two, apparently distinct functions. This is supported by the fact that Δ*pgcA* and Δ*ugtP* can suppress lethality of the Δ*whiA* Δ*zapA* double mutant strain, yet they fail to restore growth of a Δ*whiA* Δ*yabA* double mutant. Moreover, overexpression of FtsZ only partially rescues a Δ*whiA* Δ*zapA* mutant, and although cell division is restored, growth rate is still affected. So what is the function of WhiA in cell division? WhiA acts early during the cell division process and promotes the FtsZ ring assembly (see chapter 3.3). As yet it is unclear how exactly WhiA cooperates in this process. FtsZ levels remain constant in a *whiA* mutant, therefore we assume that other cell division proteins acting on FtsZ polymerization may be affected. WhiA is also involved in chromosome dynamics possibly at the level of chromosome segregation, and/or architecture. It might be that this role indirectly influences cell division. One example is induction of SOS response protein YneA (Kawai *et al.*, 2003), although this is not likely since the phenotype of *whiA* mutant is YneA independent. The other possibility is the DnaA-directed expression of FtsL which is an essential component of the divisome (Goranov *et al.*, 2005). This is supported by the fact that WhiA interacts with Spo0J and Soj proteins that modulate the activity of DnaA (Murray and Errington, 2008). This would make WhiA one of the few proteins that link chromosome replication with cell division and it would be interesting to study this possibility.

7.3 Future prospects

Since the structure of $WhiA^{Tm}$ (from *T. maritima*) is available (Kaiser *et al.*, 2009), it may now be feasible to find mutants in WhiA that can separate both activities, one in cell division and one in chromosome dynamics. This might shed more light into pleiotropic effects of WhiA.

Since WhiA is a conserved protein, solving its function in *B. subtilis* might make possible further investigation of cell division and development in other Gram-positive bacteria such as *Streptomyces* spp.

References

Aarsman, M.E., Piette, A., Fraipont, C., Vinkenvleugel, T.M., Nguyen-Disteche, M., and den Blaauwen, T. (2005). Maturation of the Escherichia coli divisome occurs in two steps. Molecular microbiology *55*, 1631-1645.

Abuhammad, A.M., Lowe, E.D., Fullam, E., Noble, M., Garman, E.F., and Sim, E. (2010). Probing the architecture of the Mycobacterium marinum arylamine N-acetyltransferase active site. Protein Cell *1*, 384-392.

Adams, D.W., and Errington, J. (2009). Bacterial cell division: assembly, maintenance and disassembly of the Z ring. Nature reviews *7*, 642-653.

Ainsa, J.A., Parry, H.D., and Chater, K.F. (1999). A response regulator-like protein that functions at an intermediate stage of sporulation in Streptomyces coelicolor A3(2). Molecular microbiology *34*, 607-619.

Ainsa, J.A., Ryding, N.J., Hartley, N., Findlay, K.C., Bruton, C.J., and Chater, K.F. (2000). WhiA, a protein of unknown function conserved among gram-positive bacteria, is essential for sporulation in Streptomyces coelicolor A3(2). Journal of bacteriology *182*, 5470-5478.

Anderson, D.E., Gueiros-Filho, F.J., and Erickson, H.P. (2004). Assembly dynamics of FtsZ rings in Bacillus subtilis and Escherichia coli and effects of FtsZ-regulating proteins. Journal of bacteriology *186*, 5775-5781.

Arigoni, F., Duncan, L., Alper, S., Losick, R., and Stragier, P. (1996). SpoIIE governs the phosphorylation state of a protein regulating transcription factor sigma F during sporulation in Bacillus subtilis. Proc Natl Acad Sci U S A *93*, 3238-3242.

Arigoni, F., Pogliano, K., Webb, C.D., Stragier, P., and Losick, R. (1995). Localization of protein implicated in establishment of cell type to sites of asymmetric division. Science *270*, 637-640.

Augustin, L.B., Jacobson, B.A., and Fuchs, J.A. (1994). Escherichia coli Fis and DnaA proteins bind specifically to the nrd promoter region and affect expression of an nrd-lac fusion. Journal of bacteriology *176*, 378-387.

Austin, S., and Abeles, A. (1983). Partition of unit-copy miniplasmids to daughter cells. I. P1 and F miniplasmids contain discrete, interchangeable sequences sufficient to promote equipartition. J Mol Biol *169*, 353-372.

Autret, S., Levine, A., Holland, I.B., and Seror, S.J. (1997). Cell cycle checkpoints in bacteria. Biochimie *79*, 549-554.

Autret, S., Nair, R., and Errington, J. (2001). Genetic analysis of the chromosome segregation protein Spo0J of Bacillus subtilis: evidence for separate domains involved in DNA binding and interactions with Soj protein. Molecular microbiology *41*, 743-755.

Bailey, T.L., Boden, M., Buske, F.A., Frith, M., Grant, C.E., Clementi, L., Ren, J., Li, W.W., and Noble, W.S. (2009). MEME SUITE: tools for motif discovery and searching. Nucleic acids research *37*, W202-208.

Barak, I., Behari, J., Olmedo, G., Guzman, P., Brown, D.P., Castro, E., Walker, D., Westpheling, J., and Youngman, P. (1996). Structure and function of the Bacillus

SpoIIE protein and its localization to sites of sporulation septum assembly. Molecular microbiology *19*, 1047-1060.

Barak, I., and Wilkinson, A.J. (2005). Where asymmetry in gene expression originates. Molecular microbiology *57*, 611-620.

Barak, I., and Wilkinson, A.J. (2007). Division site recognition in Escherichia coli and Bacillus subtilis. FEMS Microbiol Rev *31*, 311-326.

Barak, I., and Youngman, P. (1996). SpoIIE mutants of Bacillus subtilis comprise two distinct phenotypic classes consistent with a dual functional role for the SpoIIE protein. Journal of bacteriology *178*, 4984-4989.

Bates, D., and Kleckner, N. (2005). Chromosome and replisome dynamics in E. coli: loss of sister cohesion triggers global chromosome movement and mediates chromosome segregation. Cell *121*, 899-911.

Bath, J., Wu, L.J., Errington, J., and Wang, J.C. (2000). Role of Bacillus subtilis SpoIIIE in DNA transport across the mother cell-prespore division septum. Science *290*, 995-997.

Beall, B., and Lutkenhaus, J. (1992). Impaired cell division and sporulation of a Bacillus subtilis strain with the ftsA gene deleted. Journal of bacteriology *174*, 2398-2403.

Ben-Yehuda, S., Fujita, M., Liu, X.S., Gorbatyuk, B., Skoko, D., Yan, J., Marko, J.F., Liu, J.S., Eichenberger, P., Rudner, D.Z*., et al.* (2005). Defining a centromere-like element in Bacillus subtilis by Identifying the binding sites for the chromosome-anchoring protein RacA. Mol Cell *17*, 773-782.

Ben-Yehuda, S., and Losick, R. (2002). Asymmetric cell division in B. subtilis involves a spiral-like intermediate of the cytokinetic protein FtsZ. Cell *109*, 257-266.

Ben-Yehuda, S., Rudner, D.Z., and Losick, R. (2003). RacA, a bacterial protein that anchors chromosomes to the cell poles. Science *299*, 532-536.

Bender, A., and Pringle, J.R. (1991). Use of a screen for synthetic lethal and multicopy suppressee mutants to identify two new genes involved in morphogenesis in Saccharomyces cerevisiae. Mol Cell Biol *11*, 1295-1305.

Bernard, R., Marquis, K.A., and Rudner, D.Z. (2010). Nucleoid occlusion prevents cell division during replication fork arrest in Bacillus subtilis. Molecular microbiology *78*, 866-882.

Bernhardt, J., Volker, U., Volker, A., Antelmann, H., Schmid, R., Mach, H., and Hecker, M. (1997). Specific and general stress proteins in Bacillus subtilis--a two-deimensional protein electrophoresis study. Microbiology (Reading, England) *143*, 999-1017.

Bernhardt, T.G., and de Boer, P.A. (2004). Screening for synthetic lethal mutants in Escherichia coli and identification of EnvC (YibP) as a periplasmic septal ring factor with murein hydrolase activity. Molecular microbiology *52*, 1255-1269.

Bernhardt, T.G., and de Boer, P.A. (2005). SlmA, a nucleoid-associated, FtsZ binding protein required for blocking septal ring assembly over Chromosomes in E. coli. Mol Cell *18*, 555-564.

Beuria, T.K., Mullapudi, S., Mileykovskaya, E., Sadasivam, M., Dowhan, W., and Margolin, W. (2009). Adenine nucleotide-dependent regulation of assembly of bacterial tubulin-like FtsZ by a hypermorph of bacterial actin-like FtsA. The Journal of biological chemistry *284*, 14079-14086.

Bi, E., and Lutkenhaus, J. (1993). Cell division inhibitors SulA and MinCD prevent formation of the FtsZ ring. Journal of bacteriology *175*, 1118-1125.

Bigot, S., Sivanathan, V., Possoz, C., Barre, F.X., and Cornet, F. (2007). FtsK, a literate chromosome segregation machine. Molecular microbiology *64*, 1434-1441.

Biller, S.J., and Burkholder, W.F. (2009). The Bacillus subtilis SftA (YtpS) and SpoIIIE DNA translocases play distinct roles in growing cells to ensure faithful chromosome partitioning. Molecular microbiology *74*, 790-809.

Bowman, G.R., Comolli, L.R., Zhu, J., Eckart, M., Koenig, M., Downing, K.H., Moerner, W.E., Earnest, T., and Shapiro, L. (2008). A polymeric protein anchors the chromosomal origin/ParB complex at a bacterial cell pole. Cell *134*, 945-955.

Bramhill, D., and Thompson, C.M. (1994). GTP-dependent polymerization of Escherichia coli FtsZ protein to form tubules. Proceedings of the National Academy of Sciences of the United States of America *91*, 5813-5817.

Bramkamp, M., Emmins, R., Weston, L., Donovan, C., Daniel, R.A., and Errington, J. (2008). A novel component of the division-site selection system of Bacillus subtilis and a new mode of action for the division inhibitor MinCD. Molecular microbiology *70*, 1556-1569.

Branda, S.S., Chu, F., Kearns, D.B., Losick, R., and Kolter, R. (2006). A major protein component of the Bacillus subtilis biofilm matrix. Molecular microbiology *59*, 1229-1238.

Breier, A.M., and Grossman, A.D. (2007). Whole-genome analysis of the chromosome partitioning and sporulation protein Spo0J (ParB) reveals spreading and origin-distal sites on the Bacillus subtilis chromosome. Molecular microbiology *64*, 703-718.

Britton, R.A., and Grossman, A.D. (1999). Synthetic lethal phenotypes caused by mutations affecting chromosome partitioning in Bacillus subtilis. Journal of bacteriology *181*, 5860-5864.

Buddelmeijer, N., and Beckwith, J. (2004). A complex of the Escherichia coli cell division proteins FtsL, FtsB and FtsQ forms independently of its localization to the septal region. Molecular microbiology *52*, 1315-1327.

Burbulys, D., Trach, K.A., and Hoch, J.A. (1991). Initiation of sporulation in B. subtilis is controlled by a multicomponent phosphorelay. Cell *64*, 545-552.

Burton, B.M., Marquis, K.A., Sullivan, N.L., Rapoport, T.A., and Rudner, D.Z. (2007). The ATPase SpoIIIE transports DNA across fused septal membranes during sporulation in Bacillus subtilis. Cell *131*, 1301-1312.

Bylund, J.E., Haines, M.A., Piggot, P.J., and Higgins, M.L. (1993). Axial filament formation in Bacillus subtilis: induction of nucleoids of increasing length after addition of chloramphenicol to exponential-phase cultures approaching stationary phase. Journal of bacteriology *175*, 1886-1890.

Cabrera, J.E., and Jin, D.J. (2003). The distribution of RNA polymerase in Escherichia coli is dynamic and sensitive to environmental cues. Molecular microbiology *50*, 1493-1505.

Camberg, J.L., Hoskins, J.R., and Wickner, S. (2009). ClpXP protease degrades the cytoskeletal protein, FtsZ, and modulates FtsZ polymer dynamics. Proc Natl Acad Sci U S A *106*, 10614-10619.

Camberg, J.L., Hoskins, J.R., and Wickner, S. (2011). The interplay of ClpXP with the cell division machinery in Escherichia coli. Journal of bacteriology *193*, 1911-1918.

Cha, J.H., and Stewart, G.C. (1997). The divIVA minicell locus of Bacillus subtilis. Journal of bacteriology *179*, 1671-1683.

Chater, K.F. (1972). A morphological and genetic mapping study of white colony mutants of Streptomyces coelicolor. J Gen Microbiol *72*, 9-28.

Chater, K.F. (1975). Construction and phenotypes of double sporulation deficient mutants in Streptomyces coelicolor A3(2). Journal of general microbiology *87*, 312-325.

Chater, K.F. (2001). Regulation of sporulation in Streptomyces coelicolor A3(2): a checkpoint multiplex? Current opinion in microbiology *4*, 667-673.

Chater, K.F., Bruton, C.J., Plaskitt, K.A., Buttner, M.J., Mendez, C., and Helmann, J.D. (1989). The developmental fate of S. coelicolor hyphae depends upon a gene product homologous with the motility sigma factor of B. subtilis. Cell *59*, 133-143.

Chen, R., Guttenplan, S.B., Blair, K.M., and Kearns, D.B. (2009). Role of the sigmaD-dependent autolysins in Bacillus subtilis population heterogeneity. Journal of bacteriology *191*, 5775-5784.

Chiaramello, A.E., and Zyskind, J.W. (1990). Coupling of DNA replication to growth rate in Escherichia coli: a possible role for guanosine tetraphosphate. Journal of bacteriology *172*, 2013-2019.

Cho, E., Ogasawara, N., and Ishikawa, S. (2008). The functional analysis of YabA, which interacts with DnaA and regulates initiation of chromosome replication in Bacillus subtils. Genes Genet Syst *83*, 111-125.

Chung, K.M., Hsu, H.H., Govindan, S., and Chang, B.Y. (2004). Transcription regulation of ezrA and its effect on cell division of Bacillus subtilis. Journal of bacteriology *186*, 5926-5932.

Claessen, D., Emmins, R., Hamoen, L.W., Daniel, R.A., Errington, J., and Edwards, D.H. (2008). Control of the cell elongation-division cycle by shuttling of PBP1 protein in Bacillus subtilis. Molecular microbiology *68*, 1029-1046.

Cooper, S., and Helmstetter, C.E. (1968). Chromosome replication and the division cycle of Escherichia coli B/r. J Mol Biol *31*, 519-540.

Corbin, B.D., Yu, X.C., and Margolin, W. (2002). Exploring intracellular space: function of the Min system in round-shaped Escherichia coli. EMBO J *21*, 1998-2008.

Cordell, S.C., Anderson, R.E., and Lowe, J. (2001). Crystal structure of the bacterial cell division inhibitor MinC. The EMBO journal *20*, 2454-2461.

Cordell, S.C., Robinson, E.J., and Lowe, J. (2003). Crystal structure of the SOS cell division inhibitor SulA and in complex with FtsZ. Proc Natl Acad Sci U S A *100*, 7889-7894.

Costes, A., Lecointe, F., McGovern, S., Quevillon-Cheruel, S., and Polard, P. (2010). The C-terminal domain of the bacterial SSB protein acts as a DNA maintenance hub at active chromosome replication forks. PLoS genetics *6*, e1001238.

Cox, M.M., Goodman, M.F., Kreuzer, K.N., Sherratt, D.J., Sandler, S.J., and Marians, K.J. (2000). The importance of repairing stalled replication forks. Nature *404*, 37-41.

Dai, K., and Lutkenhaus, J. (1992). The proper ratio of FtsZ to FtsA is required for cell division to occur in Escherichia coli. Journal of bacteriology *174*, 6145-6151.

Dajkovic, A., Lan, G., Sun, S.X., Wirtz, D., and Lutkenhaus, J. (2008). MinC spatially controls bacterial cytokinesis by antagonizing the scaffolding function of FtsZ. Curr Biol *18*, 235-244.

Dame, R.T. (2005). The role of nucleoid-associated proteins in the organization and compaction of bacterial chromatin. Molecular microbiology *56*, 858-870.

Dame, R.T., Wyman, C., and Goosen, N. (2000). H-NS mediated compaction of DNA visualised by atomic force microscopy. Nucleic Acids Res *28*, 3504-3510.

Daniel, R.A., and Errington, J. (2000). Intrinsic instability of the essential cell division protein FtsL of Bacillus subtilis and a role for DivIB protein in FtsL turnover. Molecular microbiology *36*, 278-289.

Daniel, R.A., Harry, E.J., Katis, V.L., Wake, R.G., and Errington, J. (1998). Characterization of the essential cell division gene ftsL(yIID) of Bacillus subtilis and its role in the assembly of the division apparatus. Molecular microbiology *29*, 593-604.

Daniel, R.A., Noirot-Gros, M.F., Noirot, P., and Errington, J. (2006). Multiple interactions between the transmembrane division proteins of Bacillus subtilis and

the role of FtsL instability in divisome assembly. Journal of bacteriology *188*, 7396-7404.

de Boer, P., Crossley, R., and Rothfield, L. (1992). The essential bacterial cell-division protein FtsZ is a GTPase. Nature *359*, 254-256.

de Boer, P.A., Crossley, R.E., Hand, A.R., and Rothfield, L.I. (1991). The MinD protein is a membrane ATPase required for the correct placement of the Escherichia coli division site. The EMBO journal *10*, 4371-4380.

de Boer, P.A., Crossley, R.E., and Rothfield, L.I. (1989). A division inhibitor and a topological specificity factor coded for by the minicell locus determine proper placement of the division septum in E. coli. Cell *56*, 641-649.

Delius, H., and Worcel, A. (1974). Electron microscopic studies on the folded chromosome of Escherichia coli. Cold Spring Harb Symp Quant Biol *38*, 53-58.

Den Blaauwen, T., Buddelmeijer, N., Aarsman, M.E., Hameete, C.M., and Nanninga, N. (1999). Timing of FtsZ assembly in Escherichia coli. Journal of bacteriology *181*, 5167-5175.

Deng, S., Stein, R.A., and Higgins, N.P. (2004). Transcription-induced barriers to supercoil diffusion in the Salmonella typhimurium chromosome. Proc Natl Acad Sci U S A *101*, 3398-3403.

Deng, S., Stein, R.A., and Higgins, N.P. (2005). Organization of supercoil domains and their reorganization by transcription. Molecular microbiology *57*, 1511-1521.

Dereeper, A., Guignon, V., Blanc, G., Audic, S., Buffet, S., Chevenet, F., Dufayard, J.F., Guindon, S., Lefort, V., Lescot, M*., et al.* (2008). Phylogeny.fr: robust phylogenetic analysis for the non-specialist. Nucleic acids research *36*, W465-469.

Dervyn, E., Suski, C., Daniel, R., Bruand, C., Chapuis, J., Errington, J., Janniere, L., and Ehrlich, S.D. (2001). Two essential DNA polymerases at the bacterial replication fork. Science *294*, 1716-1719.

Dewar, S.J., Begg, K.J., and Donachie, W.D. (1992). Inhibition of cell division initiation by an imbalance in the ratio of FtsA to FtsZ. Journal of bacteriology *174*, 6314-6316.

Drzewiecki, K., Eymann, C., Mittenhuber, G., and Hecker, M. (1998). The yvyD gene of Bacillus subtilis is under dual control of sigmaB and sigmaH. Journal of bacteriology *180*, 6674-6680.

Dubarry, N., Pasta, F., and Lane, D. (2006). ParABS systems of the four replicons of Burkholderia cenocepacia: new chromosome centromeres confer partition specificity. Journal of bacteriology *188*, 1489-1496.

Duncan, L., Alper, S., Arigoni, F., Losick, R., and Stragier, P. (1995). Activation of cell-specific transcription by a serine phosphatase at the site of asymmetric division. Science *270*, 641-644.

Dunn, G., and Mandelstam, J. (1977). Cell polarity in Bacillus subtilis: effect of growth conditions on spore positions in sister cells. J Gen Microbiol *103*, 201-205.

Durand-Heredia, J.M., Yu, H.H., De Carlo, S., Lesser, C.F., and Janakiraman, A. (2011). Identification and characterization of ZapC, a stabilizer of the FtsZ ring in Escherichia coli. Journal of bacteriology *193*, 1405-1413.

Ebersbach, G., Briegel, A., Jensen, G.J., and Jacobs-Wagner, C. (2008a). A self-associating protein critical for chromosome attachment, division, and polar organization in caulobacter. Cell *134*, 956-968.

Ebersbach, G., Galli, E., Moller-Jensen, J., Lowe, J., and Gerdes, K. (2008b). Novel coiled-coil cell division factor ZapB stimulates Z ring assembly and cell division. Molecular microbiology *68*, 720-735.

Edwards, D.H., and Errington, J. (1997). The Bacillus subtilis DivIVA protein targets to the division septum and controls the site specificity of cell division. Molecular microbiology *24*, 905-915.

Erickson, H.P. (1995). FtsZ, a prokaryotic homolog of tubulin? Cell *80*, 367-370.

Erickson, H.P., Taylor, D.W., Taylor, K.A., and Bramhill, D. (1996). Bacterial cell division protein FtsZ assembles into protofilament sheets and minirings, structural homologs of tubulin polymers. Proceedings of the National Academy of Sciences of the United States of America *93*, 519-523.

Errington, J. (2003). Regulation of endospore formation in Bacillus subtilis. Nature reviews Microbiology *1*, 117-126.

Errington, J., Daniel, R.A., and Scheffers, D.J. (2003a). Cytokinesis in bacteria. Microbiol Mol Biol Rev *67*, 52-65, table of contents.

Errington, J., Daniel, R.A., and Scheffers, D.J. (2003b). Cytokinesis in bacteria. Microbiology and molecular biology reviews : MMBR *67*, 52-65, table of contents.

Fang, L., Davey, M.J., and O'Donnell, M. (1999). Replisome assembly at oriC, the replication origin of E. coli, reveals an explanation for initiation sites outside an origin. Mol Cell *4*, 541-553.

Feucht, A., and Errington, J. (2005). ftsZ mutations affecting cell division frequency, placement and morphology in Bacillus subtilis. Microbiology (Reading, England) *151*, 2053-2064.

Feucht, A., Lucet, I., Yudkin, M.D., and Errington, J. (2001). Cytological and biochemical characterization of the FtsA cell division protein of Bacillus subtilis. Molecular microbiology *40*, 115-125.

Feucht, A., Magnin, T., Yudkin, M.D., and Errington, J. (1996). Bifunctional protein required for asymmetric cell division and cell-specific transcription in Bacillus subtilis. Genes & development *10*, 794-803.

Figge, R.M., Easter, J., and Gober, J.W. (2003). Productive interaction between the chromosome partitioning proteins, ParA and ParB, is required for the progression of the cell cycle in Caulobacter crescentus. Molecular microbiology *47*, 1225-1237.

Flardh, K. (2003). Growth polarity and cell division in Streptomyces. Curr Opin Microbiol *6*, 564-571.

Flardh, K., Findlay, K.C., and Chater, K.F. (1999). Association of early sporulation genes with suggested developmental decision points in Streptomyces coelicolor A3(2). Microbiology (Reading, England) *145 (Pt 9)*, 2229-2243.

Flardh, K., Leibovitz, E., Buttner, M.J., and Chater, K.F. (2000). Generation of a non-sporulating strain of Streptomyces coelicolor A3(2) by the manipulation of a developmentally controlled ftsZ promoter. Molecular microbiology *38*, 737-749.

Fleming, T.C., Shin, J.Y., Lee, S.H., Becker, E., Huang, K.C., Bustamante, C., and Pogliano, K. (2010). Dynamic SpoIIIE assembly mediates septal membrane fission during Bacillus subtilis sporulation. Genes & development *24*, 1160-1172.

Foulquier, E., Pompeo, F., Bernadac, A., Espinosa, L., and Galinier, A. (2011). The YvcK protein is required for morphogenesis via localization of PBP1 under gluconeogenic growth conditions in Bacillus subtilis. Molecular microbiology *80*, 309-318.

Freymond, P.P., Lazarevic, V., Soldo, B., and Karamata, D. (2006). Poly(glucosyl-N-acetylgalactosamine 1-phosphate), a wall teichoic acid of Bacillus subtilis 168: its biosynthetic pathway and mode of attachment to peptidoglycan. Microbiology (Reading, England) *152*, 1709-1718.

Fujita, Y. (2009). Carbon catabolite control of the metabolic network in Bacillus subtilis. Biosci Biotechnol Biochem *73*, 245-259.

Fukushima, T., Yamamoto, H., Atrih, A., Foster, S.J., and Sekiguchi, J. (2002). A polysaccharide deacetylase gene (pdaA) is required for germination and for production of muramic delta-lactam residues in the spore cortex of Bacillus subtilis. Journal of bacteriology *184*, 6007-6015.

Galinier, A., Haiech, J., Kilhoffer, M.C., Jaquinod, M., Stulke, J., Deutscher, J., and Martin-Verstraete, I. (1997). The Bacillus subtilis crh gene encodes a HPr-like protein involved in carbon catabolite repression. Proceedings of the National Academy of Sciences of the United States of America *94*, 8439-8444.

Galli, E., and Gerdes, K. (2010). Spatial resolution of two bacterial cell division proteins: ZapA recruits ZapB to the inner face of the Z-ring. Molecular microbiology *76*, 1514-1526.

Gamba, P., Veening, J.W., Saunders, N.J., Hamoen, L.W., and Daniel, R.A. (2009). Two-step assembly dynamics of the Bacillus subtilis divisome. Journal of bacteriology *191*, 4186-4194.

Gellert, M., O'Dea, M.H., Itoh, T., and Tomizawa, J. (1976). Novobiocin and coumermycin inhibit DNA supercoiling catalyzed by DNA gyrase. Proc Natl Acad Sci U S A *73*, 4474-4478.

Gerdes, K., Howard, M., and Szardenings, F. (2010). Pushing and pulling in prokaryotic DNA segregation. Cell *141*, 927-942.

Gerdes, K., Larsen, J.E., and Molin, S. (1985). Stable inheritance of plasmid R1 requires two different loci. Journal of bacteriology *161*, 292-298.

Gerdes, K., Moller-Jensen, J., and Bugge Jensen, R. (2000). Plasmid and chromosome partitioning: surprises from phylogeny. Molecular microbiology *37*, 455-466.

Gholamhoseinian, A., Shen, Z., Wu, J.J., and Piggot, P. (1992). Regulation of transcription of the cell division gene ftsA during sporulation of Bacillus subtilis. Journal of bacteriology *174*, 4647-4656.

Gitai, Z., Dye, N.A., Reisenauer, A., Wachi, M., and Shapiro, L. (2005). MreB actin-mediated segregation of a specific region of a bacterial chromosome. Cell *120*, 329-341.

Godfrin-Estevenon, A.M., Pasta, F., and Lane, D. (2002). The parAB gene products of Pseudomonas putida exhibit partition activity in both P. putida and Escherichia coli. Molecular microbiology *43*, 39-49.

Gon, S., Camara, J.E., Klungsoyr, H.K., Crooke, E., Skarstad, K., and Beckwith, J. (2006). A novel regulatory mechanism couples deoxyribonucleotide synthesis and DNA replication in Escherichia coli. EMBO J *25*, 1137-1147.

Gonzy-Treboul, G., Karmazyn-Campelli, C., and Stragier, P. (1992). Developmental regulation of transcription of the Bacillus subtilis ftsAZ operon. J Mol Biol *224*, 967-979.

Goodell, E.W., and Higgins, C.F. (1987). Uptake of cell wall peptides by Salmonella typhimurium and Escherichia coli. Journal of bacteriology *169*, 3861-3865.

Goranov, A.I., Katz, L., Breier, A.M., Burge, C.B., and Grossman, A.D. (2005). A transcriptional response to replication status mediated by the conserved bacterial replication protein DnaA. Proceedings of the National Academy of Sciences of the United States of America *102*, 12932-12937.

Gorke, B., Foulquier, E., and Galinier, A. (2005). YvcK of Bacillus subtilis is required for a normal cell shape and for growth on Krebs cycle intermediates and substrates of the pentose phosphate pathway. Microbiology (Reading, England) *151*, 3777-3791.

Grainge, I., Lesterlin, C., and Sherratt, D.J. (2011). Activation of XerCD-dif recombination by the FtsK DNA translocase. Nucleic acids research.

Grantcharova, N., Lustig, U., and Flardh, K. (2005). Dynamics of FtsZ assembly during sporulation in Streptomyces coelicolor A3(2). Journal of bacteriology *187*, 3227-3237.

Gregory, J.A., Becker, E.C., and Pogliano, K. (2008). Bacillus subtilis MinC destabilizes FtsZ-rings at new cell poles and contributes to the timing of cell division. Genes & development *22*, 3475-3488.

Gruber, S., and Errington, J. (2009). Recruitment of condensin to replication origin regions by ParB/SpoOJ promotes chromosome segregation in B. subtilis. Cell *137*, 685-696.

Gueiros-Filho, F.J., and Losick, R. (2002). A widely conserved bacterial cell division protein that promotes assembly of the tubulin-like protein FtsZ. Genes & development *16*, 2544-2556.

Gundogdu, M.E., Kawai, Y., Pavlendova, N., Ogasawara, N., Errington, J., Scheffers, D.J., and Hamoen, L.W. (2011). Large ring polymers align FtsZ polymers for normal septum formation. The EMBO journal *30*, 617-626.

Haering, C.H., Lowe, J., Hochwagen, A., and Nasmyth, K. (2002). Molecular architecture of SMC proteins and the yeast cohesin complex. Mol Cell *9*, 773-788.

Haeusser, D.P., Garza, A.C., Buscher, A.Z., and Levin, P.A. (2007). The division inhibitor EzrA contains a seven-residue patch required for maintaining the dynamic nature of the medial FtsZ ring. Journal of bacteriology *189*, 9001-9010.

Haeusser, D.P., Lee, A.H., Weart, R.B., and Levin, P.A. (2009). ClpX inhibits FtsZ assembly in a manner that does not require its ATP hydrolysis-dependent chaperone activity. Journal of bacteriology *191*, 1986-1991.

Haeusser, D.P., Schwartz, R.L., Smith, A.M., Oates, M.E., and Levin, P.A. (2004). EzrA prevents aberrant cell division by modulating assembly of the cytoskeletal protein FtsZ. Molecular microbiology *52*, 801-814.

Hale, C.A., and de Boer, P.A. (1997). Direct binding of FtsZ to ZipA, an essential component of the septal ring structure that mediates cell division in E. coli. Cell *88*, 175-185.

Hale, C.A., and de Boer, P.A. (1999). Recruitment of ZipA to the septal ring of Escherichia coli is dependent on FtsZ and independent of FtsA. Journal of bacteriology *181*, 167-176.

Hale, C.A., and de Boer, P.A. (2002). ZipA is required for recruitment of FtsK, FtsQ, FtsL, and FtsN to the septal ring in Escherichia coli. Journal of bacteriology *184*, 2552-2556.

Hale, C.A., Rhee, A.C., and de Boer, P.A. (2000). ZipA-induced bundling of FtsZ polymers mediated by an interaction between C-terminal domains. Journal of bacteriology *182*, 5153-5166.

Hamoen, L.W., and Errington, J. (2003). Polar targeting of DivIVA in Bacillus subtilis is not directly dependent on FtsZ or PBP 2B. Journal of bacteriology *185*, 693-697.

Hamoen, L.W., Meile, J.C., de Jong, W., Noirot, P., and Errington, J. (2006). SepF, a novel FtsZ-interacting protein required for a late step in cell division. Molecular microbiology *59*, 989-999.

Harry, E.J., Rodwell, J., and Wake, R.G. (1999). Co-ordinating DNA replication with cell division in bacteria: a link between the early stages of a round of replication and mid-cell Z ring assembly. Molecular microbiology *33*, 33-40.

Hayashi, I., Oyama, T., and Morikawa, K. (2001). Structural and functional studies of MinD ATPase: implications for the molecular recognition of the bacterial cell division apparatus. The EMBO journal *20*, 1819-1828.

Henriques, A.O., and Moran, C.P., Jr. (2000). Structure and assembly of the bacterial endospore coat. Methods *20*, 95-110.

Henriques, A.O., and Moran, C.P., Jr. (2007). Structure, assembly, and function of the spore surface layers. Annu Rev Microbiol *61*, 555-588.

Hilbert, D.W., and Piggot, P.J. (2004). Compartmentalization of gene expression during Bacillus subtilis spore formation. Microbiology and molecular biology reviews : MMBR *68*, 234-262.

Hirano, M., and Hirano, T. (2002). Hinge-mediated dimerization of SMC protein is essential for its dynamic interaction with DNA. EMBO J *21*, 5733-5744.

Hirano, T. (2002). The ABCs of SMC proteins: two-armed ATPases for chromosome condensation, cohesion, and repair. Genes & development *16*, 399-414.

Hirano, T. (2006). At the heart of the chromosome: SMC proteins in action. Nat Rev Mol Cell Biol *7*, 311-322.

Honeyman, A.L., and Stewart, G.C. (1989). The nucleotide sequence of the rodC operon of Bacillus subtilis. Molecular microbiology *3*, 1257-1268.

Howard-Flanders, P., Theriot, L., and Stedeford, J.B. (1969). Some properties of excision-defective recombination-deficient mutants of Escherichia coli K-12. Journal of bacteriology *97*, 1134-1141.

Hu, Z., and Lutkenhaus, J. (1999). Topological regulation of cell division in Escherichia coli involves rapid pole to pole oscillation of the division inhibitor MinC under the control of MinD and MinE. Molecular microbiology *34*, 82-90.

Hu, Z., Mukherjee, A., Pichoff, S., and Lutkenhaus, J. (1999). The MinC component of the division site selection system in Escherichia coli interacts with FtsZ to prevent polymerization. Proc Natl Acad Sci U S A *96*, 14819-14824.

Huecas, S., and Andreu, J.M. (2004). Polymerization of nucleotide-free, GDP- and GTP-bound cell division protein FtsZ: GDP makes the difference. FEBS Lett *569*, 43-48.

Huecas, S., Llorca, O., Boskovic, J., Martin-Benito, J., Valpuesta, J.M., and Andreu, J.M. (2008). Energetics and geometry of FtsZ polymers: nucleated self-assembly of single protofilaments. Biophys J *94*, 1796-1806.

Hueck, C.J., Hillen, W., and Saier, M.H., Jr. (1994). Analysis of a cis-active sequence mediating catabolite repression in gram-positive bacteria. Research in microbiology *145*, 503-518.

Huisman, O., and D'Ari, R. (1981). An inducible DNA replication-cell division coupling mechanism in E. coli. Nature *290*, 797-799.

Huisman, O., D'Ari, R., and Gottesman, S. (1984). Cell-division control in Escherichia coli: specific induction of the SOS function SfiA protein is sufficient to block septation. Proc Natl Acad Sci U S A *81*, 4490-4494.

Hullo, M.F., Auger, S., Dassa, E., Danchin, A., and Martin-Verstraete, I. (2004). The metNPQ operon of Bacillus subtilis encodes an ABC permease transporting methionine sulfoxide, D- and L-methionine. Research in microbiology *155*, 80-86.

Illing, N., and Errington, J. (1991). Genetic regulation of morphogenesis in Bacillus subtilis: roles of sigma E and sigma F in prespore engulfment. Journal of bacteriology *173*, 3159-3169.

Inoue, H., Nojima, H., and Okayama, H. (1990). High efficiency transformation of Escherichia coli with plasmids. Gene *96*, 23-28.

Ireton, K., Gunther, N.W.t., and Grossman, A.D. (1994). spo0J is required for normal chromosome segregation as well as the initiation of sporulation in Bacillus subtilis. Journal of bacteriology *176*, 5320-5329.

Ishikawa, S., Kawai, Y., Hiramatsu, K., Kuwano, M., and Ogasawara, N. (2006). A new FtsZ-interacting protein, YlmF, complements the activity of FtsA during progression of cell division in Bacillus subtilis. Molecular microbiology *60*, 1364-1380.

Itaya, M., Kondo, K., and Tanaka, T. (1989). A neomycin resistance gene cassette selectable in a single copy state in the Bacillus subtilis chromosome. Nucleic Acids Res *17*, 4410.

Jacobs, C., Domian, I.J., Maddock, J.R., and Shapiro, L. (1999). Cell cycle-dependent polar localization of an essential bacterial histidine kinase that controls DNA replication and cell division. Cell *97*, 111-120.

Jakimowicz, D., Mouz, S., Zakrzewska-Czerwinska, J., and Chater, K.F. (2006). Developmental control of a parAB promoter leads to formation of sporulation-

associated ParB complexes in Streptomyces coelicolor. Journal of bacteriology *188*, 1710-1720.

Janniere, L., Canceill, D., Suski, C., Kanga, S., Dalmais, B., Lestini, R., Monnier, A.F., Chapuis, J., Bolotin, A., Titok, M.*, et al.* (2007). Genetic evidence for a link between glycolysis and DNA replication. PLoS One *2*, e447.

Jensen, R.B., and Shapiro, L. (1999). The Caulobacter crescentus smc gene is required for cell cycle progression and chromosome segregation. Proc Natl Acad Sci U S A *96*, 10661-10666.

Jensen, R.B., Wang, S.C., and Shapiro, L. (2001). A moving DNA replication factory in Caulobacter crescentus. EMBO J *20*, 4952-4963.

Jensen, S.O., Thompson, L.S., and Harry, E.J. (2005). Cell division in Bacillus subtilis: FtsZ and FtsA association is Z-ring independent, and FtsA is required for efficient midcell Z-Ring assembly. Journal of bacteriology *187*, 6536-6544.

Jones, L.J., Carballido-Lopez, R., and Errington, J. (2001). Control of cell shape in bacteria: helical, actin-like filaments in Bacillus subtilis. Cell *104*, 913-922.

Jorasch, P., Wolter, F.P., Zahringer, U., and Heinz, E. (1998). A UDP glucosyltransferase from Bacillus subtilis successively transfers up to four glucose residues to 1,2-diacylglycerol: expression of ypfP in Escherichia coli and structural analysis of its reaction products. Molecular microbiology *29*, 419-430.

Juarez, J.R., and Margolin, W. (2010). Changes in the Min oscillation pattern before and after cell birth. Journal of bacteriology *192*, 4134-4142.

Justice, S.S., Garcia-Lara, J., and Rothfield, L.I. (2000). Cell division inhibitors SulA and MinC/MinD block septum formation at different steps in the assembly of the Escherichia coli division machinery. Molecular microbiology *37*, 410-423.

Kaimer, C., Gonzalez-Pastor, J.E., and Graumann, P.L. (2009). SpoIIIE and a novel type of DNA translocase, SftA, couple chromosome segregation with cell division in Bacillus subtilis. Molecular microbiology *74*, 810-825.

Kaiser, B.K., Clifton, M.C., Shen, B.W., and Stoddard, B.L. (2009). The structure of a bacterial DUF199/WhiA protein: domestication of an invasive endonuclease. Structure *17*, 1368-1376.

Karimova, G., Pidoux, J., Ullmann, A., and Ladant, D. (1998). A bacterial two-hybrid system based on a reconstituted signal transduction pathway. Proceedings of the National Academy of Sciences of the United States of America *95*, 5752-5756.

Karow, M.L., Glaser, P., and Piggot, P.J. (1995). Identification of a gene, spoIIR, that links the activation of sigma E to the transcriptional activity of sigma F during sporulation in Bacillus subtilis. Proc Natl Acad Sci U S A *92*, 2012-2016.

Kavenoff, R., and Bowen, B.C. (1976). Electron microscopy of membrane-free folded chromosomes from Escherichia coli. Chromosoma *59*, 89-101.

Kavenoff, R., and Ryder, O.A. (1976). Electron microscopy of membrane-associated folded chromosomes of Escherichia coli. Chromosoma *55*, 13-25.

Kawai, Y., Moriya, S., and Ogasawara, N. (2003). Identification of a protein, YneA, responsible for cell division suppression during the SOS response in Bacillus subtilis. Molecular microbiology *47*, 1113-1122.

Kawai, Y., and Ogasawara, N. (2006). Bacillus subtilis EzrA and FtsL synergistically regulate FtsZ ring dynamics during cell division. Microbiology (Reading, England) *152*, 1129-1141.

Kelemen, G.H., Brian, P., Flardh, K., Chamberlin, L., Chater, K.F., and Buttner, M.J. (1998). Developmental regulation of transcription of whiE, a locus specifying the polyketide spore pigment in Streptomyces coelicolor A3 (2). Journal of bacteriology *180*, 2515-2521.

Kelemen, G.H., Brown, G.L., Kormanec, J., Potuckova, L., Chater, K.F., and Buttner, M.J. (1996). The positions of the sigma-factor genes, whiG and sigF, in the

hierarchy controlling the development of spore chains in the aerial hyphae of Streptomyces coelicolor A3(2). Molecular microbiology *21*, 593-603.

Keyamura, K., Fujikawa, N., Ishida, T., Ozaki, S., Su'etsugu, M., Fujimitsu, K., Kagawa, W., Yokoyama, S., Kurumizaka, H., and Katayama, T. (2007). The interaction of DiaA and DnaA regulates the replication cycle in E. coli by directly promoting ATP DnaA-specific initiation complexes. Genes & development *21*, 2083-2099.

Kim, H.J., Calcutt, M.J., Schmidt, F.J., and Chater, K.F. (2000). Partitioning of the linear chromosome during sporulation of Streptomyces coelicolor A3(2) involves an oriC-linked parAB locus. Journal of bacteriology *182*, 1313-1320.

Knizewski, L., and Ginalski, K. (2007). Bacterial DUF199/COG1481 proteins including sporulation regulator WhiA are distant homologs of LAGLIDADG homing endonucleases that retained only DNA binding. Cell cycle (Georgetown, Tex *6*, 1666-1670.

Kohler, P., and Marahiel, M.A. (1997). Association of the histone-like protein HBsu with the nucleoid of Bacillus subtilis. Journal of bacteriology *179*, 2060-2064.

Krauhs, E., Little, M., Kempf, T., Hofer-Warbinek, R., Ade, W., and Ponstingl, H. (1981). Complete amino acid sequence of beta-tubulin from porcine brain. Proc Natl Acad Sci U S A *78*, 4156-4160.

Kreuzer, K.N. (2005). Interplay between DNA replication and recombination in prokaryotes. Annual review of microbiology *59*, 43-67.

Kruse, T., Blagoev, B., Lobner-Olesen, A., Wachi, M., Sasaki, K., Iwai, N., Mann, M., and Gerdes, K. (2006). Actin homolog MreB and RNA polymerase interact and are both required for chromosome segregation in Escherichia coli. Genes & development *20*, 113-124.

Kuempel, P.L., Henson, J.M., Dircks, L., Tecklenburg, M., and Lim, D.F. (1991). dif, a recA-independent recombination site in the terminus region of the chromosome of Escherichia coli. New Biol *3*, 799-811.

Kwak, J., Dharmatilake, A.J., Jiang, H., and Kendrick, K.E. (2001). Differential regulation of ftsZ transcription during septation of Streptomyces griseus. Journal of bacteriology *183*, 5092-5101.

Lara, B., Rico, A.I., Petruzzelli, S., Santona, A., Dumas, J., Biton, J., Vicente, M., Mingorance, J., and Massidda, O. (2005). Cell division in cocci: localization and properties of the Streptococcus pneumoniae FtsA protein. Molecular microbiology *55*, 699-711.

Lazarevic, V., Abellan, F.X., Moller, S.B., Karamata, D., and Mauel, C. (2002). Comparison of ribitol and glycerol teichoic acid genes in Bacillus subtilis W23 and 168: identical function, similar divergent organization, but different regulation. Microbiology (Reading, England) *148*, 815-824.

Lazarevic, V., Soldo, B., Medico, N., Pooley, H., Bron, S., and Karamata, D. (2005). Bacillus subtilis alpha-phosphoglucomutase is required for normal cell morphology and biofilm formation. Applied and environmental microbiology *71*, 39-45.

Le Breton, Y., Mohapatra, N.P., and Haldenwang, W.G. (2006). In vivo random mutagenesis of Bacillus subtilis by use of TnYLB-1, a mariner-based transposon. Applied and environmental microbiology *72*, 327-333.

Leaver, M., Dominguez-Cuevas, P., Coxhead, J.M., Daniel, R.A., and Errington, J. (2009). Life without a wall or division machine in Bacillus subtilis. Nature *457*, 849-853.

LeDeaux, J.R., Solomon, J.M., and Grossman, A.D. (1997). Analysis of non-polar deletion mutations in the genes of the spo0K (opp) operon of Bacillus subtilis. FEMS microbiology letters *153*, 63-69.

Lemon, K.P., and Grossman, A.D. (1998). Localization of bacterial DNA polymerase: evidence for a factory model of replication. Science *282*, 1516-1519.

Lemon, K.P., Kurtser, I., and Grossman, A.D. (2001). Effects of replication termination mutants on chromosome partitioning in Bacillus subtilis. Proc Natl Acad Sci U S A *98*, 212-217.

Lenarcic, R., Halbedel, S., Visser, L., Shaw, M., Wu, L.J., Errington, J., Marenduzzo, D., and Hamoen, L.W. (2009). Localisation of DivIVA by targeting to negatively curved membranes. EMBO J *28*, 2272-2282.

Levin, P.A., Kurtser, I.G., and Grossman, A.D. (1999). Identification and characterization of a negative regulator of FtsZ ring formation in Bacillus subtilis. Proc Natl Acad Sci U S A *96*, 9642-9647.

Levin, P.A., and Losick, R. (1996). Transcription factor Spo0A switches the localization of the cell division protein FtsZ from a medial to a bipolar pattern in Bacillus subtilis. Genes & development *10*, 478-488.

Levin, P.A., Losick, R., Stragier, P., and Arigoni, F. (1997). Localization of the sporulation protein SpoIIE in Bacillus subtilis is dependent upon the cell division protein FtsZ. Molecular microbiology *25*, 839-846.

Levin, P.A., Schwartz, R.L., and Grossman, A.D. (2001). Polymer stability plays an important role in the positional regulation of FtsZ. Journal of bacteriology *183*, 5449-5452.

Lewis, P.J., and Marston, A.L. (1999). GFP vectors for controlled expression and dual labelling of protein fusions in Bacillus subtilis. Gene *227*, 101-110.

Li, H., DeRosier, D.J., Nicholson, W.V., Nogales, E., and Downing, K.H. (2002). Microtubule structure at 8 A resolution. Structure *10*, 1317-1328.

Li, Z., Trimble, M.J., Brun, Y.V., and Jensen, G.J. (2007). The structure of FtsZ filaments in vivo suggests a force-generating role in cell division. EMBO J *26*, 4694-4708.

Lin, D.C., and Grossman, A.D. (1998). Identification and characterization of a bacterial chromosome partitioning site. Cell *92*, 675-685.

Lin, D.C., Levin, P.A., and Grossman, A.D. (1997). Bipolar localization of a chromosome partition protein in Bacillus subtilis. Proc Natl Acad Sci U S A *94*, 4721-4726.

Liu, N.J., Dutton, R.J., and Pogliano, K. (2006). Evidence that the SpoIIIE DNA translocase participates in membrane fusion during cytokinesis and engulfment. Molecular microbiology *59*, 1097-1113.

Liu, Z., Mukherjee, A., and Lutkenhaus, J. (1999). Recruitment of ZipA to the division site by interaction with FtsZ. Molecular microbiology *31*, 1853-1861.

Livny, J., Yamaichi, Y., and Waldor, M.K. (2007). Distribution of centromere-like parS sites in bacteria: insights from comparative genomics. Journal of bacteriology *189*, 8693-8703.

Londono-Vallejo, J.A., Frehel, C., and Stragier, P. (1997). SpoIIQ, a forespore-expressed gene required for engulfment in Bacillus subtilis. Molecular microbiology *24*, 29-39.

Londono-Vallejo, J.A., and Stragier, P. (1995). Cell-cell signaling pathway activating a developmental transcription factor in Bacillus subtilis. Genes & development *9*, 503-508.

Loose, M., Fischer-Friedrich, E., Ries, J., Kruse, K., and Schwille, P. (2008). Spatial regulators for bacterial cell division self-organize into surface waves in vitro. Science *320*, 789-792.

Lorca, G.L., Chung, Y.J., Barabote, R.D., Weyler, W., Schilling, C.H., and Saier, M.H., Jr. (2005). Catabolite repression and activation in Bacillus subtilis: dependency on CcpA, HPr, and HprK. Journal of bacteriology *187*, 7826-7839.

Losick, R., Youngman, P., and Piggot, P.J. (1986). Genetics of endospore formation in Bacillus subtilis. Annual review of genetics *20*, 625-669.

Low, H.H., Moncrieffe, M.C., and Lowe, J. (2004). The crystal structure of ZapA and its modulation of FtsZ polymerisation. J Mol Biol *341*, 839-852.

Lowe, J., and Amos, L.A. (1998). Crystal structure of the bacterial cell-division protein FtsZ. Nature *391*, 203-206.

Lowe, J., and Amos, L.A. (1999). Tubulin-like protofilaments in Ca2+-induced FtsZ sheets. The EMBO journal *18*, 2364-2371.

Lowe, J., Li, H., Downing, K.H., and Nogales, E. (2001). Refined structure of alpha beta-tubulin at 3.5 A resolution. J Mol Biol *313*, 1045-1057.

Lucet, I., Feucht, A., Yudkin, M.D., and Errington, J. (2000). Direct interaction between the cell division protein FtsZ and the cell differentiation protein SpoIIE. EMBO J *19*, 1467-1475.

Luciano, J., Foulquier, E., Fantino, J.R., Galinier, A., and Pompeo, F. (2009). Characterization of YvcJ, a conserved P-loop-containing protein, and its implication in competence in Bacillus subtilis. Journal of bacteriology *191*, 1556-1564.

Lutkenhaus, J. (2009). FtsN--trigger for septation. Journal of bacteriology *191*, 7381-7382.

Lynch, A.S., and Wang, J.C. (1993). Anchoring of DNA to the bacterial cytoplasmic membrane through cotranscriptional synthesis of polypeptides encoding membrane proteins or proteins for export: a mechanism of plasmid hypernegative supercoiling in mutants deficient in DNA topoisomerase I. Journal of bacteriology *175*, 1645-1655.

Mader, U., Hennig, S., Hecker, M., and Homuth, G. (2004). Transcriptional organization and posttranscriptional regulation of the Bacillus subtilis branched-chain amino acid biosynthesis genes. Journal of bacteriology *186*, 2240-2252.

Marczynski, G.T. (1999). Chromosome methylation and measurement of faithful, once and only once per cell cycle chromosome replication in Caulobacter crescentus. Journal of bacteriology *181*, 1984-1993.

Margolin, W. (2000). Organelle division: Self-assembling GTPase caught in the middle. Curr Biol *10*, R328-330.

Marston, A.L., and Errington, J. (1999). Selection of the midcell division site in Bacillus subtilis through MinD-dependent polar localization and activation of MinC. Molecular microbiology *33*, 84-96.

Marston, A.L., Thomaides, H.B., Edwards, D.H., Sharpe, M.E., and Errington, J. (1998). Polar localization of the MinD protein of Bacillus subtilis and its role in selection of the mid-cell division site. Genes & development *12*, 3419-3430.

Marszalek, J., and Kaguni, J.M. (1994). DnaA protein directs the binding of DnaB protein in initiation of DNA replication in Escherichia coli. J Biol Chem *269*, 4883-4890.

Mascarenhas, J., Soppa, J., Strunnikov, A.V., and Graumann, P.L. (2002). Cell cycle-dependent localization of two novel prokaryotic chromosome segregation and condensation proteins in Bacillus subtilis that interact with SMC protein. EMBO J *21*, 3108-3118.

Mauel, C., Young, M., and Karamata, D. (1991). Genes concerned with synthesis of poly(glycerol phosphate), the essential teichoic acid in Bacillus subtilis strain 168, are organized in two divergent transcription units. Journal of general microbiology *137*, 929-941.

McLennan, A.G. (2006). The Nudix hydrolase superfamily. Cell Mol Life Sci *63*, 123-143.

Merrikh, H., and Grossman, A.D. (2011). Control of the replication initiator DnaA by an anti-cooperativity factor. Molecular microbiology.

Micka, B., Groch, N., Heinemann, U., and Marahiel, M.A. (1991). Molecular cloning, nucleotide sequence, and characterization of the Bacillus subtilis gene encoding the DNA-binding protein HBsu. Journal of bacteriology *173*, 3191-3198.

Migocki, M.D., Lewis, P.J., Wake, R.G., and Harry, E.J. (2004). The midcell replication factory in Bacillus subtilis is highly mobile: implications for coordinating chromosome replication with other cell cycle events. Molecular microbiology *54*, 452-463.

Mingorance, J., Rueda, S., Gomez-Puertas, P., Valencia, A., and Vicente, M. (2001). Escherichia coli FtsZ polymers contain mostly GTP and have a high nucleotide turnover. Molecular microbiology *41*, 83-91.

Mingorance, J., Tadros, M., Vicente, M., Gonzalez, J.M., Rivas, G., and Velez, M. (2005). Visualization of single Escherichia coli FtsZ filament dynamics with atomic force microscopy. The Journal of biological chemistry *280*, 20909-20914.

Miwa, Y., Nakata, A., Ogiwara, A., Yamamoto, M., and Fujita, Y. (2000). Evaluation and characterization of catabolite-responsive elements (cre) of Bacillus subtilis. Nucleic acids research *28*, 1206-1210.

Mo, A.H., and Burkholder, W.F. (2010). YneA, an SOS-induced inhibitor of cell division in Bacillus subtilis, is regulated posttranslationally and requires the transmembrane region for activity. Journal of bacteriology *192*, 3159-3173.

Mohammadi, T., Ploeger, G.E., Verheul, J., Comvalius, A.D., Martos, A., Alfonso, C., van Marle, J., Rivas, G., and den Blaauwen, T. (2009). The GTPase activity of Escherichia coli FtsZ determines the magnitude of the FtsZ polymer bundling by ZapA in vitro. Biochemistry *48*, 11056-11066.

Mohammadi, T., van Dam, V., Sijbrandi, R., Vernet, T., Zapun, A., Bouhss, A., Diepeveen-de Bruin, M., Nguyen-Disteche, M., de Kruijff, B., and Breukink, E. (2011). Identification of FtsW as a transporter of lipid-linked cell wall precursors across the membrane. The EMBO journal *30*, 1425-1432.

Mohl, D.A., and Gober, J.W. (1997). Cell cycle-dependent polar localization of chromosome partitioning proteins in Caulobacter crescentus. Cell *88*, 675-684.

Molle, V., Fujita, M., Jensen, S.T., Eichenberger, P., Gonzalez-Pastor, J.E., Liu, J.S., and Losick, R. (2003a). The Spo0A regulon of Bacillus subtilis. Molecular microbiology *50*, 1683-1701.

Molle, V., Nakaura, Y., Shivers, R.P., Yamaguchi, H., Losick, R., Fujita, Y., and Sonenshein, A.L. (2003b). Additional targets of the Bacillus subtilis global regulator CodY identified by chromatin immunoprecipitation and genome-wide transcript analysis. Journal of bacteriology *185*, 1911-1922.

Monahan, L.G., Robinson, A., and Harry, E.J. (2009). Lateral FtsZ association and the assembly of the cytokinetic Z ring in bacteria. Molecular microbiology *74*, 1004-1017.

Morimoto, T., Loh, P.C., Hirai, T., Asai, K., Kobayashi, K., Moriya, S., and Ogasawara, N. (2002). Six GTP-binding proteins of the Era/Obg family are essential for cell growth in Bacillus subtilis. Microbiology (Reading, England) *148*, 3539-3552.

Mukherjee, A., Cao, C., and Lutkenhaus, J. (1998). Inhibition of FtsZ polymerization by SulA, an inhibitor of septation in Escherichia coli. Proc Natl Acad Sci U S A *95*, 2885-2890.

Mukherjee, A., and Lutkenhaus, J. (1994). Guanine nucleotide-dependent assembly of FtsZ into filaments. Journal of bacteriology *176*, 2754-2758.

Mulder, E., and Woldringh, C.L. (1989). Actively replicating nucleoids influence positioning of division sites in Escherichia coli filaments forming cells lacking DNA. Journal of bacteriology *171*, 4303-4314.

Munakata, N. (1974). Ultraviolet sensitivity of Bacillus subtilis spores upon germination and outgrowth. Journal of bacteriology *120*, 59-65.

Murphy, L.D., and Zimmerman, S.B. (1997). Isolation and characterization of spermidine nucleoids from Escherichia coli. J Struct Biol *119*, 321-335.

Murray, H., and Errington, J. (2008). Dynamic control of the DNA replication initiation protein DnaA by Soj/ParA. Cell *135*, 74-84.

Murray, H., Ferreira, H., and Errington, J. (2006). The bacterial chromosome segregation protein Spo0J spreads along DNA from parS nucleation sites. Molecular microbiology *61*, 1352-1361.

Nasmyth, K., and Haering, C.H. (2005). The structure and function of SMC and kleisin complexes. Annu Rev Biochem *74*, 595-648.

Nguyen-Disteche, M., Fraipont, C., Buddelmeijer, N., and Nanninga, N. (1998). The structure and function of Escherichia coli penicillin-binding protein 3. Cell Mol Life Sci *54*, 309-316.

Nielsen, H.J., Li, Y., Youngren, B., Hansen, F.G., and Austin, S. (2006a). Progressive segregation of the Escherichia coli chromosome. Molecular microbiology *61*, 383-393.

Nielsen, H.J., Ottesen, J.R., Youngren, B., Austin, S.J., and Hansen, F.G. (2006b). The Escherichia coli chromosome is organized with the left and right chromosome arms in separate cell halves. Molecular microbiology *62*, 331-338.

Nikolaichik, Y.A., and Donachie, W.D. (2000). Conservation of gene order amongst cell wall and cell division genes in Eubacteria, and ribosomal genes in Eubacteria and Eukaryotic organelles. Genetica *108*, 1-7.

Nishibori, A., Kusaka, J., Hara, H., Umeda, M., and Matsumoto, K. (2005). Phosphatidylethanolamine domains and localization of phospholipid synthases in Bacillus subtilis membranes. Journal of bacteriology *187*, 2163-2174.

Nogales, E., Wolf, S.G., and Downing, K.H. (1998). Structure of the alpha beta tubulin dimer by electron crystallography. Nature *391*, 199-203.

Noirot-Gros, M.F., Dervyn, E., Wu, L.J., Mervelet, P., Errington, J., Ehrlich, S.D., and Noirot, P. (2002). An expanded view of bacterial DNA replication. Proc Natl Acad Sci U S A *99*, 8342-8347.

Noirot-Gros, M.F., Velten, M., Yoshimura, M., McGovern, S., Morimoto, T., Ehrlich, S.D., Ogasawara, N., Polard, P., and Noirot, P. (2006). Functional dissection of YabA, a negative regulator of DNA replication initiation in Bacillus subtilis. Proc Natl Acad Sci U S A *103*, 2368-2373.

Norris, V. (1995). Hypothesis: chromosome separation in Escherichia coli involves autocatalytic gene expression, transertion and membrane-domain formation. Molecular microbiology *16*, 1051-1057.

Ogasawara, N., and Yoshikawa, H. (1992). Genes and their organization in the replication origin region of the bacterial chromosome. Molecular microbiology *6*, 629-634.

Ogura, T., and Hiraga, S. (1983). Partition mechanism of F plasmid: two plasmid gene-encoded products and a cis-acting region are involved in partition. Cell *32*, 351-360.

Ogura, Y., Imai, Y., Ogasawara, N., and Moriya, S. (2001). Autoregulation of the dnaA-dnaN operon and effects of DnaA protein levels on replication initiation in Bacillus subtilis. Journal of bacteriology *183*, 3833-3841.

Oliva, M.A., Cordell, S.C., and Lowe, J. (2004a). Structural insights into FtsZ protofilament formation. Nature structural & molecular biology *11*, 1243-1250.

Oliva, M.A., Cordell, S.C., and Lowe, J. (2004b). Structural insights into FtsZ protofilament formation. Nat Struct Mol Biol *11*, 1243-1250.

Osteryoung, K.W., and Pyke, K.A. (1998). Plastid division: evidence for a prokaryotically derived mechanism. Current opinion in plant biology *1*, 475-479.

Osteryoung, K.W., Stokes, K.D., Rutherford, S.M., Percival, A.L., and Lee, W.Y. (1998). Chloroplast division in higher plants requires members of two functionally

divergent gene families with homology to bacterial ftsZ. The Plant cell *10*, 1991-2004.

Paez, A., Mateos-Gil, P., Horger, I., Mingorance, J., Rivas, G., Vicente, M., Velez, M., and Tarazona, P. (2009). Simple modeling of FtsZ polymers on flat and curved surfaces: correlation with experimental in vitro observations. PMC Biophys *2*, 8.

Patrick, J.E., and Kearns, D.B. (2008). MinJ (YvjD) is a topological determinant of cell division in Bacillus subtilis. Molecular microbiology *70*, 1166-1179.

Pedersen, L.B., Angert, E.R., and Setlow, P. (1999). Septal localization of penicillin-binding protein 1 in Bacillus subtilis. Journal of bacteriology *181*, 3201-3211.

Perego, M., Higgins, C.F., Pearce, S.R., Gallagher, M.P., and Hoch, J.A. (1991). The oligopeptide transport system of Bacillus subtilis plays a role in the initiation of sporulation. Molecular microbiology *5*, 173-185.

Peters, P.C., Migocki, M.D., Thoni, C., and Harry, E.J. (2007). A new assembly pathway for the cytokinetic Z ring from a dynamic helical structure in vegetatively growing cells of Bacillus subtilis. Molecular microbiology *64*, 487-499.

Petit, M.A., Dervyn, E., Rose, M., Entian, K.D., McGovern, S., Ehrlich, S.D., and Bruand, C. (1998). PcrA is an essential DNA helicase of Bacillus subtilis fulfilling functions both in repair and rolling-circle replication. Molecular microbiology *29*, 261-273.

Pichoff, S., and Lutkenhaus, J. (2002). Unique and overlapping roles for ZipA and FtsA in septal ring assembly in Escherichia coli. EMBO J *21*, 685-693.

Pichoff, S., and Lutkenhaus, J. (2005). Tethering the Z ring to the membrane through a conserved membrane targeting sequence in FtsA. Molecular microbiology *55*, 1722-1734.

Pichoff, S., Vollrath, B., Touriol, C., and Bouche, J.P. (1995). Deletion analysis of gene minE which encodes the topological specificity factor of cell division in Escherichia coli. Molecular microbiology *18*, 321-329.

Piggot, P.J., and Coote, J.G. (1976). Genetic aspects of bacterial endospore formation. Bacteriological reviews *40*, 908-962.

Polard, P., Marsin, S., McGovern, S., Velten, M., Wigley, D.B., Ehrlich, S.D., and Bruand, C. (2002). Restart of DNA replication in Gram-positive bacteria: functional characterisation of the Bacillus subtilis PriA initiator. Nucleic acids research *30*, 1593-1605.

Ponstingl, H., Krauhs, E., Little, M., and Kempf, T. (1981). Complete amino acid sequence of alpha-tubulin from porcine brain. Proc Natl Acad Sci U S A *78*, 2757-2761.

Postow, L., Hardy, C.D., Arsuaga, J., and Cozzarelli, N.R. (2004). Topological domain structure of the Escherichia coli chromosome. Genes & development *18*, 1766-1779.

Potuckova, L., Kelemen, G.H., Findlay, K.C., Lonetto, M.A., Buttner, M.J., and Kormanec, J. (1995). A new RNA polymerase sigma factor, sigma F, is required for the late stages of morphological differentiation in Streptomyces spp. Molecular microbiology *17*, 37-48.

Price, K.D., Roels, S., and Losick, R. (1997). A Bacillus subtilis gene encoding a protein similar to nucleotide sugar transferases influences cell shape and viability. Journal of bacteriology *179*, 4959-4961.

Ptacin, J.L., Lee, S.F., Garner, E.C., Toro, E., Eckart, M., Comolli, L.R., Moerner, W.E., and Shapiro, L. (2010). A spindle-like apparatus guides bacterial chromosome segregation. Nat Cell Biol *12*, 791-798.

Quardokus, E.M., and Brun, Y.V. (2002). DNA replication initiation is required for mid-cell positioning of FtsZ rings in Caulobacter crescentus. Molecular microbiology *45*, 605-616.

Ramamurthi, K.S., and Losick, R. (2009). Negative membrane curvature as a cue for subcellular localization of a bacterial protein. Proc Natl Acad Sci U S A *106*, 13541-13545.

Raskin, D.M., and de Boer, P.A. (1997). The MinE ring: an FtsZ-independent cell structure required for selection of the correct division site in E. coli. Cell *91*, 685-694.

RayChaudhuri, D. (1999). ZipA is a MAP-Tau homolog and is essential for structural integrity of the cytokinetic FtsZ ring during bacterial cell division. EMBO J *18*, 2372-2383.

RayChaudhuri, D., and Park, J.T. (1992). Escherichia coli cell-division gene ftsZ encodes a novel GTP-binding protein. Nature *359*, 251-254.

Regamey, A., Harry, E.J., and Wake, R.G. (2000). Mid-cell Z ring assembly in the absence of entry into the elongation phase of the round of replication in bacteria: co-ordinating chromosome replication with cell division. Molecular microbiology *38*, 423-434.

Rodionov, O., and Yarmolinsky, M. (2004). Plasmid partitioning and the spreading of P1 partition protein ParB. Molecular microbiology *52*, 1215-1223.

Romberg, L., and Levin, P.A. (2003). Assembly dynamics of the bacterial cell division protein FTSZ: poised at the edge of stability. Annual review of microbiology *57*, 125-154.

Romberg, L., and Mitchison, T.J. (2004). Rate-limiting guanosine 5'-triphosphate hydrolysis during nucleotide turnover by FtsZ, a prokaryotic tubulin homologue involved in bacterial cell division. Biochemistry *43*, 282-288.

Romberg, L., Simon, M., and Erickson, H.P. (2001). Polymerization of Ftsz, a bacterial homolog of tubulin. is assembly cooperative? J Biol Chem *276*, 11743-11753.

Rothfield, L., Justice, S., and Garcia-Lara, J. (1999). Bacterial cell division. Annual review of genetics *33*, 423-448.

Rothfield, L.I., and Zhao, C.R. (1996). How do bacteria decide where to divide? Cell *84*, 183-186.

Rouviere-Yaniv, J., Yaniv, M., and Germond, J.E. (1979). E. coli DNA binding protein HU forms nucleosomelike structure with circular double-stranded DNA. Cell *17*, 265-274.

Rowland, S.J., Boocock, M.R., and Stark, W.M. (2005). Regulation of Sin recombinase by accessory proteins. Molecular microbiology *56*, 371-382.

Rowland, S.L., Wadsworth, K.D., Robson, S.A., Robichon, C., Beckwith, J., and King, G.F. (2010). Evidence from artificial septal targeting and site-directed mutagenesis that residues in the extracytoplasmic beta domain of DivIB mediate its interaction with the divisomal transpeptidase PBP 2B. Journal of bacteriology *192*, 6116-6125.

Rudner, D.Z., LeDeaux, J.R., Ireton, K., and Grossman, A.D. (1991). The spo0K locus of Bacillus subtilis is homologous to the oligopeptide permease locus and is required for sporulation and competence. Journal of bacteriology *173*, 1388-1398.

Rueda, S., Vicente, M., and Mingorance, J. (2003). Concentration and assembly of the division ring proteins FtsZ, FtsA, and ZipA during the Escherichia coli cell cycle. Journal of bacteriology *185*, 3344-3351.

Ryding, N.J., Kelemen, G.H., Whatling, C.A., Flardh, K., Buttner, M.J., and Chater, K.F. (1998). A developmentally regulated gene encoding a repressor-like protein is essential for sporulation in Streptomyces coelicolor A3(2). Molecular microbiology *29*, 343-357.

Sahoo, T., Mohanty, B.K., Lobert, M., Manna, A.C., and Bastia, D. (1995). The contrahelicase activities of the replication terminator proteins of Escherichia coli and Bacillus subtilis are helicase-specific and impede both helicase translocation

and authentic DNA unwinding. The Journal of biological chemistry *270*, 29138-29144.

Sakai, N., Yao, M., Itou, H., Watanabe, N., Yumoto, F., Tanokura, M., and Tanaka, I. (2001). The three-dimensional structure of septum site-determining protein MinD from Pyrococcus horikoshii OT3 in complex with Mg-ADP. Structure *9*, 817-826.

Sanders, G.M., Dallmann, H.G., and McHenry, C.S. (2010). Reconstitution of the B. subtilis replisome with 13 proteins including two distinct replicases. Mol Cell *37*, 273-281.

Sargent, M.G. (1975). Control of cell length in Bacillus subtilis. Journal of bacteriology *123*, 7-19.

Schaechter, M., Maaloe, O., and Kjeldgaard, N.O. (1958). Dependency on medium and temperature of cell size and chemical composition during balanced grown of Salmonella typhimurium. J Gen Microbiol *19*, 592-606.

Schaeffer, P., Millet, J., and Aubert, J.P. (1965). Catabolic repression of bacterial sporulation. Proc Natl Acad Sci U S A *54*, 704-711.

Scheffers, D.J., de Wit, J.G., den Blaauwen, T., and Driessen, A.J. (2002). GTP hydrolysis of cell division protein FtsZ: evidence that the active site is formed by the association of monomers. Biochemistry *41*, 521-529.

Scheffers, D.J., and Driessen, A.J. (2002). Immediate GTP hydrolysis upon FtsZ polymerization. Molecular microbiology *43*, 1517-1521.

Scheffers, D.J., and Errington, J. (2004). PBP1 is a component of the Bacillus subtilis cell division machinery. Journal of bacteriology *186*, 5153-5156.

Schleiffer, A., Kaitna, S., Maurer-Stroh, S., Glotzer, M., Nasmyth, K., and Eisenhaber, F. (2003). Kleisins: a superfamily of bacterial and eukaryotic SMC protein partners. Mol Cell *11*, 571-575.

Schwedock, J., McCormick, J.R., Angert, E.R., Nodwell, J.R., and Losick, R. (1997). Assembly of the cell division protein FtsZ into ladder-like structures in the aerial hyphae of Streptomyces coelicolor. Molecular microbiology *25*, 847-858.

Sciochetti, S.A., Piggot, P.J., and Blakely, G.W. (2001). Identification and characterization of the dif Site from Bacillus subtilis. Journal of bacteriology *183*, 1058-1068.

Sciochetti, S.A., Piggot, P.J., Sherratt, D.J., and Blakely, G. (1999). The ripX locus of Bacillus subtilis encodes a site-specific recombinase involved in proper chromosome partitioning. Journal of bacteriology *181*, 6053-6062.

Sekowska, A., Coppee, J.Y., Le Caer, J.P., Martin-Verstraete, I., and Danchin, A. (2000). S-adenosylmethionine decarboxylase of Bacillus subtilis is closely related to archaebacterial counterparts. Molecular microbiology *36*, 1135-1147.

Shaevitz, J.W., and Gitai, Z. (2010). The Structure and Function of Bacterial Actin Homologs. Cold Spring Harb Perspect Biol.

Sharp, M.D., and Pogliano, K. (2003). The membrane domain of SpoIIIE is required for membrane fusion during Bacillus subtilis sporulation. Journal of bacteriology *185*, 2005-2008.

Sharpe, M.E., and Errington, J. (1995). Postseptational chromosome partitioning in bacteria. Proceedings of the National Academy of Sciences of the United States of America *92*, 8630-8634.

Sharpe, M.E., Hauser, P.M., Sharpe, R.G., and Errington, J. (1998). Bacillus subtilis cell cycle as studied by fluorescence microscopy: constancy of cell length at initiation of DNA replication and evidence for active nucleoid partitioning. Journal of bacteriology *180*, 547-555.

Shiomi, D., and Margolin, W. (2008). Compensation for the loss of the conserved membrane targeting sequence of FtsA provides new insights into its function. Molecular microbiology *67*, 558-569.

Shivers, R.P., and Sonenshein, A.L. (2004). Activation of the Bacillus subtilis global regulator CodY by direct interaction with branched-chain amino acids. Molecular microbiology *53*, 599-611.

Sievers, J., and Errington, J. (2000). The Bacillus subtilis cell division protein FtsL localizes to sites of septation and interacts with DivIC. Molecular microbiology *36*, 846-855.

Sim, E., Walters, K., and Boukouvala, S. (2008). Arylamine N-acetyltransferases: from structure to function. Drug metabolism reviews *40*, 479-510.

Singh, J.K., Makde, R.D., Kumar, V., and Panda, D. (2008). SepF increases the assembly and bundling of FtsZ polymers and stabilizes FtsZ protofilaments by binding along its length. J Biol Chem *283*, 31116-31124.

Skarstad, K., Lobner-Olesen, A., Atlung, T., von Meyenburg, K., and Boye, E. (1989). Initiation of DNA replication in Escherichia coli after overproduction of the DnaA protein. Mol Gen Genet *218*, 50-56.

Small, E., Marrington, R., Rodger, A., Scott, D.J., Sloan, K., Roper, D., Dafforn, T.R., and Addinall, S.G. (2007). FtsZ polymer-bundling by the Escherichia coli ZapA orthologue, YgfE, involves a conformational change in bound GTP. J Mol Biol *369*, 210-221.

Smith, T.J., Blackman, S.A., and Foster, S.J. (2000). Autolysins of Bacillus subtilis: multiple enzymes with multiple functions. Microbiology (Reading, England) *146 (Pt 2)*, 249-262.

Soppa, J. (2001). Prokaryotic structural maintenance of chromosomes (SMC) proteins: distribution, phylogeny, and comparison with MukBs and additional prokaryotic and eukaryotic coiled-coil proteins. Gene *278*, 253-264.

Soppa, J., Kobayashi, K., Noirot-Gros, M.F., Oesterhelt, D., Ehrlich, S.D., Dervyn, E., Ogasawara, N., and Moriya, S. (2002). Discovery of two novel families of proteins that are proposed to interact with prokaryotic SMC proteins, and characterization of the Bacillus subtilis family members ScpA and ScpB. Molecular microbiology *45*, 59-71.

Soufo, C.D., Soufo, H.J., Noirot-Gros, M.F., Steindorf, A., Noirot, P., and Graumann, P.L. (2008). Cell-cycle-dependent spatial sequestration of the DnaA replication initiator protein in Bacillus subtilis. Dev Cell *15*, 935-941.

Steele, V.R., Bottomley, A.L., Garcia-Lara, J., Kasturiarachchi, J., and Foster, S.J. (2011). Multiple essential roles for EzrA in cell division of Staphylococcus aureus. Molecular microbiology *80*, 542-555.

Stragier, P., Bonamy, C., and Karmazyn-Campelli, C. (1988). Processing of a sporulation sigma factor in Bacillus subtilis: how morphological structure could control gene expression. Cell *52*, 697-704.

Stricker, J., Maddox, P., Salmon, E.D., and Erickson, H.P. (2002). Rapid assembly dynamics of the Escherichia coli FtsZ-ring demonstrated by fluorescence recovery after photobleaching. Proc Natl Acad Sci U S A *99*, 3171-3175.

Sullivan, N.L., Marquis, K.A., and Rudner, D.Z. (2009). Recruitment of SMC by ParB-parS organizes the origin region and promotes efficient chromosome segregation. Cell *137*, 697-707.

Sun, L., and Fuchs, J.A. (1994). Regulation of the Escherichia coli nrd operon: role of DNA supercoiling. Journal of bacteriology *176*, 4617-4626.

Tan, H., Yang, H., Tian, Y., Wu, W., Whatling, C.A., Chamberlin, L.C., Buttner, M.J., Nodwell, J., and Chater, K.F. (1998). The Streptomyces coelicolor sporulation-specific sigma WhiG form of RNA polymerase transcribes a gene encoding a ProX-like protein that is dispensable for sporulation. Gene *212*, 137-146.

Tanaka, I., Appelt, K., Dijk, J., White, S.W., and Wilson, K.S. (1984). 3-A resolution structure of a protein with histone-like properties in prokaryotes. Nature *310*, 376-381.

Tapias, A., Lopez, G., and Ayora, S. (2000). Bacillus subtilis LrpC is a sequence-independent DNA-binding and DNA-bending protein which bridges DNA. Nucleic Acids Res *28*, 552-559.

Teleman, A.A., Graumann, P.L., Lin, D.C., Grossman, A.D., and Losick, R. (1998). Chromosome arrangement within a bacterium. Curr Biol *8*, 1102-1109.

Thanbichler, M., and Shapiro, L. (2006). MipZ, a spatial regulator coordinating chromosome segregation with cell division in Caulobacter. Cell *126*, 147-162.

Thanedar, S., and Margolin, W. (2004). FtsZ exhibits rapid movement and oscillation waves in helix-like patterns in Escherichia coli. Curr Biol *14*, 1167-1173.

Tojo, S., Satomura, T., Morisaki, K., Deutscher, J., Hirooka, K., and Fujita, Y. (2005). Elaborate transcription regulation of the Bacillus subtilis ilv-leu operon involved in the biosynthesis of branched-chain amino acids through global regulators of CcpA, CodY and TnrA. Molecular microbiology *56*, 1560-1573.

Trucksis, M., and Depew, R.E. (1981). Identification and localization of a gene that specifies production of Escherichia coli DNA topoisomerase I. Proc Natl Acad Sci U S A *78*, 2164-2168.

Vagner, V., Dervyn, E., and Ehrlich, S.D. (1998). A vector for systematic gene inactivation in Bacillus subtilis. Microbiology (Reading, England) *144 (Pt 11)*, 3097-3104.

van den Ent, F., Amos, L.A., and Lowe, J. (2001). Prokaryotic origin of the actin cytoskeleton. Nature *413*, 39-44.

van den Ent, F., and Lowe, J. (2000). Crystal structure of the cell division protein FtsA from Thermotoga maritima. EMBO J *19*, 5300-5307.

Varshavsky, A.J., Nedospasov, S.A., Bakayev, V.V., Bakayeva, T.G., and Georgiev, G.P. (1977). Histone-like proteins in the purified Escherichia coli deoxyribonucleoprotein. Nucleic Acids Res *4*, 2725-2745.

Vicente, M., and Rico, A.I. (2006). The order of the ring: assembly of Escherichia coli cell division components. Molecular microbiology *61*, 5-8.

Viollier, P.H., Thanbichler, M., McGrath, P.T., West, L., Meewan, M., McAdams, H.H., and Shapiro, L. (2004). Rapid and sequential movement of individual chromosomal loci to specific subcellular locations during bacterial DNA replication. Proc Natl Acad Sci U S A *101*, 9257-9262.

Vologodskii, A.V., and Cozzarelli, N.R. (1994). Conformational and thermodynamic properties of supercoiled DNA. Annu Rev Biophys Biomol Struct *23*, 609-643.

Wahle, E., Lasken, R.S., and Kornberg, A. (1989). The dnaB-dnaC replication protein complex of Escherichia coli. I. Formation and properties. J Biol Chem *264*, 2463-2468.

Wang, J.C. (1971). Interaction between DNA and an Escherichia coli protein omega. J Mol Biol *55*, 523-533.

Wang, J.D., and Levin, P.A. (2009). Metabolism, cell growth and the bacterial cell cycle. Nature reviews *7*, 822-827.

Wang, J.D., Sanders, G.M., and Grossman, A.D. (2007). Nutritional control of elongation of DNA replication by (p)ppGpp. Cell *128*, 865-875.

Wang, X., Liu, X., Possoz, C., and Sherratt, D.J. (2006). The two Escherichia coli chromosome arms locate to separate cell halves. Genes & development *20*, 1727-1731.

Warner, J.B., and Lolkema, J.S. (2003). A Crh-specific function in carbon catabolite repression in Bacillus subtilis. FEMS microbiology letters *220*, 277-280.

Waterhouse, A.M., Procter, J.B., Martin, D.M., Clamp, M., and Barton, G.J. (2009). Jalview Version 2--a multiple sequence alignment editor and analysis workbench. Bioinformatics *25*, 1189-1191.

Weart, R.B., Lee, A.H., Chien, A.C., Haeusser, D.P., Hill, N.S., and Levin, P.A. (2007). A metabolic sensor governing cell size in bacteria. Cell *130*, 335-347.

Weart, R.B., and Levin, P.A. (2003). Growth rate-dependent regulation of medial FtsZ ring formation. Journal of bacteriology *185*, 2826-2834.

Weart, R.B., Nakano, S., Lane, B.E., Zuber, P., and Levin, P.A. (2005). The ClpX chaperone modulates assembly of the tubulin-like protein FtsZ. Molecular microbiology *57*, 238-249.

Webb, C.D., Teleman, A., Gordon, S., Straight, A., Belmont, A., Lin, D.C., Grossman, A.D., Wright, A., and Losick, R. (1997). Bipolar localization of the replication origin regions of chromosomes in vegetative and sporulating cells of B. subtilis. Cell *88*, 667-674.

Weiss, D.S. (2004). Bacterial cell division and the septal ring. Molecular microbiology *54*, 588-597.

Wendrich, T.M., and Marahiel, M.A. (1997). Cloning and characterization of a relA/spoT homologue from Bacillus subtilis. Molecular microbiology *26*, 65-79.

Whitehead, R.N., Overton, T.W., Snyder, L.A., McGowan, S.J., Smith, H., Cole, J.A., and Saunders, N.J. (2007). The small FNR regulon of Neisseria gonorrhoeae: comparison with the larger Escherichia coli FNR regulon and interaction with the NarQ-NarP regulon. BMC Genomics *8*, 35.

Willemse, J., Borst, J.W., de Waal, E., Bisseling, T., and van Wezel, G.P. (2011). Positive control of cell division: FtsZ is recruited by SsgB during sporulation of Streptomyces. Genes & development *25*, 89-99.

Witz, G., and Stasiak, A. (2010). DNA supercoiling and its role in DNA decatenation and unknotting. Nucleic Acids Res *38*, 2119-2133.

Woldringh, C.L., Mulder, E., Valkenburg, J.A., Wientjes, F.B., Zaritsky, A., and Nanninga, N. (1990). Role of the nucleoid in the toporegulation of division. Research in microbiology *141*, 39-49.

Woo, J.S., Lim, J.H., Shin, H.C., Suh, M.K., Ku, B., Lee, K.H., Joo, K., Robinson, H., Lee, J., Park, S.Y*., et al.* (2009). Structural studies of a bacterial condensin complex reveal ATP-dependent disruption of intersubunit interactions. Cell *136*, 85-96.

Worcel, A., and Burgi, E. (1972). On the structure of the folded chromosome of Escherichia coli. J Mol Biol *71*, 127-147.

Wu, L.J., and Errington, J. (1994). Bacillus subtilis SpoIIIE protein required for DNA segregation during asymmetric cell division. Science *264*, 572-575.

Wu, L.J., and Errington, J. (2003). RacA and the Soj-Spo0J system combine to effect polar chromosome segregation in sporulating Bacillus subtilis. Molecular microbiology *49*, 1463-1475.

Wu, L.J., and Errington, J. (2004). Coordination of cell division and chromosome segregation by a nucleoid occlusion protein in Bacillus subtilis. Cell *117*, 915-925.

Wu, L.J., Ishikawa, S., Kawai, Y., Oshima, T., Ogasawara, N., and Errington, J. (2009). Noc protein binds to specific DNA sequences to coordinate cell division with chromosome segregation. EMBO J *28*, 1940-1952.

Xie, Z., Li, W., Tian, Y., Liu, G., and Tan, H. (2007). Identification and characterization of sawC, a whiA-like gene, essential for sporulation in Streptomyces ansochromogenes. Archives of microbiology *188*, 575-582.

Xu, Y.C., and Bremer, H. (1988). Chromosome replication in Escherichia coli induced by oversupply of DnaA. Mol Gen Genet *211*, 138-142.

Yamaichi, Y., and Niki, H. (2000). Active segregation by the Bacillus subtilis partitioning system in Escherichia coli. Proc Natl Acad Sci U S A *97*, 14656-14661.

Yates, J., Zhekov, I., Baker, R., Eklund, B., Sherratt, D.J., and Arciszewska, L.K. (2006). Dissection of a functional interaction between the DNA translocase, FtsK, and the XerD recombinase. Molecular microbiology *59*, 1754-1766.

Yu, X.C., and Margolin, W. (1999). FtsZ ring clusters in min and partition mutants: role of both the Min system and the nucleoid in regulating FtsZ ring localization. Molecular microbiology *32*, 315-326.

Zechiedrich, E.L., Khodursky, A.B., and Cozzarelli, N.R. (1997). Topoisomerase IV, not gyrase, decatenates products of site-specific recombination in Escherichia coli. Genes & development *11*, 2580-2592.

Zhang, Y., Rowland, S., King, G., Braswell, E., and Rothfield, L. (1998). The relationship between hetero-oligomer formation and function of the topological specificity domain of the Escherichia coli MinE protein. Molecular microbiology *30*, 265-273.

Zyskind, J.W., and Smith, D.W. (1992). DNA replication, the bacterial cell cycle, and cell growth. Cell *69*, 5-8.

Appendices

Appendix 1 Solutions

4x Binding buffer	40% glycerol 80 mM Tris HCl, pH 8.0 400 mM KCl 20 mM $MgCl_2$ 2 µM DTT 100 µg/ml BSA
Blocking buffer	5% Milk powder in PBS 0.1% Tween
Buffer A	50 mM Tris·HCl, pH 8.0 100 mM NaCl
Buffer AK	100 mM KCl 50 mM Tris·HCl, pH 8.0 20 mM imidazole 5% glycerol
Buffer BK	1 M KCl 50 mM Tris·HCl, pH 8.0 20 mM imidazole 5% glycerole
CAA (casamino acids)	20% casamino acids
Ferric ammonium citrate	2.2 mg/ml Ferric ammonium citrate
PBST	0.1% Tween20 in PBS
PBSTM	0.25% skimmed milk in PBST
pronase solution	10 mg/ml protease type VI (Sigma) in TES
2 x sample buffer	125 mM Tris HCl, pH 6.8 20 % glycerol 10 % β-mercaptoethanol 4 % SDS 0.005 % bromphenol blue
10x SDS running buffer for WB	0.25 M Tris 1.92M glycine 1% SDS
SMM (Spizizen minimal medium)	0.2% $(NH_4)_2SO_4$ 1.4% K_2HPO_4 0.6% KH_2PO_4

0.1% sodium citrate
0.02% $MgSO_4$
adjust the volume to 1 l with dH_2O

Solution D 0.1 M $CaCl_2$

Solution E 40% D-glucose

Solution F 1 M $MgSO_4$

Solution G 25 g Oxoid Casein hydrolysate
11.7 g sodium glutamate
3.125 g L-alanine
3.48 g L-asparagine
3.4 g KH_2PO_4
1.34 g NH_4Cl_2
0.27 g Na_2SO_4
0.24 g NH_4NO_3
2.45 g $FeCl_3 \cdot 6H_2O$
adjust the volume to 1 l with dH_2O

Solution H 50 mM $MnSO_4$
fill up to 1 l with dH_2O

Solution P 40% methanol
12% acetic acid

STOP dye (6x DNA loading dye) 0.04% bromphenol blue
50% glycerol

TB buffer 10 mM PIPES (or HEPES)
55 mM $MnCl_2$
15 mM $CaCl_2$
250 mM KCl
adjust the pH 6.7
add $MnCl_2$ to a final concentration of 55 mM and filter sterilize

50× TAE buffer 2 M Tris pH 8
50 mM acetic acid
100 mM EDTA

TE buffer 10 mM Tris, pH 8
1 mM EDTA

10× TES buffer 0.2 M Tris pH 7.5
5 mM EDTA
100 mM NaCl

Transfer Buffer 0.5 x SDS running buffer
20% methanol
dH_2O

Tryptophan solution 2 mg/ml tryptophan

Appendix 2 Growth media

CH medium	200 ml solution G 2 ml tryptophan solution 0.4 ml solution H 0.2 ml solution D 0.08 ml solution F
Competence medium	10 ml SMM
SMM+	0.125 ml solution E 0.1 ml tryptophan solution 0.06 ml solution F 0.01 ml CAA 0.005 ml ferric ammonium citrate
DSM medium	modified after (Schaeffer *et al.*, 1965) 8 g Nutrient Broth powder (Difco) 1 ml solution F 1 g KCl adjust the volume to 1 l with dH_2O, autoclave add the following: 10 ml solution D 2 ml solution H
LB medium	10 g Tryptone 5 g Yeast extract 10 g NaCl adjust the volume to 1 l and autoclave autoclave
Nutrient Agar	28 g Oxoid Nutrient Agar adjust the volume to 1 l with dH_2O and autoclave
Starvation medium	10 ml SMM 0.125 ml solution E 0.06 ml solution F